SWELLING, THERMAL, AND HYDRAULIC PROPERTIES OF A BENTONITE-SAND BARRIER IN A DEEP GEOLOGICAL REPOSITORY FOR RADIOACTIVE WASTES: EFFECT OF GROUNDWATER CHEMISTRY, TEMPERATURE AND PHYSICAL FACTORS

Mohammed Alzamel

A thesis submitted in partial fulfillment of the requirements for the
Doctor of Philosophy degree in Environmental Engineering

Ottawa-Carleton Institute for Environmental Engineering
Department of Civil and Environmental Engineering
Faculty of Engineering
University of Ottawa

Abstract

Electricity generation at nuclear power plants produces a large amount of high-level radioactive waste (HLW) every year, which has long-term detrimental effects on humans and the environment. Other applications of nuclear technology (e.g., medicine, research, nuclear weapons, industry) also produce radioactive waste (e.g., low-level radioactive waste, LLW, Intermediate-level waste, ILW). The potential of deep geological repositories (DGRs) as an option for disposal of radioactive waste (HLW, ILW, LLW) has been examined in several countries, including Bulgaria, Canada, China, Finland, France, Germany, India, Japan, Russia, Spain, Sweden, Switzerland, Ukraine and the United Kingdom and are still under discussion. In Ontario, Canada, DGRs with a multi-barrier system comprised of a sedimentary rock formation (i.e., a natural barrier) and an engineered barrier system (EBS) are currently under consideration. An EBS consists of various components, such as waste containers, buffer, backfill, and tunnel sealing materials, intended to prevent the release of radionuclides. Several engineered barrier materials, including a mixture of bentonite and sand, are currently being considered for use in DGRs for nuclear waste in Ontario. Bentonite has some advantageous physical and chemical properties, such as low permeability, high plasticity, and high swelling potential, which provide it with a good sealing ability and thus make it an effective barrier. However, interaction between the compacted bentonite–sand mixture and underground water chemistry fluids (chemical factor) in the DGR could significantly alter the favourable properties of bentonite (e.g., swelling potential), thus influencing its performance when used in an EBS and eventually jeopardizing the overall safety of DGRs. In addition, other parameters, such as the clay content, initial dry density and moisture content of the compacted barrier (physical factors), as well as the presence of salts in groundwater may affect the physical and physiochemical properties of barrier materials. Moreover, during the lifetime of a DGR for used spent fuel, the bentonite–based barrier material will not only be exposed to a broad range

of groundwaters with different chemical compositions, but also to high temperatures (heat generated by the nuclear wastes) (thermal factor). Thus, the interaction between the compacted bentonite–sand mixture, the surrounding groundwater and the heat from the nuclear waste material could jeopardize the favourable properties of the bentonite-based (bentonite-sand) barrier material.

Properties of a bentonite-sand barrier is an important characteristic to study while designing and constructing an EBS for a DGR. Thus, to understand and assess the operations of DGRs in Ontario, comprehensive studies must be performed on engineering properties like swelling behaviour, permeability, and thermal conductivity. The goal of this research study is to experimentally investigate the physical, chemical and thermal factors that influencing the engineering properties of a barrier material made up of bentonite-sand composite used in DGRs for nuclear waste in Ontario. Compacted samples are subjected to one-dimensional free swell test to understand the swelling behaviour of the material. Hydraulic conductivity was investigated using a flexible wall permeability test. Thermal conductivity and diffusivity were tested using Decangon KD2 Pro with TR-1 and and KS-1 sensors. The specimens contain different bentonite–sand mixture ratios (20:80, 30:70, 50:50, and 70:30 dry mass), and they are tested under conditions with differing bentonite content, dry density, groundwater chemistry, and temperature. Additional tests were conducted to investigate the microstructure of the specimens. These tests include X-ray diffraction (XRD) analysis, mercury intrusion porosimetry (MIP), and thermogravimetric analyses (TG/DTG).

The results reveal that the time and strain required to achieve maximum swelling of compacted bentonite–sand specimens increase with the increase of initial dry density. The simulated saline solutions of Guelph and Trenton groundwater are found to suppress the swelling of the bentonite–sand specimens. This in turn leads to the increase of hydraulic conductivity and decrease of thermal properties of the barrier material. However, the impact of

the salinity is significantly reduced by increasing the dry densities and sand content of the compacted material. Moreover, the coupled effect of salinity and temperature decreases the swelling potential of the bentonite-sand mixture. Also, some transformation of Na-montmorillonite into Ca-Montmorillonite was observed. The results also indicate that some montmorillonites might have been transformed into illites, thereby further decreasing the swelling potential of the bentonite-based barrier.

Dedication

I dedicate this work to my beloved wife, Norah Alowayridhi for her love, support, and patience during my study.

Acknowledgements

Praise be to Almighty Allah, for granting me the capability to successfully complete this work. I would like to acknowledge many people for their support in writing this manuscript and through my PhD journey.

Special appreciation to my supervisor, Professor Mamadou Fall for his guidance, encouragement, patience, insightful advice, and constructive feedback during my studies.

I am grateful to King Abdulaziz City for Science and Technology (KACST) for giving me the opportunity and providing me with sponsorship, including full financial support for my family and I to complete my postgraduate studies. In addition, thanks to the Saudi Arabian Cultural Mission in Canada and the University of Ottawa, in particular the Civil Engineering Department for their services and support. I also appreciate the support of Dr. Zaid Aldhafeeri, Dr. Khalid Aleissa and Ahmad Alowayridhi at KACST.

I would also like to express my appreciation to all of those who provided support and assistance, and those I have known and worked in the Geotechnical Lab, especially Mr. Sada Haruna, and Mr. Jean Claude Célestin. In addition, my sincere thanks as well to all my colleagues at the University of Ottawa, as they have offered invaluable guidance and support.

I have no words to express my gratitude to my parents Abdullah and Hessa for their enormous support, care and prayers. Many thanks to my wife Norah Alowayridhi for being by my side throughout; I couldn't have done it without you. I also thank my brothers and sisters: Saad, Fahad, Norah, Fatema, Amira, Mona, Khalid, Khulood and Waleed, for their endearing support.

Table of Contents

List of Figures

List of Tables

Chapter 1: Introduction

1.1 Background

The global demand and consumption of energy/electricity are rapidly increasing due to continuous growth in the world's population and economy. This in turn leads to higher consumption of fossil fuels and the release of greenhouse gases (GHG) in the atmosphere, which contributes to global warming, also referred to as climate change. The environmental imperative is to reduce the release of carbon dioxide (CO_2) by using cleaner energy sources. Nuclear energy has been established as a new way to generate electricity around the world to meet the increased demand in many countries and reduce CO2 emissions. The electricity produced by different energy sources from 1985–2020, shows that nuclear power produced by about 450 power reactors provides about 11% of the world's electricity and is the second largest source of low-carbon energy source, as shown in Figure 1.1. According to the International Atomic Energy Agency (2017), there are 225 additional reactors for research purposes. However, the generation of nuclear energy is accompanied by the production of large amounts of harmful waste, including spent fuel bundles and radioactive waste, which are a great threat to human health and the surrounding environment for thousands of years. Moreover, other applications of nuclear technology (e.g., medicine, research, nuclear weapons, and industry) also produce detrimental radioactive wastes. It is, therefore, important to find suitable methods and techniques to dispose these wastes safely. The main principle for the management of radioactive wastes is total isolation to prevent radionuclide migration from repositories (European Commission, 2011).

Currently, deep geological repositories are widely agreed to be the best solution for the disposal of radioactive waste (Yang and Fall, 2021a, b, c). This approach has a reduced impact on the economy, human health, and the environment. The option of disposing nuclear waste in deep sedimentary rock is currently being investigated across the world (e.g., in Argentina,

Australia, Belgium, Canada, Czech Republic, Finland, France, Germany, Japan, the Netherlands, Republic of Korea, Russia, Spain, Sweden, Switzerland, the UK, and the USA. Deep geological repositories (DGRs) allow for radioactive waste disposal below the earth's surface at depths of 300–1000 m, which prevents radionuclides from reaching people and the environment (Atomic Energy of Canada Limited, 1994; Japan Nuclear Cycle Development Institute, 1999; Swedish Nuclear Fuel and Waste Management, 1992). The overall safety of this method of disposal is dependent upon the rock characteristics at the site (natural barrier, host rock) and a set of engineered barrier systems (EBSs), which comprises waste containers, buffer/backfill, and sealing elements (International Atomic Energy Agency [IAEA], 1981).

In Canada, DGRs are employed for disposing of nuclear waste and the process of site selection (e.g., Northern Ontario) has commenced (Nuclear Waste Management Organization [NWMO], 2012). The NWMO of Canada has put forward a proposal for the construction of a DGR in the Municipality of Kincardine in Ontario that would be 680 m deep. A sedimentary rock formation that forms a natural barrier extends throughout Southern Ontario.

The bentonite-based barrier is an important part of the DGR system. However, compacted pure bentonite has relatively low mechanical strength. For this reason, the use of bentonite-sand mixture has been the subject of various studies as a potential buffer and sealing material of EBS for Canadian DGRs and in other countries. The mixture has suitable performance properties from an engineering perspective due to its low permeability and high swelling potential. Furthermore, it is capable of retaining radionuclides if a canister should fail, causing contaminants to migrate through the barrier (Ito, 2006; Martin et al., 2000; Sato and Suzuki, 2003; Shehata et al., 2020; Stewart et al., 2003; Tripathy et al., 2004; Villar et al., 2005).

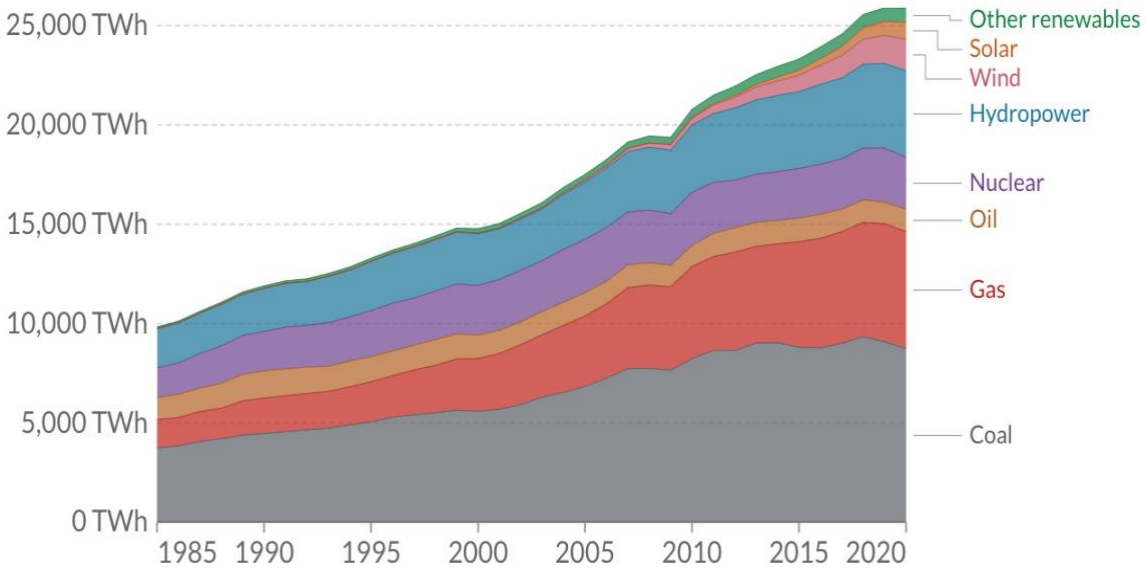

Note: Other renewables include biomass and waste, geothermal, wave and tidal

Figure 0.1. World electricity production by energy source from 1985–2020 (Our World in Data, 2021)

1.2 Problem description

There are many factors that affect the engineering performance of bentonite-based barrier material and the overall safety of a DGR. For instance, the swelling, thermal and hydraulic properties of bentonite-sand barriers can be changed by physical factors such as the dry density, and blending ratio (i.e. bentonite content) of the mixture. These properties can be significantly influenced by the chemical composition of the fluid within its pores. In particular, the interaction between the bentonite barrier and the saline water in a DGR could significantly alter its favourable properties (e.g., swelling potential) and negatively impact its long-term performance in preventing radionuclide migration, as concluded by numerous previous studies (e.g., Chen et al., 2017; Navarro et al., 2017; Liu et al., 2018; Akinwunmi et al., 2020). However, the results obtained in these previous studies are not directly transferable to a bentonite–sand barrier material in Canadian DGR conditions because Canadian groundwaters feature different chemical compositions than the groundwaters examined in these previous studies.

In Ontario, groundwater at the depth of the proposed DGR (600–700 m) is highly saline. This could impair the aforementioned properties of bentonite thereby affecting the safety of DGRs in Ontario. Thus, it is important to understand and assess the effect of the groundwater chemistry on the swelling behaviour as well as and hydraulic and thermal properties of compacted bentonite–sand barrier material. However, the effect of the groundwater chemistry on the engineering properties (swelling, hydraulic, thermal) of the bentonite-sand barrier is not fully understood. Furthermore, during the lifetime of a DGR for spent fuel, bentonite–sand barrier material will not only get exposed to a broad range of groundwaters with different chemical compositions but could also be subjected to elevated temperatures from the heat generated by the nuclear wastes. These high temperatures may intensify the groundwater chemistry-induced chemical attack on the bentonite-based barrier material. Thus, to ensure that the EBS will perform properly in all groundwater and thermal loading conditions in Ontario's or Canadian's DRGs, it is essential to understand whether and how significantly the swelling ability and other engineering properties of the barrier made with bentonite–sand is affected by the combined effects of groundwater chemistry and temperature. Due to the paucity of technical information on the coupled effect of the chemistry of Ontario's groundwater and temperature on the behaviour of bentonite-sand material, a new study is needed.

1.3 Research objectives

The overall goal of this proposed study is to provide valuable information that will ensure a better and safer design for DGRs in Ontario. To achieve that, the following specific objectives are set:

- To assess the effects of the physical factors (bentonite-sand ratio and dry density bentonite-sand mixture) on the swelling behaviour and the microstructural characteristics of potential barrier material for a DGR in Ontario (Canada).

- To assess the effects of the physical factors on the hydraulic conductivity and thermal properties of potential barrier material for a DGR in Ontario (Canada).
- To assess the effects of the physical factors and the salinity of Ontario's groundwaters on the swelling behaviour and mineralogical and microstructural characteristics of potential barrier material for a DGR in Ontario (Canada).
- To assess the effects of the physical factors and the salinity of Ontario's groundwater on the hydraulic conductivity and thermal properties of potential barrier material for a DGR in Ontario (Canada).
- To assess the effects of the physical factors, the salinity of Ontario's groundwaters, and temperature on the swelling behaviour and mineralogical and microstructural characteristics of potential barrier materials for a DGR in Ontario (Canada).
- To assess the effects of the physical factors, the salinity of groundwater and temperature on the hydraulic conductivity and thermal properties of potential barrier material for a DGR in Ontario (Canada).

1.4 Research approach and methods

In this research study, the effects of various factors (i.e., bentonite content, temperature, salinity, and dry density) on the swelling behaviour, as well as thermal, hydraulic, mineralogical, and microstructural properties of compacted mixtures of bentonite and sand with different blending ratios (20:80, 30:70, 50:50, and 70/30 dry mass) is experimentally investigated using many laboratory tests to achieve the aforementioned objectives. Figure 1.2 shows a flowchart of the research method or approach.

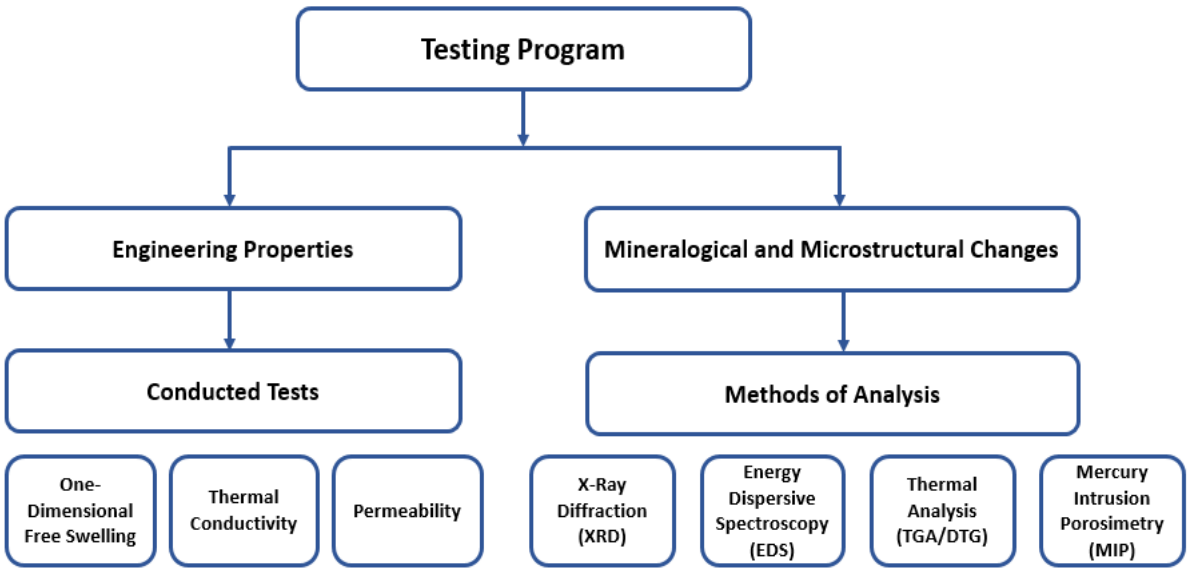

Figure 0.2. Flowchart of the research method

First, a one-dimensional free swell test (according to ASTM D-4546-08) was conducted to understand the swelling behaviour of the treated compacted bentonite–sand specimens. Second, mineralogical, and microstructural changes were assessed by conducting XRD EDS, and TGA/DTG analyses as well as MIP tests. Third, the thermal conductivity of compacted bentonite–sand mixtures exposed to Ontario's saline groundwater and/or temperatures was evaluated using a single-probe technique with Decagon KD2 Pro with a TR-1 sensor. Fourth, the hydraulic conductivity of the mixtures permeated with saline groundwater and subjected to varying thermal loadings was determined using an improved flexible wall permeability test by adding a cutting ring around the specimen to prevent sidewall leakage, which can simulate the actual stress states around the barrier system in practice.

1.5 Organization of thesis

This PhD manuscript will be organized into seven chapters, as described below. Figure 1.3 presents the organization visually.

Chapter One contains the introduction, providing a background information and stating the research problem, objectives, and methods.

Chapter Two consists of three main sections. The first section presents sources of radioactive waste and methods of classifying and managing them; the second section provides a theoretical and technical background on bentonite-based materials, the concept design of DGRs, and the characteristics of buffer/backfill and tunnel seals; and the third section reviews prior literature on the influence of salinity and other factors (temperature, dry density and bentonite content,) on the swelling behaviour and thermal, hydraulic, mineralogical, and microstructural properties of a bentonite–sand barrier in a DGR for radioactive waste.

Chapters Three to Five are three technical papers organized in a paper-based thesis format. Each technical paper includes an introduction, sections on the materials, methodology, experimental results, a discussion, and a conclusion. Because the main results are presented as technical papers, they will contain some repeated information. This is because each paper was independently written, without taking into account the content of the other papers or the rest of the document, and in accordance with the manuscript preparation instructions of the periodical in which they were published. **Chapter Six** integrates the whole results followed by a discussion. Finally, **Chapter Seven** concludes the thesis and provides recommendations for future work.

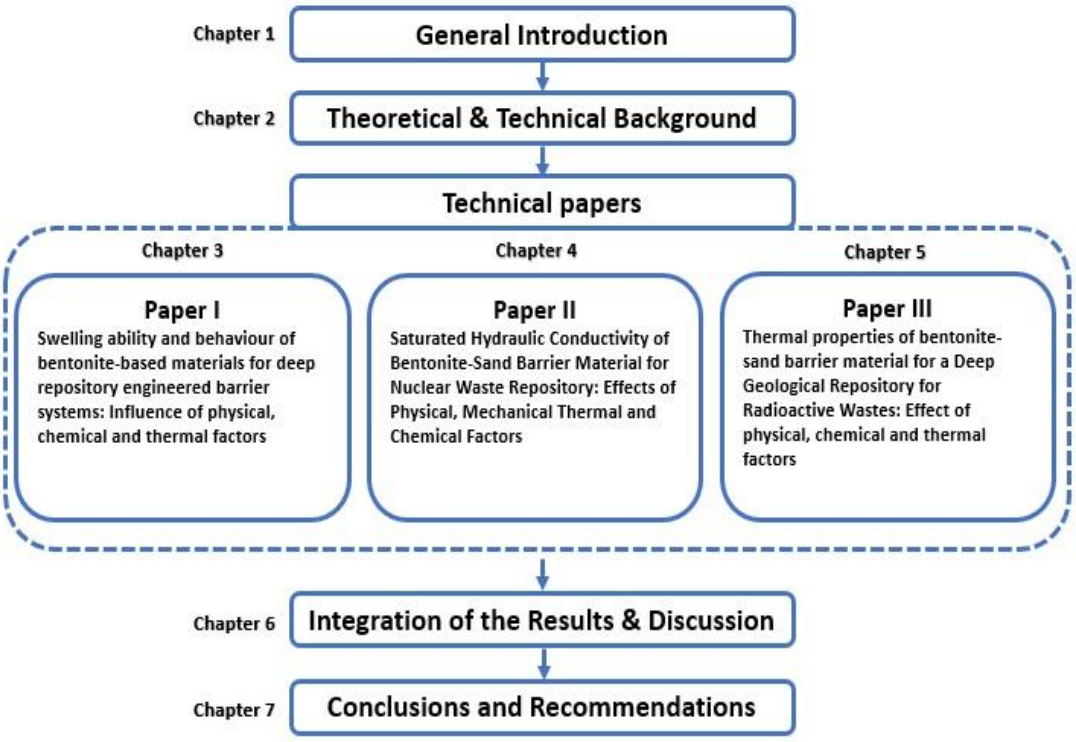

Figure 1.3. Organization of thesis

1.6 Statement of Authorship

Table 1.1 presents the summary of the technical papers produced from the current research.

Table 1.1. Technical papers from the PhD research

Title of Paper	**Journal**	**Authors**
Technical paper I: Swelling ability and behaviour of bentonite-based materials for deep repository engineered barrier systems: Influence of physical, chemical and thermal factors	Journal of Rock Mechanics and Geotechnical Engineering	Mohammed Alzamel, Mamadou Fall, Sada Haruna,
Technical paper II: Saturated Hydraulic Conductivity of Bentonite-Sand Barrier Material for Nuclear Waste Repository: Effects of Physical, Mechanical Thermal and Chemical Factors	Environmental Earth Sciences Journal	Mohammed Alzamel, Mamadou Fall, Sada Haruna,

Technical paper III: Thermal conductivity and diffusivity of bentonite-sand backfill materials for a deep geological repository exposed to saline groundwater	Journal of Rock Mechanics and Geotechnical Engineering	Mohammed Alzamel, Mamadoul Fall

Author Contributions

The contributions of each of the authors to the publications are outlined in Table 1.2. The authors have granted permissions for the publications to be included in the candidate's PhD thesis.

Table 1.2. Contributions of the authors of the technical papers

Name of Author	Designation	Contributions
Mohammed Alzamel	Principal author	Designed and constructed testing equipment, prepared samples and performed required tests; analysed and interpreted data; wrote the first draft of the manuscript.
Mamadou Fall	Co-author	Supervised conception and development of the research; provided help in data analysis and interpretation, manuscript writing and evaluation; acted as the corresponding author.
Sada Haruna	Co-author	Assisted the first author in samples preparation and testing.

1.7 References

Akinwunmi B., Hirvi J. T., Kasa S., Pakkanen T. A., 2020. Swelling pressure of Na- and Ca-montmorillonites in saline environments: A molecular dynamics study, Chemical Physics, 528,

Atomic Energy of Canada Limited, 1994. Environmental impact statement on the concept for disposal of Canada's nuclear fuel waste. AECL-10711: COG-93–COG-1, Ottawa, Ontario.

Chen Y.-G., Jia L.-Y., Li Q., Ye W.-M., Cui Y.-J., Chen B., 2017. Swelling deformation of compacted GMZ bentonite experiencing chemical cycles of sodium-calcium exchange and salinization-desalinization effect. Applied Clay Science, 141, 55-63.

European Commission, 2011. Third commission report on financing decommissioning. Available at http://ec.europa.eu/energy/sites/ener/files/documents/seventh_situation_report_corr_version_without_cover_page.pdf.

International Atomic Energy Agency, 1981. Underground Disposal of Radioactive Waste: Basic Guidance, Safety Series No. 54, IAEA, Vienna.

International Atomic Energy Agency, 2017. Energy, electricity and nuclear power estimates for the period up to 2050. Reference Data Series No. 1, Vienna, Austria.

Our World in Data (2020) Electricity production by source, World. Web. https://ourworldindata.org/grapher/electricity-prod-source-stacked. Retrieved 26 Jan. 2022.

Ito, H., 2006. Compaction properties of granular bentonite. Applied Clay Science, 31, 47–55.

Japan Nuclear Cycle Development Institute, 1999. H12: Project to establish the scientific and technical basis for HLW disposal in Japan. Supporting Report 2 (Respiratory Design and Engineering Technology), Japan Nuclear Cycle Development Institute, Tokyo, Japan.

Liu L.-N., Chen Y.-G., Ye W.-M., Cui Y.-J., Wu D.-B., 2018. Effects of hyperalkaline solutions on the swelling pressure of compacted Gaomiaozi (GMZ) bentonite from the viewpoint of Na+ cations and OH– anions, Applied Clay Science, 161, 334-342,

Martin, M., Cuevas, J., and Leguey, S., 2000. Diffusion of soluble salts under a temperature gradient after the hydration of compacted bentonites. Applied Clay Science, 17, 55–70.

Navarro V., Yustres Á., Asensio L., De la Morena G., González-Arteaga J., Laurila T., Pintado X., 2017. Modelling of compacted bentonite swelling accounting for salinity effects. Engineering Geology 223(7):48-58

Nuclear Waste Management Organization, 2012. Newsletter, Nuclear Waste Management Organization, 10, 1–4. Available at http://www.nwmo.ca/dgrprojectschedule.

Swedish Nuclear Fuel and Waste Management Company, 1992. SKB91 final disposal of spent nuclear fuel. Importance of the bedrock for safety. SKB Technical Report SKB TR 92–20, Swedish Nuclear Fuel and Waste Management Co. (SKB), Stockholm

Sato, H. and Suzuki, S., 2003. Fundamental study on the effect of an orientation of clay particles on diffusion pathway in compacted bentonites. Applied Clay Science, 23, 51–60.

Shehata, A., Fall, M., Detellier, C. 2020. Impact of groundwater chemistry and temperature on the swelling and microstructural properties of bentonite-sand mixtures for barriers for radioactive wastes repositories. Bulleting of Engineering Geology and the Environment, 80(2), 1857-1873.

Stewart, D.I., Studds, P.G., and Cousens, T.W., 2003. The factors controlling the engineering properties of bentonite-enhanced sand. Applied Clay Science, 23, 97–110.

Tripathy, S., Sridharan, A., and Schanz, T., 2004. Swelling pressures of compacted bentonites from diffuse double layer theory. Canadian Geotechnical Journal, 41, 437–450.

Villar, M., Garcia-Sineriz, J., Barcena, I., and Lloret, A., 2005. State of the bentonite barrier after five years operation of an in-situ test simulating a high-level radioactive waste repository. Engineering Geology, 81, 317–328.

Yang, J., Fall, M., 2021a. A two-scale hydro-mechanical-damage model for simulation of preferential gas flow in saturated clayey rocks. Computer & Geotechnics, 138, 104365.

Yang, J., Fall, M., 2021b. A dual porosity poroelastic model for simulation of gas flow in saturated claystone as a potential host rock for deep geological repositories. Tunnelling and Underground Space Technology, 115(4), 104049.

Yang, J., Fall, M., 2021c. A two-scale time dependent damage model for preferential gas flow in clayey rock materials. Mechanics of Materials, 158, 103853.

Chapter 2: Theoretical and Technical Background

This chapter provides a brief overview of deep geological repository (DGR) concepts, starting with a summary of the types of radioactive waste and management that are typically considered for DGR. Moreover, it provides a theoretical and technical background on bentonite-based materials and the characteristics of buffer/backfill and tunnel seals. Then, a literature review of previous works on the effects of water chemistry on the behaviour of bentonite-based barrier materials is presented.

2.1 Introduction

Nuclear waste is generated by a number of different human activities, including nuclear power production, transportation, medical treatment, agriculture, military weapon production, and scientific research. Safe management and disposal of this radioactive waste have become an issue of great importance for the protection of human health and the environment, both now and in the future. Discussion about and implementation of DGRs as a way to dispose of nuclear waste underground has begun in several countries, including Canada. A number of designs and concepts are still under discussion, and different countries have considered or adopted different designs and concepts. Numerous studies have been carried out recently to determine the best designs for storing nuclear waste safely putting into consideration the location of the DGR, host rock specifications, engineered barrier system (EBS), and nuclear waste container materials, among other factors. However, research on this topic is still limited, despite the need to understand the effects of other factors, such as the salinity of deep groundwater, dry density, temperature and clay content on the thermal, hydraulic and swelling properties of bentonite-based barrier materials to ensure the safety of DGRs.

Bentonite clay and bentonite–sand mixtures have been used as buffers between canisters containing radioactive waste and host rock, backfills, or seals in excavated disposal galleries in almost all DGRs throughout the world (Guo and Fall, 2018, 2019). These materials

are used because of their low hydraulic conductivity, excellent swelling potential, and long-term mineralogical stability. However, the aggressive environment in which DGRs are situated due to the chemical composition of deep groundwater and confining pressure, may cause changes in the mineralogy of the bentonite–sand materials and ultimately impact the physical and chemical properties of EBSs.

Divided into three sections, this chapter is intended to shed light on DGRs for radioactive waste and the behaviour of bentonite–sand mixture as an engineered barrier. The first section presents the sources and methods of classifying and managing of radioactive waste material; the second section provides a theoretical and technical background on bentonite-based materials, concept designs for DGRs, and the characteristics of buffer/backfill and tunnel seals; and the third section presents the main factors that affect the swelling behaviour and thermal, hydraulic, mineralogical, and microstructural properties of bentonite–sand barriers for DGRs. In addition, the chapter also provides a review on previous studies on the effects of pore water chemistry on the swelling behaviour and thermal, hydraulic, mineralogical, and microstructural properties of bentonite–sand barriers in DGRs for radioactive waste is performed.

2.2 Sources and classification of radioactive waste

Radioactive decay is a natural phenomenon that occurs in waste produced by various activities in industrial sectors, medicine, military weapons programs and laboratory research. Nuclear installations and reprocessing of spent fuel produce tons of radioactive waste every year. The general classification of radioactive waste is the responsibility of the International Atomic Energy Agency (IAEA) (see Figure 2.1), and such waste is usually classified according to the level of activity (Miller et al., 2000). This classification includes exempt waste (EW), very short-lived waste (VSLW), very low-level waste (VLLW), low-level waste (LLW), intermediate-level waste (ILW) and high-level waste (HLW).

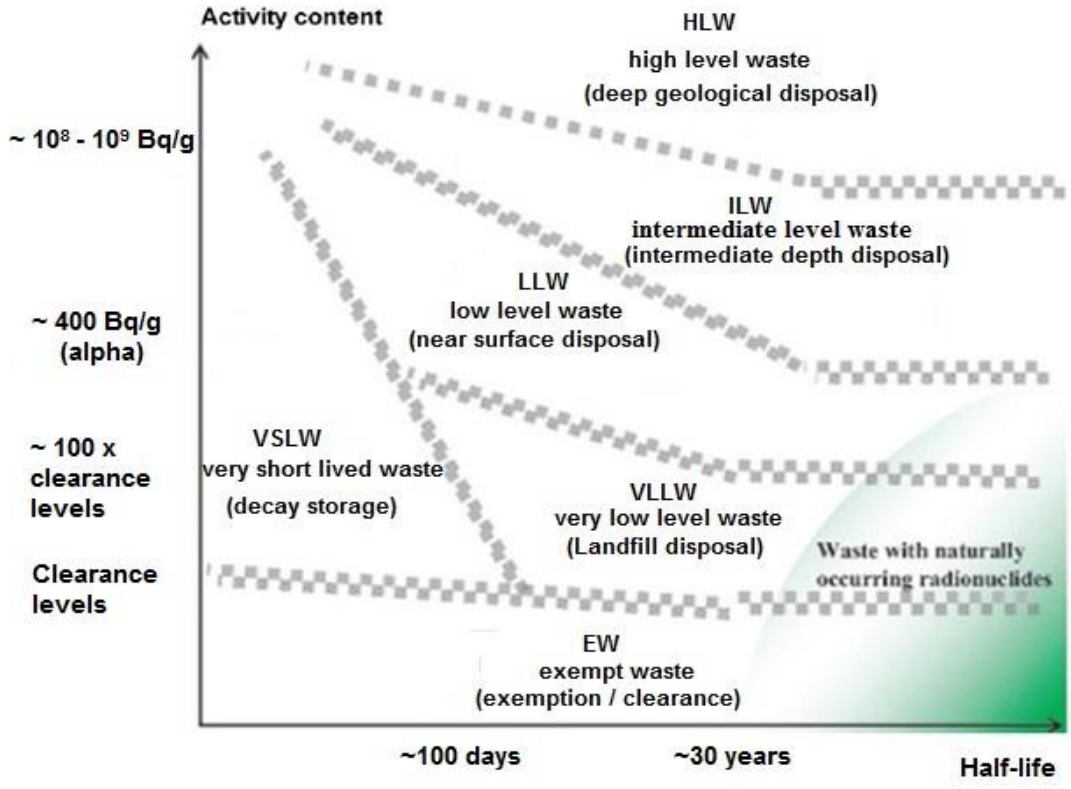

Figure 2.1. Classification scheme for radioactive wastes (IAEA, 2009)

The form of radioactive waste that is disposed of in a DGR depends on the national nuclear fuel program and classification system for radioactive waste used in the country in which the DGR is located. The Canadian Nuclear Safety Commission (CNSC) recognizes that nuclear waste falls into four broad categories (see Figure 2.2):

I. Low-level waste (IAEA classification: LLW)

LLW is a common type of nuclear waste that is mainly contaminated by short-lived radionuclides generated by industrial processes, hospitals, and nuclear reactor operations. This category of waste represents about 76% of all accumulated nuclear waste in the world but less than 1% of highly radioactive waste.

II. Intermediate-level waste (IAEA classification: ILW)

ILW, which features long-lived nuclides, is defined as materials contaminated from decommissioned reactors, such as internal reactor components, chemical sludge, and

cooling water filters. This waste category represents about 23% of all accumulated nuclear waste in the world and about 4% of highly radioactive waste.

III. High-level nuclear waste (IAEA classification: HLW)

HLW is a heat-producing waste mainly generated from nuclear fuel cycles. It includes spent fuel elements (SFs) such as uranium and plutonium. This type of waste represents less than 1% of all accumulated nuclear waste in the world but about 95% of highly radioactive waste.

IV. Uranium mine and mill waste

Uranium mine waste rock and mill tailings are a major forms of radioactive waste. Mining activities produce tons of dry mass of mineralized and clean waste rock. This waste contains significant concentrations of radioactive elements that are long-lived, namely thorium-230 and radium-226.

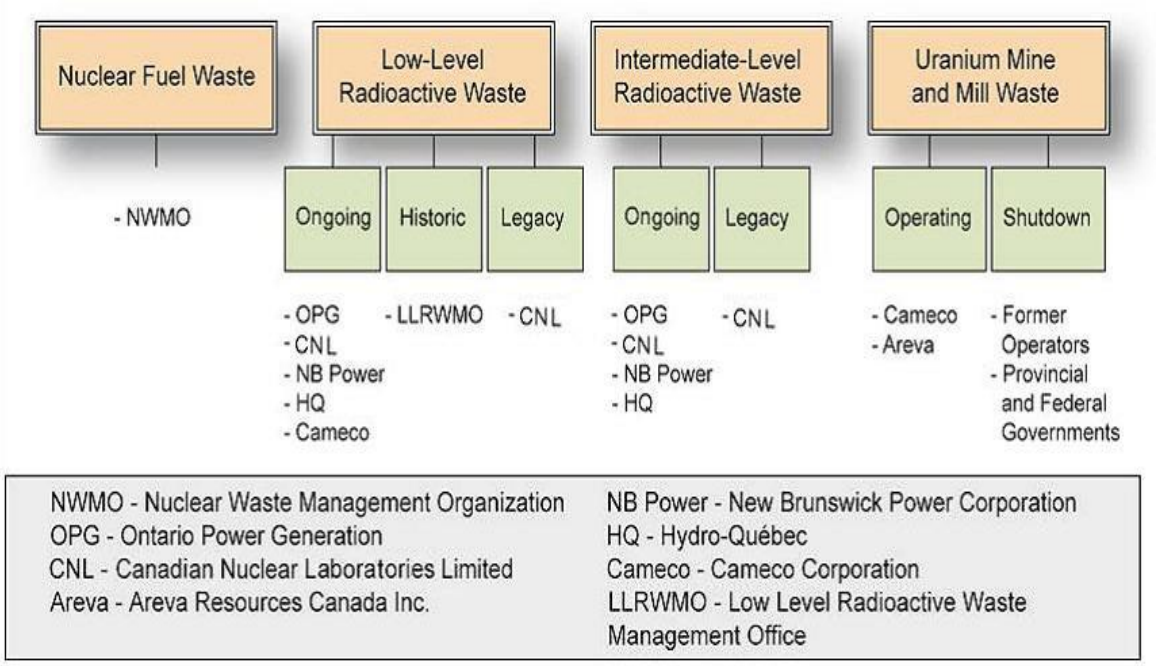

Figure 2.2. Organizations responsible for long-term management of used fuel and radioactive waste (CNSC, 2017)

2.3 Management of radioactive waste

For decades, a wide range of management strategies for the effective disposal of nuclear waste with long-lived toxicity, such as spent nuclear fuel (SNF) and HLW have been discussed. Such strategies include methods not related to geologic disposal, including seabed disposal, shooting waste into space, storage in the Antarctic ice sheet, partitioning and transmutation, long-term temporary disposal, and nuclear guardianship. However, all of these alternative disposal methods have been dismissed due to problems regarding technical realization, the high risk of accidents, ethical aspects, or costs. The international consensus (IAEA, 2003) is that geological disposal is the safest option for long-term disposal of all waste types. This involves isolating and containment of radioactive waste material in repositories located hundreds of meters below the ground surface in stable geological media that prevent the waste from interacting with the biosphere over time. Several countries have proposed building such repositories and have run extensive research for decades to develop a safe and sustainable repository for waste with long-lived toxicity. Figure 2.3 shows commonly accepted disposal and management procedures for different categories of radioactive waste materials.

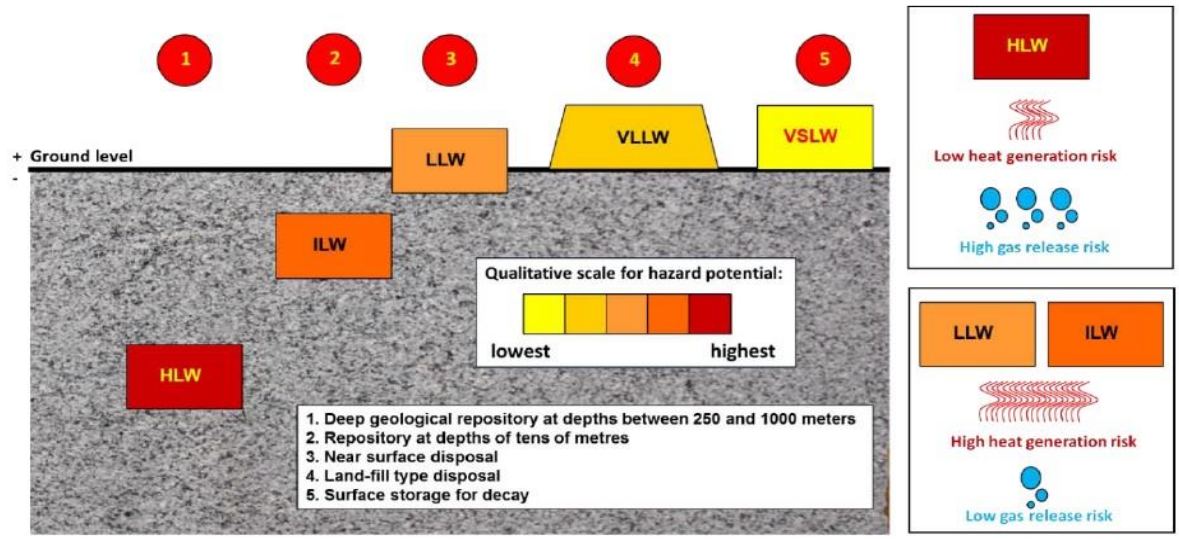

Figure 2.3. Commonly accepted management methods and storage depths of different types of radioactive waste (IAEA classification) with risks illustrations (figure on the left adapted from Bergström et al., 2011)

2.4 Background on deep geological repositories for radioactive waste

2.4.1 Description of the deep geological repository system

In a 1995 report by the NEA, the DGRs systems should be capable of the following:

(a) "*isolate the wastes from the biosphere for extremely long periods of time*" and

(b) "*ensure that residual radioactive substances reaching the biosphere will be at concentrations that are insignificant compared, for example, with the natural background levels of radioactivity*."

DGRs are permanent depositories that safely store, isolate, and contain radioactive waste for very long periods of time at depths of 300–1000 m (NWMO, 2010, 2012). Geological repositories comprise of multiple barriers (natural or geological barriers and EBSs or human-engineered materials) to isolate final waste packages from the biosphere and avoid potential disasters over long periods (see Figure 2.4; IGSC, 2012; NWMO, 2012; Nasir et al., 2013, 2014).

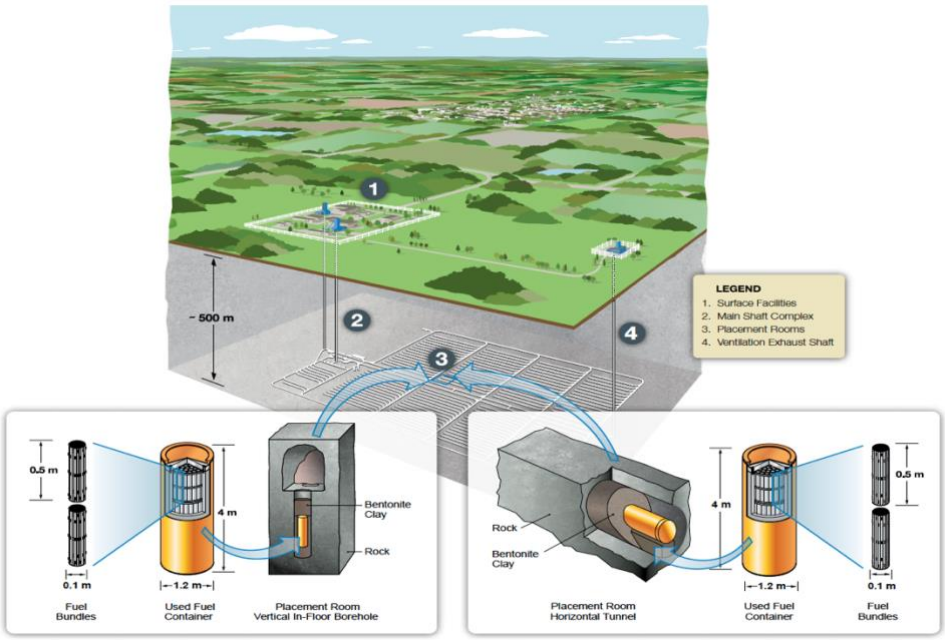

Figure 2.4. The outline of deep geological disposal in Canada (NWMO, 2010)

These multi-barrier systems include the following:

- **Natural barrier systems**

The geological or natural composition of surrounding rock mass or a competent rock layer as well as the underground water chemistry play very important roles in the selection of a DGR site to enclose the EBS (Abdi et al., 2015). Some typical rock formations include clay rocks, salt rocks, crystalline rocks, and volcanic tuffs. Clay rocks, also referred to as argillaceous rocks, are sedimentary rocks consisting mainly of clay minerals such as illite, kaolinite, and montmorillonite (Chamley, 2013; Fall et al., 2014). Salt rocks are usually found as large deposits in the Earth Cust, with simple hydroloical and structural features (Liang et al., 2005). Crystalline rocks can either be igneous or metamorphic, with their structure entirely formed by crystallized minerals rather than glassy components (DiPietro, 2018). Volcanic tuff, on the other hand, are formations formed entirely by the volcanic ash released during volcanic eruptions. Over time, the ash compacted into dense rocks by pressure acting on their formations (De La Fuente et al., 2002). Several countries have determined that different host rock types have different advantageous and disadvantageous characteristics (IAEA, 2003), as illustrated in Table 2.1. It is very important that the host rock has low permeability to limit the flow of underground water through rock layers to ensure stable and safe storage of radioactive waste for an extended period of time and to preserve the geological environment (IAEA, 2003; NWMO, 2012; Wilson et al., 2011). Other beneficial properties of a host rock as a natural barrier include high thermal conductivity, high strength and low ductility. High thermal conductivity felicitates rapid dissipation of heat generated from the waste canister (Gariette et al., 2014). Mechanical strength and low ductility are also important to avoid failure from ground movement caused by seismic activities (Lavallee and Kendrick, 2021).

Table 2. 1. Main characteristics of potential host rock formations (IAEA, 2003)

Rock Type	**Rock Characteristics**				
	Permeability	Ion Exchange	Thermal Conductivity	Strength	Ductility
Clay	Very Low	Very High	Low	Low	High
Salt	Impermeable	None	High	Low	High
Crystalline	Matrix – Low Fractures- High	None	Variable	High	Low
Volcanic Tuffs	High	High	Low	Low	Moderate

Legend

Desirable Undesirable Fairly desirable

- **EBS**

The main components of an EBS are (i) the waste form; (ii) disposal containers (i.e., waste canisters); (iii) buffer and backfill materials to surround the waste canisters; and (iv) backfill, seals, and plugs in tunnels, galleries, boreholes, and shafts intended to prevent the possible escape of radionuclides to the biosphere over time (IGSC, 2012; Radioactive Waste Management [RWM], 2003) as illustrated in Figure 2.5. The initial three components help contain the radionuclides present in the waste, especially during the period when radioactivity levels are highest. The last component isolates waste emplacement zones from other rock zones that are more susceptible to water flow.

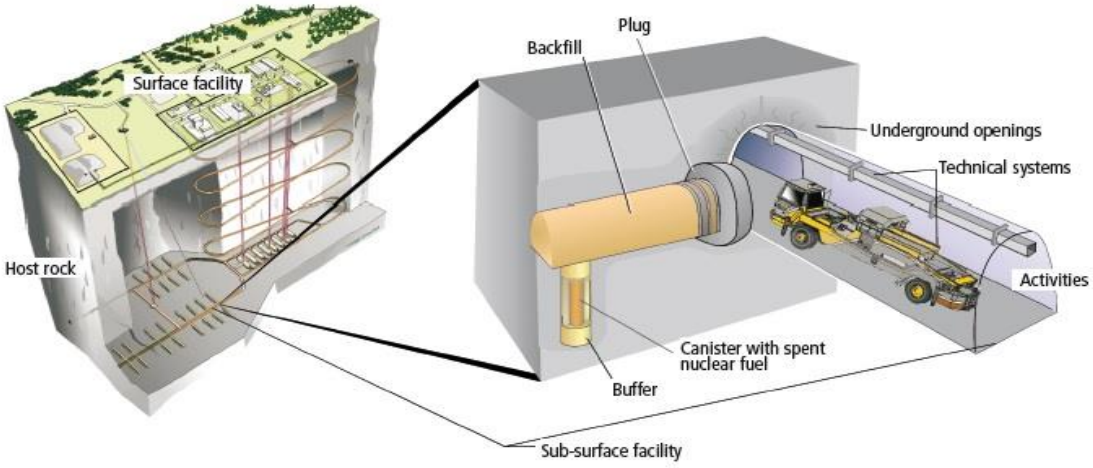

Figure 2.5. Example of an EBS within a DGR system (with the permission of SKB, Sweden; from the Integration Group for the Safety Case, 2012)

I. Waste form

There are several types of nuclear waste forms, which serve as the initial barrier. The purpose of the waste form is to isolate radionuclides in a matrix that will resist leaching and cracking and lead to a slow rate of radionuclide release in the long term. For example, spent fuel waste is formed into durable ceramic pellets enclosed in a corrosion-resistant material, such as zirconium and aluminium alloys or stainless steel (IGSC, 2012; NWMO, 2011; RWM, 2003).

II. Disposal container

Waste containers are used to enclose radioactive waste, ensure retrievability, facilitate waste handling, provide high corrosion resistance, and withstand shear loading and mechanical stress from overlying rock and earthquakes for a long period of time (1,000 years or longer, depending on what type of radioactive waste is being stored). A metal container is typically designed with either a corrosion-allowance approach (for example, carbon steel is an option for a thick-walled container that also resists deformation) or a corrosion-resistant approach (in which case copper is preferred). Many countries, including Canada, have proposed using

carbon steel inside and copper or stainless steel outside of the containers (see Figure 2.6 and Table 2; IGSC, 2012; NWMO, 2011; RWM, 2003).

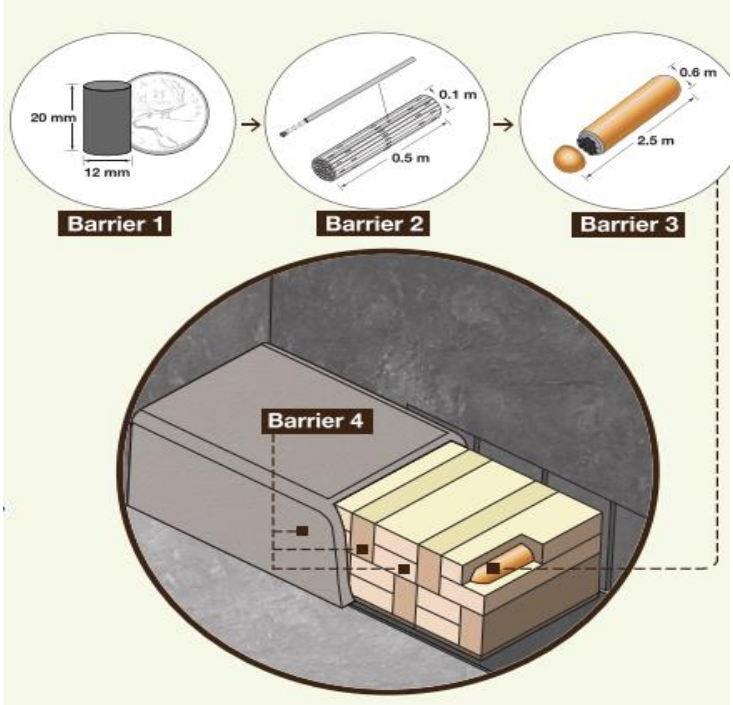

Figure 2.6. Barrier design for an EBS (NWMO, 2015)

III. Buffer

A buffer material made of bentonite is used to fill all voids between canisters and the disposal hole as well as between the canisters and the host rock. This buffer is designed to stabilize repository excavations, provide favourable thermo-hydro-mechanical-chemical (THMC) conditions for preserving disposal containers, obstruct groundwater migration to the disposal container, and prevent any radionuclide movement (Guo and Fall, 2021a,b). Bentonite materials are common candidates for buffer materials in both crystalline rock and clay formations (Nasir et al., 2011). They are often prepared in pre-compacted blocks (see Figure 2.7; Melamed and Pitkanen, 1996; Posiva, 2009).

According to the Swedish KBS-3, the target properties of a compacted bentonite buffer with regard to safety functions are as follows (Posiva, 2009; Wilson et al., 2011):

- low hydraulic conductivity < 10^{-12} m/s,
- swelling pressure higher than 2 MPa,
- range density of 1900–2050 kg/m3 in saturated conditions, and
- a buffer temperature less than 100ºC.

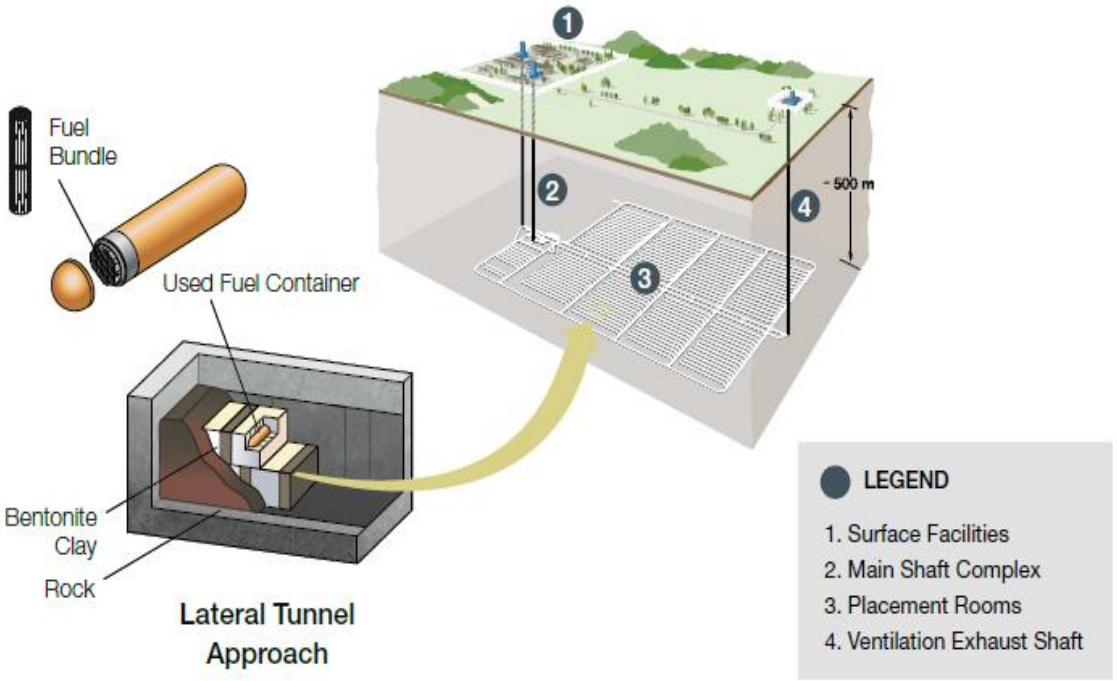

Figure 2.7. New design for an EBS (NWMO, 2015)

IV. Backfill, Seals, and Plugs

To prevent interaction between radioactive disposal areas and eliminate underground contamination, access tunnels must be sealed and the shafts of all repositories must be backfilled. Backfill, plugs and seals for repositories are usually made of bentonite clays in formations of crystalline and sedimentary rocks. Various types of seals and plugs are applied at different repository development stages. For example, seals are often placed permanently at strategic points to serve as barriers between deposition zones and rock zones that are susceptible to water flow, whereas temporary tunnel plugs are used during the operations to

protect the repository work areas from groundwater infiltration or swell pressure within wet backfill (IGSC, 2012; Wilson et al., 2011). The target material backfills for backfill, according to Wilson et al., (2011), include low hydraulic conductivity (less than $10^{-}10$ m/s) and a swelling pressure higher than 0.1 MPa.

2.4.2 Design concepts for deep geological repositories

Design concepts and standards for DGRs vary between countries depending upon the development stage of the EBSs, economy, and the nature of nuclear waste being disposed of, as illustrated in Tables 2.2 and 2.3 (RWM, 2003).

Table 2.2. Baseline assumptions underlying DGR and EBS designs across countries (RWM, 2003)

Country/ program	Baseline assumptions
Belgium	A natural geological barrier is the common isolation barrier. Overpacking provides containment during the thermal phase (500 years for vitrified HLW, 2,000 years in the case of spent fuel). In a normal evolution scenario, there would be no early failure of the overpacking method. Backfill provides an additional, but minor, contribution to safety. A disposal tube facilitates retrievability.
Canada	Constraints on the design include waste type, volume, and inventory (e.g., the age and burnup of fuel); the need for maintaining container surface temperatures under 100 °C; the need for maintaining low permeability, keeping the rock surrounding the repository saturated; and the need for keeping the bentonite protecting the spent fuel dense to ensure no microbiologically influenced corrosion of the containers.

France	Long-term isolation of waste via the EBS, which is designed to account for present-day and future conditions at the disposal location and to minimize disturbances on the rock caused during construction and operation.
Japan	Constraints on the design of the EBS include the provision of long-term isolation and barrier functions under current and future conditions and the minimization of disturbances during construction and operations.
US/WIPP	US/ Waste Isolation Pilot Plan (WIPP) Constraints on the design of the EBS include feasibility and present-day technologies.
US/YMP	US/Yucca Mountain Project (YMP), the repository should be located above the water table and be capable of supporting different stages of repository development. Additionally, it should receive waste no later than 2010, the surface temperature of the cladding should remain below 350°C, there should be flexibility in the thermal operating mode, and waste should be retrievable.

2.5 Canadian radioactive waste disposal and deep geological repository concepts

Radioactive waste material has been generated in Canada since the early 1930s. Currently, Canada has nineteen operating nuclear power plants and most of them are located in Ontario (Figures 2.8 and 2.9). These reactors produced about 15% of Canada's electricity in 2019. They have generated over 2 million used SF bundles (consisting largely of radium and uranium-contaminated soils) and tons of radioactive waste material since the 1960s, based on the report from the Canadian Nuclear Safety Commission (CNSC, 2008) and NWMO (2010), as indicated in Figure 2.10.

Table 2.3. DGR design standards of different countries (RWM, 2003)

Country/ program	Waste type	Waste matrix	Container/ overpack	Buffer/ backfill	Other
Belgium	HLW	Borosilicate glass	304 stainless steel container, 316L stainless steel overpack	FoCa clay, 60% calcium bentonite, 35% quartz sand, 5% graphite -	Disposal tube, tunnel lining
	Spent fuel	-	-		-
Canada	Spent fuel	UO2	Carbon steel inner container with a copper outer shell.	Bentonite buffer, bentonite/sand buffer, clay/crushed rock backfill	Tunnel and shaft seals.
Czech Republic	ILW	Concrete	Steel	Bentonite buffer	Clay seals
	Spent fuel	UO2			
	HLW	Glass			
Finland	Spent fuel	UO2 (not considered part of EBS)	Copper-iron	Bentonite buffer, backfill of compacted crushed rock and bentonite	Bentonite and concrete plugs
Sweden/KBS-3	Spent fuel	UO2	Copper-iron	Bentonite	Tunnel backfill.
Japan	HLW	Glass	Carbon steel overpack	Bentonite-sand mixture.	Tunnel sealing plugs and grout

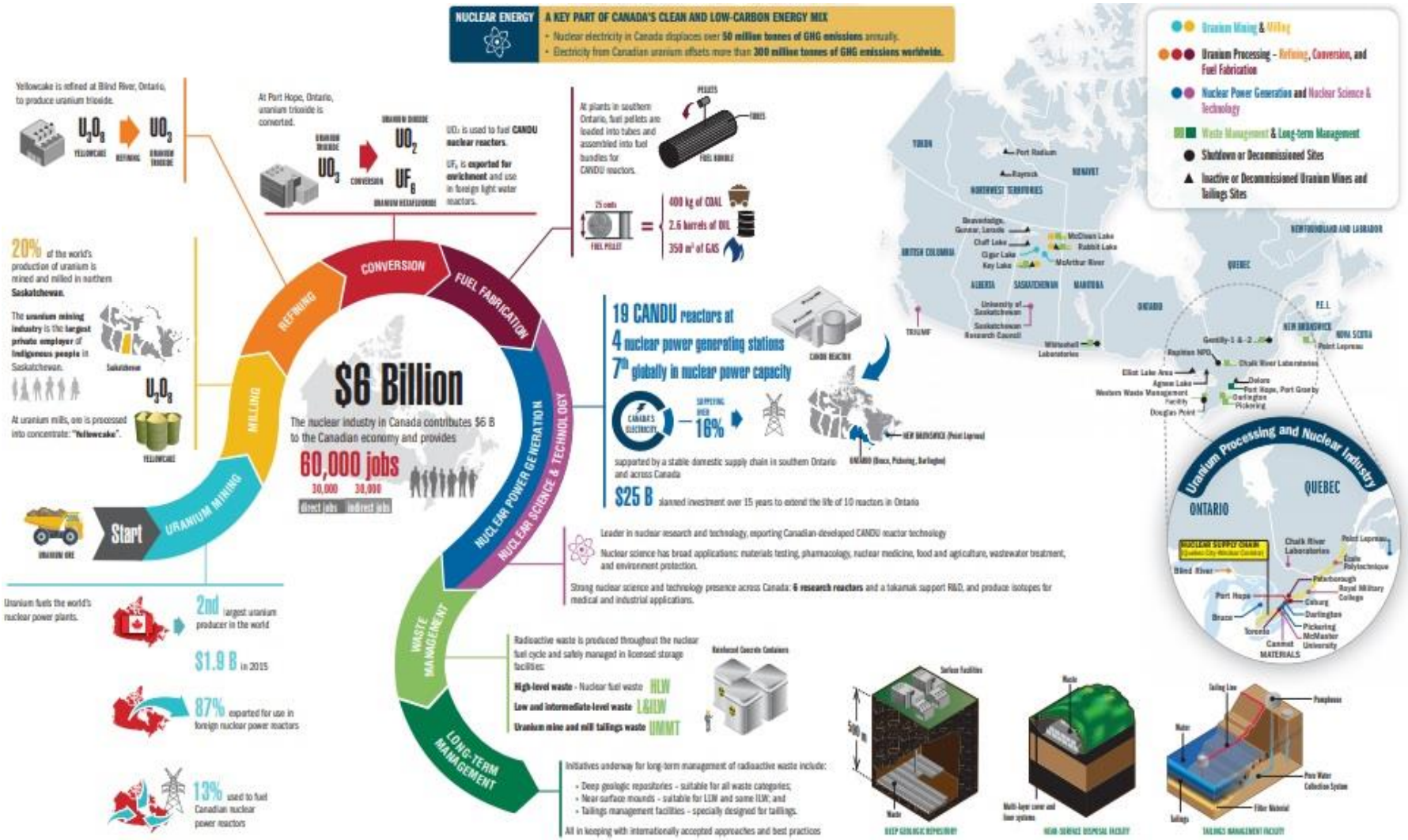

Figure 2.8. Nuclear power plants in Canada (Minister of Natural Resources, 2017)

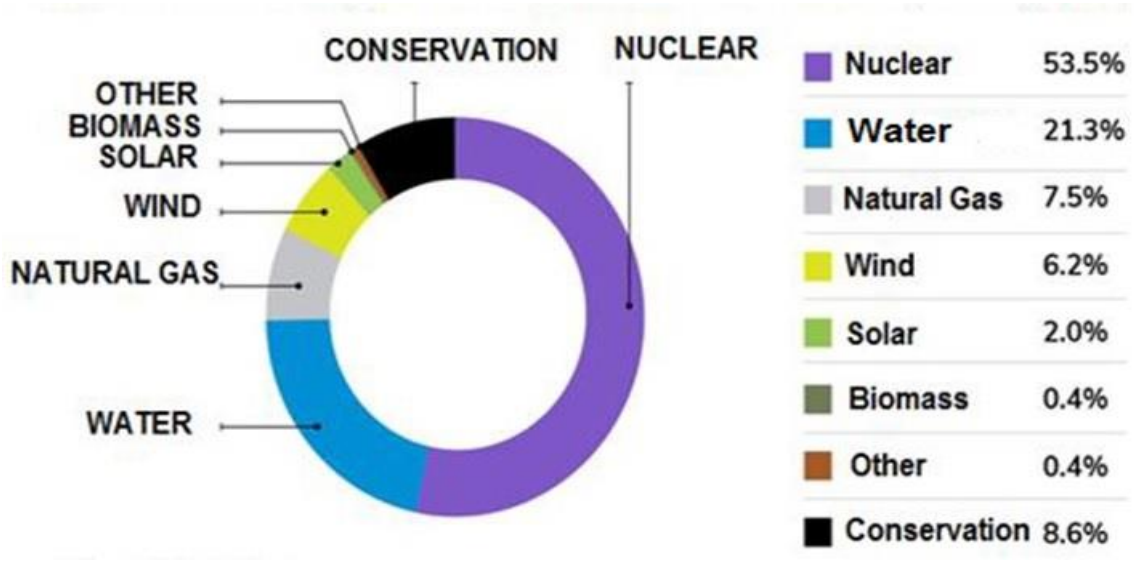

Figure 2.9. Ontario's electricity generation and conservation, 2016 (Ministry of Energy, 2017)

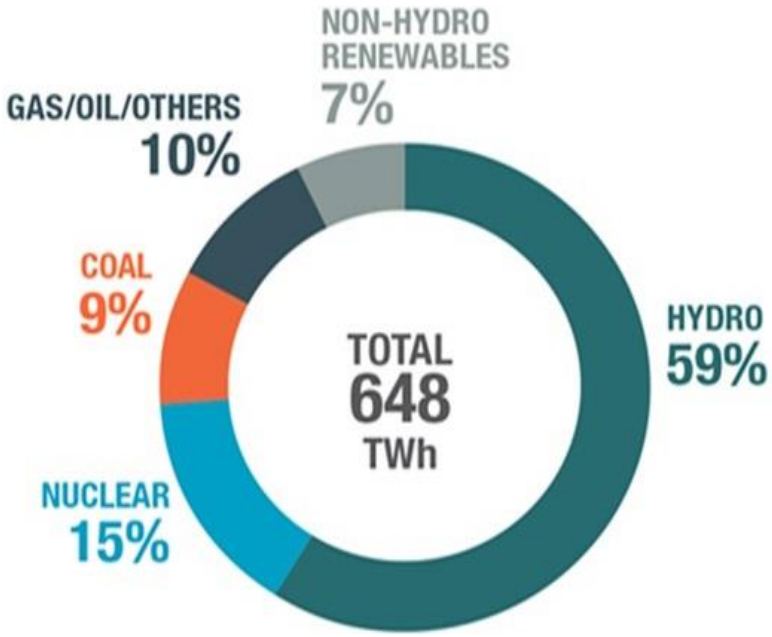

Figure 2.10. Canadian energy generation by source (Canada Ministry of Natural Resources, 2018)

DGRs contain different levels of radioactive waste (LLW, ILW, and HLW) with different uses from various stages of the nuclear fuel cycle, nuclear reactor operations, nuclear research, and radioisotope manufacture. Currently, all generated radioactive waste is stored in

a way that allows retrieval when the proposed permanent DGR management facilities become available in Kincardine, Ontario (see Figure 2.11; NWMO, 2011).

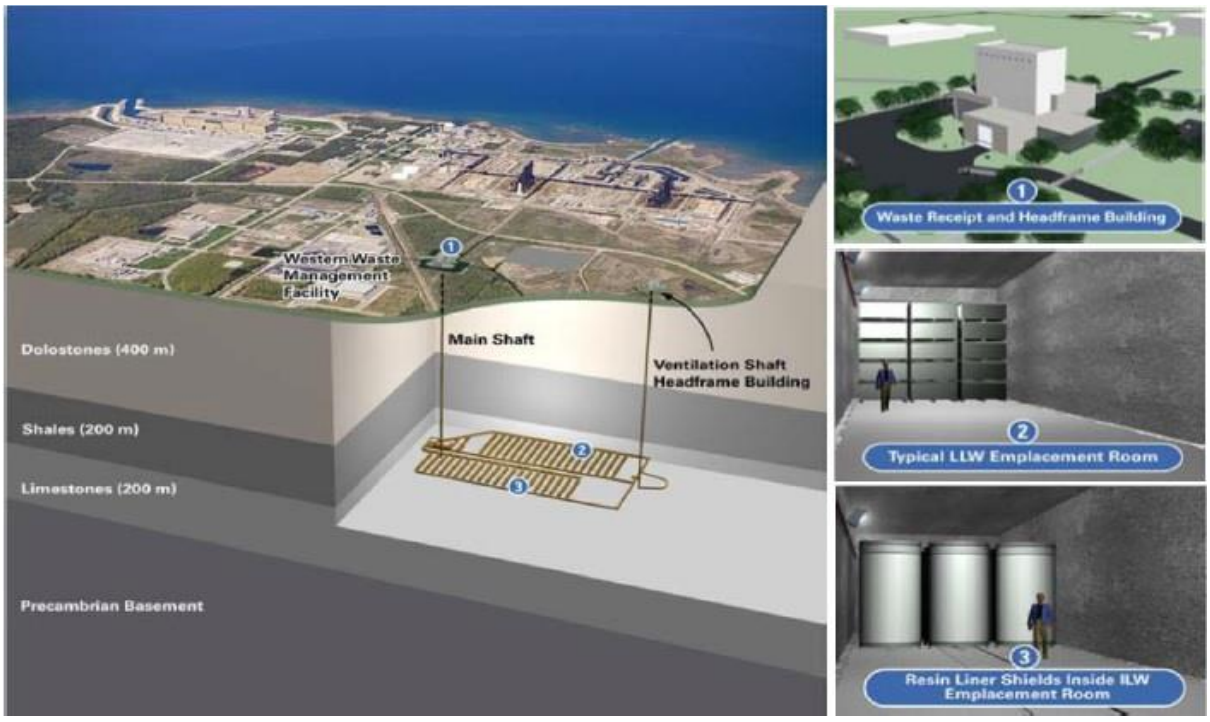

Figure 2.11. DGR for LLW and ILW in the Municipality of Kincardine, Ontario, as proposed by Ontario Power Generation (NWMO, 2011)

In Canada, DGRs are designed based on a multi-barrier system that includes crystalline or sedimentary rock to support the geological disposal of SF (Yang and Fall, 2020, 2021d). This system is still under development, and the best sites for establishing a DGR are still being studied. The NWMO has been investigating three locations in Northern Saskatchewan and 16 in Ontario (see Figure 2.12). It has proposed constructing DGRs at depths of 300–700 m (NWMO, 2012).

The design concepts for DGRs, including the components of EBSs, vary from one country to another (see Tables 2.2 and 2.3). The expectations of the DGRs in Canada are:

- Minimize the rate of radionuclide release from the spent fuel.

- Provide radionuclide containment for a minimum of 100,000 years. The containers are made of a carbon steel inner container and a copper outer shell with a total thickness of 25 mm (RWM, 2003; Rebak, 2011).
- Include EBSs consisting of a buffer made of bentonite or bentonite–sand mixture, tunnel and shaft seals and clay/crushed rock mixture backfill (IGSC, 2012; Wilson et al., 2011).
- Include buffer/backfill barriers for physical, chemical, hydraulic, and biological isolation of waste and minimization of radionuclide release into the geosphere in the long term.
- Include tunnel and shaft seals to provide mechanical support during the repository monitoring phase and hydraulic separation of rooms after repository closure.
- Keep the container surface and bentonite buffer temperature below 100 ºC (Hicks et al., 2009; RWM, 2003).

Figure 2.12. Proposed locations for Canadian DGRs (NWMO, 2012)

2.6 Conditions in a Canadian deep geological repository

There are many parameters affecting the behaviour and conditions of EBSs in DGRs within Canada, such as EBS geometry, material composition, corrosion properties, near-field temperatures, groundwater flow rates, and pore water chemistry (i.e., salinity).

2.6.1 Pore water chemistry

The groundwater conditions vary considerably within the Canadian Shield. The salinity of a site depends on the depths and location of the groundwater. It can generally be assumed that salinity will increase with depth, with full salinity of about 400 g/L achieved at depths greater than 300 m across the Canadian Shield (Gascoyne et al., 1987). The NWMO is considering sedimentary rock formations (i.e., natural barrier) throughout Southern Ontario as

potential hosts for used nuclear fuel. A DGR for LLW and ILW was proposed to be located in the Municipality of Kincardine, Ontario, at a 680 m depth.

At the regional scale, the natural geochemical systems in Ontario can be classified into two general zones based on groundwater conditions. First, a shallow system located less than 200 m the Earth's surface containing fresh to brackish waters, which could be Na-Cl, Na-Mg-Ca-Cl, Ca-SO4, Na-Ca-Cl, or Ca-Na-Cl depending on their ion concentrations. Second, an intermediate to a deep geological system located at a depth of more than 200 m containing predominantly brine with hydrocarbons in reservoirs, which could be Na-Ca-Cl or Ca-Na-Cl waters with total dissolved solids (TDSs) ranging from 200,000–400,000 mg/L (Dollar, 1988; Jensen et al., 2009; NWMO, 2011, 2012). Figure 2.13 shows the actual sedimentary formation(s) in which shallow systems occur, which vary with stratigraphy across southwestern Ontario.

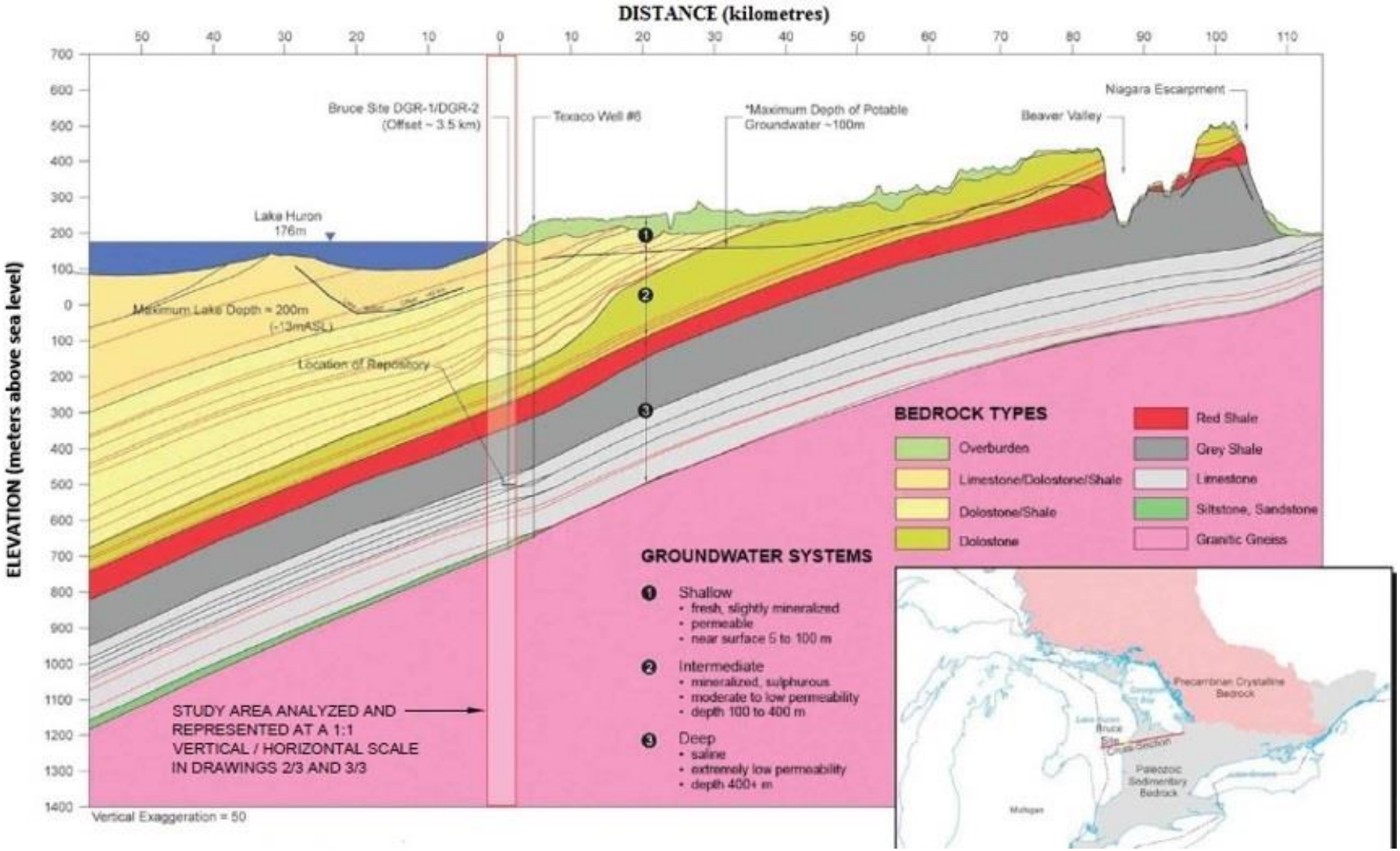

Figure 2.13. Groundwater salinity in sedimentary formations within southwestern Ontario (NWMO, 2011)

2.6.2 Temperature

The NWMO has proposed constructing DGRs for the long-term disposal of used fuel from engineered excavations at depths of 300–700 m in either crystalline or sedimentary rock (NWMO, 2005). The used-fuel container corrosion rate, the performance of the buffer material around the containers, and the mechanical stability of DGRs all depend on the temperature response and groundwater salinity around the repository. Therefore, thermal analyses are important for designing safe repositories. In Canada, a range of thermo-mechanical analyses of DGR concepts have been conducted over the past 30 years (Acres et al., 1985, 1993; Baumgartner et al., 1994; Golder Associates Ltd., 1993; Guo, 2007, 2008; Mathers, 1985; Tsui and Tsai, 1985). These studies included two- and three-dimensional thermal transient and thermo-mechanical analyses and were divided into far-field modelling (the rock mass surrounding a repository of finite dimension) and near-field modelling (the boundary condition near the placement room materials) to accurately identify at early times and the thermal response is overestimated at longer times. This previous study was revised by the NWMO (2016) and applied to a concept for a Mark II repository in crystalline rock. To investigate the effects of this boundary condition, thermal near-field modelling was performed for the Mark II repository using COMSOL modelling environment with customized physics interfaces heat transfer analysis and proposed to account for boundary condition influences. The method was validated by comparing the modified COMSOL results with a theoretical solution produced using the HOTROK analytical computer code. The modified analysis showed that a thermal peak occurs early in the repository lifetime and without any comparable peak for thousands of years. In the evaluated case, the peak container surface temperature after 45 years is 84 °C, the peak temperature between two containers after 45 years is 83 °C, and the peak temperature of rock in the roof above the top layer of containers after 65 years is 77 °C.

Figure 2.14 shows the (very uniform) rock temperature along the vertical surface near the placement room of materials after 45 years. Figure 2.15 shows the temperature along horizontal cross-sections through the axis of the containers after 45 years. The maximum container temperature was 84 °C. Figure 2.16 shows the temperature to be time-dependent at five points along a vertical line, OB4. The temperature at Point O (i.e., the centre of the tunnel below the upper layer of containers) reaches a maximum peak of 83 °C at 45.8 years after placement and a second peak of 83 °C at 1,480 years. The roof temperature of the placement tunnel (Point B1) reaches 77 °C at 65 years and 82 °C at 1,550 years. After 1,590 years, the temperature 1.0 m over the tunnel roof (B2) reaches 74 °C at 76 years and then 81 °C. After 1,660 years, the temperature at 5 m (B3) and 10 m (B4) from the tunnel centre (O) reaches 80 °C and 79 °C, respectively.

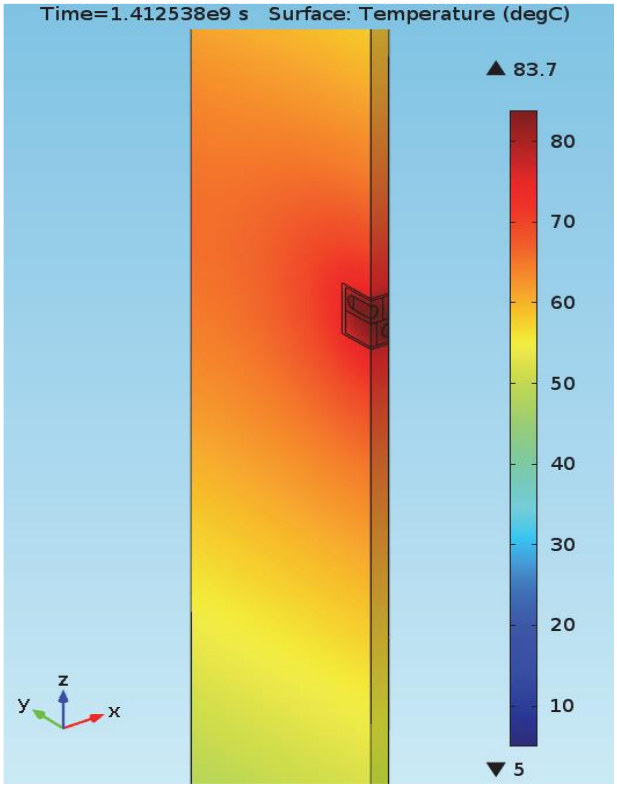

Figure 2.14. Temperatures in the rock along the vertical surface near a tunnel at 45 years after placement (NWMO, 2016)

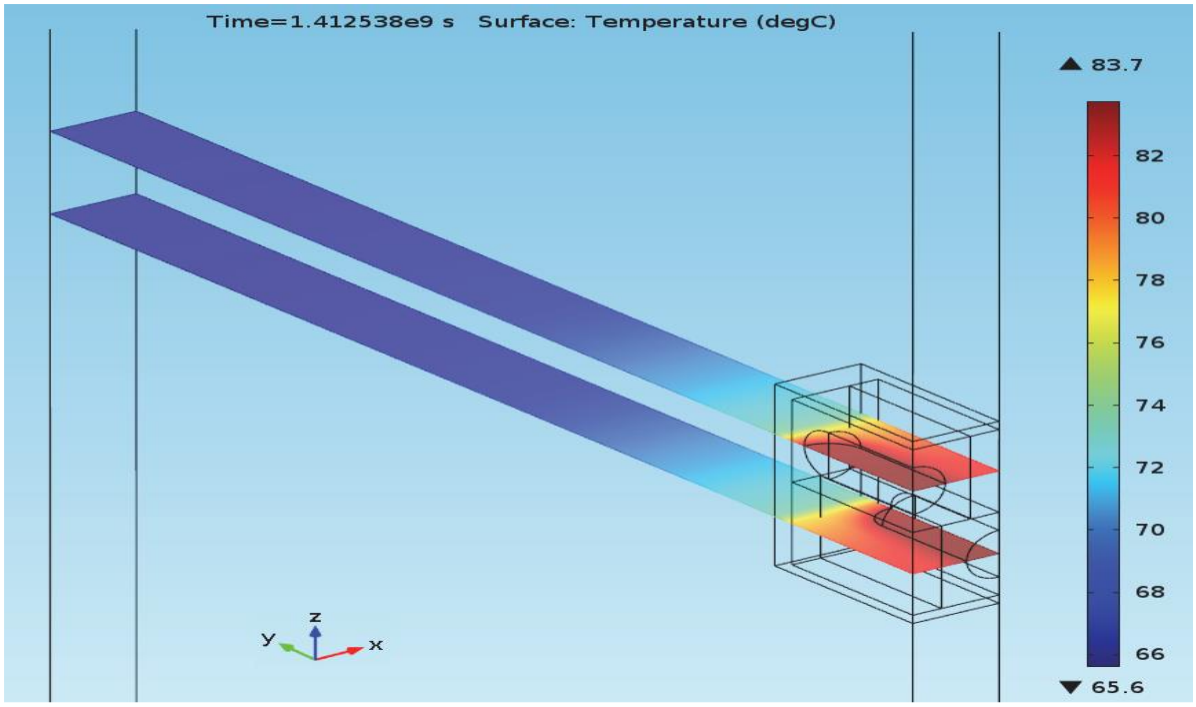

Figure 2.15. Temperatures in the rock along a horizontal cross-section through the container axis at 45 years after placement (NWMO, 2016)

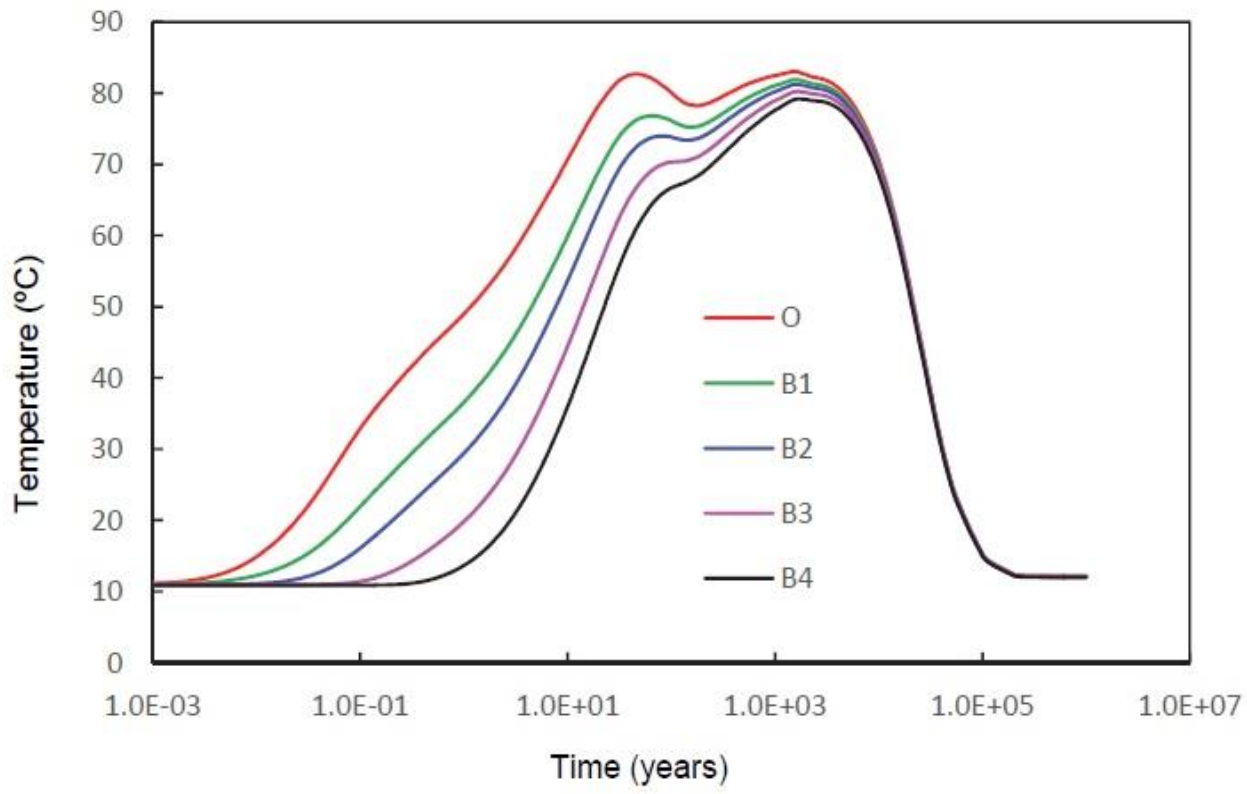

Figure 2.16. Temperatures as a function of time at five points along a vertical line (NWMO, 2016)

2.7 Background information on bentonite

Natural bentonite was formed millions of years ago when volcanic ash transformed from rhyolite to dacite and was deposited into saltwater or freshwater and then crystals grew in saline water using the glassy components of the volcanic ash as source material (Figure 2.17). There are bentonite types (Meunier, 2005), which are named after their dominant element:

- Sodium (Na) bentonite is created when volcanic ash is deposited into saltwater rich with sodium Na^{+}. It has higher swelling potentials and compressibility than Ca-bentonite.
- Calcium (Ca) bentonite is created when volcanic ash is deposited into freshwater rich with calcium (Ca^{2+}). It has a relatively higher permeability than Na-bentonite with equivalent dry density.

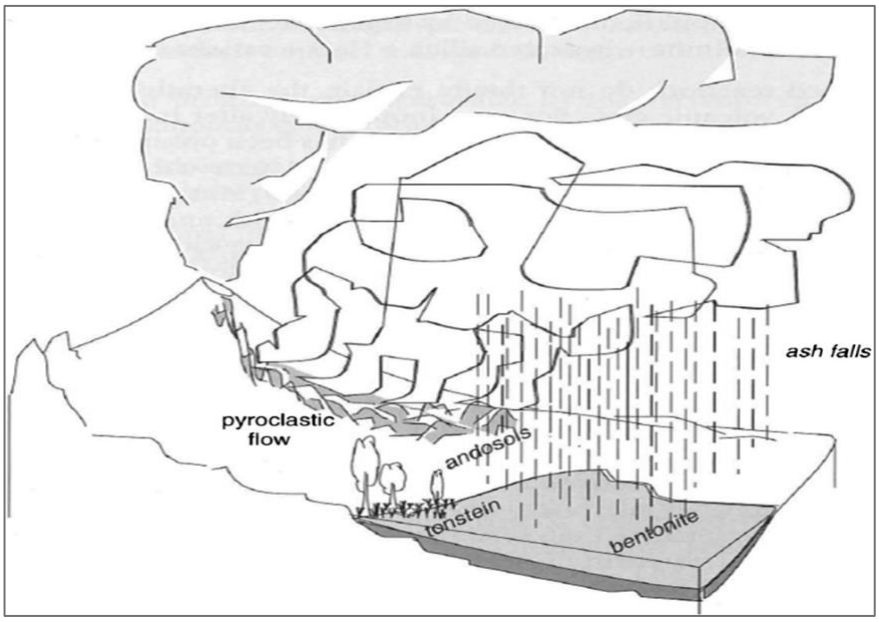

Figure 2.17. Schematic presentation of the alteration environment of ash (Meunier, 2005)

Each bentonite type has different properties that are dependent on the availability of montmorillonite and major exchangeable cations (Athanassopoulos, 2011; Liu et al., 2011). It

has various industrial applications and can be mixed at different ratios to form compounds with specific properties (Grim and Güven, 1978).

Bentonite is an expansive clay material and belongs to the smectite mineral group with 2:1 clay mineral (consisting of an octahedral sheet located between two silica sheets) (see Figure 2.18). Montmorillonite is the main component in bentonite clay materials (which features some substitution of Al for Si in the silica sheet and Fe and Mg for Al in the alumina sheet) along with other accessory minerals, such as quartz, feldspar, calcite, pyrite and gypsum (Melamed and Pitkanen, 1996). Bentonite interlayer bonding is by van der Waals forces, expands or contracts based on the quantity of water and interlayer cations present, when combined with water the generated negative charges are balanced by exchangeable cations found between the unit layers. The bonds are weak and easily separated by absorption of water or other polar liquids. Bentonite has low hydraulic conductivity. The specific surface of smectites is very large (ranges from 50–120 m^2/g. Up to 840 m^2/g of the surface which could be exposed when the lattice expands). Moreover, due to the high number of unbalanced substitutions, smectites have a high CEC, generally 80–150 meq/100 g, including both external and internal surfaces. This has a tremendous impact on swelling, plasticity, and other physical properties (Mitchell, 1993).

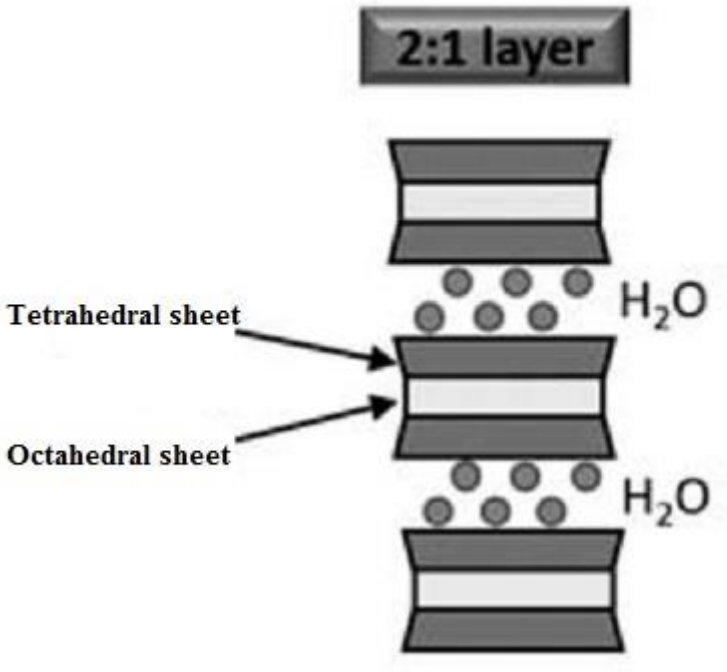

Figure 2.18. Schematic representation of montmorillonite structure (Zhang, 2016)

2.7.1 Types of bentonite

The characteristics of bentonite vary based on the location in which it was formed. It is often light yellow or green, but sometimes it can be bluish due to the oxidation of iron or the leaching replacement of exchangeable sodium by calcium at significant depths. Increased fractions of montmorillonite lead to higher-quality bentonite. Mx-80 Wyoming bentonite is obtained from the US, Kunigel clay is obtained from Japan, Kinnekulle is obtained from Sweden, Busachi is obtained from Sardinia, The Milos clay Deponit CA-N is obtained from the isle of Milos, FEBEX is obtained from Spain, and FoCa7 is obtained from France (Grim and Güven 1978; Rautioaho and Korkiala-Tanttu, 2009; Sandra, 2013). These are shown and described in Figure 2.19 and Table 2.4.

Figure 2.19. Appearance of a different bentonite clays (Svensson et al., 2011)

Table 2.4. Mineral compositions (wt.%) of different types of potential clay barrier materials (Hicks et al., 2009)

Mineral	MX-80	Avonseal	Kyungju	Deponit CA-N	FEBEX	Friedland
Montmorillonite	87	79	69.5	81	89-95	30
Quartz / Chalcedony	3	5	1.4	1	1-3	20.2
Christobalite	2		6.9	1	1-3	0.1
Feldspar	3	1.5	22.2	2	1-3	1.1
Calcite / Siderite				10	0.6	0.5
Dolomite				3		
Analcite						
Pyrite	0.25			0.5	0.02	1.2
Mica	4					7.2
Ilite	1.6	9.5				26
Gypsum	0.7	2			0.14	0.7
Rutile / Anatase	0.26					0.6
Organic Matter	0.2	0.3		0.2	~0.3	
Other					0.8	10.7 (Kaolin)

2.7.1.1 Mx-80 bentonite

Mx-80 bentonite was formed by in situ alterations of volcanic ash deposited in Wyoming, USA, hundreds of millions of years ago. It has a particularly good reputation because it has montmorillonite content that could reach 75–85% (Carlson, 2004) and sodium

is the primary adsorbed cation (leading to very high CEC). This produces extraordinarily good colloidal, plasticity, and bonding properties (self-sealing properties) and low hydraulic conductivity. Mx-80 bentonite also contains accessory minerals, such as quartz and feldspar, and traces of illite, cristobalite, pyrite, gypsum, calcite, and amphibole (Carlson, 2004; Grim and Güven, 1978; Wilson et al., 2011), as illustrated in Table 2.4. The CEC of bentonite ranges from 74–110 meq/100 g, liquid limit of 526%, plastic limit of 46%, and specific gravity of 2.82 (Villar and Gómez-Espina, 2008). A sample of Mx-80 bentonite is presented in Figure 2.20.

Figure 2.20. MX-80 Wyoming bentonite (Carlson, 2004)

2.7.1.2 FEBEX bentonite

FEBEX bentonites comes from Almería, Spain. It was formed by the transformation of acidic volcanic rocks through hydrothermal processes. FEBEX bentonite is considered to be of excellent quality because it features a high CEC (96–102 meq/100 g) and contains more than 92% montmorillonite. FEBEX bentonite also contains accessory minerals, such as quartz (about 2%), feldspar, plagioclase, calcite, potassic, cristobalite, and trydimite, which are shown in Table 2.3. The liquid limit is 102%, the plastic limit is 53%, and the specific gravity is 2.70.

FEBEX bentonite was used as a buffer material in a Spanish DGR for nuclear waste (García-Gutiérrez et al., 2011; Hicks et al., 2009; Villar and Gómez-Espina 2008; Villar and Lloret 2007).

2.7.1.3 Asha bentonite

Asha bentonite was formed by hydrothermal alteration of volcanic ash in saline water. The clay is found on the northwest coast of India and was deposited in the Kutch district millions of years ago (Karnland et al., 2006). The average content of expandable minerals is 60–65%, and the liquid limit is180% (Johannesson and Nilsson, 2006). A sample of Asha bentonite is presented in Figure 2.21.

Figure 2.21. Asha bentonite sample (Karnland et al., 2006)

2.7.1.4 Friedland bentonite

Friedland bentonite was formed in situ through hydrothermal alteration, sedimentation, and weathering. The clay is of tertiary origin and was deposited in Neubrandenburg in Northeast Germany millions of years ago (Karnland et al., 2006; Schomburg, 1997). It has an average expandable mineral content of 50–60% and a montmorillonite content of 30% (Pusch

1998). The rest comprises mixed-layer minerals, such as quartz (20%), mica (7.2%), and feldspar (1.1%), as illustrated in Table 2.3 (Carlson, 2004; Hicks et al., 2009; Karnland et al., 2006). Its CEC varies from 35–45 meq/100 g (Carlson, 2004), and the liquid limit of 109% (Johannesson and Nilsson, 2006). Friedland bentonite is a suitable candidate for backfilling drifts and shafts in DGRs for nuclear waste (Schomburg, 1997). A sample of Friedland bentonite is shown in Figure 2.22.

Figure 2.22. Friedland bentonite sample (Carlson, 2004)

2.7.2 Bentonite swelling behaviour

The swelling behaviour of bentonite has both positive and negative effects. The swelling behaviour of bentonite was described by Komine and Ogata (1996) as shown in Figures 2.23 and 2.24. It is mainly controlled by water content and hydrological properties. Furthermore, the magnitude of swelling in bentonite depends upon the active clay minerals. Compacted bentonite mainly consists of montmorillonite and other accessory minerals, such as quartz, feldspar, calcite, pyrite, gypsum and voids. The water content in saturated bentonite

varies based on the level of compaction and available space since bentonite swells to fill in any void in the presence of water. The voids between mineral and Na-montmorillonite particles are occupied by air and free water. Water molecules are adsorbed at active sites on layers of Na-bentonite, and when the interlayer space is filled with only one layer of water molecules, it expands and swelling begins. The hydration of exchangeable cations is largely responsible for this adsorption and the accompanied increase in the interlayer spacing. Therefore, at low relative humidity, hydration of Na-montmorillonite begins on external surfaces and diffuses double layer (DDLs) of water with one layer of water molecules. As water adsorption continues, relative humidity increases and water enters between elementary clay layers, resulting in the development of water layers and increasing the interlayer spacing and the volume of porosity (Komine and Ogata, 1996; Salles et al., 2009).

If compacted bentonite can swell freely at constant vertical pressure, its volume increases during water uptake as the volume of montmorillonite minerals increases. This process continues until the swelling pressure of montmorillonite equals the applied vertical pressure (see Figure 2.23).

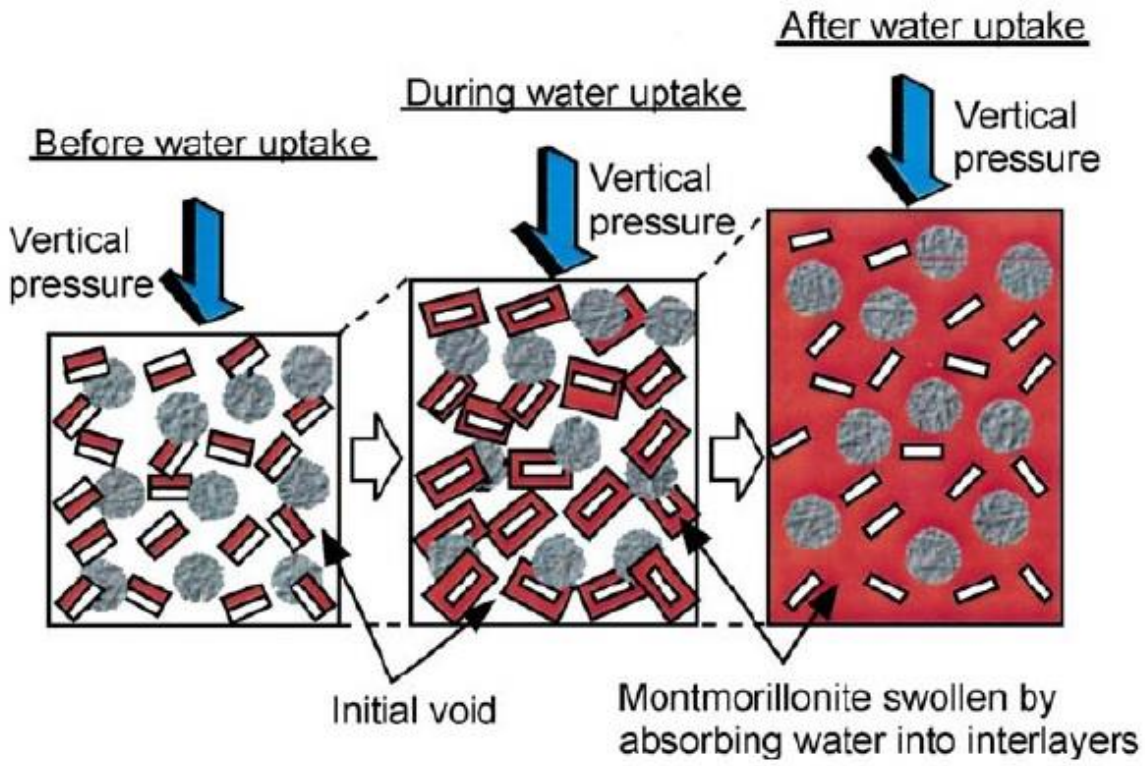

Figure 2.23. Swelling behaviour of compacted bentonite under constant vertical stress (Komine, 2004b)

If the vertical and horizontal deformation of the compacted clay is restricted to a constant volume, montmorillonite minerals swell during water uptake and fill most part of the voids in the compacted bentonite. When the voids are filled, the volume of bentonite cannot increase further and the pressure from the swelling of montmorillonite minerals would be the corresponding swelling pressure of the bentonite (see Figure 2.24).

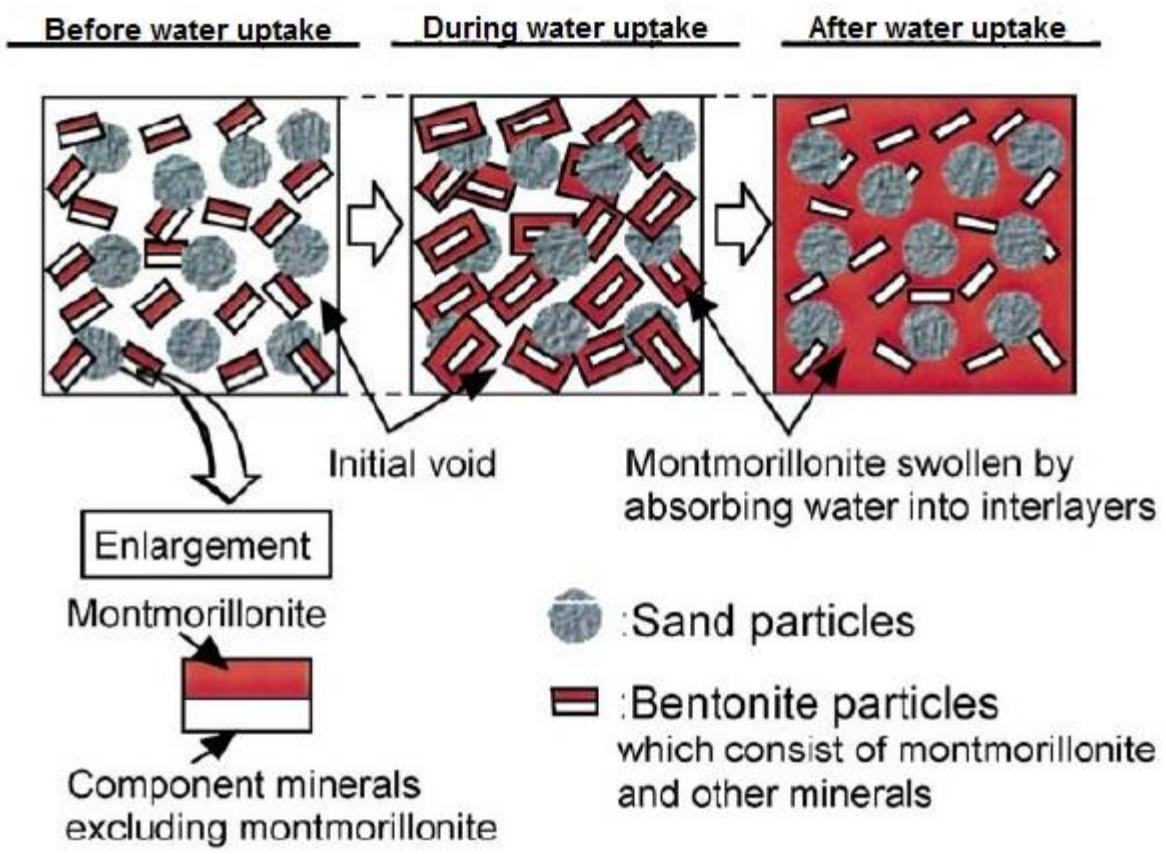

Figure 2.24. Swelling behaviour of compacted bentonite with a constant volume (Komine, 2004a)

2.7.3 Bentonite mineralogy

There are two atomic structural units from which most clay minerals, including smectites, are formed (Grim, 1968). The first is an octahedral sheet consisting of Al^{3+}, Fe^{3+}, Fe^{2+}, or Mg^{2+} cations surrounded by O^{2-} or OH^{-} anions in an octahedral configuration. The aluminium (Al^{3+}) octahedral unit is composed of one Al^{3+} atom bound with six OH^{-} atoms, composing $Al_2(OH)_6$ (Grim, 1968), as shown in Figure 2.25.a. The second is a sheet consisting of predominantly silicate tetrahedrons. The silica tetrahedral unit is composed of one silica atom bound with four O^{2-} atoms, composing $(Si_4O_{10})^{4-}$. These units are connected in a hexagonal sheet (Grim, 1968), as presented in Figure 2.25.b. Hydrous phyllosilicate minerals are classified depending on the structure of the linkages between octahedral and tetrahedral sheets as 1:1, 2:1, or modulated layers, as shown in Figure 2.26, with further sub-divisions

based on the charge deficit across the 2:1 structural layer, the occupancy of the octahedral layer, the structure of the interlayer region, and its chemical composition (Bailey, 1988).

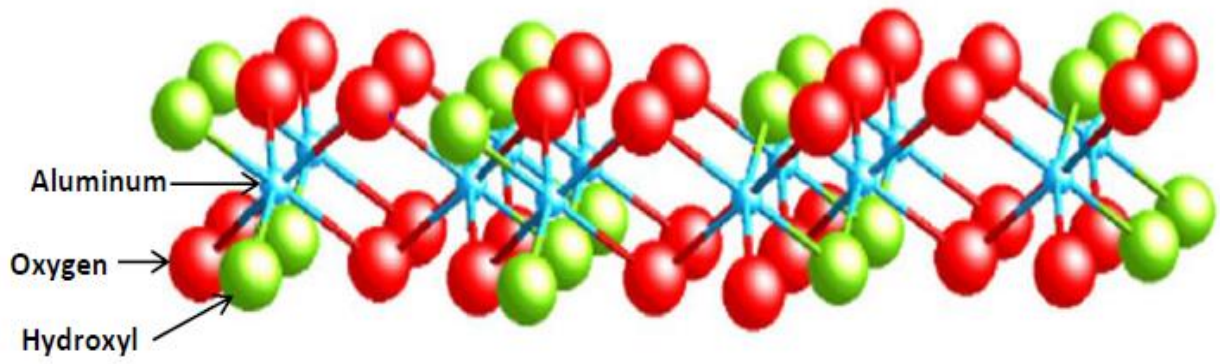

a. Octahedral unit and octahedral structure

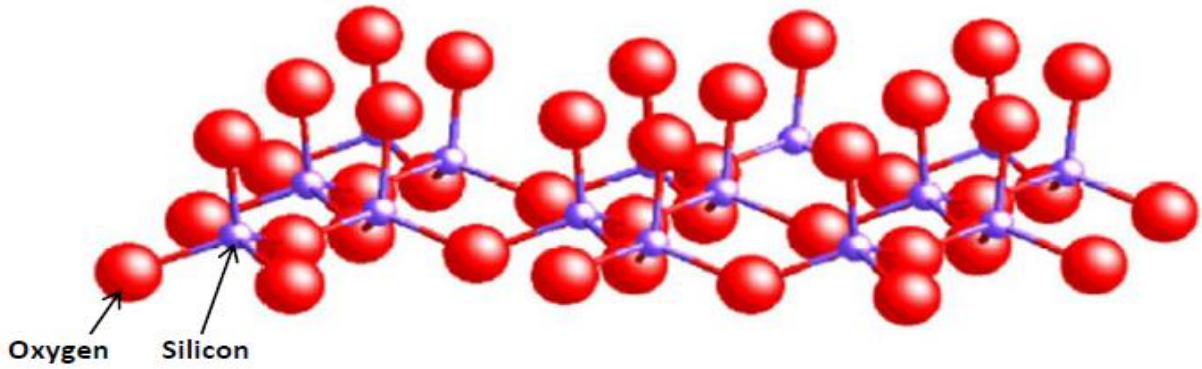

b. Silicon tetrahedron and tetrahedral structure

Figure 2.25. Clay mineral structure: (a) octahedral unit and octahedral structure and (b) silicon tetrahedron and tetrahedral structure (Wilson et al., 2011)

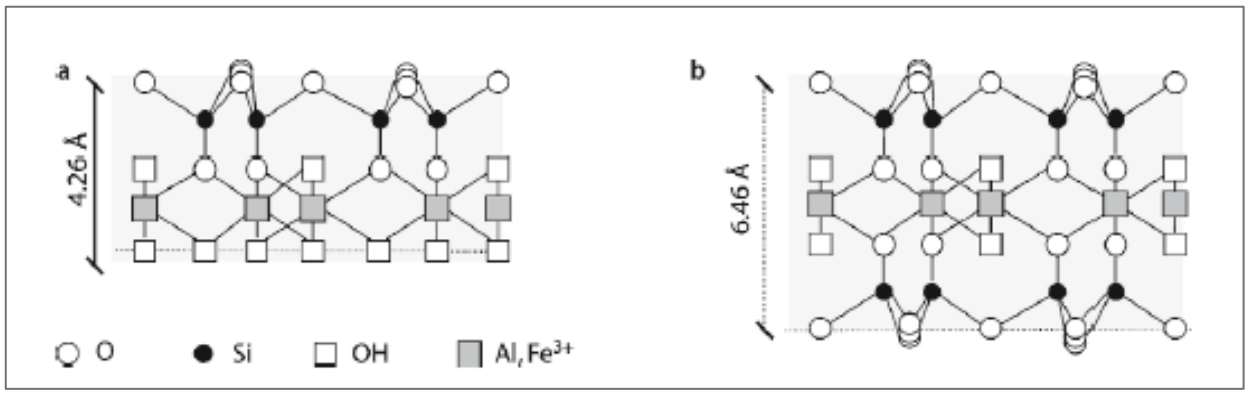

Figure 2.26. The two crystal structures of dioctahedral phyllosilicates: (a) 1:1 layer and (b) 2:1 layer (Meunier, 2005)

Montmorillonite is a swelling clay mineral that consists of parallel stacks of 2:1 layers. It has a very small crystal size in the lengthwise direction. The crystals are arranged in very

thin layers (about 1 nm thick) that extend 10 nm in both directions (Murata and Saito, 2003). A montmorillonite crystal consists of an aluminium octahedral sheet that is covalently coordinated and located between two silica tetrahedral sheets, as shown in Figure 2.27.

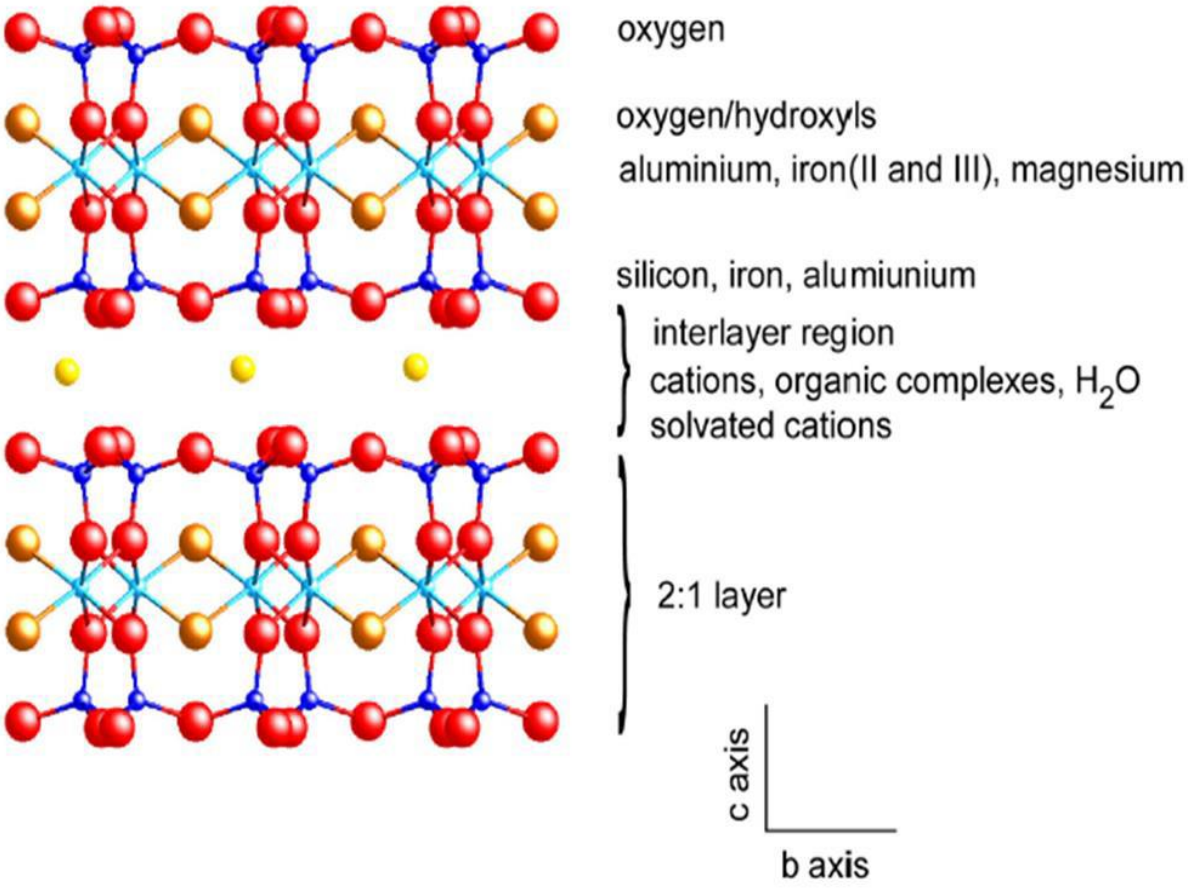

Figure 2.27. Sketch of montmorillonite structure (Wilson et al., 2011)

The silica tetrahedral sheets connect with the Al^{3+} octahedral sheet through a very strong bond that is formed from the ionic bonds (Mitchell et al., 1993). Montmorillonite layers, however, are weakly connected and easily disconnect when they combine with water or any other polar liquids or cleavage caused by van der Waals forces and exchangeable cations (Mitchell et al., 1993). Mica, chlorite and other minerals from the talc-pyrophyllite group also have atomic structures based on 2:1 layers (Bailey, 1988).

2.7.4 Bentonite microstructure

In design concepts of DGRs for nuclear waste, bentonites are often utilized as buffer and sealing materials. The general safety of the storage system is very important because expected thermo-hydro-mechanical-chemical (THMC) loadings it may undergo over a long period of time. To understand the THMC behaviour of bentonite, the changes in the bentonite microstructures need to be studied (Cui et al., 2002; Delage, 2007). Bentonite is made up of structural units known as laminae, which pile up, forming elementary particle arrangements (Villar et al., 2012). These particles aggregate together in face-to-face, face-to-edge, and edge-to-edge manners (Delage, 2006; Gens and Alonso, 1992; Meunier, 2005), as presented in Figure 2.28. The organization of laminae, particles, and aggregates creates varying forms of pore structure (inter-layer or inter-laminar pores, which are usually smaller than 2 nm, inter-particle pores, or inter-aggregate pores (larger than 0.002 μm) (Stepkowska, 1990). Inter-layer or inter-laminar pores and inter-particle pores are also called micro-pores, as shown in Figure 2.29. Inter-aggregate pores are classified into macro-pores (which are larger than 0.05 μm) and meso-pores (which are less than 0.05 μm), which depends on the compacted dry density, as shown in Figure 2.30 (Villar et al., 2012).

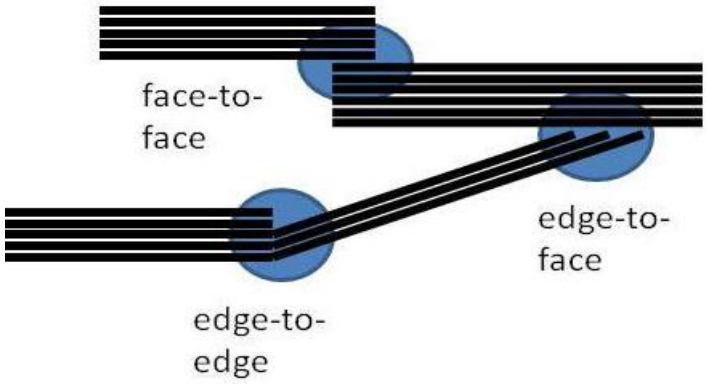

Figure 2.28. Particle contact types (modified from Meunier, 2005)

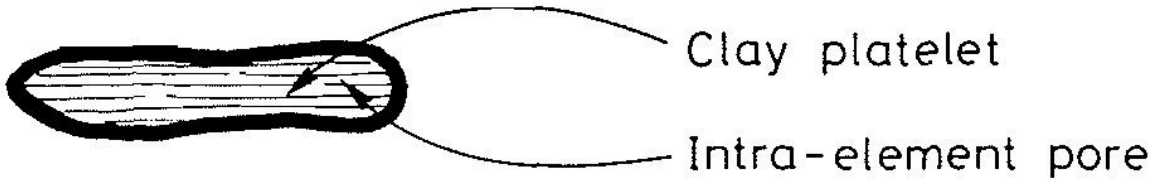

Figure 2.29. Microstructure of clay consisting of elementary particle arrangements (Gens and Alonso, 1992)

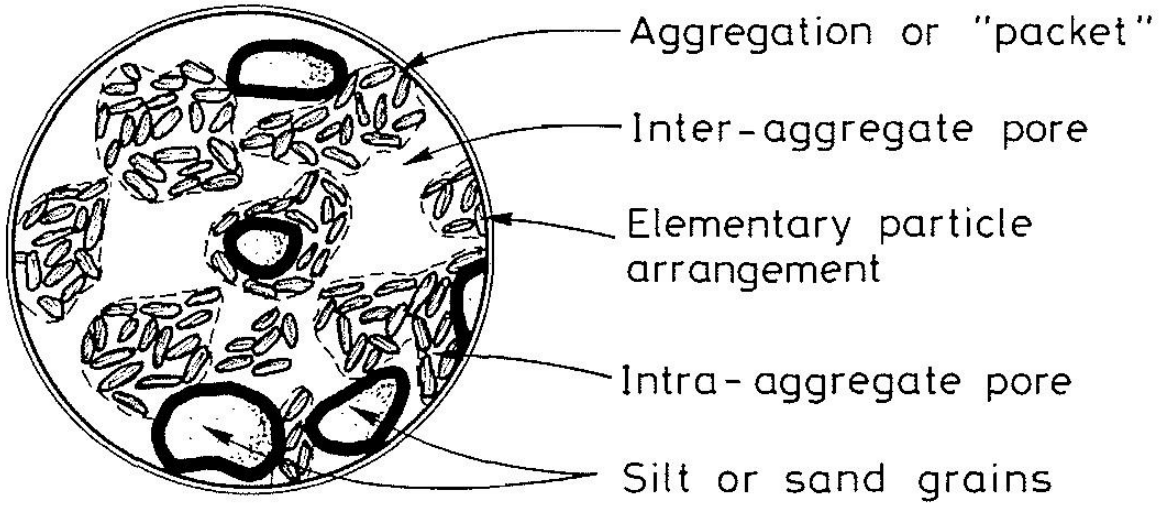

Figure 2.30. Macrostructure of a clay that predominantly consists of aggregations of elementary particle arrangements (Gens and Alonso, 1992)

2.7.5 Cation exchange capacity of bentonite (CEC)

Smectite minerals have exchangeable cations that can be found on the edges and outer surfaces, as well as in the interlayers. The negative charges on the edges and outer surfaces are balanced in part by pH. The characteristic properties of bentonite clay could be changed based on the composition of the exchangeable cations. In clay minerals with 2:1 layers, the most exchangeable cations are hydrated and situated in interlayer positions. In general, divalent cations, which have higher charges, are usually substituted for univalent cations, which have lower charges, in the interlayer position. Positive ions are adsorbed on the clay minerals' surface in order to balance negative charges. The CEC of bentonite is defined as the total amount of cations that could be exchanged. The quantities of NH_4^+, Ba^{2+}, and Na^+ ions are the

standard parameters for determining CEC of the clay. Montmorillonite has a very high CEC. In general, high-power cations replace low-power cations (Meunier, 2005), as follows: $Li^+ < Na^+ < K^+ < Ca^{2+} < Mg^{2+} < Ba^{2+} < Al^{3+} < NH_4^+$.

Previous experimental research has shown that the replaceability of cations varies according to the clay minerals, the cations that are implicated, and the experimental situations. Other factors include ion concentration, the nature of the anions in the replacement solutions, cation type, cation valency, and particle size. According to Meunier (2005), the internal CEC (permanent charges) of montmorillonite is given as:

Internal CEC (permanent charges) = (charge/mass) *1000 *100

CEC = internal CEC variable charges + external CEC (permanent charges)

The external exchange capacity of the main clay mineral (CEC variable charges) can be used to obtain the total CEC of montmorillonite, The CEC of the various clay minerals as given in Table 2.5can be determined using the external exchange capacity.

Table 2.5. Total CEC of the major clay minerals (Meunier, 2005)

Mineral	**CEC (meq/100 g)**
Kaolinite	5–15
Illite	25–40
Vermiculite	100–120
Montmorillonite	80–120
Chlorite	5–15

2.7.6 Mechanisms of bentonite–water interaction

The smectite component of bentonite is responsible for its swelling potential. There are two main swelling processes: crystalline and osmotic swelling. In the former, water molecules are adsorbed at the surface of the clay particles over an inter-layer separation of 10 to 22 Å. In

osmotic swelling, the adsorption occurs over an inter-layer separation of over 22 Å (Savage, 2005; Rao et al., 2013). The general swelling mechanism is depicted in Figure 2.31.

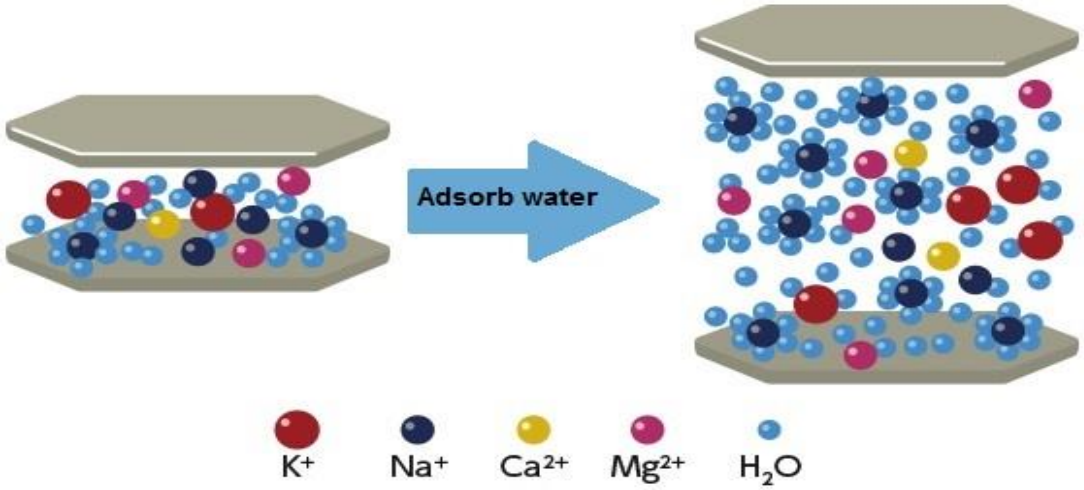

Figure 2.31. Schematic diagram of the swelling mechanism in montmorillonite (Kunimine Industries)

When water molecules penetrate the crystalline structure of dry Na-montmorillonite, the separation between the crystalline structure and two water layers increases (Meunier, 2005), as depicted in Figure 2.32.

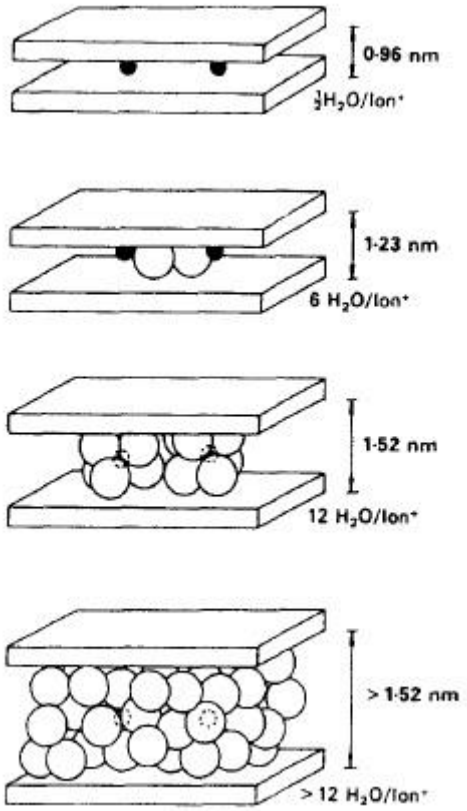

Figure 2.32. Water molecules penetrating the inner crystalline structure of Na-montmorillonite and increasing the basal spacing (d-space) (Madsen and Müller-Vonmoos, 1989)

The water adsorption mechanism depends on the degree of water saturation and the amounts of cations in the interlayers. Moreover, they act within the pore space of the minerals. These mechanisms are influenced by the breakup of montmorillonite particles and the de-mixing of ions and cations (Sandra, 2013). Montmorillonite consists of silica and alumina in a 2:1 ratio. Therefore, it has a negative layer charge caused by the isomorphic replacement of Al^{3+} by Si^{4+} ions and Mg^{2+} for Al^{3+} ions within the tetrahedral layer and Al octahedral layer, respectively. The total charge of the octahedral layer is much more than that of the tetrahedral layer (Laine and Karttunen, 2010). The cations between the interlayers balance the layer with a negative charge and the water molecules adsorbed within the montmorillonite layers (Karnland et al., 2006), as shown in Figure 2.33.

Generally, the crystalline swelling differs from the osmotic swelling based on the hydration structure of the adsorbed water (Yong, 1999). Montmorillonite particles can attract water molecules by bonding the negative layer of oxygen on the surface of the clay with the positive hydrogen ions of the bipolar water molecule or between the layer of positive hydroxyls on the surface of the clay and negative oxygen ions in water, as shown in Figure 2.34.a. Also, montmorillonite particles could attract water molecules by the hydration of cations in the interlayer between the Al octahedral sheet and the two Si tetrahedral sheets, as shown in Figure 2.34.b. Furthermore, montmorillonite particles can attract water molecules by osmosis attraction, which results from the difference in concentration between ions close to the layer surfaces of montmorillonite and in the pore water, as shown in Figure 2.34.c., and dipole attraction from the large net negative charge on the montmorillonite particle surface, which attracts the positive poles of the water. This leads water to orient with its positive poles towards the clay surface and connects with other water molecules, thus forming several layers of water dipoles, as shown in Figure 2.34.d (Sandra, 2013; Shehata, 2015).

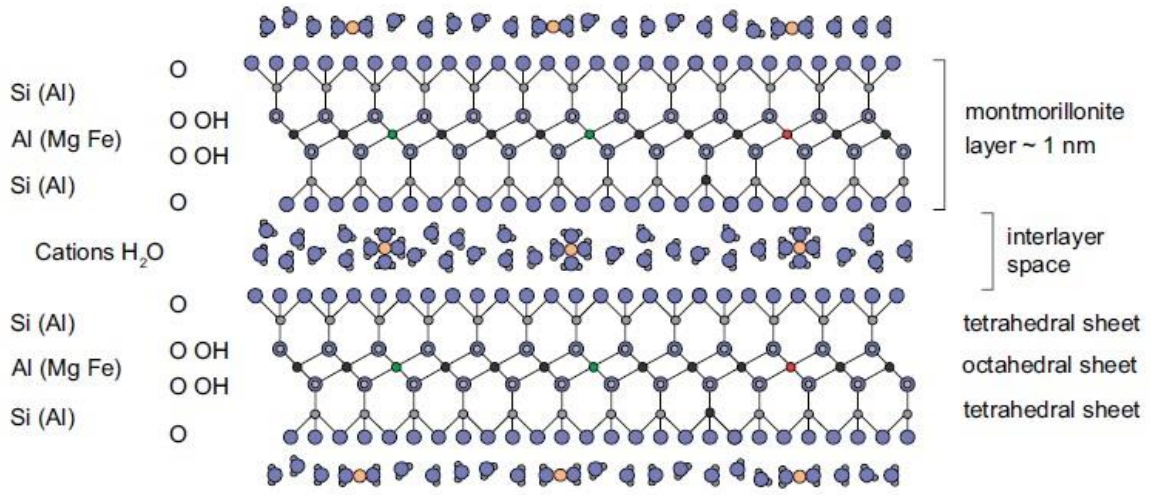

Figure 2.33. Montmorillonite layers showing interlayer cations and water molecules (Karnland et al., 2006)

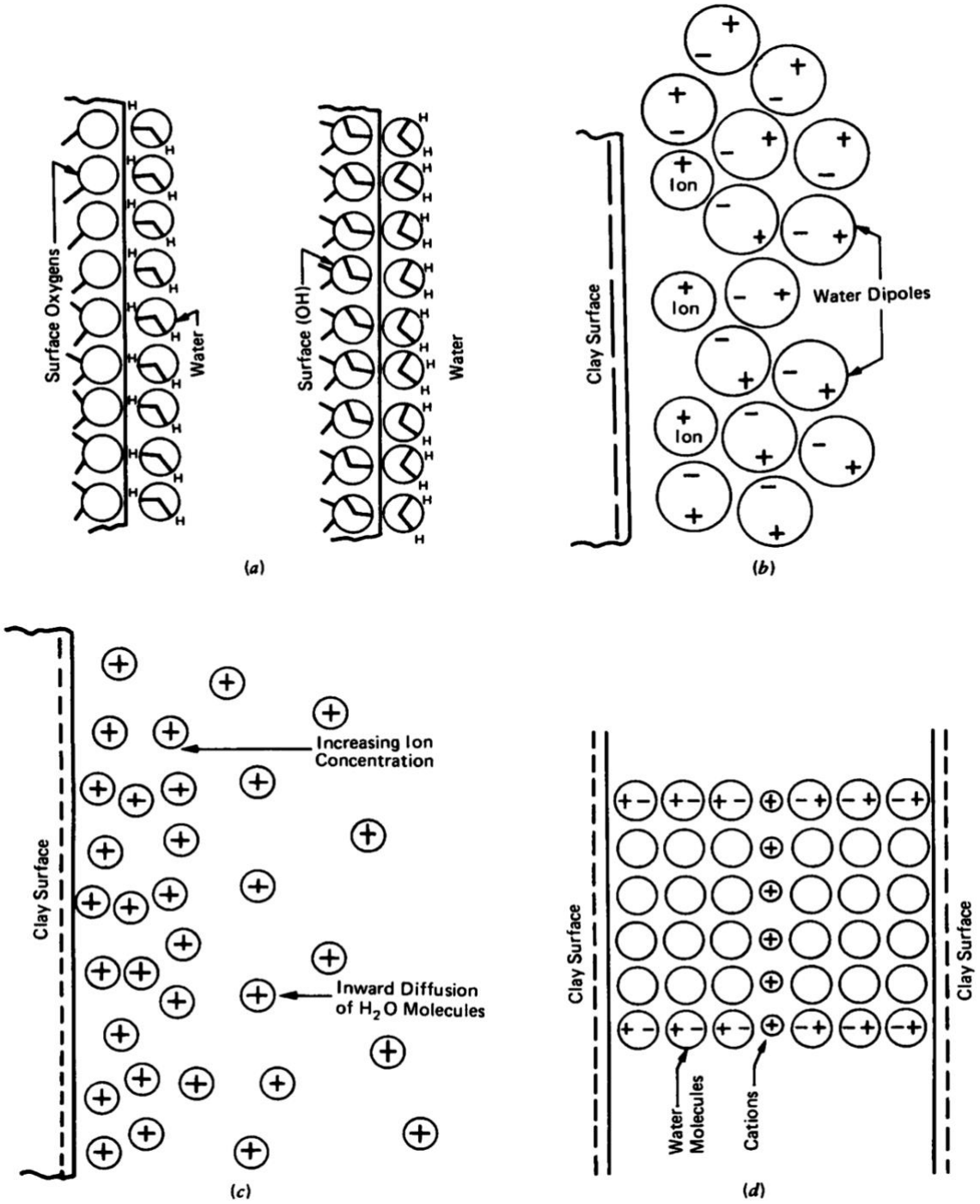

Figure 2.34. Interactions of clay minerals with water: (a) attraction by hydrogen bonding, (b) interlayer cations interactions (c) attraction by osmosis, and (d) dipole attraction (Mitchell et al., 1993)

2.8 Main factors that affect the swelling behaviour and thermal, hydraulic, mineralogical, and microstructural properties of bentonite–sand barriers in deep geological repositories

In most countries, bentonite-based materials are used as an engineered barrier material because of bentonite's high swelling potential, low hydraulic conductivity, long-term mineralogical stability, and ability to keep radionuclides in the event of canister failure (Cho et al., 1999, 2011; Melamed and Pitkanen, 1996; Wilson et al., 2011). However, as bentonite is active clay, changes in water content, dry density, solvents and salts in the groundwater and high temperature can affect its properties and, thus, the stability of repositories (Cho et al., 2011; Herbert et al., 2008; Karnland et al., 2007; Villar and Lloret, 2004). The sections below discuss the nature of the impact of these factors.

2.8.1 Dry density

Compaction of soil is defined as a method of increasing soil density by applying mechanical energy to reduce voids between soil particles. High dry density of compacted bentonite improves the performance of engineered bentonite barrier systems. In all bentonite, the swelling strain increases proportionately according to the initial dry density (Komine, 2004a). Chen (1988) cited dry density as an important factor governing swelling behaviour. Rao et al., (2004) studied the influence of dry density on swelling potential, and the results from their experiments confirmed that the swelling potential is significantly affected by the dry density; however, other influences, including stress state and moisture content, also contribute to swelling potential, as shown in Figure 2.35. Later, Ahn and Jo (2008) experimentally investigated two different bentonite types with varying dry densities (0.8–1.3 Mg/m^3). The results show that the hydraulic conductivity of the compacted material decreased with increasing final dry density. Also, Cho et al., (2009) studied the influence of dry density (1.4, 1.6, and 1.8 Mg/m^3) on the hydraulic conductivity of Kyungju Ca-bentonite at a 25 ºC

temperature. The results demonstrated that hydraulic conductivity decreases with increasing dry density, as presented in Figure 2.36. ENRESA (2006) investigated the thermo-hydro-mechanical (THM) properties of FEBEX bentonite and discovered that the dependence of thermal conductivity on temperature was least important, and at the same time, water content and bulk density had a significant influence. Thermal conductivity increased from 0.69 to 1.12 W/m·K with increasing dry density from 1.54–1.71 g/cm^3 for intact blocks with natural water content.

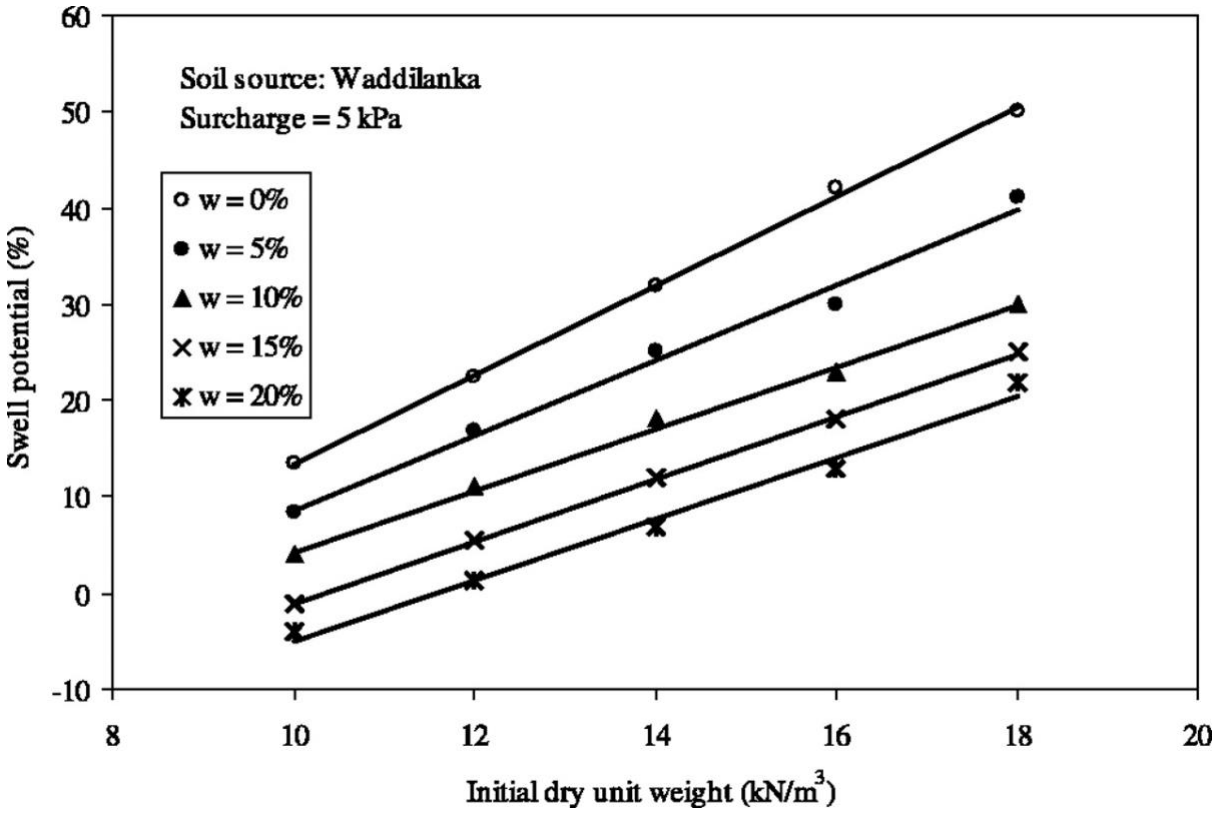

Figure 2.35. Increases in swelling potential with increasing dry density (Rao et al., 2004)

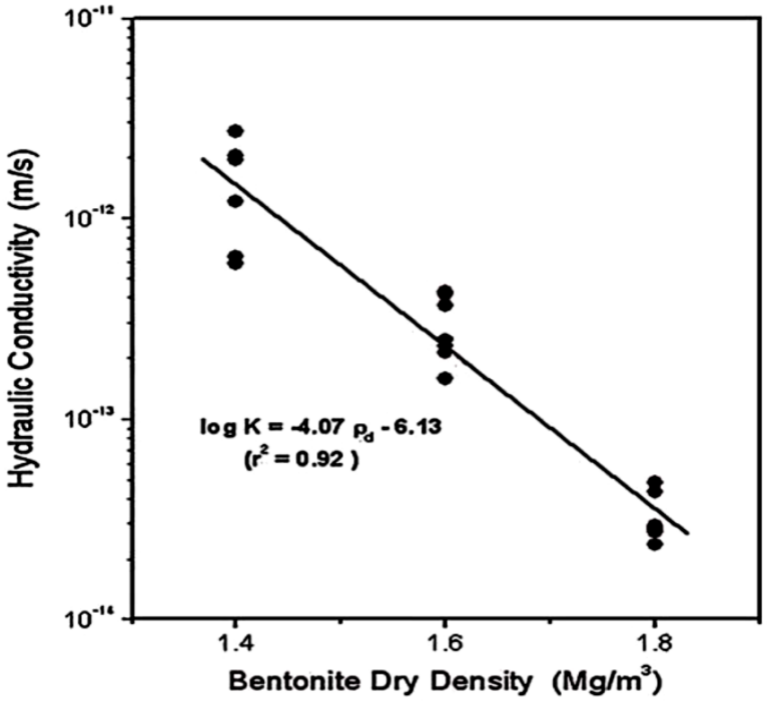

Figure 2.36. Influence of bentonite compaction on hydraulic conductivity (Cho et al., 2009)

2.8.2 Initial water content

The deformation characteristics of buffer and backfill materials in DGRs are mainly controlled by swelling properties, which are closely connected to the water content and its hydrological properties. Several authors have observed that the initial water content has a remarkable influence on the swelling potential of a compacted bentonite barrier (i.e., swelling behaviour decreases as the water content increases with high dry density). However, this is the case for compacted bentonite barriers with low dry density (Kassiff and Ben Shalom, 1971; Villar and Lloret, 2008). Kassiff et al., (1971) studied the impact of different initial water contents with a dry density of 1.5 Mg/m^3 on the swelling strain of plastic clay subjected to different vertical loads. The test results indicated that the swelling strain decreases as the initial water content is increased. In another study by Villar and Lloret (2008), the swelling capacity of highly compacted FEBEX bentonite specimens is significantly decreased as initial water content increases (Fig 2.37a). Moreover, as shown in Figure 2.37.b, the influence of the initial water content is less evident as vertical pressure increases. Thus, initial water content has an

insignificant impact on the swelling strain for compacted bentonite with low dry density and high vertical loads. Its impact is also negligible when the vertical loads are close to the swelling pressure. Komine and Ogata (1994) also investigated the effects of the initial water content on the swelling deformation of Na-bentonite compacted to dry densities of 1.24–1.99 Mg/m^3, finding that the deformation is more or less independent of the water content but increased proportionately based on the initial dry density with vertical pressure being constant. In addition, the swelling pressure increased exponentially with respect to the initial dry density but independently with respect to the initial water content.

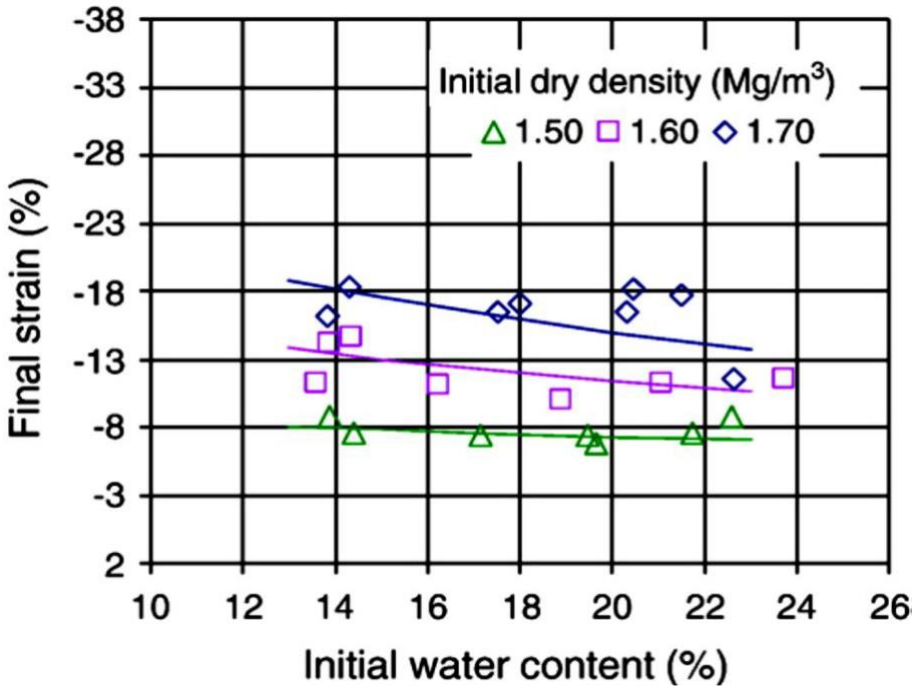

(a)

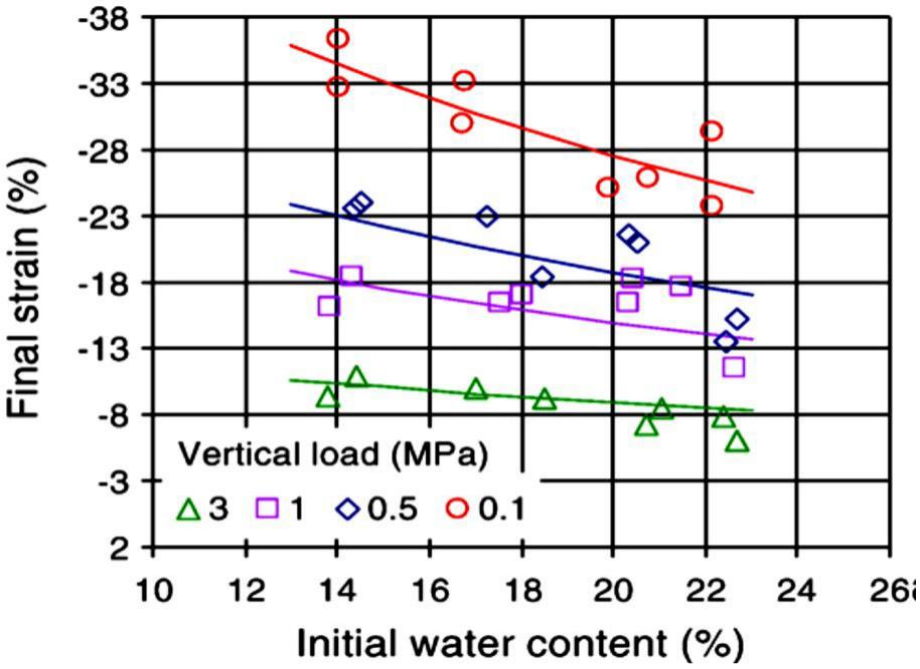

(b)

Figure 2.37. Impact of initial water content in bentonite on its swelling properties under (a) different dry densities (b) different vertical stresses (Villar and Lloret, 2008)

Figure 2.38 shows that the initial water content and dry density have a significant influence on thermal conductivity values measured in blocks from Grimsel underground laboratory in Switzerland (Villar and Lloret, 2007). Increase in thermal conductivity with an increase in water content has been noted by numerous other studies as well (e.g., Börgesson et al., 2001; ENRESA, 2006; Tang and Cui, 2006). ENRESA (2006) found that while the natural water content in intact blocks varied from 12–29%, thermal conductivity increased with respect to water content from 0.69 to 1.12 W/m·K. In partly dried samples, the water content was between 8–12%, the mean dry density was 1.66 g/cm^3, and thermal conductivity ranged from 0.62–0.82 W/m·K

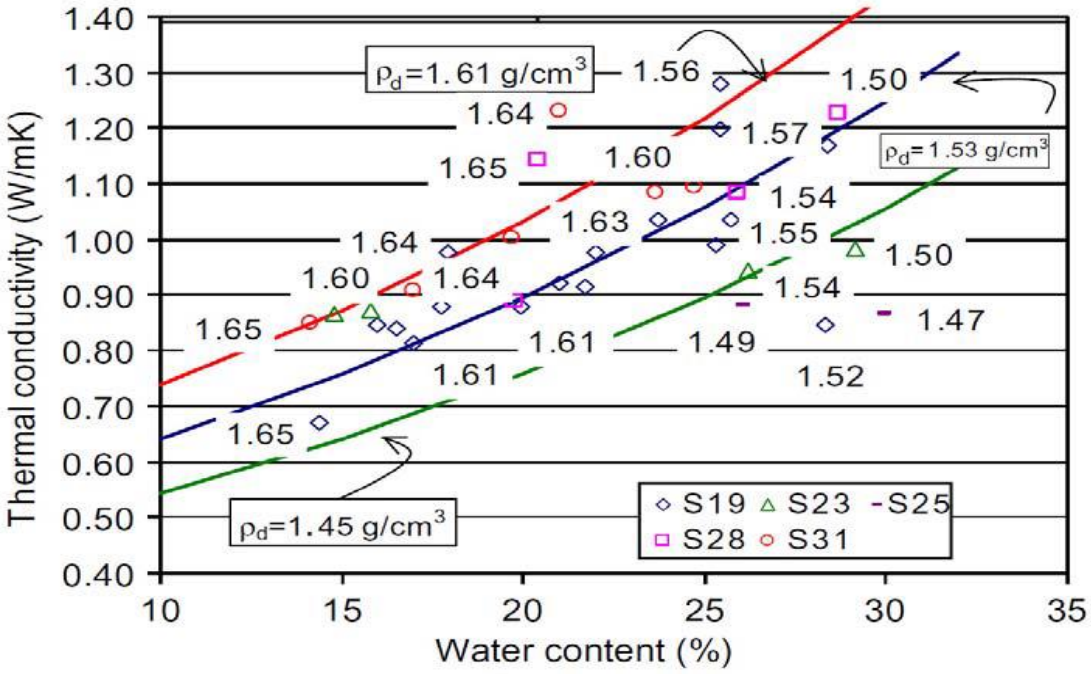

Figure 2.38. Thermal conductivity values measured in blocks from Grimsel (dry density indicated in g/cm3) and fittings obtained from theoretical evaluation (Villar and Lloret, 2007)

2.8.3 Bentonite content

It has been shown that adding bentonite to a specific amount of sand results in a mixture with improved properties that could increase the stability and decrease the hydraulic conductivity of excavated water channels. Furthermore, partial sizes of bentonite clay are very fine and occupy the pore space between individual grains of sand to perform better than properties of clayey mixtures in the buffer performance (Cho et al., 2011; Wilson et al., 2011; RWM, 2003). The swelling pressure and hydraulic conductivity of a bentonite–sand mixture depend on the bentonite content ratio and dry density of the mixture (Cho et al., 2000, 2011; Cui et al., 2012). The addition of small quantities of bentonite allows the fulfilment of the permeability requirement without failing in mechanical stability. The maximum swelling pressure increases with an increase in the dry density and decreases with an increase in sand content ratio, according to Cui et al.'s (2012) experimental results for GMZ Na-bentonite (Figure 2.39). The sand content ratio (R_s) is the mass proportion of the sand in the mixture. On

the contrary, the hydraulic conductivity and void ratio were observed to decrease with increasing bentonite content, according to Cho et al.'s (2000, 2011) experimental results for Kyungju Ca-bentonite.

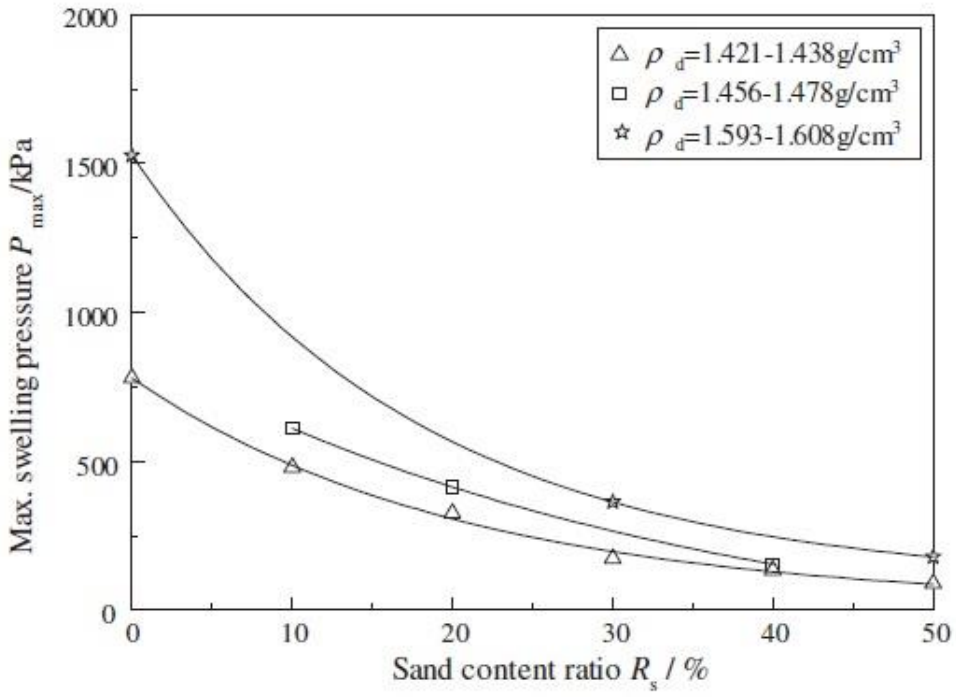

Figure 2.39. Maximum swelling pressure vs. sand content ratio (Cui et al., 2012)

Pusch (2008) and Wilson et al., (2011) showed that adding bentonite to a specific amount of sand results in both advantages and disadvantages. The advantages include the following:

- increased thermal conductivity when bentonite is mixed with silica sand with high thermal conductivity (which increases the ability of the buffer to transfer heat);
- reduced impact of groundwater salinity on the swelling capacity and hydraulic conductivity of the buffer material;
- reduced risk of increasing swelling pressure more than anticipated, which would result in an increase in the mechanical stress on the canisters and host rocks; and
- a cheaper price than pure bentonite.

The disadvantages are as follows:

- increased hydraulic conductivity (although this can be controlled by increasing the dry density) and
- reduced swelling capacity (but still within an acceptable range).

2.8.4 Pore water chemistry

Bentonite is composed of a mixture of montmorillonite, non-swelling minerals (e.g. quartz) and voids. When the montmorillonite swells by absorbing water into interlayers occupying the voids in the bentonite, the volume of montmorillonite increases and swelling pressure is produced (Sandra, 2013). The chemical evolution and physico-chemical properties of bentonite-buffer material are affected by several factors, such as groundwater salinity and chemicals in the groundwater. Therefore, the swelling properties of the material can be affected by the chemical composition of the saturating water. Fast chemical processes occur for buffer with water trapped inside its pores in a saturated state, and slow processes affect its mineral structure (Pastina and Hellä, 2006). The chemical transformations that occur in the external pores of bentonite are illustrated in Figure 2.40 (Itälä, 2009).

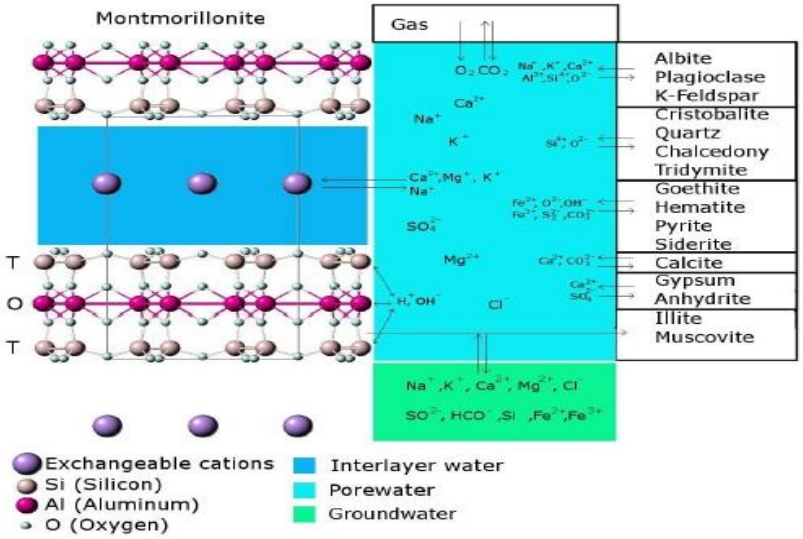

Figure 2.40. Schematic illustration of geochemical processes in a bentonite-water system in final repository conditions (Itälä, 2009); the montmorillonite layering and interlayer sites are on the left, while the mineral equilibria are on the right and the entrapped

High water salinity could affect the mineralogical stability of bentonite buffer material used as a component of an EBS, causing mineral alterations and a smectite-to-illite transformation. Many studies have found that the swelling potential of bentonite diminishes as the salinity of the saturating water increases, although the effect is less significant at higher densities (Karnland et al., 2007). Moreover, pore water chemistry is the major factor that governs the transformation of smectite to illite (Shehata, 2015).

2.8.5 Temperature

Highly elevated temperature is attributed to mineralogical instability of bentonite buffer material and may cause mineral alterations when used as a component of an EBS. In addition, they may lead to the transformation of smectite into illite, smectite into Fe-rich clay, or other types of transformation.

- **Smectite to illite transformation**

Smectite is not stable at higher temperatures and begins to alter to a more stable form, which may reduce the swelling of silicate phases such as illite, chlorite, mica, and zeolite as the temperature rises, as shown in Figure 2.41. Many scholars have discussed the illitization process. Temperature, the concentration of K^+ ions in pore water, the pH of the pore water, and pressure are the factors identified to play role in the transformation of smectite to illite (Laine and Karttunen, 2010). Linares et al., (1992) indicated that the transformation is independent on temperature time, temperature and the concentration of potassium. Kascandes et al., (1991) found that the main parameters that affect the illitization process are the solid/liquid ratio; low amounts of liquid and high amounts of reacting smectite inhibit illitization. Cuardos and Linares (1996) and Amouric and Olive (1991) concluded that the illitization process is accompanied by changes in the charge of the tetrahedral layer and changes in the mineral lattice due to decreasing contents of Si^{4+}, Mg^{2+}, and Fe^{2+} and increasing Al^{3+}, Fe^{2+}, and K^+ contents.

According to Wersin et al., (2007), smectite is naturally converted to illite at a very slow rate under heat conditions and in the presence of K^+. Finally, Wilson et al., (2011) indicated that temperature and time are the most important factors that enable the transformation of smectite to illite

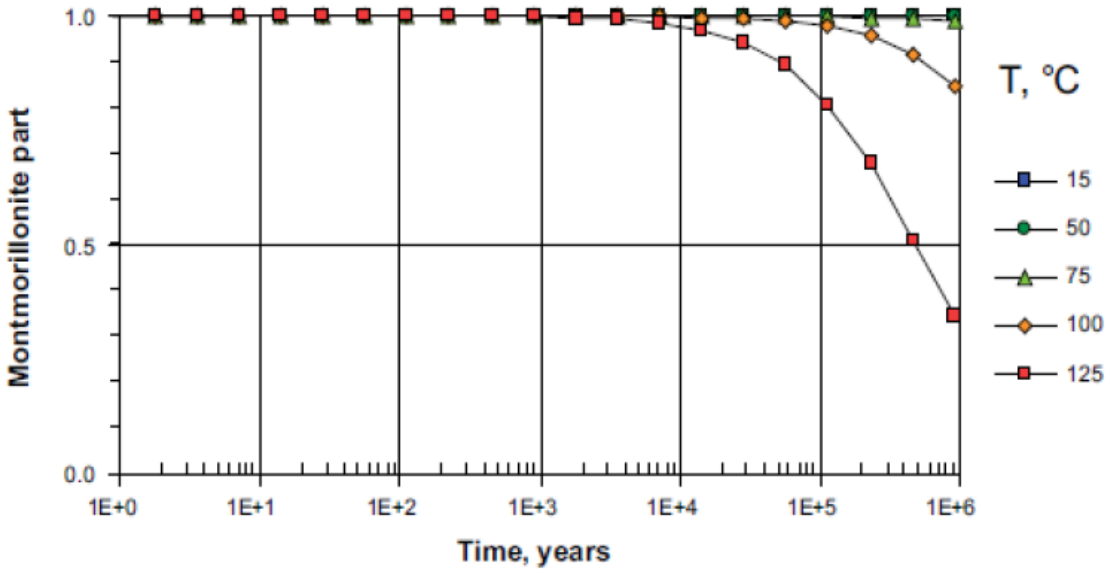

Figure 2.41. Model of smectite illitization that shows the remaining montmorillonite part for different temperatures with [K^+] = 0.002 mole/litre (80 ppm) according to Huang et al.'s (1993) kinetic model and laboratory-determined constants (from Karnland and Birger

- **Smectite to Fe-rich clay transformation**

Many countries are considering multi-barrier concepts for long-term underground repositories for SF and HLW. Waste containers are designed to isolate radioactive waste, provide high corrosion resistance, and withstand shear loading and mechanical stresses. Containers may be made of copper, iron, or steel depending on the country, while bentonite is universally considered the major component of EBSs (Gates et al., 2009; RWM, 2003). Corrosion of the waste container may occur when it comes in contact with saline underground water and heat decay conditions over a long period of time, leading to the release of iron (Fe) as a corrosion product (Wersin et al., 2008; NWMO, 2007; Smart et al., 2002). The interaction between bentonite and Fe in the presence of highly saline water and high temperatures may

result in mineralogical changes in the bentonite over a long period of time (Drief et al., 2001; Guillaume et al., 2003; Mosser-Ruck et al., 2010; Osacký et al., 2010). Some experiments have found that higher temperatures (>250 °C) resulted in chlorite formation, whereas lower temperatures tend to not result in significant alterations or the formation of a 1:1 mineral or altered Fe-rich saponite-type smectite (Wilson et al., 2011).

Many studies have focused on the interaction between bentonitic clays and Fe, with findings such as the reaction pathways depending on the temperature, pH, liquid to clay ratio, Fe to clay ratio, and nature of the initial bentonite as shown in Figure 2.42 (Mosser-Ruck et al., 2010; Osacký et al., 2010; Savage et al., 2010; Shehata, 2015). Expected reaction pathways for bentonitic clays and waste containers include the transformation of montmorillonite into Fe-rich smectite through an ion exchange reaction and the conversion of montmorillonite into non-swelling Fe-rich under very high temperature conditions (Shehata, 2015).

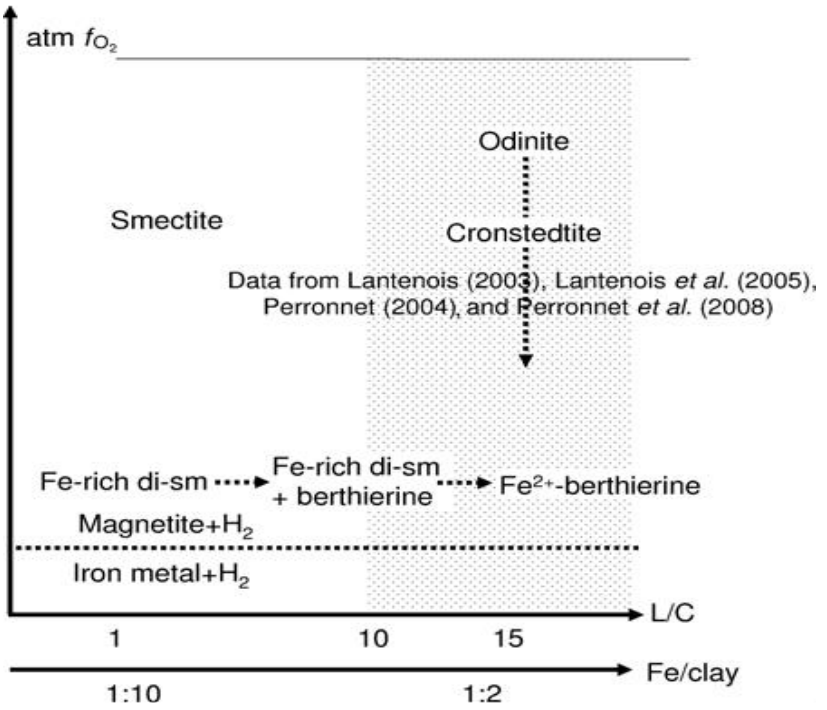

Figure 2.42. Smectite and Fe reaction pathway, which depends on the redox state, availability of Fe, and liquid to clay ratio at low temperatures (Mosser-Ruck, 2010)

- **Other types of alteration (such as chloritization)**

Chloritization is a parallel reaction to illitization, and their resulting effects are similar (i.e., reduction of expandability). Chloritization may occur from buffer alteration processes in the absence of K^+ and access to Mg, Fe, or Al, or it may occur in cases without illitization (Karnland and Birgersson, 2006). The test results of one experiment showed that the formation of chlorite from pure smectite takes place at 0.5 M KOH at 35 °C after 270 days (Eberl et al., 1993).

2.9 Review of previous studies on the effect of pore water chemistry, physical factors and temperature on the swelling behaviour and thermal, hydraulic, mineralogical, and microstructural properties of bentonite–based barrier material in deep geological repositories for radioactive waste

Bentonite is composed of a mixture of montmorillonite, voids, non-swelling minerals, and sand particles. When montmorillonite adsorbs water into interlayers, occupying voids in the bentonite, the volume of bentonite increases and swelling pressure is produced (Sandra, 2013). The chemical composition of deep groundwater (i.e., pore water), in combination with high temperatures, can affect the physical and chemical properties of EBS and may limit the potential of bentonite particles to expand. Thus, saline pore water may compromise the ability of a bentonite-based material to fulfil its role as a swelling and self-sealing barrier. Many studies have found that the swelling capacity of bentonite decreases with an increase in the salinity of the saturating water at low compacted dry densities (Karnland et al., 2007). Moreover, swelling potential may decrease with time due to the rearrangement of the clay particles over time (Delage et al., 2006; Herbert et al., 2008). Johannesson and Nilsson (2006) investigated the effect of pore water salinity with different dry densities on the THMC properties of Friedland clay. The experimental results indicated a large variation in the

measured swelling pressure, most of which can be explained by differences in the polarity of the permeating fluid, as shown in Figure 2.43.

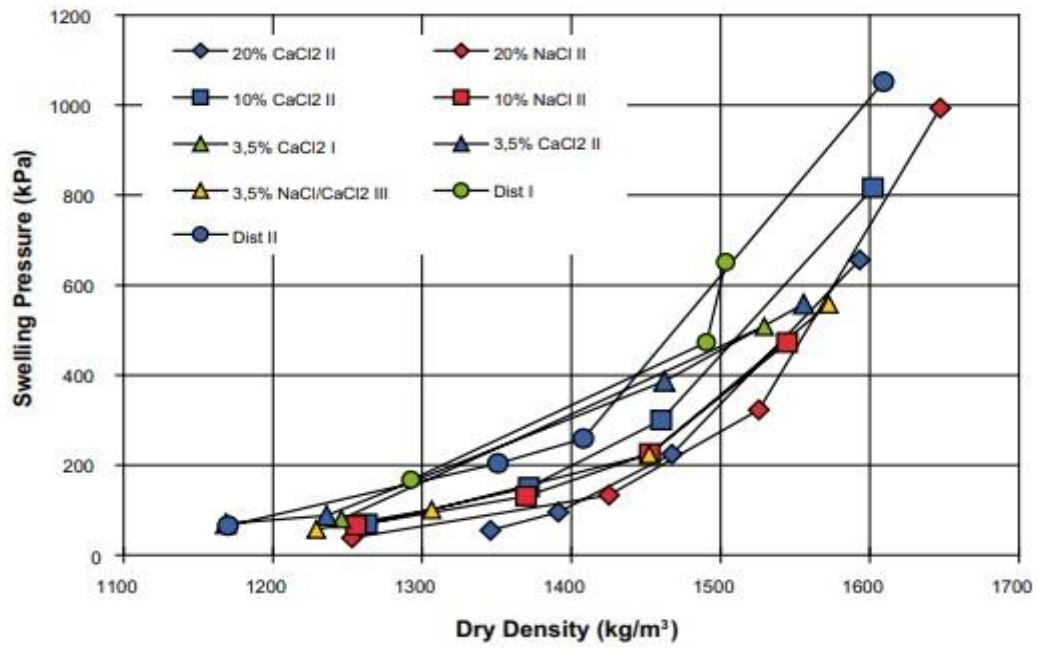

Figure 2.43. Swelling pressure in Friedland clay as a function of dry density with different salinities of pore water (Johannesson and Nilsson, 2006)

Karnland et al., (2007) investigated highly compacted MX-bentonite containing 83% montmorillonite by mass. The compacted bentonite was saturated with four solutions: de-ionized water, 1.0 M NaCl, 1.0 M NaOH, and 1.0 M NaCl. These solutions were replaced with 1.0 M NaOH after 15 days, as shown in Figure 2.44. The results showed that the average swelling pressure of the samples treated with 1.0 M NaOH was lower than that of the samples treated with 1.0 M NaCl and those treated with de-ionized water. Thus, the swelling pressure of MX-bentonite differs between solutions with regard to ionic strength as well as between chemical concentrations of the same solution.

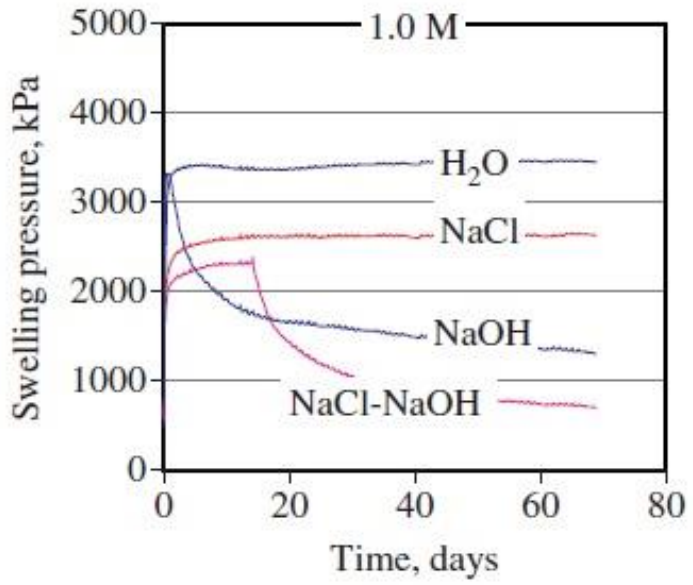

Figure 2. 44. Swelling pressure response in four individual MX-80 samples (Karnland et al., 2007)

Wang et al., (2012) investigated the effect of pore water chemistry on swelling pressure under constant-volume conditions for 700 days. Distilled water and synthetic water with chemical compositions similar to that of in situ pore water were used for hydration. The results obtained during the first 100 days indicated that the water types have no significant influence on the evolution of the swelling pressure, and the maximum swelling pressure observed was close to 4.30 MPa. Over time, however, swelling pressure was observed to decrease for all samples, and this decrease is more pronounced in the samples subjected to synthetic water. All the results were analyzed by considering the physico-chemical interactions between the minerals in the claystone, minerals in the bentonite, and different fluids.

Chen and Huang (2013) investigated the free swelling properties of Zhisin clay as a potential buffer material under varying groundwater conditions (i.e., immersion in $CaCl_2$, NaCl, and Na_2SO4 solutions at various concentrations). The experimental results indicated that Zhisin clay, as a Ca-bentonite, exhibited reduced swelling strain in saline solutions. The extent to which the swelling strain decreases when exposed to saline water was affected by both the concentration and type of electrolytes. At a constant concentration, swelling strain in the $CaCl_2$

solution was lower than in the NaCl solution due to the quasi-crystals formation in the presence of calcium ions. Also, the swelling in the Na_2SO_4 solution was lower than in the NaCl solution. Chen et al., (2017) studied the swelling behaviour of compacted GMZ bentonite experiencing chemical cycles of sodium-calcium exchange and salinization-desalinization effect. Experimental results show that the salinity of groundwater has an influence on the swelling properties of compacted bentonite and Na-bentonite is partly transformed into Ca-bentonite once NaCl solution is replaced with $CaCl^2$ solution. Liu et al., (2018) studied the swelling pressure of compacted Gaomiaozi (GMZ) bentonite exposed to hyperalkaline solutions from the viewpoint of Na+ cations and OH– anions. They found out that high concentrations of Na+ cations inhibit the crystalline swelling as well as the double-layer swelling; while high OH– anions concentration facilitates the double-layer swelling and fabric re-arrangement. Furthermore, Akinwunmi et al., (2020) observed a decrease in the swelling pressure of both Na- and Ca-montmorillonites when subjected to saline water.

Another important parameter is the hydraulic conductivity, which depends on the montmorillonite content, pore water chemistry, particle size, dry density, swelling pressure, temperature, and void ratio, but the most important factors are pore water chemistry and dry density (Pastina and Hellä, 2006). The physio-chemical interaction of pore water with a soil particle system occurs particularly close to particles' surface (Terzaghi, 1925). Particle spacing, particle size (influenced by aggregation or dispersion particle rearrangement), adsorbed layers, and inter-lamellar swelling all influence hydraulic conductivity and the transportation of contaminants (Macey, 1942). Michaels and Lin (1954) suggested that the major influence of the water chemistry was expressed as control over the tendency of clay particles to disperse or form aggregates, and they experimentally investigated the influence of different permeating fluids on the hydraulic conductivity of kaolinite. The results indicated that the hydraulic conductivity of kaolinite markedly decreases as the polarity of the permeating fluid increases

and that the most important factor affecting hydraulic conductivity was the degree of dispersion of kaolinite in the permeating fluid.

Mesri and Olson (1970) investigated the effect of pore water chemistry on the hydraulic conductivity of bentonite clay using several types of fluids as permeants. The test results confirmed that physio-chemical variables have significant impacts on the hydraulic conductivity of bentonite, controlling the tendency of the clay to disperse or form aggregates. They concluded that hydraulic conductivity increases with increasing the concentration of pore fluid, as shown in Figure 2.45.

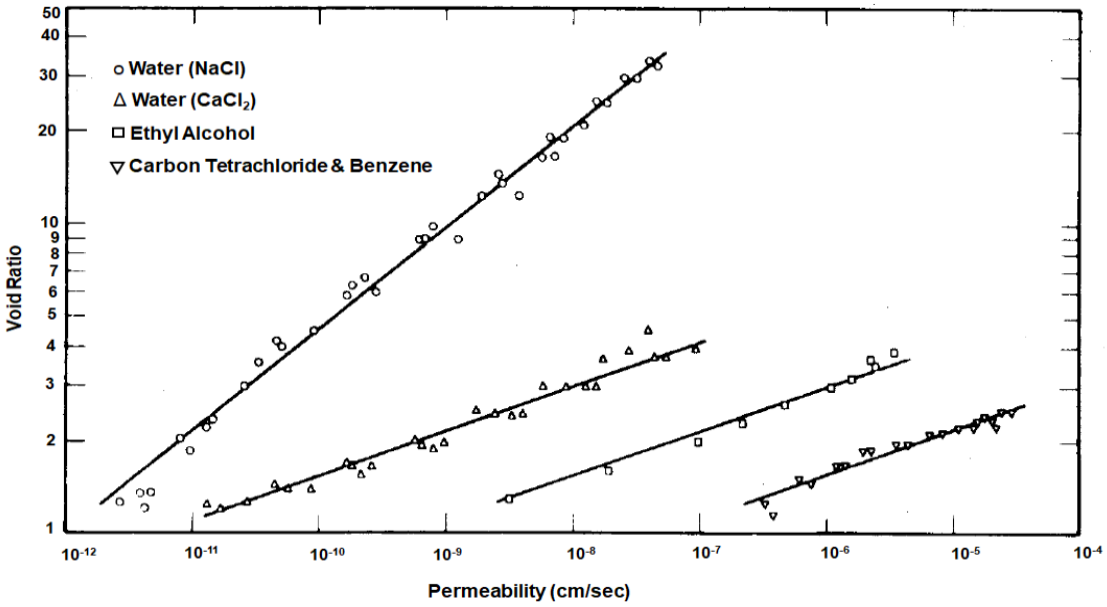

Figure 2.45. Effect of pore fluid on smectite (Mesri and Olson, 1970)

Villar et al., (2003) investigated the effect of three different types of pore water serving as permeants on the hydraulic conductivity of FEBEX bentonite. The test results revealed that higher hydraulic conductivity is achieved with saline water than for distilled water and that this effect is more significant for low densities, as shown in Figure 2.46.

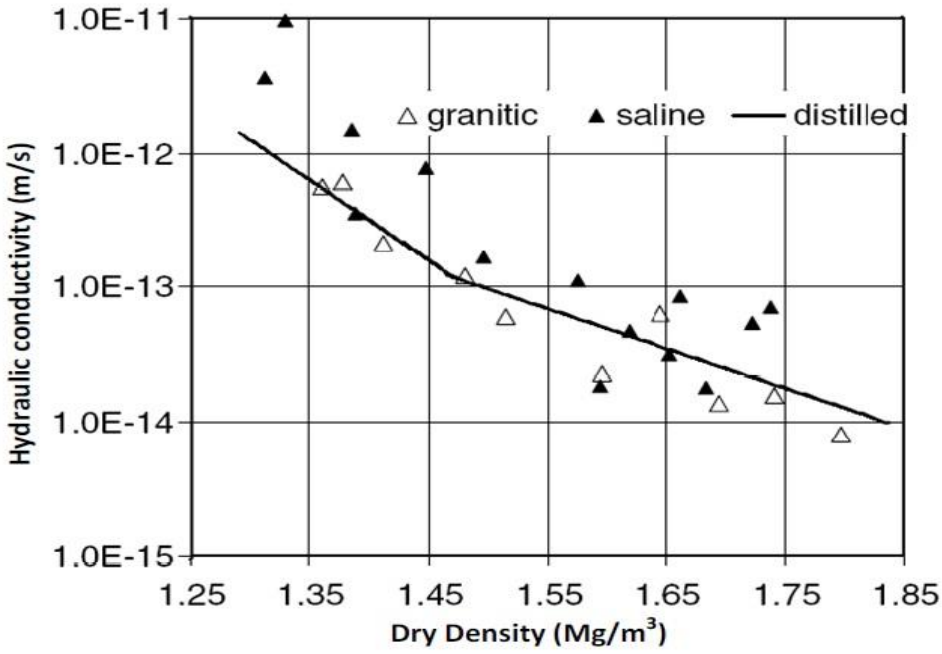

Figure 2.46. Hydraulic conductivity versus dry density of FEBEX bentonite measured with three types of pore fluids (Villar et al., 2003)

An increase in hydraulic conductivity with saline permeant fluid was also observed by Karnland et al., (1992) and Pusch (2001) for Friedland Ton clay, Mata (2003) for a granite/Na bentonite mixture, and Batenipour (2008) for MX-bentonite. Batenipour (2008) conducted a series of one-dimensional compression experiments on MX-bentonite that contained 75 wt. % montmorillonite. The experiments were performed with four different chemical solutions: distilled water, 100 g/L $CaCl_2$, 250 g/L $CaCl_2$ and constrained 250 g/L $CaCl_2$ under different effective montmorillonite dry densities (EMDDs). The test results confirmed that hydraulic conductivity increases with increasing solution salinity. The hydraulic conductivity for the experiments with 100 g/l $CaCl_2$ was several times higher than that of fresh water but less than that of the tests that used 250 g/l $CaCl_2$ for specimens with the same dry density. Furthermore, hydraulic conductivity decreased with increasing EMDD, as shown in Figure 2.47.

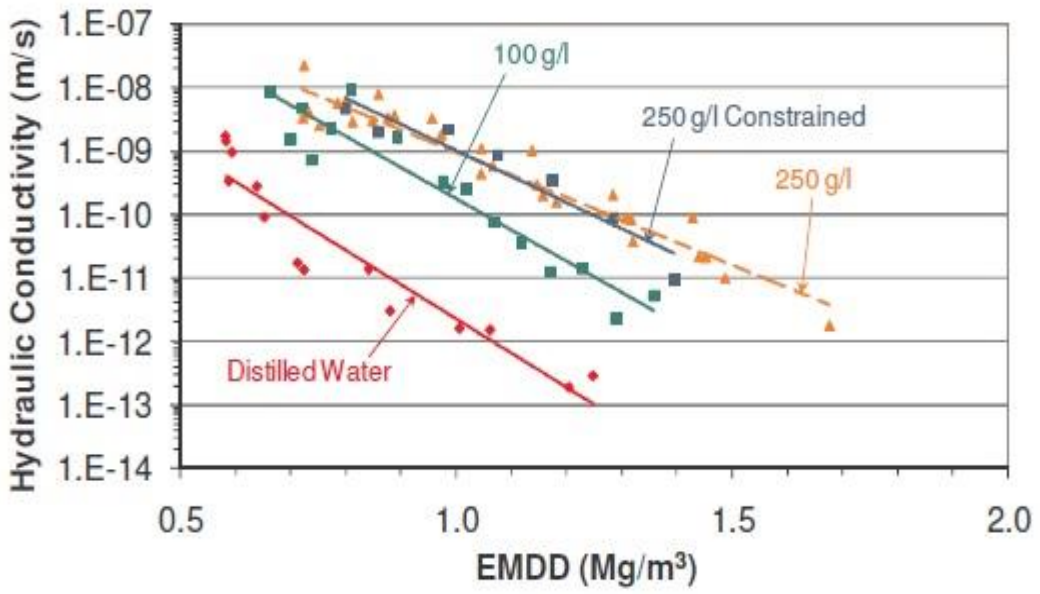

Figure 2.47. Hydraulic conductivity versus dry density of MX bentonite using three types of pore fluids (Batenipour, 2008) (EMDDs: effective montmorillonite dry densities).

During the operating life of the repository, the physical properties of bentonite are highly sensitive to the salinity of the constituent pore fluid (i.e., local groundwater) that permeates into the disposal vault from the host rock to the used fuel containers, resulting in the hydration of bentonite-based engineered barriers (Siddiqua et al., 2014). The heat dissipation rate of the designed barriers is dependent on the thermal properties of the bentonite buffer material.

Moreover, the penetration of saline groundwater into barriers changes the pore fluid chemistry in the soil-water system. This could influence the thermal conduction capability of the bentonite materials. In the past, several laboratory studies have been conducted to determine impact of salt concentrations and other factors on the thermal conductivity of soil materials or bentonite-based barrier materials (Abu-Hamdeh and Reeder, 2000, Casas et al., 2013, Siddiqua et al., 2018). Abu-Hamdeh and Reeder (2000) monitored the thermal conductivity of certain Jordanian soils with different bulk densities, moisture contents, salinity (NaCl and $CaCl_2$), and proportion of organic matter. The found that an increase in the amount of added salts at a given

moisture content resulted in the decrease in thermal conductivity and that the sandy soil has higher thermal conductivity than clay loam under the same salt type and concentration, as shown in Figure 2.48.

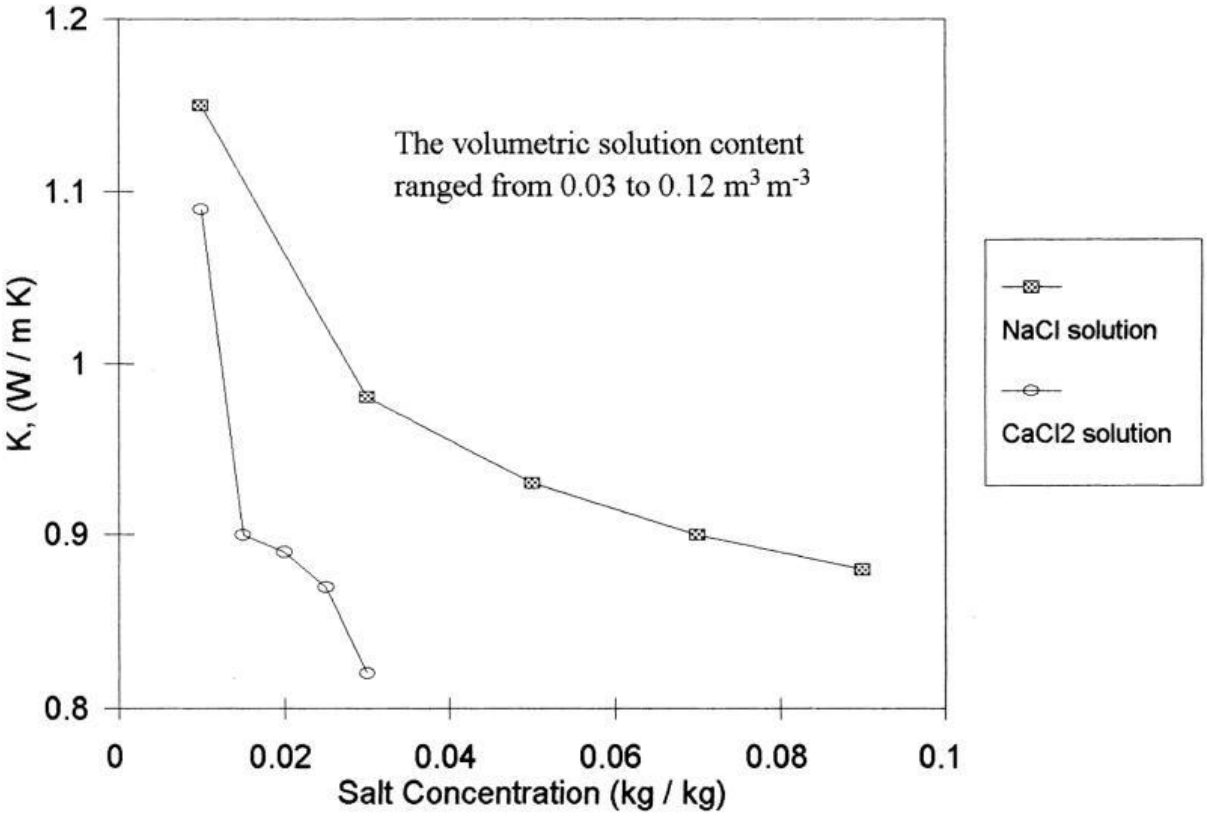

Figure 2.48. Soil thermal conductivity of sand as a function of the concentrations of both NaCl and CaCl2 solutions (Abu-Hamdeh and Reeder, 2000)

Casas et al., (2013) investigated the specific heat capacity, density, thermal conductivity, and viscosity of a bentonitic clay (composed mainly of 55% Na+- saturated trioctahedral smectite, 28% sepiolite, and 15% illite) mixed with different saline solutions (0, 1, 2, 3, and 3.5%) in a temperature range of 293.15–317.15 K. The results indicate that the mixture of bentonitic clay and seawater reached highest values of thermal conductivity while the lowest values are associated with the mixture containing distilled water. Thermal diffusivity increased with increasing temperature, as shown in Table 2.6 and Figure 2.49

Table 2.6. Experimental thermal conductivity (W·m−1·K−1), density (kg·m−3), and viscosity (mPa·s) of mixtures of bentonite and seawater solutions at 298.15 and 308.15 K (Casas et al., 2013)

T/K	M0	M1	M2	M3	M4
Thermal conductivity/W · m^{-1} · K^{-1}					
298.15	0.772	0.682	0.668	0.655	0.641
308.15	0.784	0.697	0.681	0.662	0.649
Density/kg · m^{-3}					
298.15	1330	1290	1240	1180	1130
308.15	1320	1260	1230	1170	1120
Viscosity/mPa · s					
298.15	14632	14233	13898	13814	12943
308.15	14356	14037	13427	13392	12786

M0: 35% bentonitic clay + 65% Pure sea water content (wt.%)
M1: 30% bentonitic clay + 58% Pure sea water content (wt.%)
M2: 25% bentonitic clay + 42% Pure sea water content (wt.%)
M3: 20% bentonitic clay + 22% Pure sea water content (wt.%)
M4: 15% bentonitic clay + 0% Pure sea water content (wt.%)

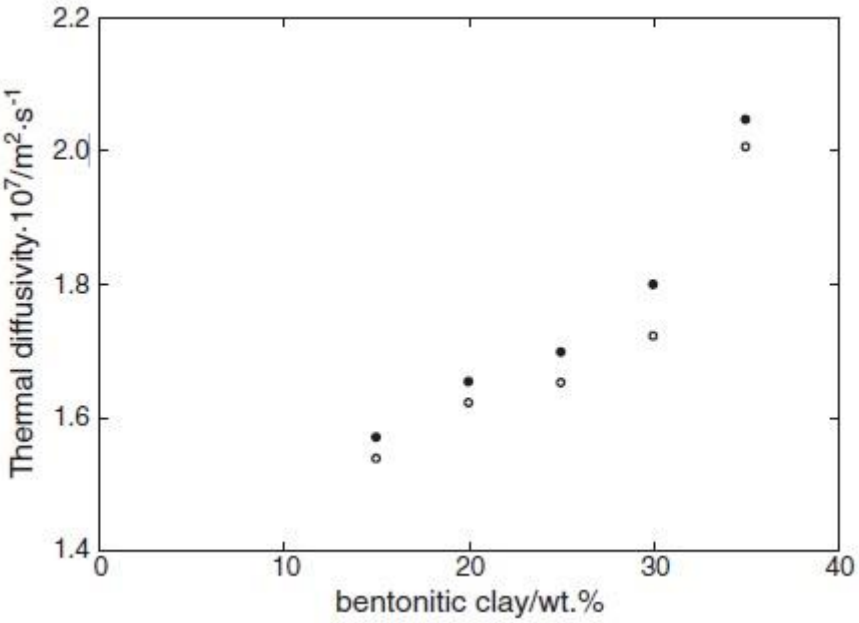

Figure 2.49. Thermal diffusivity (m2·s−1) of mixtures of bentonite with seawater solutions as a function of the clay proportion (wt.%): o 298.15 K, • 308.15 K (Casas et al., 2013)

Siddiqua et al., (2018) conducted several laboratory tests to evaluate the impact of pore fluid salinity on the thermal conductivity of a mixture of bentonite and silica sand. A thermal probe based on the hot wire technique was used for the measurement of the thermal conductivity. The test results revealed that an increase in the salt concentration in the pore fluid's leads to a decrease in the thermal conductivity of the mixture, as shown in Figure 2.50

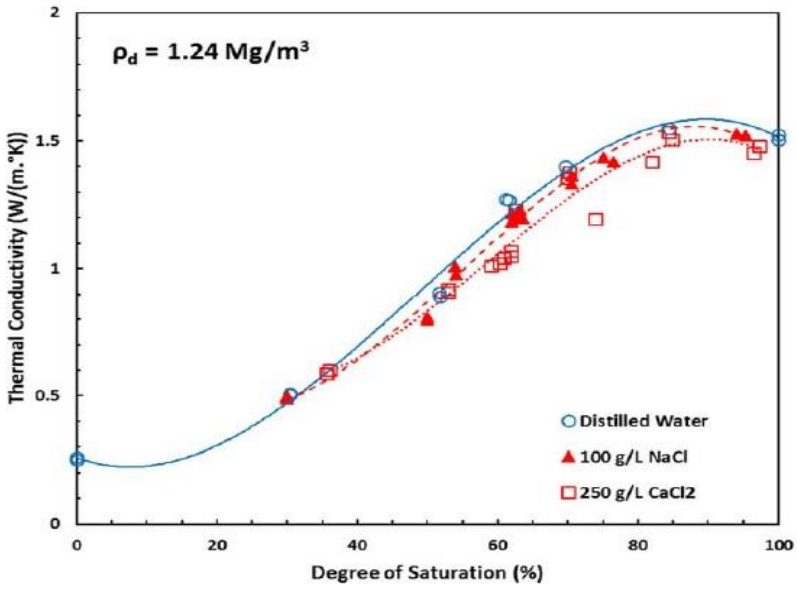

Figure 2.50. Thermal conductivity values for the specimens with a target dry density of 1.24

The properties of bentonite depend on the amount of smectite minerals in the bulk material and on the exchangeable cations in the interlayer position. These properties could be affected when compacted bentonite interacts with saline groundwater and absorbs this water into the inter-lamellar spaces. In particular, the type of hydrated cations present in the solution has a significant influence (Mitchell, 1993). In the hydration process, water molecules are absorbed between elementary clay layers to develop water layers. The thicknesses of dehydrated montmorillonite crystals and complete hydrate layers depend on the CEC of the clay and could affect the mineralogical stability of bentonite buffer-based material. Montmorillonite layers are naturally converted to illite layers very slowly in the presence of high concentrations of potassium (Garrels, 1984). Eberl et al., (1993) indicated that pore water

chemistry and pH are the main factors that control montmorillonite–illite conversion and that illitization takes place in the presence of NaOH and KOH solutions at a temperature of 35 ºC. Moreover, Ureana et al., (2013) confirmed that the montmorillonite–illite conversion takes place within 15–30 days of curing with magnesium hydroxide, seawater, or olive mill wastewater with different concentrations. Honty et al., (2004) asserted that water chemistry and temperature are the most important parameters controlling illite formation. Karnland and Birgersson (2006) concluded that bentonite that contains at least 75% montmorillonite by mass requires the availability of 5% potassium by mass in order to achieve full illitization of the buffer material. According to Wersin et al., (2007), smectite is naturally converted to illite at a very slow rate under heat conditions and in the presence of potassium.

2.10 Conclusions

Nuclear power generation has become an important source of energy in many countries, but it is associated with large amounts of high-level radioactive nuclear waste every year, which is detrimental to humans and the environment. Canada and other countries have agreed that the most appropriate solution is to construct DGRs to isolate and dispose of radioactive waste at depths of 300–1000 m. Canadian DGRs are based on multi-barrier concept, and the overall safety of the DGR depends on its stability and that of the natural host rock. Bentonite-based material is typically used as a buffer material to provide mechanical and chemical protection, dissipate heat, and retard radionuclide diffusion in the event of canister failure. A composite compacted barrier made of bentonite and sand has been proposed as a suitable buffer and sealing material of EBS for Canadian DGRs as well as in other countries. However, the current literature indicates that the swelling behaviour and mineralogical and microstructural properties of bentonite-based materials and their hydraulic and thermal properties are generally affected by the chemical composition of fluid within its pores. It is also suggested that combined effects of groundwater chemistry and the heat generated by the radioactive waste

could also negatively impact the long-term performance of the bentonite-based barrier materials.

However, most of the aforementioned previous studies focused on pure bentonite. The effects of chemical composition or high salinity of pore water on the engineering (swelling, hydraulic, thermal) properties of compacted bentionite-sand barrier material (with different blending ratios of bentonite and sand, as well as with different dry densities) are not well understood. Moreover, the findings from previous studies on the effects of salinity on the engineering properties of other bentonite-based materials are not directly transferable to a bentonite–sand barrier material in Ontario's DGR conditions because Ontarios' groundwaters feature different chemical compositions than the groundwaters examined in previous studies. In addition, no previous studies have investigated the coupled effect of the chemistry of Ontario's groundwater at potential DGR sites in Canada (specifically, the Trenton and Guelph regions in Ontario) and the heat generated by the nuclear waste material on the swelling behaviour and thermal and hydraulic properties of compacted bentonite–sand barrier (with different blending ratios of bentonite and sand, as well as with different dry densities). This research gap is addressed in this thesis.

2.11 References

Abdi, H., Labrie, D., Nguyen, T. S., Barnichon, J. D., Su, G., Evgin, E., ... & Fall, M. (2015). Laboratory investigation on the mechanical behaviour of Tournemire argillite. Canadian Geotechnical Journal, 52(3), 268-282.

Abu-Hamdeh, N. H., & Reeder, R. C. (2000). Soil thermal conductivity effects of density, moisture, salt concentration, and organic matter. Soil science society of America Journal, 64(4), 1285-1290.

Acres Consulting Services Ltd. and RE/SPEC Ltd., (1985). A feasibility study of the multilevel

vault concept. Atomic Energy of Canada Limited Technical Report, TR-297.

Acres Consulting Services Ltd. (1993). A preliminary study of long-hole emplacement alternatives. Atomic Energy of Canada Limited Technical Report, TR-346.

Ahn, H. S., & Jo, H. Y. (2009). Influence of exchangeable cations on hydraulic conductivity of compacted bentonite. *Applied Clay Science*, *44*(1-2), 144-150.

Akinwunmi, B., Hirvi, J. T., Kasa, S., & Pakkanen, T. A. (2020). Swelling pressure of Na-and Ca-montmorillonites in saline environments: A molecular dynamics study. *Chemical Physics*, *528*, 110511.

Amouric, M., & Olives, J. (1981). Illitization of smectite as seen by high-resolution transmission electron microscopy. *European Journal of Mineralogy*, 831-836.

Athanassopoulos, C. (2011). Natural sodium versus activated calcium bentonite in geosynthetic clay liners (GCLs). In *Proceedings of the solid waste and recycling conference*.

Atomic Energy of Canada Limited. (1994). Environmental impact statement on the concept for disposal of Canada's nuclear fuel waste. Atomic Energy of Canada Limited, Ottawa, Ont AECL-10711: COG-93–COG-1.

Bailey, S. W. (1988). Odinite, a new dioctahedral-trioctahedral Fe3+-rich 1: 1 clay mineral. *Clay minerals*, *23*(3), 237-247.

Batenipour, H., 2008. Effect of water salinity on the hydro-mechanical behaviour of granular bentonite as light backfill material. (2008) *61st Canadian Geotechnical Conference Edmonton, Alberta.* Volume 1, 499-505.

Baumgartner, P., Tran, T.V., & Burgher, R. (1994). Sensitivity analyses for the thermal response of a nuclear fuel waste disposal vault. Atomic Energy of Canada Limited Technical Report, TR-621, COG-94-258.

Bergström, U., Pers, K., & Almén, Y. (2011). *International perspective on repositories for low level waste* (No. SKB-R--11-16). Swedish Nuclear Fuel and Waste Management Co..

Börgesson, L., Chijimatsu, M., Fujita, T., Nguyen, T. S., Rutqvist, J., & Jing, L. (2001). Thermo-hydro-mechanical characterisation of a bentonite-based buffer material by laboratory tests and numerical back analyses. *International Journal of Rock Mechanics and Mining Sciences*, *38*(1), 95-104.

Canadian Nuclear Safety Commission. (2008). October. Canadian national report for the Joint Convention for the Safety of Spent Fuel Management and on the Safety of Radioactive Waste Management: Third report. Minister of Public Works and Government Services, Government of Canada. http://www.nuclearsafety.gc.ca/pubs_catalogue/uploads/joint_convention_2009_third_national_report_e.pdf.

Canadian Nuclear Safety Commission (2017). Canadian National Report for the Joint Convention on the Safety of Spent Fuel Management and on the Safety of Radioactive Waste Management. PWGSC catalogue number CC172-23/2014E-PDF. ISSN 2368-4828.

Carlson, L. (2004). Bentonite mineralogy. Part 1. Methods of investigation—a literature review & Part 2. Mineralogical research of selected bentonites. *Posiva Oy, Olkiluoto. Working Report*.

Casás, L. M., Pozo, M., Gómez, C. P., Pozo, E., Bessières, L. D., Plantier, F., & Legido, J. L. (2013). Thermal behaviour of mixtures of bentonitic clay and saline solutions. *Applied Clay Science*, *72*, 18-25.

Chamley, H. (2013). *Clay sedimentology*. Springer Science & Business Media.

Chen, F.H. (1988). Foundations on Expansive Soils, Development in Geotechnical Engineering. Elsevier, New York.

Chen, Y. G., Jia, L. Y., Li, Q., Ye, W. M., Cui, Y. J., & Chen, B. (2017). Swelling deformation of compacted GMZ bentonite experiencing chemical cycles of sodium-calcium exchange and salinization-desalinization effect. *Applied Clay Science*, *141*, 55-63.

Chen, W. C., & Huang, W. H. (2013). Effect of groundwater chemistry on the swelling behaviour of a Ca-bentonite for deep geological repository. *Physics and Chemistry of the Earth, Parts A/B/C*, *65*, 42-49.

Cho, W. J., Kim, J. S., & Choi, J. W. (2011). Influence of water salinity on the hydraulic conductivity of compacted bentonite. *Journal of Nuclear Fuel Cycle and Waste Technology (JNFCWT)*, *9*(4), 199-206.

Cho, W.J., & Lee, J. O. (1999). Basic physicochemical and mechanical properties of domestic bentonite for use as a buffer material in a high-level radioactive waste repository. *Nuclear Engineering and Technology*, *31*(6), 39-50.

Cho, W. J., Lee, J. O., & Kwon, S. (2009). Simulation of heat and water counterflow in unsaturated compacted bentonite. *Environmental engineering science*, *26*(3), 589-599.

Cuadros, J. and Linares, J. (1996). Experimental kinetic study of the smectite-to-illite transformation. Geochimica et Cosmochimica Acta 60, 439–453.

Cui, S. L., Zhang, H. Y., & Zhang, M. (2012). Swelling characteristics of compacted GMZ bentonite–sand mixtures as a buffer/backfill material in China. *Engineering Geology*, *141*, 65-73.

Cui, Y. J., Yahia-Aissa, M., & Delage, P. (2002). A model for the volume change behaviour of heavily compacted swelling clays. *Engineering geology*, *64*(2-3), 233-250.

De La Fuente, S., Cuadros, J., & Linares, J. (2002). Early stages of volcanic tuff alteration in hydrothermal experiments: Formation of mixed-layer illite-smectite. Clays and Clay Minerals, 50(5), 578-590.

Delage, P. (2007). Microstructure features in the behaviour of engineered barriers for nuclear waste disposal. In *Experimental unsaturated soil mechanics* (pp. 11-32). Springer, Berlin, Heidelberg.

Dollar, P.S. (1988). Geochemistry of Formation Waters, Southwestern Ontario, Canada and Southern Michigan, U.S.A.: Implications for Origin and Evolution. M.Sc. Thesis. University of Waterloo, Canada.

Drief, A., Nieto, F., and Sanchez-Navas, A. (2001). Experimental clay-mineral formation from a subvolcanic rock by interaction with 1 m naoh solution at room temperature. *Clays and Clay Minerals* 49(1), 92–106.

Eberl, D. D., Velde, B., & McCormick, T. (1993). Synthesis of illite-smectite from smectite at earth surface temperatures and high pH. *Clay Minerals*, *28*(1), 49-60.

ENRESA (2006). FEBEX Project. Final Report. Post-mortem bentonite analysis Enresa publicación técnica 05-1/2006, Spain.

European Commission (2011). Third commission report on financing decommissioning. http://ec.europa.eu/energy/sites/ener/files/documents/seventh_situation_report_corr_version_without_cover_page.pdf.

Fall, M., Nasir, O., & Nguyen, T. S. (2014). A coupled hydro-mechanical model for simulation of gas migration in host sedimentary rocks for nuclear waste repositories. *Engineering Geology*, *176*, 24-44.

García-Gutiérrez, M., Cormenzana, J. L., Missana, T., Alonso, U., & Mingarro, M. (2011). Diffusion of strongly sorbing cations (60Co and 152Eu) in compacted FEBEX bentonite. *Physics and Chemistry of the Earth, Parts A/B/C*, *36*(17-18), 1708-1713.

Garrels, R. M. (1984). Montmorillonite/illite stability diagrams. *Clays and Clay minerals*, *32*(3), 161-166.

Garitte, B., Gens, A., Vaunat, J., & Armand, G. (2014). Thermal conductivity of argillaceous rocks: determination methodology using in situ heating tests. *Rock mechanics and rock engineering*, *47*(1), 111-129.

Gascoyne, M., Davison, C. C., Ross, J. D., and Pearson, R. (1987) Saline groundwaters and brines in plutons in the Canadian Shield. In: Saline Water and Gases in Crystalline Rocks, 53–68. Fritz, P. and Frape, S. K. (editors), Geological Association of Canada Special Paper, 33. The Runge Press Limited: Ottawa.

Gates, W. P., Bouazza, A., & Churchman, G. J. (2009). Bentonite clay keeps pollutants at bay. Elements 5 (2), 105–110.

Gens, A., & Alonso, E. E. (1992). A framework for the behaviour of unsaturated expansive clays. *Canadian Geotechnical Journal*, *29*(6), 1013-1032.

Golder Associates Ltd. (1993). Used-fuel disposal vault far-field thermal and thermal-mechanical analysis. Atomic Energy of Canada Limited Report, TR-M-015.

Grim, R. (1968). Clay Mineralogy, 2nd edition. McGraw-Hill, New York.

Grim, R. and Güven, N. (1978). Bentonite: Geology, Clay Mineralogy Properties and Users. Vol. 24, Developments in Sedimentology. Elsevier, Amsterdam, 256.

Guillaume, D., Neaman, A., Cathelineau, M., Mosser-Ruck, R., Peiffert, C., Abdelmoula, M., Dubessy, J., Villi E.F., Baronnet, A., and Michau, N. (2003). Experimental synthesis of chlorite from smectite at 300ºC in the presence of metallic Fe. *Clay Minerals* 38, 281–302.

Guo, R. (2007). Numerical modelling of a deep geological repository using the in-floor borehole placement method. Nuclear Waste Management Organization, TR-2007-14.

Guo, R. (2008). Sensitivity analyses to investigate the influence of the container spacing and tunnel spacing on the thermal response in a deep geological repository. Nuclear Waste Management Organization, TR-2008-24.

Guo, G., & Fall, M. (2018). Modelling of dilatancy-controlled gas flow in saturated bentonite with double porosity and double effective stress concepts. *Engineering Geology*, *243*, 253-271.

Guo, G., & Fall, M. (2021a). Advances in modelling of hydro-mechanical processes in gas migration within saturated bentonite: A state-of-art review. *Engineering Geology*, *287*, 106-123.

Guo, G., & Fall, M. (2021b). A Thermodynamically Consistent Phase Field Model for Gas Transport in Saturated Bentonite Accounting for Initial Stress State. *Transport in Porous Media*, *137*(1), 157-194.

Herbert, H. J., Kasbohm, J., Moog, H. C., & Henning, K. H. (2004). Long-term behaviour of the Wyoming bentonite MX-80 in high saline solutions. *Applied Clay Science*, *26*(1-4), 275-291.

Hicks, T. W., White, M. J., & Hooker, P. J. (2009). Role of bentonite in determination of thermal limits on geological disposal facility design. *Galson Sciences Limited: Oakham, UK*.

Honty, M., Uhlík, P., Sucha, V., Caplovicová, M., Franců, J., & Biron, A. (2004). Smectite-to-illite alteration in salt-bearing bentonites (the East Slovak Basin). *Clays and clay Minerals*, *52*(5), 533-551.

Huang, W. L., Longo, J. M., & Pevear, D. R. (1993). An experimentally derived kinetic model for smectite-to-illite conversion and its use as a geothermometer. *Clays and Clay Minerals*, *41*(2), 162-177.

International Atomic Energy Agency (1981). Underground disposal of radioactive waste: Basic Guidance, Safety Series No. 54, IAEA, Vienna.

International Atomic Energy Agency (2003). Scientific and technical basis for the geological disposal of radioactive wastes. Technical Report Series, No. 413, Vienna, Austria.

International Atomic Energy Agency (2009). Geological disposal of radioactive waste: Technological implications for retrievability. Nuclear Energy Series No. NW-T-1.19, Vienna, Austria.

International Atomic Energy Agency (2017). Energy, electricity and nuclear power estimates for the period up to 2050. Reference Data Series No. 1, Vienna, Austria.

Integration Group for the Safety Case (2012). Engineered Barriers and Geological Disposal.

Itälä, A., & Olin, M. (2011). Chemical evolution of bentonite buffer in a final repository of spent nuclear fuel during the thermal phase. *Nuclear technology*, *174*(3), 342-352.

Ito, H. (2006). Compaction properties of granular bentonites. *Applied Clay Science*, *31*(1-2), 47-55.

Japan Nuclear Cycle Development Institute (1999). H12: Project to establish the scientific and technical basis for HLW disposal in Japan. Supporting Report 2 (Respiratory Design and Engineering Technology). Japan Nuclear Cycle Development Institute, Tokyo.

Jensen, M., Lam, T., Luhowy, D., McLay, J., Semec, B., & Frizzell, R. (2009). Ontario power generation's proposed L&ILW deep geologic repository: an overview of geoscientific studies. *Nuclear Waste Management Organization, GeoHalifax2009/GéoHalifax2009*.

Johannesson, L. E., & Nilsson, U. (2006). *Deep Repository-Engineered Barrier Systems: Geotechnical Behaviour of Candidate Backfill Materials: Laboratory Tests and Calculations for Determining Performance of the Backfill*. SKB.

Karnland, O. and Birgersson, M. (2006). Montmorillonite stability with special respect to KBS-3 conditions. SKB TR-06-11, Svensk Kärnbränslehantering AB.

Karnland, O., Olsson, S., Nilsson, U., & Sellin, P. (2007). Experimentally determined swelling pressures and geochemical interactions of compacted Wyoming bentonite with highly alkaline solutions. *Physics and Chemistry of the Earth, Parts A/B/C*, *32*(1-7), 275-286.

Karnland, O., Pusch, R., & Sandén, T. (1992). The importance of electrolyte on the physical properties of MX-80 bentonite. *Swedish Nuclear Fuel and Waste Management Company (SKB International AB), Stockholm, Sweden. Report AR*, 92-35.

Kacandes, G. H., Barnes, H. L., & Kump, L. R. (1991). The Smectite to Illite Reaction: Fluid &Solids Evolution Under Flow-Through Conditions. In *Clay Minerals Society 28th Annual Meeting* (Vol. 773, p. 85).

Kassiff, G. and Ben Shalom, A. (1971). Experimental relationship between swell pressure and suction. *Géotechnique* 21(3), 245–255.

Komine, H. (2004a). Simplified evaluation for swelling characteristics of bentonites. *Engineering Geology* 71, 265–279.

Komine, H. (2004b). Simplified evaluation on hydraulic conductivities of sand-bentonite mixture backfill. *Applied Clay Science* 26, 13–19.

Komine, H. and Ogata, N. (1994). Experimental study on swelling characteristics of compacted bentonite. Canadian Geotechnical Journal 31(4), 478–490.

Kunimine Industries Co., Ltd. https://www.kunimine.co.jp/english/bent/basic.html

Laine, H., and Karttunen, P. (2010). Long-term stability of bentonite - a literature review. Posiva Working Report 2010-53, Posiva Oy, Olkiluoto, Finland.

Lavallée, Y., & Kendrick, J. E. (2021). A review of the physical and mechanical properties of volcanic rocks and magmas in the brittle and ductile regimes. *Forecasting and planning for volcanic hazards, risks, and disasters*, 153-238.

Liang, W. G., Xu, S. G., & Zhao, Y. S. (2006). Experimental study of temperature effects on physical and mechanical characteristics of salt rock. *Rock mechanics and rock engineering*, *39*(5), 469-482.

Linares, J., Huertas, F., and Barahona, E. (1992). Conversion time from smectite to illite: A preliminary study. *Applied Clay Science* 7, 125–130.

Liu, L.-N., Chen, Y.-G., Ye, W.-M., Cui, Y.-Ju., Wu, D.-B. (2018). Effects of hyperalkaline solutions on the swelling pressure of compacted Gaomiaozi (GMZ) bentonite from the viewpoint of Na+ cations and OH– anions. *Applied Clay Science* 161, 334-342,

Liu, L., Neretnieks, I., and Moreno, L. (2011). Permeability and expansibility of natural bentonite MX-80 in distilled water. *Physics and Chemistry of the Earth* 36, 1783–1791.

Macey, H.H. (1942). Clay-water relationship and the internal mechanisms of drying. *Transactions of the Indian Ceramic Society* 41, 73–141.

Madsen, F.T., and Müller-Vonmoos, M. (1989). The swelling behaviour of clay. Applied Clay Science 4, 143–156.

Martın, M., Cuevas, J., & Leguey, S. (2000). Diffusion of soluble salts under a temperature gradient after the hydration of compacted bentonite. *Applied clay science*, *17*(1-2), 55-70.

Mata Mena, C. (2003). *Hydraulic behaviour of bentonite based mixtures in engineered barriers: The Backfill and Plug Test at the Äspö HRL (Sweden)*. Universitat Politècnica de Catalunya.

Mathers, W.G. (1985). HOTROK, a program for calculating the transient temperature field from an underground nuclear waste disposal vault. Atomic Energy of Canada Limited Technical Report, TR-366.

Melamed, A. and Pitkanen, P. (1996). Chemical and mineralogical aspects of water-bentonite interaction in nuclear fuel disposal conditions, VTT Communities and Infrastructure. Technical Research Centre of Finland, Espoo

Mesri G. and Olson R.E. (1970). Mechanisms controlling the permeability of clays. *Clays and Clay Minerals* 19(3), 151–158.

Meunier, A. (2005). *Clays*. Springer-Verlag, Berlin and Heidenberg.

Michaels A. S., & Lin C.S. (1954). The permeability of kaolinite. *Industrial and Engineering Chemistry* 46, 1239–1246.

Miller, W., Alexander, R., Chapman, N., McKinley, J. C., & Smellie, J. A. T. (Eds.). (2000). *Geological disposal of radioactive wastes and natural analogues* (Vol. 2). Elsevier.

Ministry of Energy (2017). Long-Term Energy Plan. https://www.ontario.ca/document/2017-long-term-energy-plan.

Ministry of Natural Resources Canada (2017). Nuclear in Canada. https://www.nrcan.gc.ca/our-natural-resources/minerals-mining/minerals-metals-facts/uranium-and-nuclear-power-facts/20070.

Ministry of Natural Resources Canada, 2018. Electricity facts. https://www.nrcan.gc.ca/sites/www.nrcan.gc.ca/files/energy/pdf/energy-factbook-oct2-2018%20(1).pdf.

Mitchell, J. K. (1993). *Fundamentals of Soil Behaviour*, 2nd edition. Wiley, New York.

Mosser-Ruck, R., Cathelineau, M., Guillaume, D., Charpentier, D., Rousset, D., Barres, O., & Michau, N. (2010). Effects of temperature, pH, and iron/clay and liquid/clay ratios on experimental conversion of dioctahedral smectite to berthierine, chlorite, vermiculite, or saponite. *Clays and Clay Minerals*, *58*(2), 280-291.

Murata, S., & Saito, T. (Eds.). (2003). *Environmental Rock Engineering: Proceedings of the First Kyoto International Symposium on Underground Environment, Kyoto, Japan, 17-18 March 2003*. CRC Press.

Nasir, O., Fall, M., Evgin, E. (2014). A Simulator for Modeling of Porosity and Permeability Changes in Near Field Sedimentary Host Rocks under Climate Changes Influences. *Tunnelling and Underground Space Technology*, 42, 122-135.

Nasir, O., Fall, M., Nguyen, S., Evgin, E. (2013). Modeling of the thermo-hydro-mechanical-chemical response of sedimentary rocks of Ontario to past glaciations. *International Journal of Rock Mechanics and Mining Sciences*, 64, 160-174.

Nasir, O., Fall, M., Nguyen, S., Evgin, E. (2011). Modeling of the hydro-mechanical response of sedimentary rocks of Southern Ontario to past glaciations. *Engineering Geology,* 123(4), 271-287.

Nuclear Waste Management Organization (2005). Choosing a way forward: The future management of Canada's used nuclear fuel. Final study. Nuclear Waste Management Organization Report APM-REF-00680-23833.

Nuclear Waste Management Organization (2010). Moving Forward Together: Process for Selecting a Site for Canada's Deep Geological Repository for Used Nuclear Fuel. Nuclear Waste Management Organization. Toronto, Canada.

Nuclear Waste Management Organization (2011). Regional hydrogeochemistry – Southern Ontario. NWMO DGR-TR-2011-12.

Nuclear Waste Management Organization (2012). Newsletter, Nuclear Waste Management Organization 10, 1–4. http://www.nwmo.ca/dgrprojectschedule.

Nuclear Waste Management Organization (2015). Newsletter, Nuclear Waste Management Organization 13 (2 and 4).

Nuclear Waste Management Organization (2016). Thermal response of a mark II conceptual deep geological repository in crystalline rock. NWMO-TR-2016-03.

Osacký, M., Šucha, V., Czímerová, A., and Madejová, J. (2010). Reaction of smectites with iron in a nitrogen atmosphere at 75 °C. *Applied Clay Science* 50, 237–244.

Pastina, B. and Hellä, P. (2006). Expected evolution of a spent nuclear fuel repository at Olkiluoto. Posiva report 2006-05, Posiva Oy, Olkiluoto, Finland.

Pierre, D. (2006). Some microstructure effects on the behaviour of compacted swelling clays used for engineered barriers. *Chinese Journal of Rock Mechanics and Engineering, Science Press* 25(4): 721–732.

Posiva (2009). TKS-2009 Olkiluodon ja Loviisan voimalaitosten ydinjätehuolto: Selvitys suunnitelluista toimenpiteistä ja niiden valmistelusta vuosina 2010-2012. Posiva Oy muu julkaisu.

Pusch, R. (1998). Backfilling with mixtures of bentonite/ballast materials or natural smectitic clay. Swedish Nuclear Fuel and Waste Management Co (SKB), Stockholm. Technical Report TR-98-16, 52 p.

Pusch, R. (2001). The microstructure of MX-80 clay with respect to its bulk physical properties under different environmental conditions. SKB Technical Report, TR-01-08. Swedish Nuclear Fuel and Waste Management Company, Stockholm, Sweden.

Pucsh, R. (2008). Geological Storage of Highly Radioactive Waste: Current Concepts and Plans for Radioactive Waste Disposal. *Springer-Verlag Berlin Heidelberg*. doi:10.1007/978-3-540-77333-7

Rao, A.S., Phanikumar, B.R., and Sharma, R.D. (2004). Prediction of swelling characteristics of remoulded and compacted expansive soils using free swell index. *Quarterly Journal of Engineering Geology and Hydrogeology* 37, 217–226.

Rao, S. M., Thyagaraj, T., & Rao, P. R. (2013). Crystalline and osmotic swelling of an expansive clay inundated with sodium chloride solutions. *Geotechnical and Geological Engineering, 31*(4), 1399-1404.

Rautioaho, E. and Korkiala-Tanttu, L. (2009). Bentomap: Survey of bentonite and tunnel backfill knowledge. 1459-7683, VTT Technical Research Centre of Finland.

Rebak, R. B. (2011). Environmental Degradation of Engineered Barrier Materials in Nuclear Waste Repositories. *Chapter*, *36*, 503-516.

RWM (2003). Engineered Barrier Systems and the Safety of Deep Geological Repositories, Radioactive Waste Management, ISBN 92-64-18498-8

Salles, F., Douillard, J. M., Denoyel, R., Bildstein, O., Jullien, M., Beurroies, I., & Van Damme, H. (2009). Hydration sequence of swelling clays: Evolutions of specific surface area and hydration energy. *Journal of colloid and interface science*, *333*(2), 510-522.

Sandra, S.G. (2013). The Swelling Pressure of Bentonite and Sand Mixtures. Master's thesis in Chemical Engineering and Technology, at Royal Institute of Technology (KTH) in Stockholm, Sweden.

Sato, H. and Suzuki, S. (2003). Fundamental study on the effect of an orientation of clay particles on diffusion pathway in compacted bentonites. *Applied Clay Science,* 23, 51–60.

Savage, D. (2005). The effects of high salinity groundwater on the performance of clay barriers. SKI Report 2005-54, Swedish Nuclear Power Inspectorate, Stockholm, Sweden.

Savage, D., Watson, C., Benbow, S., and Wilson, J. (2010). Modelling iron-bentonite interactions. *Applied Clay Science,* 47, 91–98.

Schomburg, J. (1997). Data and literature collection "Friedland clay". Int. Rep. DURTEC Co., Neubrandenburg, Germany

Siddiqua, S., Siemens G., Blatz, J., Man, A., and Lim B.F. (2014). Influence of pore fluid chemistry on the mechanical properties of day-based materials. *Geotechnical Geology Engineering,* 32, 1029–1042.

Siddiqua, S., Tabiatnejad, B., & Siemens, G. (2018). Impact of pore fluid chemistry on the thermal conductivity of bentonite–sand mixture. *Environmental earth sciences*, *77*(1), 1-11.

Smart, N. R., Blackwood, D. J., & Werme, L. (2002). Anaerobic corrosion of carbon steel and cast iron in artificial groundwaters: part 1—electrochemical aspects. *Corrosion*, *58*(7), 547-559.

Stçepkowska, E. T. (1990). Aspects of the clay/electrolyte/water system with special reference to the geotechnical properties of clays. *engineering geology*, *28*(3-4), 249-267.

Stewart, D. I., Studds, P. G., & Cousens, T. W. (2003). The factors controlling the engineering properties of bentonite-enhanced sand. *Applied Clay Science*, *23*(1-4), 97-110.

Svensson, D., Dueck, A., Nilsson, U., Olsson, S., Sanden, T., Lydmark, S., ... & Hansen, S. (2011). Alternative buffer material. Status of the ongoing laboratory investigation of reference materials and test package 1.

Swedish Nuclear Fuel and Waste Management Company (1992). SKB91 final disposal of spent nuclear fuel. Importance of the bedrock for safety. SKB Technical Report SKB TR 92–20, Swedish Nuclear Fuel and Waste Management Co. (SKB), Stockholm

Tang, A. M., & Cui, Y. J. (2006). Determining the thermal conductivity of compacted MX80 clay. In *Unsaturated Soils 2006* (pp. 1695-1706).

Terzaghi C. (1925). Determination of the permeability of clay, Engineering News Record 95, 832–836.

Tripathy, S., Sridharan, A., and Schanz, T. (2004). Swelling pressures of compacted bentonites from diffuse double layer theory. *Canadian Geotechnical Journal* 41, 437–450.

Tsui, K.K. and Tsai, A. (1985). Thermal analyses for different options of nuclear fuel waste placement. Atomic Energy of Canada Limited Report, AECL-7823.

Ureana, C., Azañón, J.M., Corpas, F., Nieto, F., León, C., and Pérez, L. (2013). Magnesium hydroxide, seawater and olive mill wastewater to reduce swelling potential and plasticity of bentonite soil. *Construction and Building Materials*, 45, 289–297.

Villar,M., Garcia-Sineriz, J., Barcena, I., and Lloret, A. (2005). State of the bentonite barrier after five years operation of an in situ test simulating a high level radioactive waste repository. *Engineering Geology,* 81, 317–328.

Villar, M.V., Gómez-Espina, R., Campos, R., Barrios, I., and Gutiérrez-Nebot, L. (2012). Porosity changes due to hydration of compacted bentonite. In: Mancuso, C., Jommi, C., and D'Onza, F. (Eds.), Unsaturated Soils: Research and Applications, volume 1. Springer, Berlin, pp. 137–144.

Villar, M.V. & Lloret, A. (2004). Influence of temperature on the hydro-mechanical behaviour of a compacted bentonite. *Applied Clay Science*, 26, 337–350.

Villar, M.V. & Lloret, A. (2007). Dismantling of the first section of the FEBEX in situ test: THM laboratory tests on the bentonite blocks retrieved. *Physics and Chemistry of the Earth,* 32, 716–729.

Villar, M.V. and Lloret, A. (2008). Influence of dry density and water content on the swelling of a compacted bentonite. *Applied Clay Science*, 39, 38–49.

Villar, M.V.; Lloret, A. & Romero, E. (2003). Thermo-mechanical and geochemical effects on the permeability of high-density clays. Proc. Int. Workshop Large scale field tests in granite. Advances in understanding and research needs. Universitat Politècnica de Catalunya-ENRESA. Sitges, November 12-14th 2003.

Wang, Q., Tang, A., Cui, Y., Delage, P., & Gatmiri, B. (2012). Experimental study on the swelling behaviour of bentonite/claystone mixture. *Engineering Geology*, 124, 59–66.

Wersin, P. (2002). Geochemical modelling of bentonite porewater in high-level waste repositories. *Journal of Contaminant Hydrology,* 61, 405–422.

Wersin, P., Curti, E., & Appelo, C.A.J. (2004). Modelling bentonite–water interactions at high solid/liquid ratios: Swelling and diffuse double layer effects. *Applied Clay Science,* 26(1–4): 249–257.

Wersin, P., Birgersson, M., Olsson, S., Karnland, O., & Snellman, M. (2008). Impact of corrosion-derived iron on the bentonite buffer within the KBS-3H disposal concept. *The Olkiluoto site as case study*.

Wersin, P., Johnson, L.H., and McKinley, I.G. (2007). Performance of the bentonite barrier at temperatures beyond 100ºC: A critical review. *Physics and Chemistry of the Earth,* 32, 780–788.

Wilson, J., Savage, D., Bond, A., Watson, S., Pusch, R., Bennett, D. (2011). Bentonite: a review of key properties, processes and issues for consideration in the UK context. Quintessa Report QRS-1378ZG-1.1., Henley-on-Thames: Quintessa.

Yang, J., Fall, M. (2021). Coupled hydro-mechanical modelling of dilatancy controlled gas flow and gas induced fracturing in saturated claystone. *International Journal of Rock Mechanics and Mining Sciences,* 138, 104584.

Yang, J., Fall, M, Guo, G. (2020). A Three-Dimensional Hydro-mechanical Model for Simulation of Dilatancy Controlled Gas Flow in Anisotropic Claystone. *Rock Mechanics and Rocks Engineering,* 53, 4091–4116.

Yong, R.N. (1999). Overview of modeling of clay microstructure and interactions for prediction of waste isolation barrier performance. *Engineering Geology* 54, 83–91.

Zhang, M. (2016). "The effect of clay minerals on copper and gold flotation." PhD Thesis, The University of Queensland.

Chapter 3: Technical paper I: Swelling ability and behaviour of bentonite-based materials for deep repository engineered barrier systems: Influence of physical, chemical and thermal factors

Journal of Rock Mechanics and Geotechnical Engineering 2022, 14(3):689-702

Mohammed Alzamel, Mamadou Fall, Sada Haruna

Abstract

Compacted bentonite-sand (B/S) mixtures have been used as a barrier material in engineered barrier systems (EBSs) of deep geological repositories (DGR) to store nuclear wastes. This study investigates the individual and combined effect of different chemical compositions of deep groundwater (chemical factor) at potential repository sites in Canada (the Trenton and Guelph regions in Ontario), heat generated in DGRs (thermal factor), dry densities and mass ratios of bentonite and sand mixtures (physical factors) on the swelling behaviour and ability of bentonite-based materials. In this study, swelling tests are conducted on B/S mixture with different B/S mix ratios (20/80 to 70/30), compacted at different dry densities (1.6 to 2.0 g/cm^3), saturated with different types of water (distilled water and simulated deep groundwaters of Trenton and Guelph) and exposed to different temperatures (20°C to 80°C). Moreover, scanning electron microscopy analyses, mercury intrusion porosimetry tests and x-ray diffractometry analyses are carried out to evaluate the morphological, microstructural and mineralogical characteristics of the B/S mixture. The test results indicate that the swelling potential of the B/S mixture is significantly affected by these physical and chemical factors as well as the combined effects of the chemical and thermal factors. A significant decrease in the swelling capacity is observed when the B/S material is exposed to the aforementioned groundwaters. A large decrease in the swelling capacity is observed for higher bentonite content in the mixture. Moreover, higher temperatures intensify the chemically-induced reduction of the swelling capacity of the B/S barrier materials. This decrease in the swelling capacity is caused by the chemical and/or microstructural changes of the materials. The results from this research will help engineers to design and build EBSs for DGRs with similar groundwater and thermal conditions.

Keywords: Deep Geological Repository; Engineered Barrier; Bentonite-Sand Material; Nuclear Waste; Swelling capacity; Swelling strain

3.1 Introduction

Continuous growth in the world's population and economy, combined with rapid urbanisation, has led to an increase in global energy consumption and demand. Many countries not only face the challenge of meeting energy demands but also have to reduce the release of greenhouse gases into the atmosphere to restrict their contribution to global warming, which is also known as climate change. Preserving the global environment is important since Earth is the only home that humans currently have.

Nuclear energy is a low-carbon energy resource which provides about 10% of the electricity needs worldwide with one of the lowest carbon dioxide emissions per unit of energy produced based on the total life-cycle of energy production (International Energy Agency, 2019). However, generating electricity using nuclear power produces a large amount of hazardous nuclear waste. Other applications of nuclear technology, such as those in the medical, industrial, and agricultural industries, also produce radioactive waste. Since nuclear wastes pose serious threat to human health and the environment for thousands of years, it is important to find suitable methods and techniques to safely dispose the waste. Currently, deep geological repositories (DGRs) are proposed to store radioactive waste by isolating the waste from the surrounding environment (European Commission, 2011; Nuclear Waste Management Organization, 2011; Yang et al., 2020).

Several countries, including Canada, believe that DGRs are the most appropriate solution for radioactive waste management in terms of safety, economics, environmental impact, and practicality (Fall et al., 2014; Nasir et al., 2015). DGRs preserve the environment and human health by disposing radioactive waste at a depth of 300 to 1000 m. The waste is stored in canisters placed in a multi-barrier system that consists of natural rock and engineered barrier systems (EBSs; e.g., waste containers, buffers, and sealing elements) (Nasir et al., 2013, 2014; Yang and Fall, 2021). There are many factors to be considered in the design, construction

and operation of DGRs, such as the location of the repository, properties of the host rock, design and construction of the EBS, and materials used for the waste containers (Organisation for Economic Co-operation and Development and European Commission, 2003; Wilson et al., 2011; Crowe et al., 2017; Guo and Fall, 2020).

In Canada, DGRs that are based on a multi-barrier system have been studied for many years. EBSs are considered to be one of the most important components of the multi-barrier system. Bentonite-based buffer and sealing materials are critical components of the EBSs of many DGRs designs for different types of host rock where it provides numerous important functions in a DGR system (Guo and Fall, 2018, 2019, 2021). For instance, the barrier material must be able to (i) contain and isolate the radionuclides, (ii) provide mechanical support to the containers, (iii) provide a thermal conductive medium to transfer heat from the waste to the surrounding natural (rock) barrier, and (iv) seal the access shaft to the repository to ensure that it will not serve as a rapid pathway for migration of radioactive gas or groundwater to the biosphere after the closure of a repository. Moreover, the buffer material should contribute to reducing the risk of microbiologically influenced corrosion of the used fuel containers (Zhang et al., 2019). A mixture of compacted bentonite and sand has been proposed as a potential buffer and sealing material for the EBS in Canadian DGRs as well as in other countries (Guo and Fall, 2018). Figure 3.1 shows an example of the Canadian DGR design concept for the management of nuclear waste.

Bentonite is a clay that consists of mostly clay minerals from the smectite group (i.e., montmorillonite). It is considered as a suitable buffer and sealing barrier material due its high swelling capacity, high water absorption, low hydraulic conductivity, self-sealing characteristic, and good ability to contain radionuclides if canisters fail (Cho et al., 1999; Karnland and Birgersson, 2006; Ye et al., 2010; Wilson et al., 2011; Rawat et al., 2019). However, compacted pure bentonite has relatively low mechanical strength. This is one of the

key reasons why a bentonite–sand (B/S) mixture is a preferred material than pure bentonite to seal the access shafts. Moreover, in addition to have better control on the swelling pressure, the B/S mixture costs less than pure bentonite, and is easier to compact with higher thermal conductivity which facilitates the transfer of heat from the nuclear wastes to the surrounding rock as opposed to pure bentonite (Villar and Lloret, 2008; Sun et al., 2009; Komine et al., 2009; Kim et al., 2011; Wang et al., 2012; Cui, 2019).

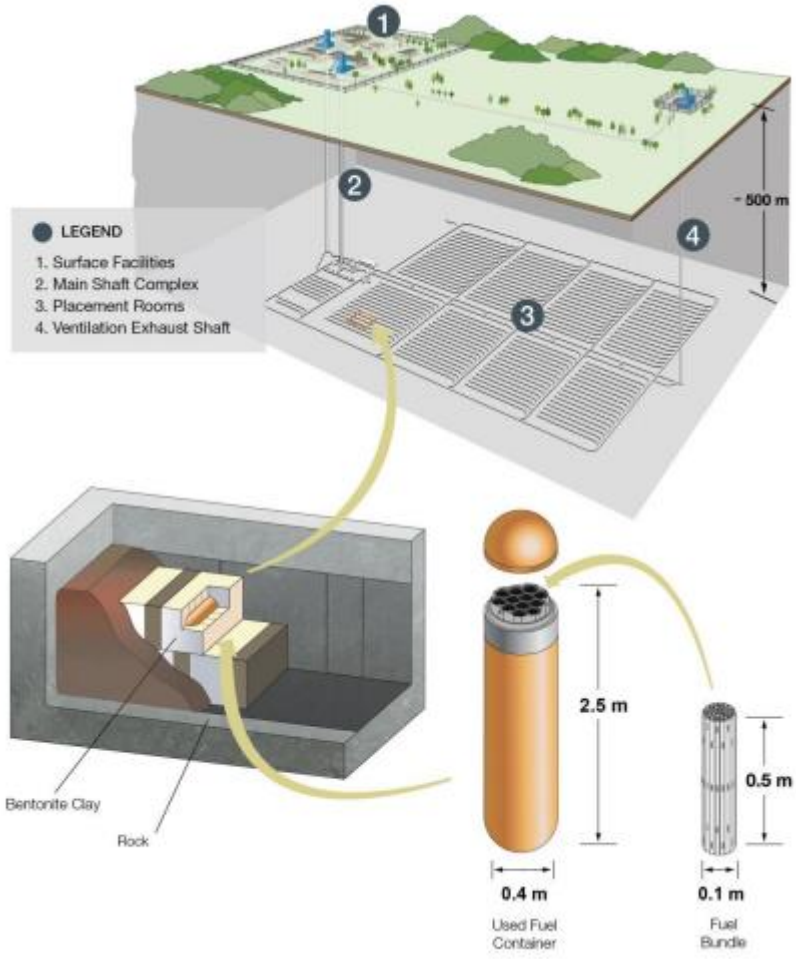

Figure 3.1. Conceptual design of a deep geological repository in Canada for the long-term disposal of used or spent nuclear fuel (Crowe et al., 2017)

The Canadian Nuclear Waste Management Organization (NWMO) has been considering and assessing several locations in Ontario (Canada) as potential DGR sites based

on safety and a number of other criteria (Crowe et al., 2010; Nuclear Waste Management Organization, 2011, 2017). For instance, the NWMO has been assessing whether to build a DGR at a depth of 680 m in the Municipality of Kincardine, Ontario. However, the chemical composition of the deep underground water in the Kincardine area, like many locations in Ontario, is significantly different from that of fresh water (Jensen et al., 2009; Hobbs et al., 2012). This means that, during the lifetime of the DRG, the B/S barrier material will react with different chemical components in the groundwater. Therefore, to ensure that the EBS will perform well in all groundwater conditions, it is important to understand whether and how significantly the swelling potential of the B/S barrier medium is affected by groundwater composition.

Numerous studies have shown that increases in the salinity of the groundwater can considerably decrease the expansion capacity of bentonite which may jeopardize its use as a barrier material (Suzuki et al., 2005; Villar 2006; Karnland et al., 2007; Castellanos et al., 2008; Zhang et al., 2012; Chen et al., 2015, 2017; Sun et al., 2015; Zheng et al., 2015, 2017; Navarro et al., 2017; Liu et al., 2018; He et al., 2019; Akinwunmi et al., 2020; Shehata et al., 2020; Xu et al., 2021). For example, Chen et al. (2017) investigated the swelling behaviour of Gaomiaozi (GMZ) bentonite under different cycles of cation exchange and salinization and desalinization. The experimental results show that the salinity of the water has an influence on the swelling properties of compacted bentonite since the sodium (Na)-bentonite is partly transformed into calcium (Ca)-bentonite once the sodium chloride (NaCl) solution is replaced with a calcium dichloride (CaCl2) solution. These findings are in agreement with Chen et al. (2015) who concluded that the salinization process results in a reduction in the swelling potential of compacted GMZ bentonite. Moreover, Navarro et al. (2017) observed that there is an increase in the rate of swelling of compacted bentonite with a corresponding decrease in the swelling strain as the salinity of the solution is increased. In addition, Liu et al. (2018) investigated the

effects of hyperalkaline solutions on the swelling pressure of compacted GMZ bentonite by examining the sodium ion (Na+) cations and hydroxide (OH–) anions in the solution. The results indicate that high concentrations of Na+ cations can inhibit crystalline swelling and double-layer swelling, and high concentration of OH– anions makes it easier for double-layer swelling and changes in the fabric structure or arrangement of soil. Also, Akinwunmi et al. (2020) observed a decrease in the swelling pressure of Na- and Ca-montmorillonites as the salinity of the solution is increased. He et al. (2019) observed in their experimental studies that the infiltration of potassium ion (K+) salt/alkaline solutions considerably reduces the swelling pressure of compacted GMZ bentonite. However, these findings cannot be directly applied in a bentonite–based material, such as a B/S mixture, which is used in Canadian repositories since the properties of the groundwaters are different from the chemical compositions used in previous studies. Moreover, most of these studies are focussed on pure bentonite. The effects of the chemical composition and salinity in the groundwater on the swelling characteristics of compacted B/S mixture with different B/S ratios and different dry densities have not been examined in detail. Therefore, our understanding on the swelling potential of compacted B/S materials with different mix ratios and dry densities with chemical compounds in the groundwaters in potential Ontario DGR sites is limited. There is a need to address this knowledge gap to ensure the safety of the DGR sites.

Furthermore, during the lifetime of a DGR for storing used or spent nuclear fuel or high-level waste (HLW), the barrier material will not only be exposed to a broad range of groundwater conditions with different chemical compounds, but also subjected to high temperatures due to heat generated by the nuclear waste (Ye et al., 2013, 2014). These high temperatures may intensify chemical reactions in the groundwater and induce chemical attacks on the bentonite-based barrier material. Therefore, to ensure that the EBS will perform properly in all groundwater and thermal conditions in the Canadian's DRGs, it is important to

understand the effects of temperature and chemical reactions on the swelling properties of B/S material. However, there is a paucity of information on the coupled effects of groundwater chemistry and temperature on the swelling capacity and mechanical behaviour of compacted B/S material with different mix ratios and dry densities. Therefore, there is a need to address this issue for the safe operation of DGRs.

The objective of this study is to investigate the individual and coupled effects of the physical characteristics of the B/S mixture (B/S ratios and densities), chemical properties of the groundwater and temperature on the swelling behaviour of the B/S mixture used in the EBS of a DGR to store nuclear waste materials.

3.2 Materials and Testing Methods

3.2.1 Solid materials

The testing program examined different mix ratios of bentonite and sand (dry mass percentage of bentonite:sand 20:80, 30:70, 50:50, and 70:30) of commercial MX-80 Na-bentonite (from Wyoming, USA) and quartz sand (GS-20 silica sand) compacted to different dry densities (1.4, 1.6, 1.8, and 2.0 g/cm3). The MX-80 bentonite is a smectite clay that predominantly consists of Na-montmorillonite. Its chemical composition is listed in Table 3.1. X-ray diffraction (XRD) tests were performed with a Scintag XDS 2000 diffractometer (Scintag, Cupertino, CA) to characterize the mineralogical composition of the MX-80 bentonite powder. The XRD patterns (Figure 3.2) show that the MX-80 bentonite contains predominantly montmorillonite (92%) and a small amount of other minerals, including quartz, calcite, and feldspar. The main physical and chemical characteristics of the MX-80 bentonite are listed in Table 3.2. Sieve analysis and sedimentation tests (i.e., hydrometer tests) were carried out to determine the grain size distribution of the bentonite by following ASTM standard D422-63, see Figure 3.3. The analysis reveals that all the bentonite particles (fully dispersed material)

can pass through the No. 100 sieve (0.150 mm) and 98% pass through the No. 200 sieve (0.075 mm; Figure 3.3). The quartz sand contains 99.99% silica (SiO2) with a specific gravity of 2.65. Based on a sieve analysis following ASTM standard D6913-04, the particle sizes of the sand range from 0.2 to 1.9 mm.

Table 3.1. Chemical composition of MX-80 bentonite

Chemical Element	Composition	%
Silicon dioxide	SiO_2	63.59
Aluminium oxide	Al_2O_3	21.43
Iron oxide	Fe_2O_3	3.78
Calcium oxide	CaO	0.66
Magnesium oxide	MgO	2.03
Sodium oxide	Na_2O	2.70
Potassium oxide	K_2O	0.31
Bound water	H_2O	5.50

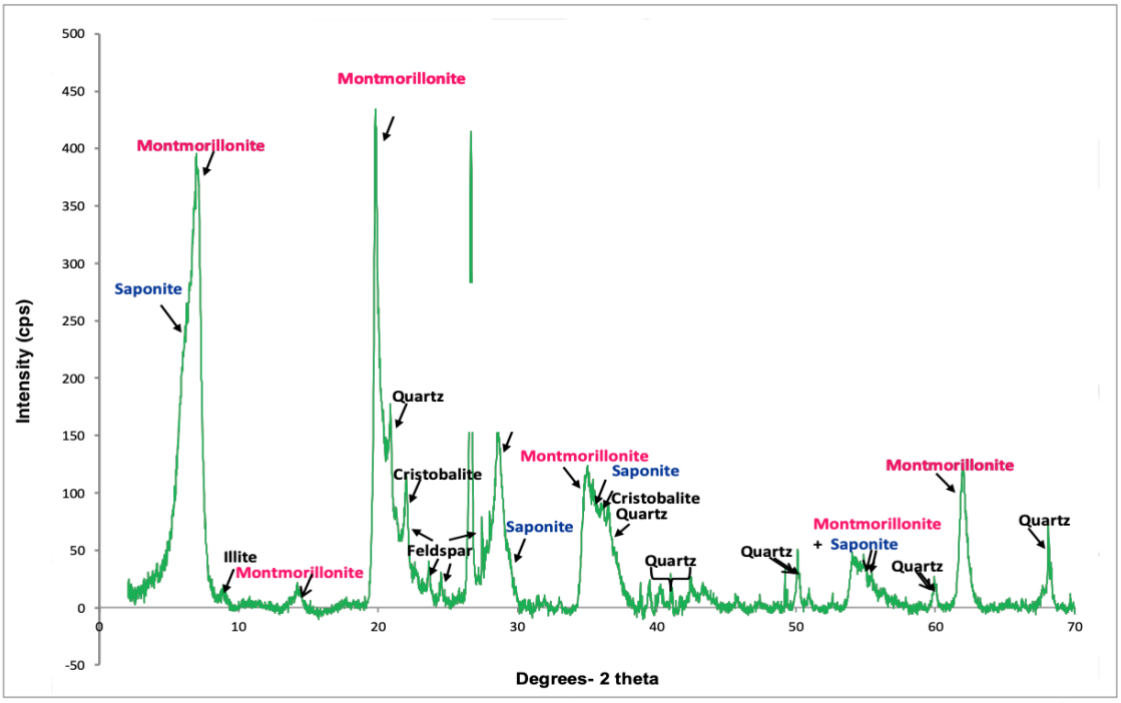

Figure 3.2. XRD pattern of the MX-80 bentonite

Table 3.2. Physical and chemical properties of MX-80 bentonite powder

Property	**Bentonite**
Average specific gravity, G	2.76
Material passing sieve number 200	>98%
Liquid limit, (%)	530
Total cation exchange capacity (meq/100 g)	105
Montmorillonite (%)	92
Plastic limit, (%)	48.5

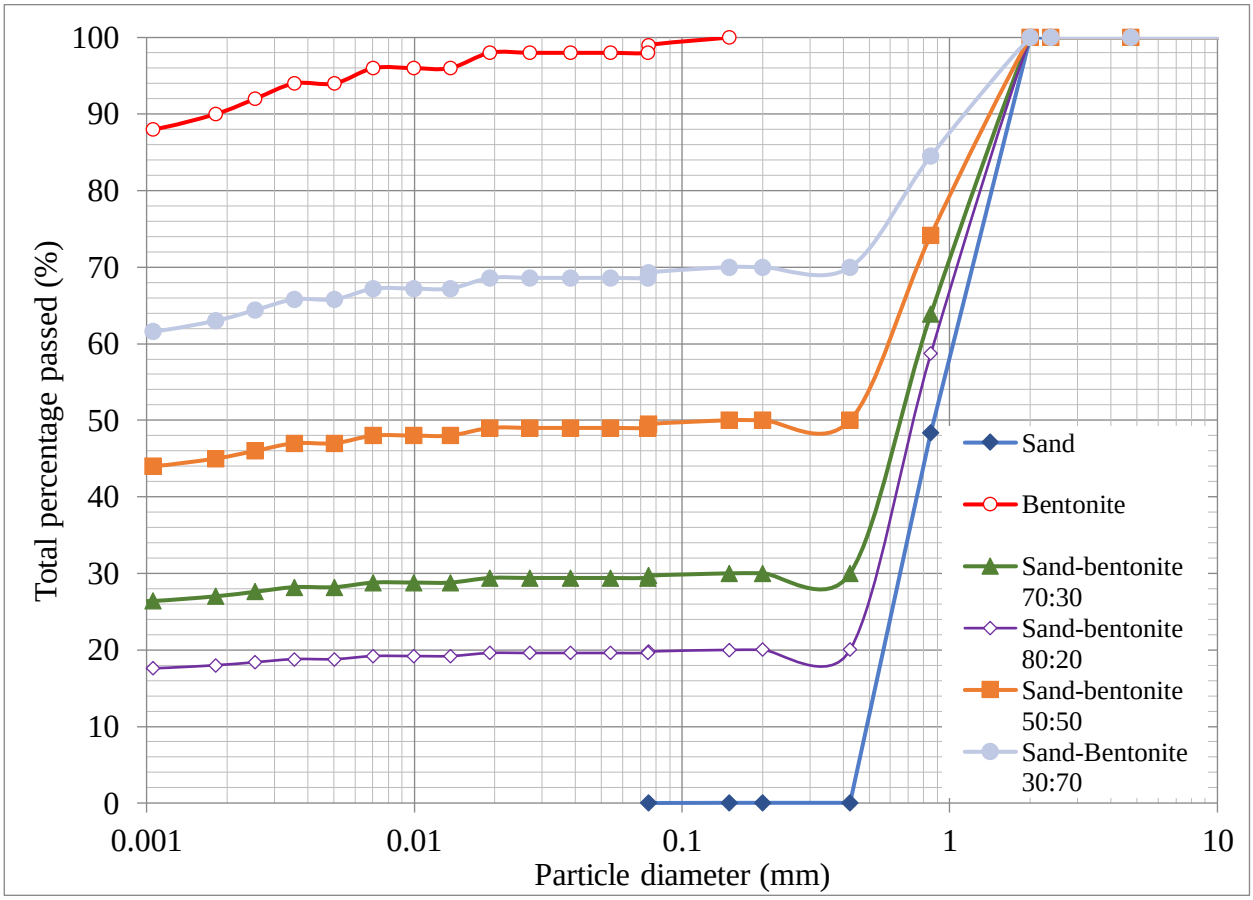

Figure 3.3. Grain size distribution curves of the MX-80 bentonite powder, quartz sand, and bentonite–sand mixtures with different bentonite:sand mix ratios (20:80, 30:70, 50:50, and 70:30)

3.2.1.1 Solutions

To investigate the effects of the water chemistry on the B/S mixtures, three different water solutions were used to simulate the chemistry of different groundwater conditions from potential DGR sites in Ontario, Canada. The control solution is the DW (DW), which simulates fresh groundwater close to the ground surface. The other two solutions were made to simulate the chemical compositions of the groundwater in the Trenton and Guelph regions. The main chemical characteristics (i.e., main cations and anions, pH, total dissolved solids (TDS)) of the synthetic groundwaters are listed in Table 3.3. Distilled water is labeled as DW, and groundwater from the Trenton and Guelph regions are referred to as the T and G solutions, respectively. $CaCl_2$, $NaCl_2$, and magnesium chloride ($MgCl_2$) were the main salts used to prepare the T and G solutions.

Table 3.3. Main chemical composition and properties of the synthetic groundwaters (g/l)

Element (g/l)	Distilled Water (DW)	Guelph Water (G)	Trenton Water (T)
Ca	0	57.0	23.0
Na	0	39.0	40.0
Mg	0	8.7	5.5
K	0	3.9	2.0
Cl	0	191.0	121.0
SO_4	0	0.2	0.6
TDS	0	300.0	192.0
pH	7	5.7	6.5

3.2.2 Specimen preparation and mix ratios

The MX-80 bentonite and sand were oven-dried separately at 105ºC for 24 h to eliminate any moisture accumulated during storage. Then, the required quantities of bentonite and sand were thoroughly mixed with a food mixer. Four uniform dried B/S mixtures were created with different mix ratios (bentonite:sand ratios of 20:80, 30:70, 50:50, and 70:30 percent by dry mass). The grain size distribution of each mixture is shown in Figure 3. Next, compaction tests were carried out on each B/S mixture to determine the compaction curves, optimum water contents, and maximum dry unit weights. Standard proctor compaction tests

were carried out with an automatic device in accordance with ASTM D698. The soil was placed in a mold with an inner diameter of 101.6 mm and a height of 116.4 mm. The soil was compacted in three layers with the use of a 2.5 kg (5.5 lb) hammer that falls from a height of 300 mm 25 times for each layer. The required quantities of bentonite and sand were blended dry to ensure homogeneity, as suggested by Gleason et al., (1997). Then, DW was added to the B/S mixtures to reach the desired moisture content (which ranged from 5% to 25%). The samples were stored in sealed polyethylene plastic bags and kept at room temperature (23ºC) for 72 hours prior to compaction. The compaction curves, maximum dry densities and optimum water contents of the compacted B/S mixtures were determined.

3.2.3 Testing and analysis of specimens

3.2.3.1 One-dimensional free swell test

The swelling induced volume changes of the compacted bentonite are schematically illustrated in Figure 3.4.

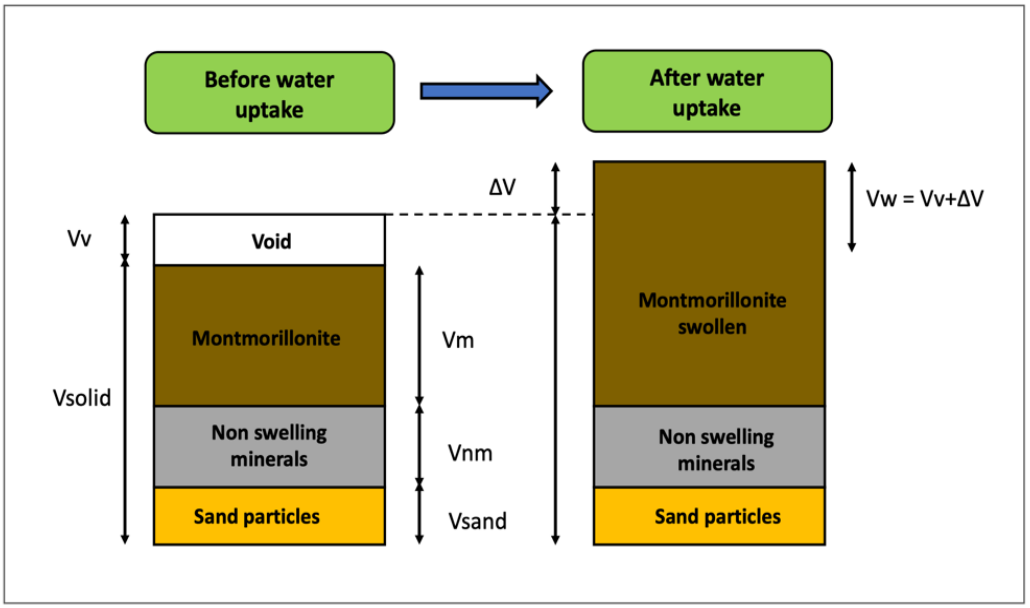

Figure 3.4. One-dimensional free swelling mechanism (modified from Liu, 1997)

Free swelling tests were carried out on the specimens (with different B/S mix ratios) compacted to the desired dry densities (1.4, 1.6, 1.8, or 2.0 g/cm^3). The water content and initial dry density were based on the different mix ratios of bentonite and sand. In accordance with ASTM standard D-4546-08, all of the specimens were compacted to a diameter of 63 mm and a height of 20 mm inside a polycarbonate tube (Figure 3.5), which has good chemical resistance. The tube has the same diameter as the specimens with a height of 120 mm, which allows the mixtures to swell vertically but not laterally. No gap at the interface between the tube and the B/S was observed. The specimens were then soaked with 150 ml of the appropriate water solutions (DW, T, or G) under approximately zero vertical stress. A digital dial gauge was used to monitor the vertical free swell strain of each specimen over time until the samples achieved full saturation and ceased expanding. At the end of the swelling tests, the degrees of saturation were determined (according to the soil mechanic approach) to ensure that the samples were fully saturated.

The free swelling tests were conducted in a temperature-controlled room under two different temperatures:

- Some tests were carried out at a temperature of 23°C. This serves as a control temperature to simulate the thermal conditions of a DGR in which no significant heating is generated due to the nuclear waste (e.g., disposal of low-level waste (LLW)).
- Some tests were carried out at a temperature of 80°C to simulate the heat generated by used or spent fuels or HWLsin a DGR. Rutqvist et al., (2014) calculated that the heat released by HWLs will increase the temperature at the interface between the host rock and the bentonite to about 80ºC. Moreover, they found that the temperature can be higher than 80°C in areas close to the canister. These results are also in agreement with the TOUGH-FLAC simulation results (Rutqvist et al., 2014). Moreover, Gobien et al.,

(2018) also found that the temperature in highly compacted bentonite around the containers could increase to 85°C after closure of the DGR.

- AT least two specimens were tested for each sample to ensure repeatability of results. As the ASTM standard D-4546 does not specify a standard error for the test due to its nature, results were accepted within a range of not more than 5% difference.

Figure 3.5. Image of one-dimensional free swell test apparatus

3.2.3.2 X-ray diffraction analysis

XRD analyses were conducted to determine the changes in the mineralogy of pure bentonite and the B/S mixture after they were immersed in different water solutions and/or exposed to different temperature conditions (23°C, 80°C). The X-ray powder diffraction data were collected by using a Philips X'Pert diffractometer (Philips Analytical, Netherlands) with a Cu tube at an operating power of 45 kV and a current of 40 mA. The XRD patterns were determined at room temperature, and the data set was collected from 2 to 70º 2θ. The step size was 0.02°, and the counting time for each step was 0.6 s.

3.2.3.3 Thermal analysis

Thermal analysis was carried out on dried pure bentonite and B/S mixture specimens after immersion in the water solutions and/or exposure to different temperatures. A TGA Q5000 V3.15 thermal gravimetric analyzer (TA Instruments, New Castle, US) was used to perform the thermogravimetric analysis (TGA) coupled with derivative thermogravimetry (DTG) analyses on several samples. The powder samples (17–20 mg) were heated up to 1000°C at a rate of 10°C/min under nitrogen purge conditions (25 mL/min). The test was performed at the Materials Characterization Core Facility, University of Ottawa.

3.2.3.4 Mercury intrusion porosimetry tests

MIP testing has been used for many decades to study the microstructure (porosity, pore size distribution (PDS)) of clays. Hence, the porosity and PSD of some of the B/S samples can be studied by using mercury intrusion porosimetry (MIP). MIP tests were performed on the specimens by using a Micromeritics Auto-Pore III 9420 mercury porosimeter (Micrometrcs, Norcross, US). AutoPore III measures the volume distribution of pores in materials by mercury intrusion or extrusion. The test was conducted at the porous materials Inc. (PMI) laboratory facility, New York, USA. It should be emphasized that because of the limited pressure range of the MIP technique, a significant pore volume (entrance diameter smaller than 6 nm) in the bentonite aggregates is not detectable. The MIP technique allows the exploration of pore diameter sizes between 0.006 and 600 μm. Since air or oven drying may lead to excessive shrinkage of the clay sample, the freeze-drying method was used which has been described and adopted by other researchers (e.g., Wang et al., 2014). This method minimizes the microstructure disturbance during dehydration which improves the quality of the MIP results (Delage et al., 2006; Tang et al., 2011). In this method, a B/S sample is cut into small pieces (approximately 1.5 g) and immersed into liquid nitrogen which has been vacuum-cooled to its

freezing point (-210°C). Then, the frozen specimen is transferred to the vacuumed chamber of a freeze dryer for sublimation for approximately 24 h.

However, some researchers (e.g., Sills et al., 1973; Simms and Yanful, 2004) have questioned the applicability of the MIP test in determining the PSD of clay sample, particularly on whether the sample is a good representation of the material due to its small sample size and disturbance during sample preparation. Another possible disturbance of the microstructure can be caused by the high injection pressure and pore accessibility. However, it should be noted that other studies (e.g., Lawrence 1978; Sills et al., 1973; Delage and Lefebvre 1984; Penumadu and Dean 2000) have concluded that the clay pore structure or microstructure is not affected by high injection pressure since the pore structure is mostly filled with incompressible mercury in the test.

3.2.3.5 SEM analyses

The microstructure of some of the dried B/S samples was also examined by using a scanning electron microscope. Scanning electron microscopy (SEM) analysis was performed by using a JSM-6610LV scanning electron microscope (JEOL Technics, Tokyo, Japan) to study the pore structure and morphology of the samples. The test was conducted at the Microanalysis lab, University of Ottawa.

3.3 Results and discussion

3.3.1 Effect of the physical factors of the bentonite-sand barrier material in distilled water

The swelling strain versus time of the compacted B/S mixtures (with different mix ratios and dry densities) exposed to DW at a temperature of 23ºC are shown in Figure 6. The final or maximum swelling strains of the B/S samples with different initial dry densities are shown in Figure 7. In this study, the swelling strain (ε, in percent) is calculated from:

$$\varepsilon = \frac{\Delta H}{H_0} x100$$

where ΔH is the swelling deformation or change in height and H_0 is the initial height of the sample.

As shown in Figures 3.6 and 3.7, it can be seen that the rate of swelling and the maximum swelling strain depend on both the initial dry density and the mix ratio. Figure 3.6 shows that, for all cases in this study, the maximum swelling strains are reached between 48 and 88 days. Samples with lower initial dry densities or higher sand contents reach the maximum swelling strain earlier. It is also observed that, regardless of the initial dry density and blending ratio, the measured swelling strain follows a sigmoid relationship with log time (Figure 3.6). The initial increase in strain is slow and less pronounced for the sample with a lower mix ratio (30/70). This is followed by a rapid increase in strain with time which represents approximately 80% of the total observed deformation. Subsequently, the strain increases slowly until reaching an asymptotic value (the maximum swelling strain). From Figure 3.7, it is obvious that the maximum swelling strain increases as the initial dry density or the mix ratio increases. For a 70:30 mix ratio, the maximum swelling strains are 266%, 277%, 286%, and 304% for dry densities of 1.4, 1.6, 1.8, and 2.0 g/cm^3, respectively. For a 30:70 mix ratio, the maximum swelling strains are 137%, 163%, 176%, and 191% for dry densities of 1.4, 1.6, 1.8, and 2.0 g/cm^3, respectively. Figure 3.7 shows that the maximum swelling strain and the dry densities follow a linear relationship, $\varepsilon_{max} = a\ \rho_d + b$, ($R^2 > 0.97$) with a positive slope over the ranges of densities. This confirms that increase in the dry density of the B/S increases the swelling potential.

The observed sigmoidal behaviour of the swelling strain vs log time is the result of the swelling process of the mixture of bentonite and coarser non-swelling particles (sand particles in this study). Indeed, it is well known that the swelling mechanism of B/S mixtures can be divided into three stages: initial swelling (inter-void swelling), primary swelling, and

secondary swelling (Suzuki et al., 2005; Rao and Thyagaraj, 2007; Cui et al., 2012). The initial swelling occurs when a B/S sample comes into contact with water and expansive minerals such as montmorillonite swell into voids (i.e., macropores) created by the coarser, non-swelling sand particles. The swelling of montmorillonite into the macropores will depend on the boundary conditions as well as the dry density of the material. However, at a low bentonite content (i.e., low mix ratio in this study), the inter-particle voids of the skeleton occupy large space, in which the bentonite can swell freely during the absorption of water without inducing a significant amount of expansion during the initial phase of swelling (Sun et al., 2013). This means that the swelling potential of the bentonite is reduced by filling the inter-particle voids. Therefore, the swelling strain of the specimens with low B/S ratio is less pronounced as shown in Figure 6b. Most of the swelling occurs during the primary stage of swelling which is caused by the hydration of the cations exchanged between the crystal layers. A sudden change in the swelling curve at 0.1 days in Figure 3.6b marks the beginning of the primary stage of swelling. The secondary stage of swelling occurs when crystalline swelling is completed and a double layer is created. During this stage, swelling follows a linear relationship with log time (Suzuki et al., 2005; Cui et al., 2012; Cui, 2019; Rawat et al, 2019).

The dependency of both the maximum swelling strain and swelling rate on the mix ratio and initial dry density can be explained by the fact that the swelling potential of the B/S mixtures is highly related to the volume of bentonite in the unit volume of mixture (Komine et al., 2009; Cui et al., 2012; Shehata et al., 2021). This means that, for a given dry density, an increase in the bentonite content or B/S ratio will lead to an increase in the volume of bentonite per unit volume of the mixture, thereby increasing the swelling strain and the rate of swelling. This explanation is consistent with the results from the SEM analyses presented in Figure 3.8. This figure shows the scanning electron microscope images magnified 14 times for B/S mixtures of 30% (B/S:70/30) and 70% (B/S:30/70) sand contents. It is seen that, with an

increase in the bentonite content, the sand particles are further apart. In other words, there is an increase in the volume of bentonite per unit volume of the mixture material.

Moreover, for a given B/S ratio, a higher dry density is associated with a smaller volume of voids (smaller size of pores) in the B/S mixture. Consequently, the volume ratio of bentonite to void in the mixture increases with increasing dry density of the B/S material, which in turn increases the swelling strain and swelling rate. The refinement of the pore structure or reduction of the volume of voids in the B/S mixture due to higher dry density is experimentally supported by the results from the MIP tests performed on two samples with a mix ratio of 70/30 and dry densities of 1.63 g/cm3 and 2.00 g/cm3, see Figure 3.9. This figure shows that an increase in the dry density does not change the range pore sizes but it significantly decreases the amount of intruded pores (Figure 3.9a, 3.9b). Moreover, the sample with a higher dry density has a lower total porosity (Figure 3.9b) and finer PSD (Figure 3.9a) than that with a lower dry density.

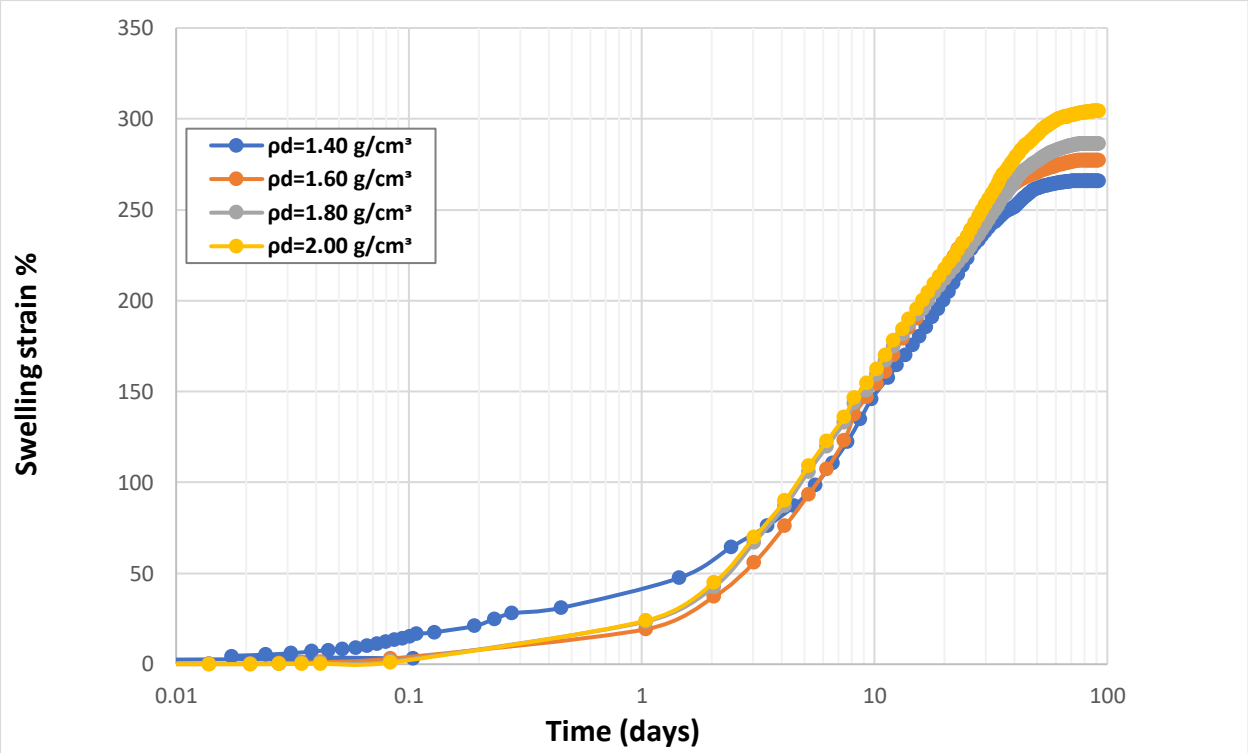

(a)

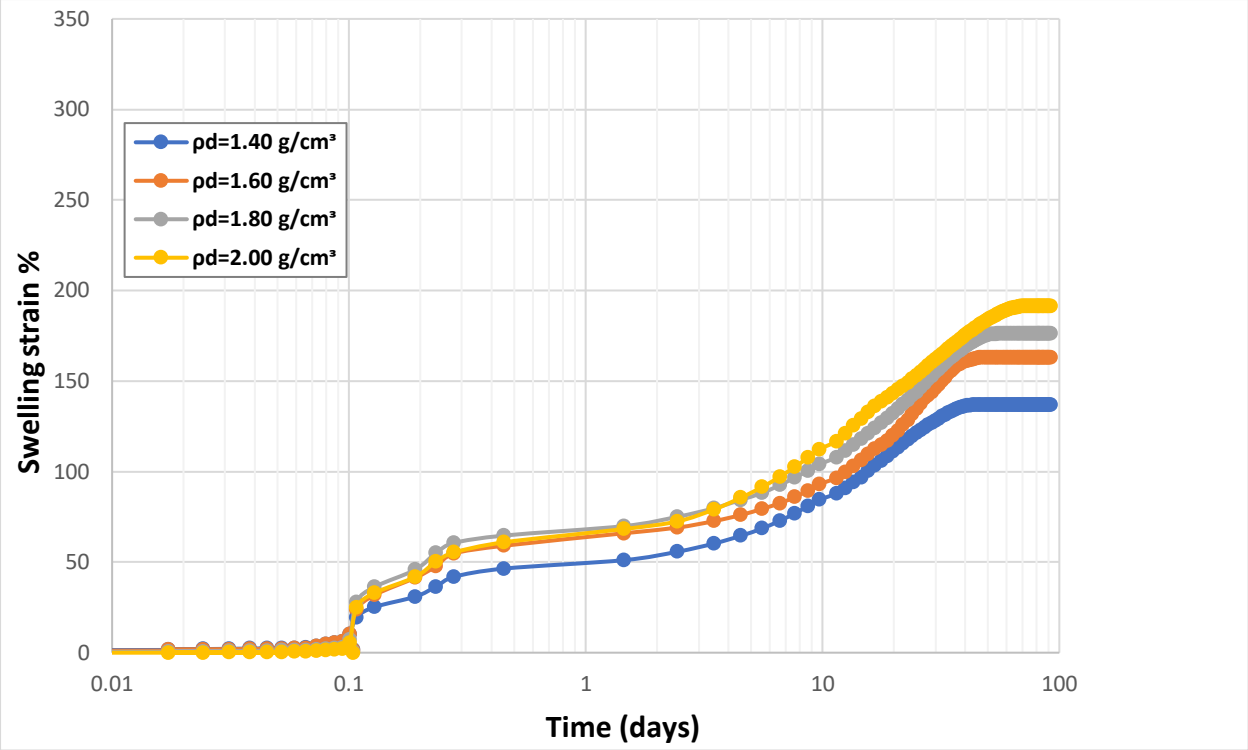

(b)

Figure 3.6. Effect of dry densities on the swelling strain of (a) 70:30 bentonite–sand mixtures and (b) 30:70 bentonite–sand mixtures immersed in DW

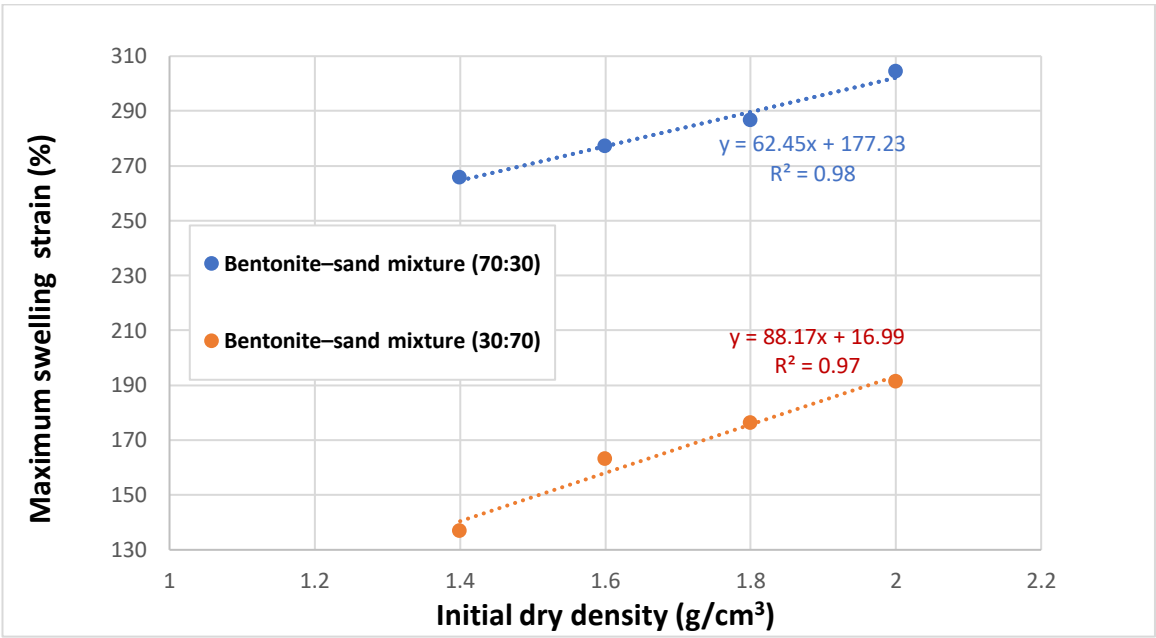

Figure 3.7. Final swelling strain for bentonite-sand specimens with different mix ratios at different initial dry densities

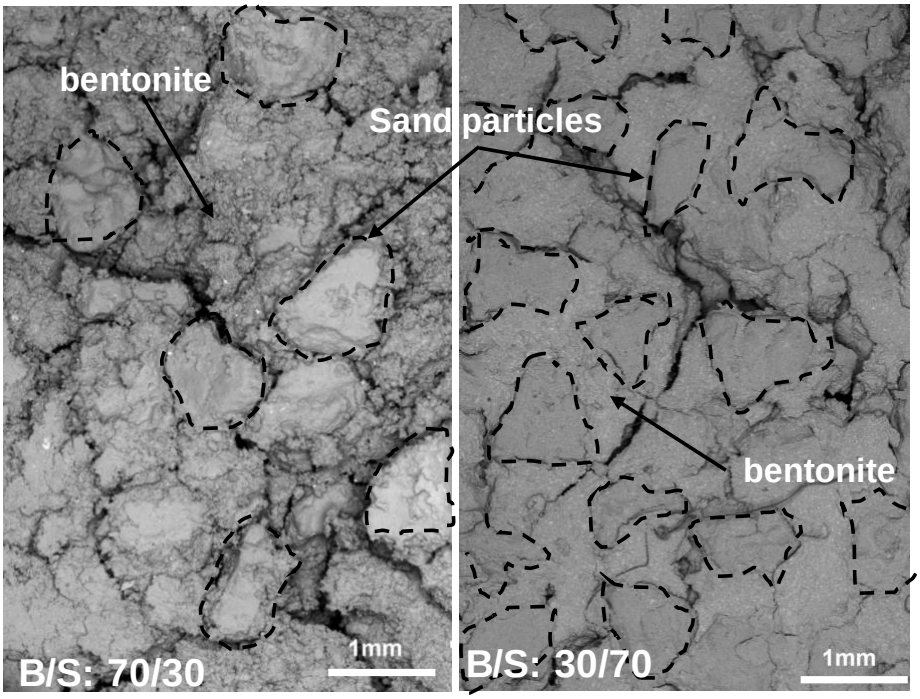

Figure 3.8. SEM images of bentonite–sand mixtures with 30% (B/S:70/30) and 70% (B/S:30/70) sand contents

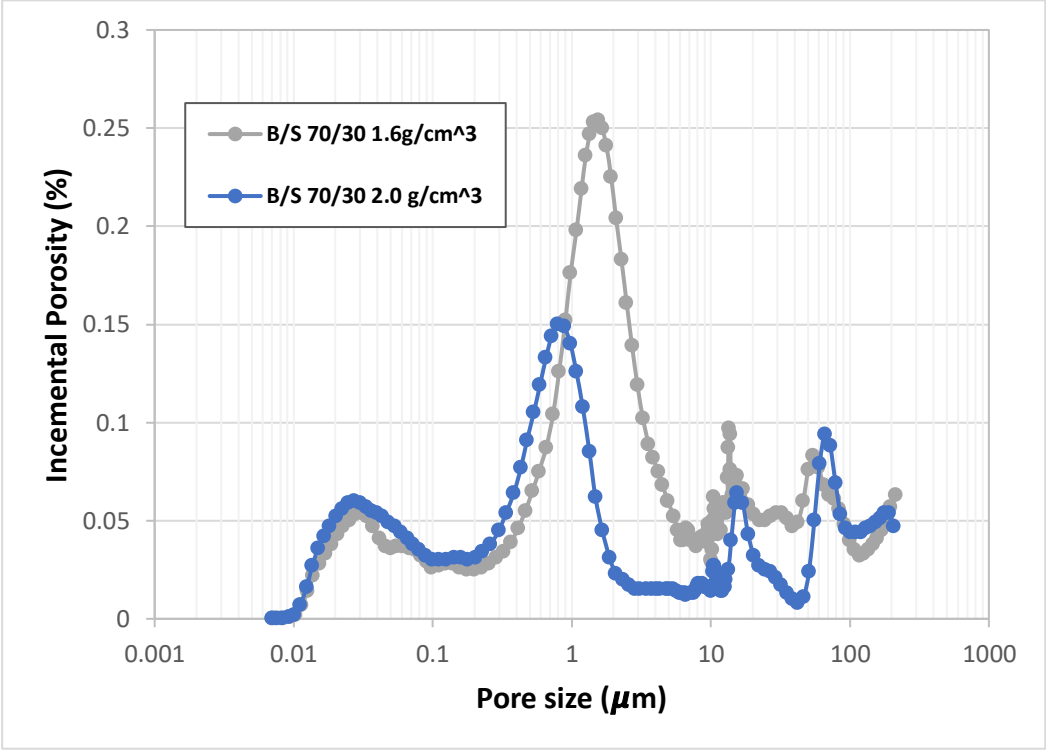

(a)

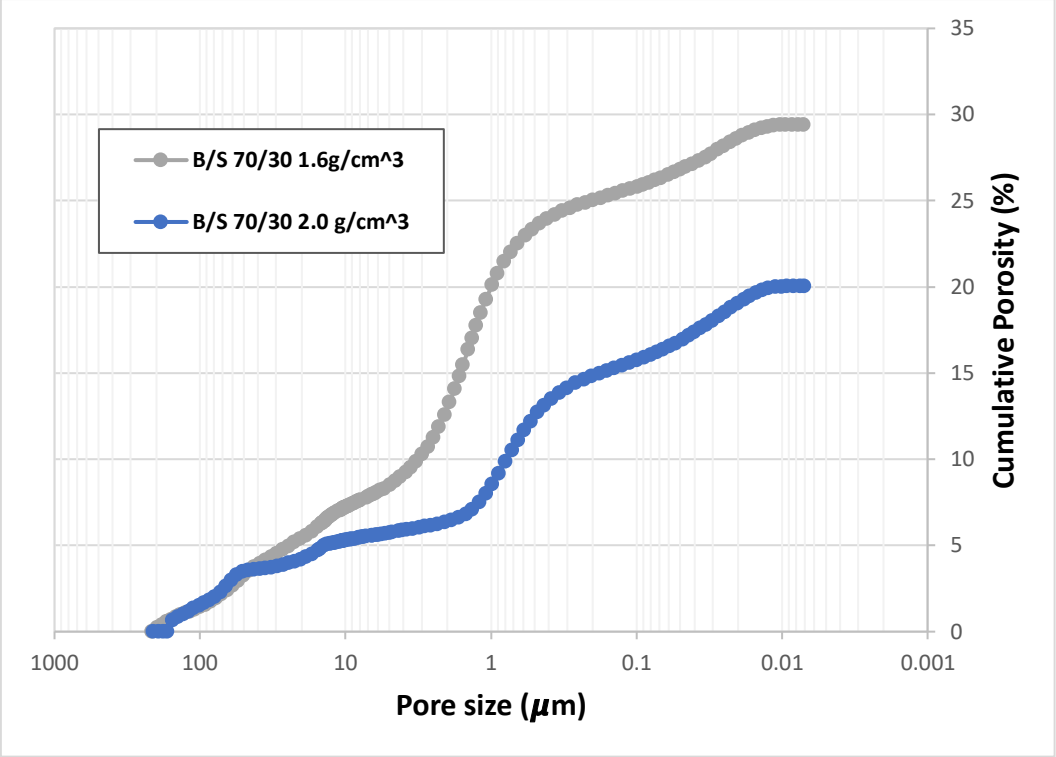

(b)

Figure 3.9. Results of MIP tests on two samples with 70/30 bentonite-sand and dry densities of 1.63 g/cm^3 and 2.00 g/cm^3

3.3.2 Influence of the chemistry of groundwaters on the bentonite-sand mixture with different dry densities and mix ratios

The changes in swelling strain with time for the compacted B/S mixture saturated with DW and G and T solutions with different concentrations of TDS are shown in Figures 3.10 to 3.13. Figures 3.10 and 3.11 show the relationship between the swelling strain and time for the B/S mixtures with the same initial dry density (1.63 g/cm^3) and different mix ratios in T solution and DW (Figure 3.10) and G solution and DW (Figure 3.11), respectively. Figures 3.12 and 3.13 show the effect of the chemistry of the T and G solutions on the swelling strain with different mix ratios and initial dry densities.

The results show that, in general, at low dry densities, the rate of swelling is slow but increases gradually with increase in dry density, regardless of the chemistry of the solution. Moreover, swelling develops more rapidly in specimens with higher dry densities, irrespective

of the type of water. Furthermore, the swelling rate is time-dependent. Initially, the increase in swelling deformation with time is slow. After that, swelling increases rapidly with time followed by a decrease in the strain rate until reaching the maximum swelling strain. The mechanisms responsible for these behaviours have been discussed earlier.

The results here indicate that the chemistry of the studied Ontario's groundwaters has a substantial effect on the swelling strain, rate of swelling and maximum swelling strain (Figure 3.14) of the B/S mixture, regardless of the initial dry density and bentonite content. However, the magnitude of this effect is a function of the chemical composition of the groundwater (particularly the TDS), see Figure 3.15, bentonite content (the B/S ratio) and the initial dry density. The specimens in DW exhibit the highest swelling rate and require the longest period of time to reach the final stage of swelling, while the specimens in T and G solutions have a lower swelling rate and shorter total swelling time, see Figures 3.10 to 3.15. The maximum swelling strain is reached at 20 to 38 days for the specimens in the G and T solutions, and 48 to 88 days for the specimens in DW, depending on the dry density, TDS, and mix ratio. Also, the mixtures saturated with DW have a greater maximum swelling deformation compared to the mixtures saturated with T and G solutions (Figures 3.10-3.15). This means that when the volume of total dissolved solids is increased, the initial swelling rate, swelling rate during the primary stage of swelling and the maximum swelling strain are decreased, see Figure 3.15. Moreover, the swelling strain is decreased significantly with increase in TDS concentration.

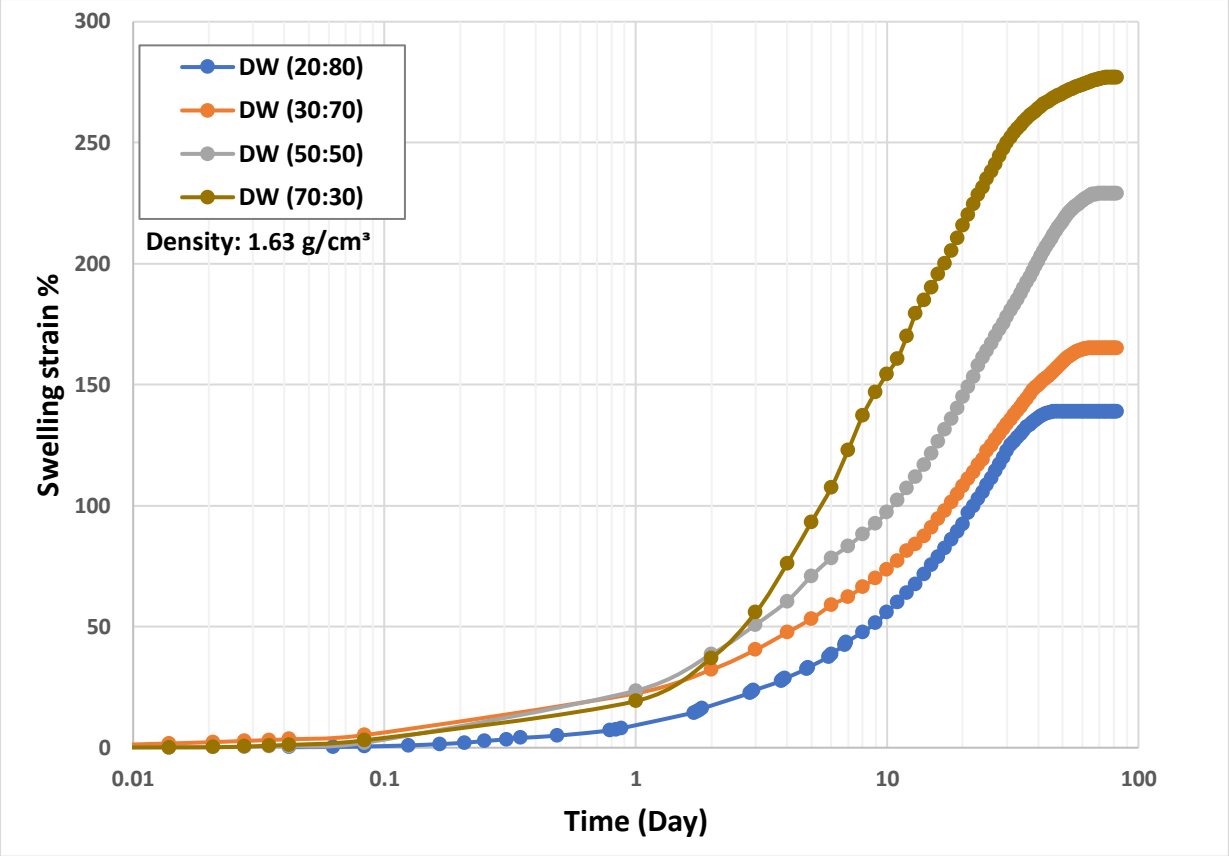

a) Swelling strain of bentonite–sand mixtures with different mix ratios immersed in distilled water

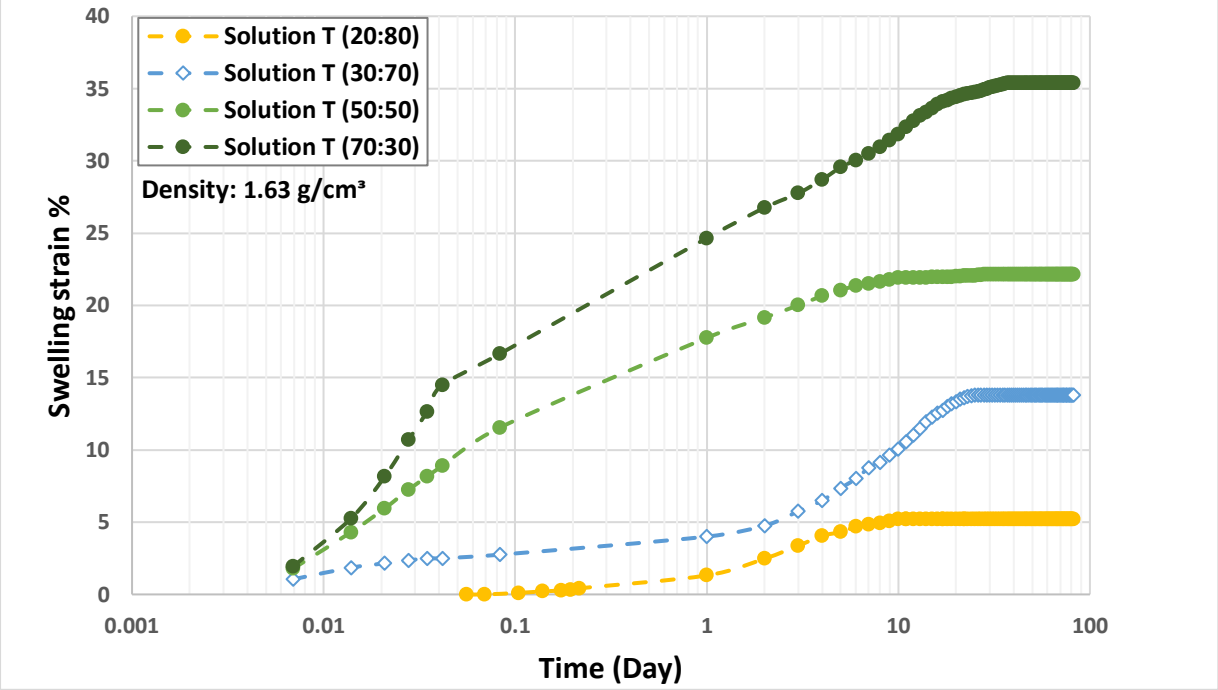

b) Swelling strain of bentonite–sand mixtures with different mix ratios immersed in water with the chemical composition of T solution

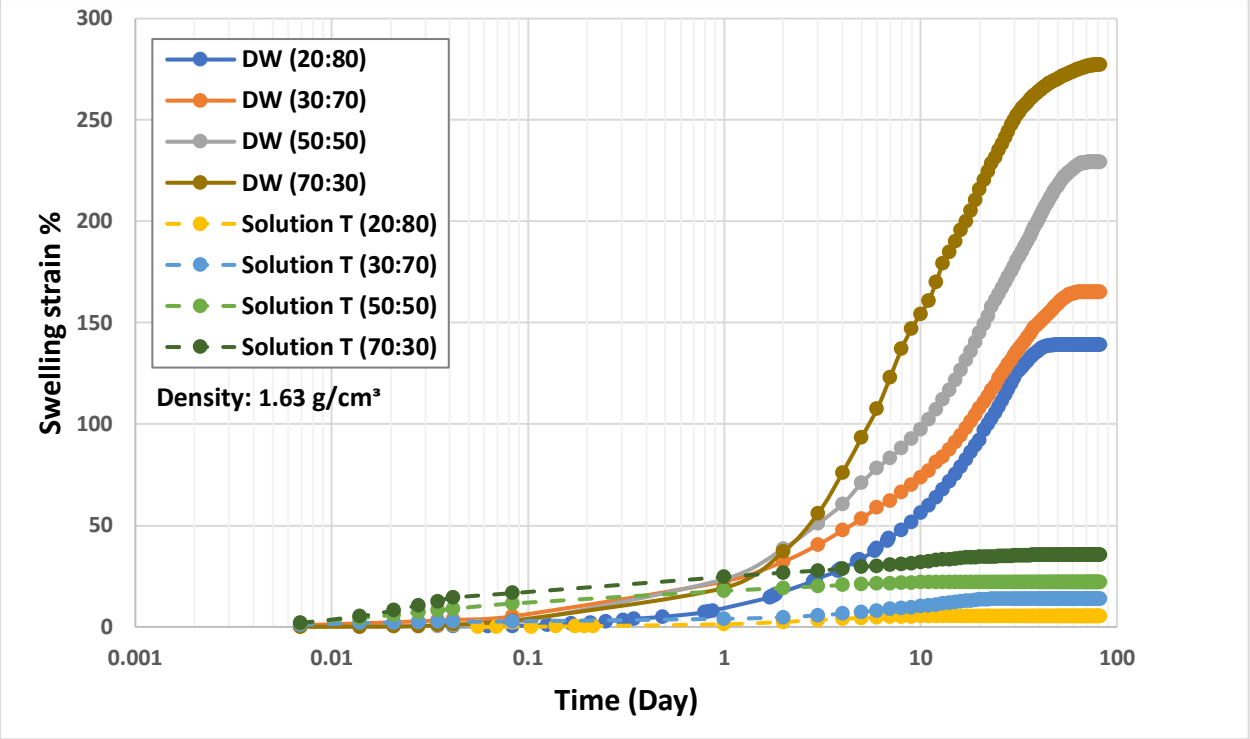

c) Comparison of the effect of DW and T solution on swelling strain of bentonite–sand mixtures with different mix ratios

Figure 3.10. Effect of distilled water and the T solution on the swelling strain of bentonite–sand mixtures with different mix ratios and a constant initial dry density (1.63 g/cm^3)

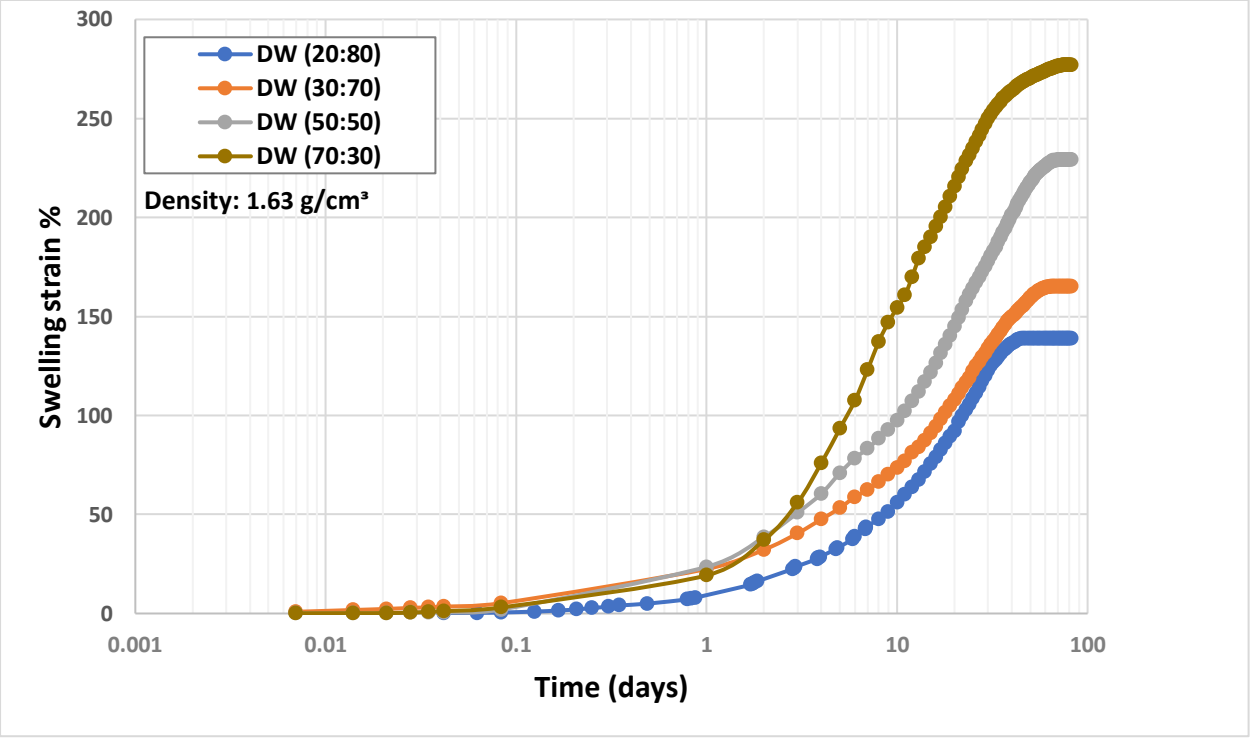

a) Swelling strain of bentonite–sand mixtures with different mix ratios immersed in distilled water

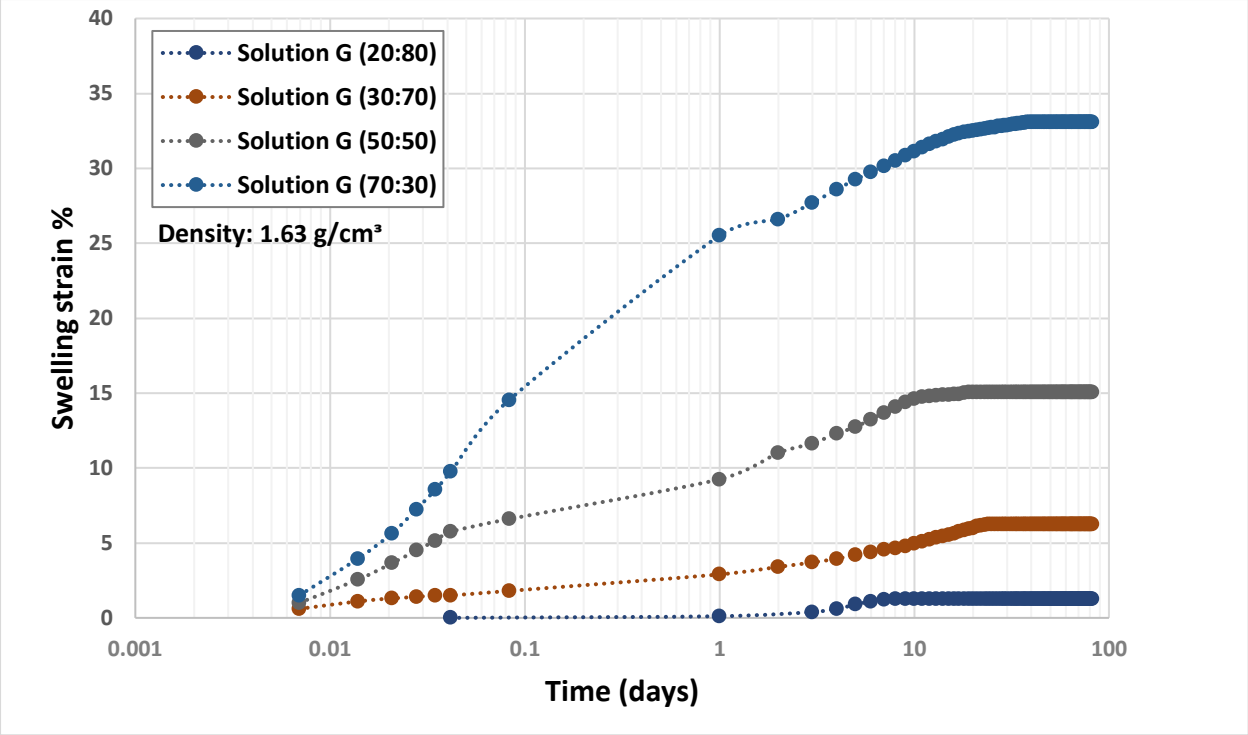

b) Swelling strain of bentonite–sand mixtures with different mix ratios immersed in water with the chemical composition of G groundwater

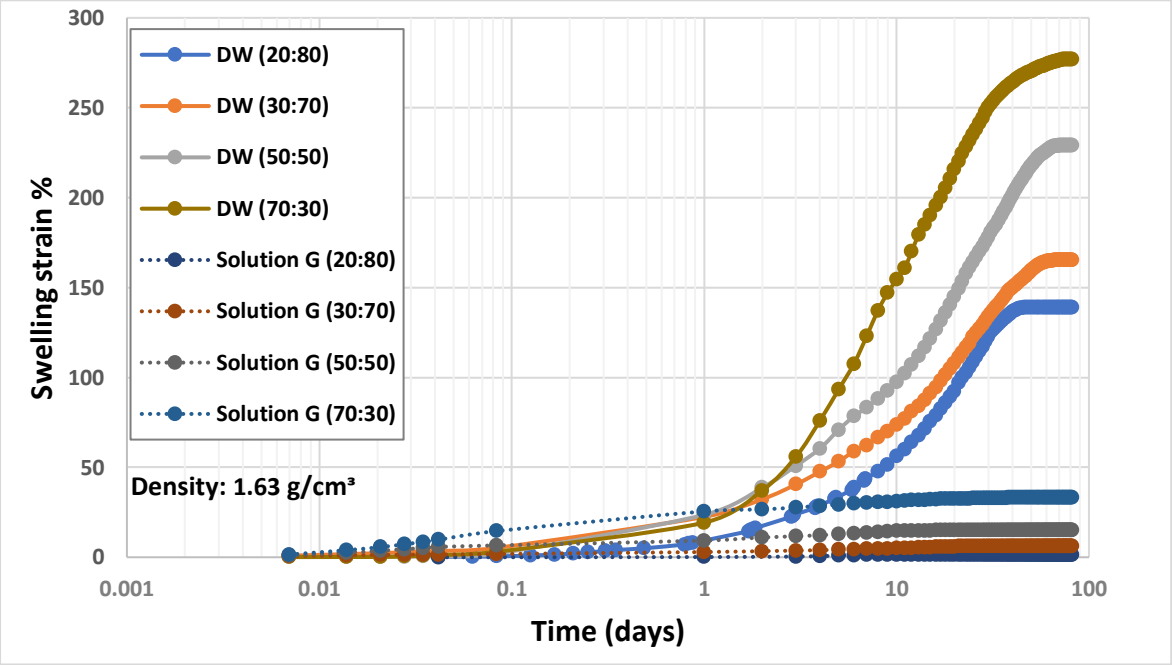

c) Comparison of the effect of DW and G solution on swelling strain of bentonite–sand mixtures with different mix ratios

Figure 3.11. Effect of distilled water and chemistry of G groundwater on the swelling strain of bentonite–sand mixtures with different mix ratios and a constant initial dry density (1.63 g/cm^3)

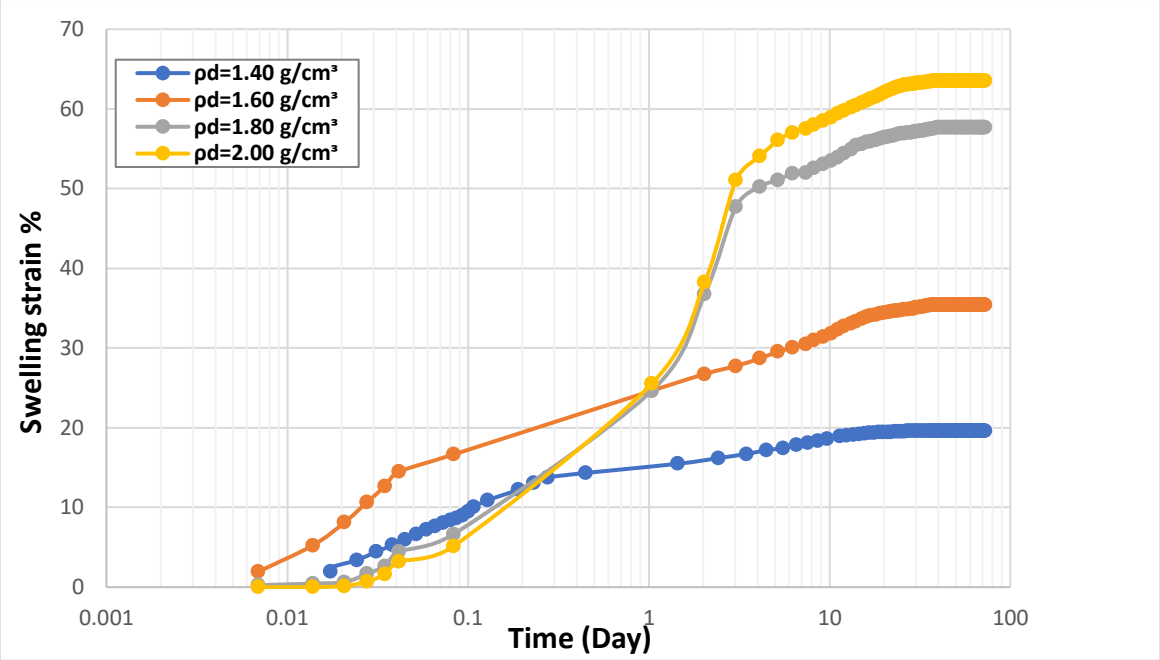

(a)

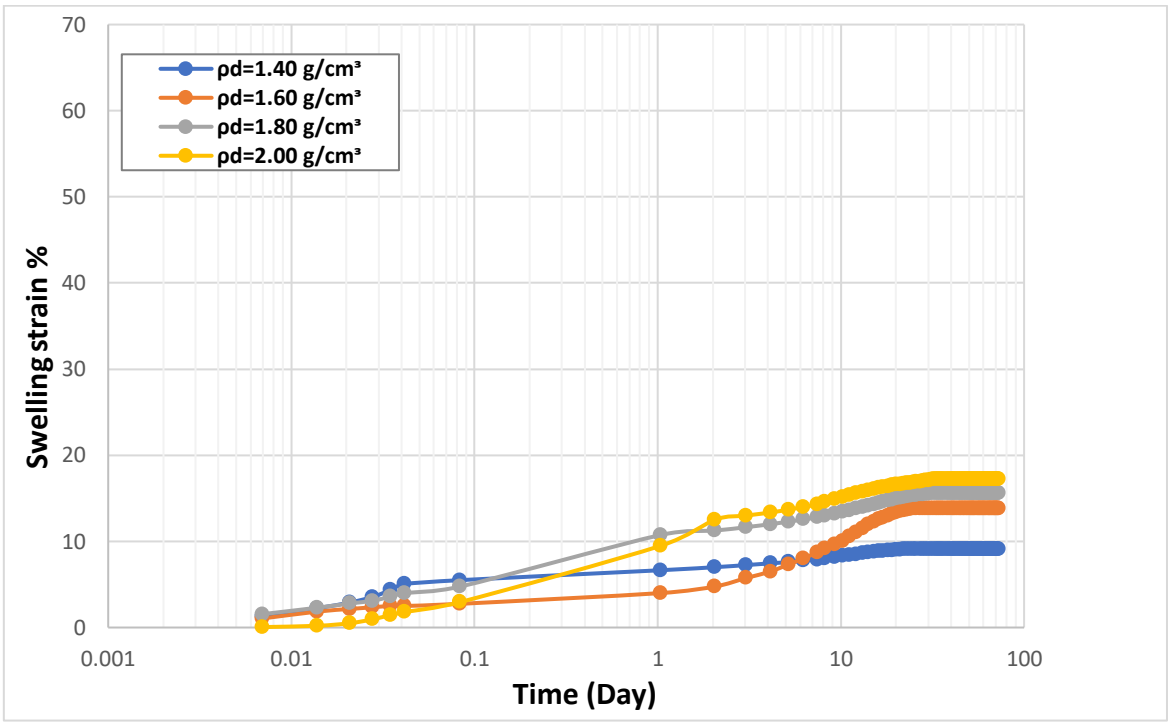

(b)

Figure 3.12. Effect of chemistry of T groundwater and initial dry density on the swelling strain of: (a) 70:30 bentonite–sand mixtures and (b) 30:70 bentonite–sand mixtures

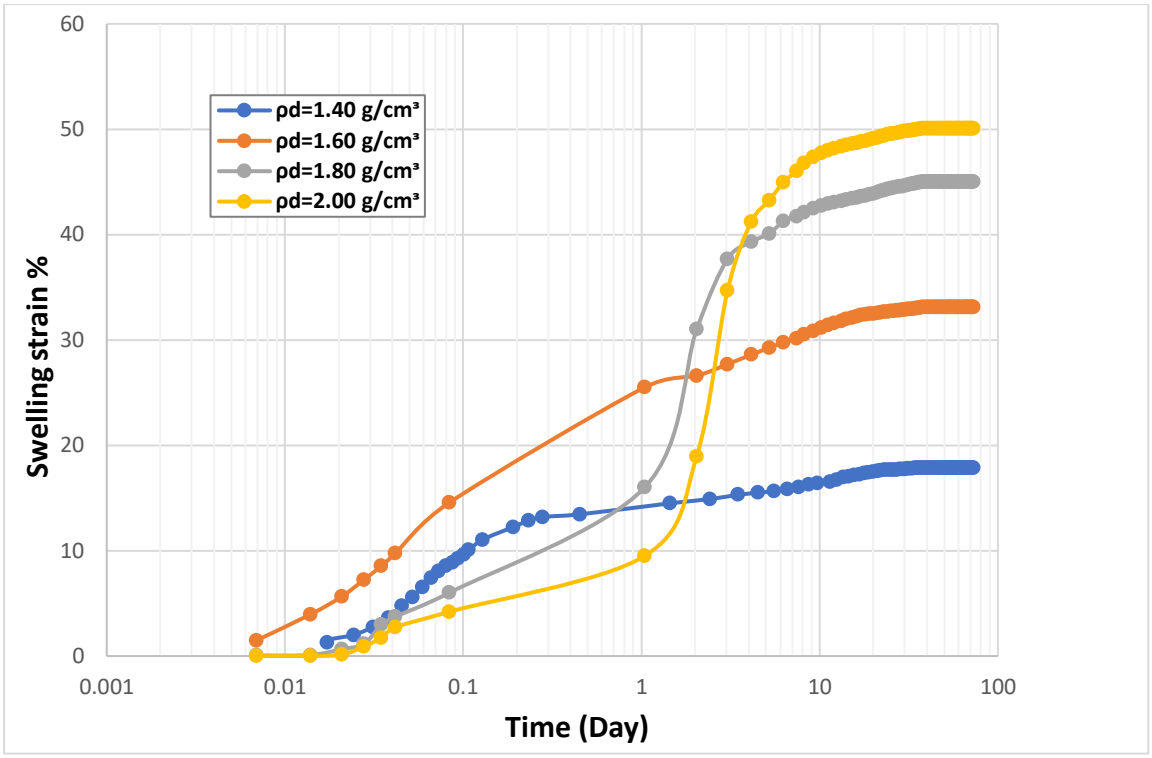

(a)

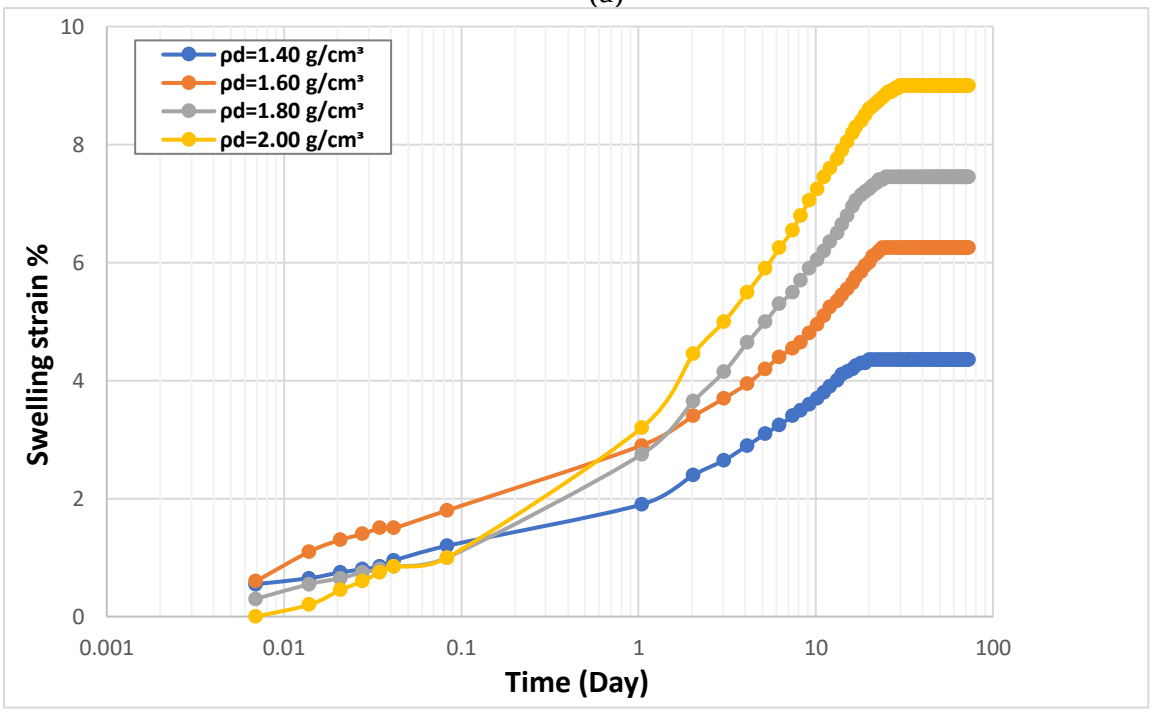

(b)

Figure 3.13. Effect of G solution and initial dry density on the swelling strain of: (a) 70:30 bentonite–sand mixtures and (b) 30:70 bentonite–sand mixtures

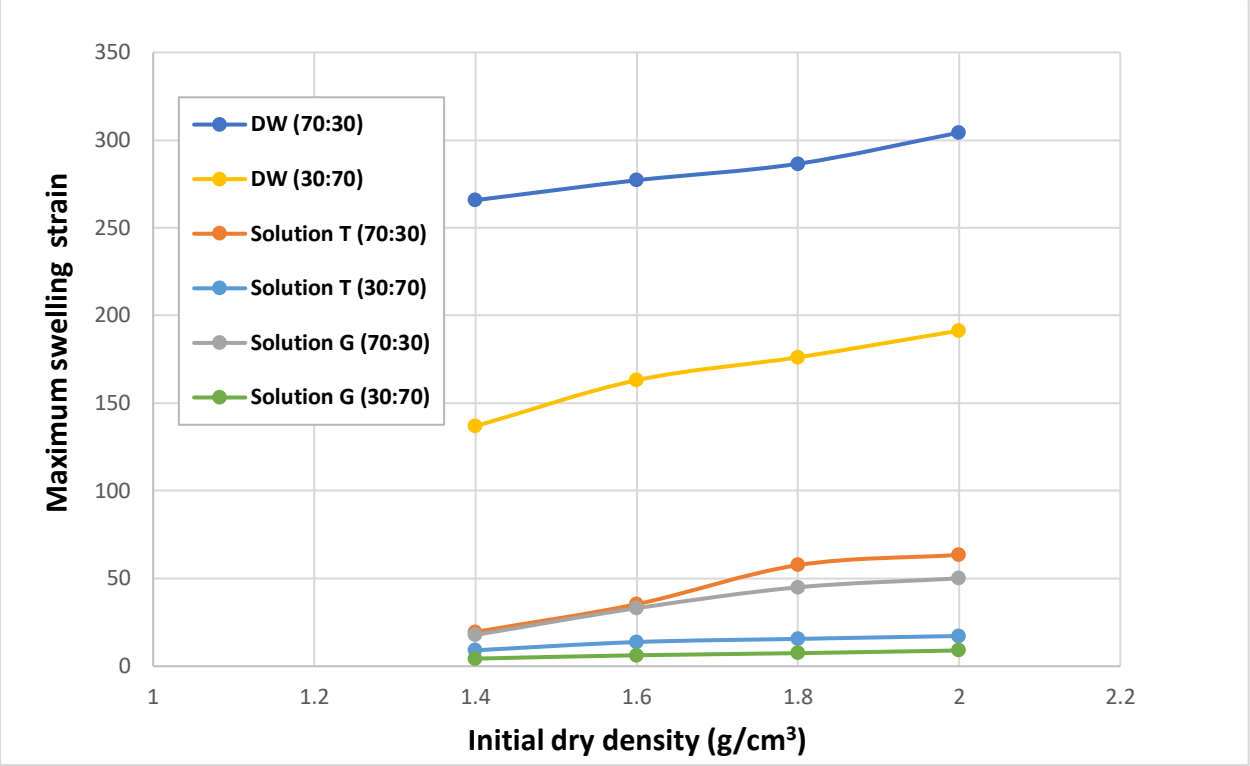

Figure 3.14. Effect of different solutions on the dry density vs swelling strain

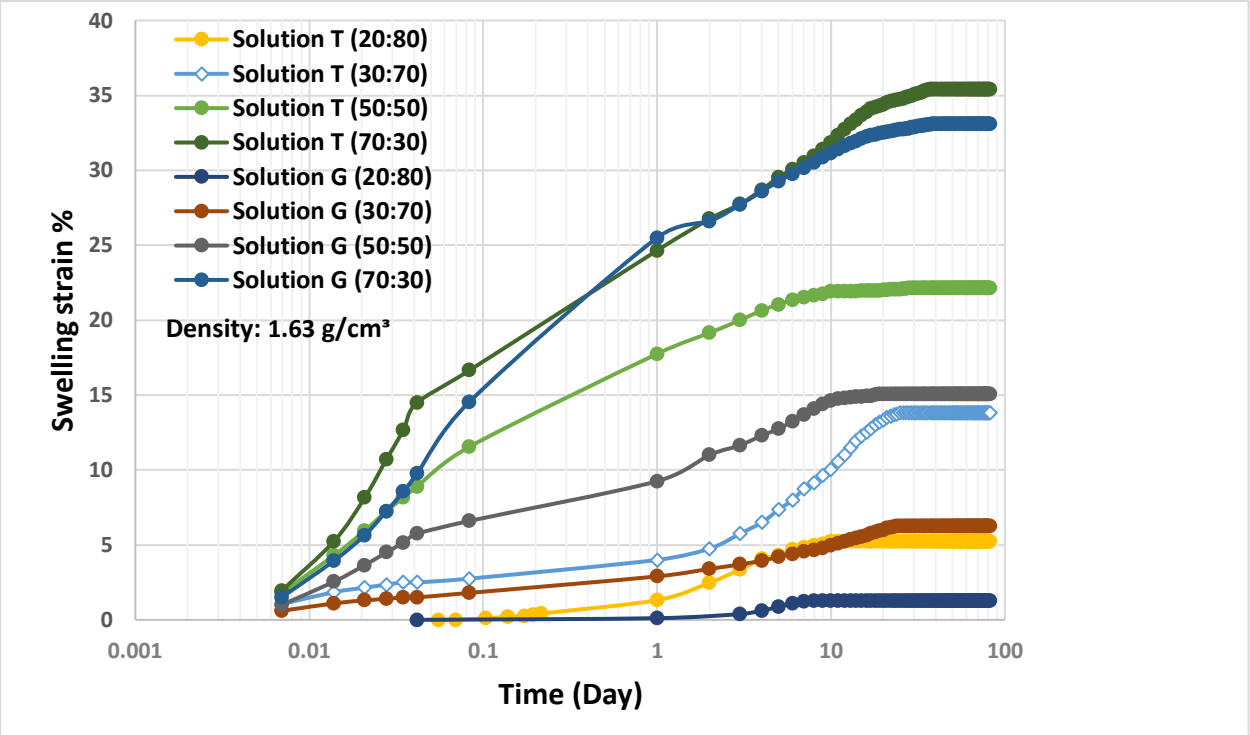

Figure 3.15. Comparison of the swelling strain of different bentonite–sand ratios exposed to groundwaters, G and T

This chemically (salinity) induced deterioration of the swelling ability of the B/S specimens is consistent with the results of the MIP tests, see Figure 3.16. MIP tests were performed on two samples with a mix ratio of 70/30 and dry density of 1.63 g/cm^3 in DW and G solution after 40 days. Figure 3.16 shows that the sample with the G solution shows higher incremental intruded pore volume and coarser pore structure than the specimen with DW. However, most of changes in the microstructure takes place in the category of macro-pores. For the sample with larger swelling strain or swelling capacity, i.e., the sample with DW, more interlayer hydration has occurred, thus resulting in a constriction of the accessible pores. These observations on the chemically induced changes of the pore structure of the Mx80 B/S mixture are in agreement with the findings by Mata (2003) who concluded that saline water has a significant influence on the macro-pores of bentonite-based material, whereas its effect on the micro-pores is not significant.

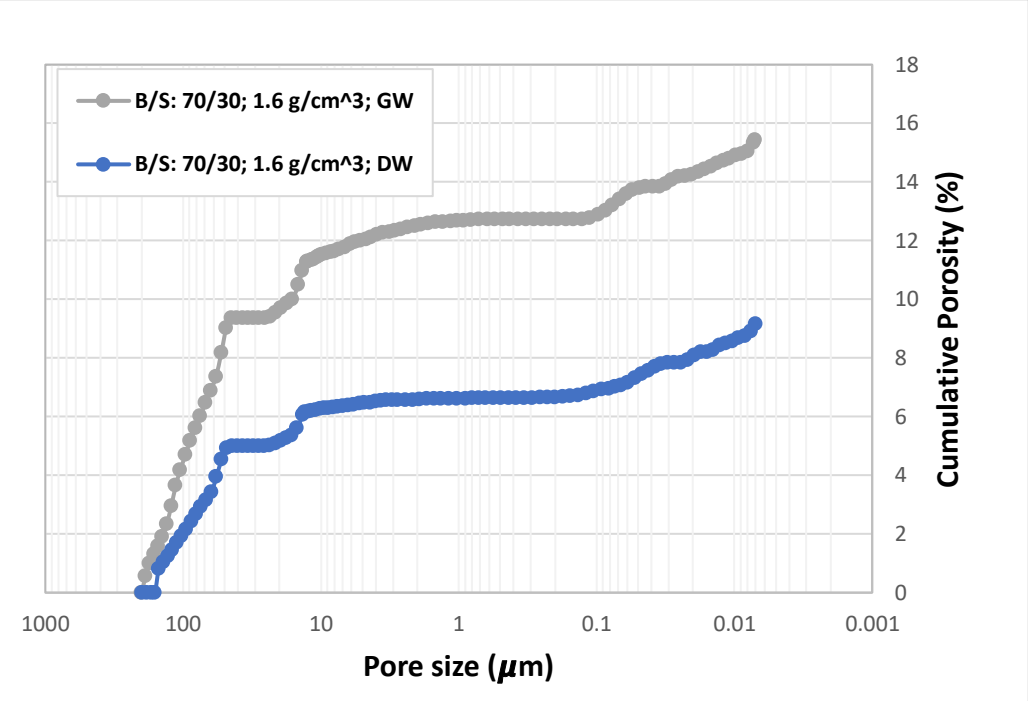

(a)

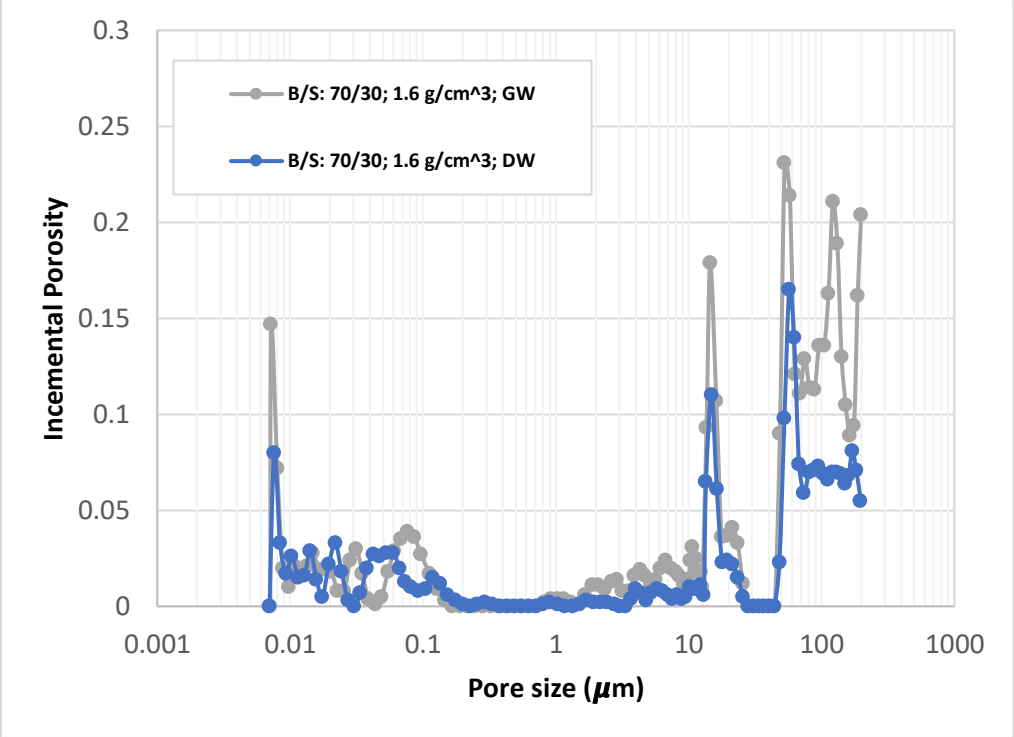

(b)

Figure 3.16. Pore size curves: (a) MIP cumulative porosity curves, (b) MIP PSD (70/30 bentonite sand; dry density is equal to 1.63 g/cm3; one sample saturated with DW, one sample saturated with the G solution; soaking time: 40 days).

The observed deterioration of the swelling characteristics (e.g., swelling strain and rate, maximum swelling strain) of the B/S mixture saturated with groundwaters T and G, irrespective of the dry density and B/S ratio, is related to the high TDS values of the groundwaters T, G. Higher dissolved salt concentrations or TDS reduce the swelling ability of bentonite (Suzuki et al., 2005; Karnland et al., 2007; Castellanos et al., 2008; Komine et al., 2009; Zhang et al., 2012; Sun et al., 2017; Shehata et al., 2021). This reduction in the swelling potential of the bentonite saturated with the G or T solutions can be explained by the two following mechanisms. First, a higher volume of TDS causes a reduction in the thickness of the double diffused layer (DDL) of the montmorillonite particles which leads to a decrease in the repulsive forces between the clay particles. Consequently, this reduces the swelling strain and swelling pressure of the material (Siddiqua et al., 2011). Secondly, chemical changes take

place in the montmorillonite minerals due the chemical attacks from the saline G and T solutions. In other words, the Na-montmorillonite minerals transform, at least partially, to Ca-montmorillonite minerals during interaction with Ca^{2+} ions in the G or T solutions, as evidenced from the results of the microstructural analyses (XRD, DT/DTG) that are shown in Figure 3.17 (XRD patterns) and Fig.18 (TG/DTG analysis results). XRD and TG/DTG analyses were performed on 30:70 bentonite–sand mixtures saturated with DW and the G solution, respectively. The results of the microstructural analyses indicate that cation exchange took place in the specimens saturated with the G (G23) solution due the presence of divalent cations (Ca^{2+}, Mg^{2+}) in the porewater of the bentonite (Table 3.3), which in turn led to the transformation of Na-montmorillonites to Ca-montmorillonites. The cation, Ca^{2+}, has a much greater affinity for montmorillonite than the Na^{+} cation and the substitution of the Na^{+} cation in the Na-montmorillonite creates the Ca-montmorillonite with reduced swelling capacity (Akinwunmi et al., 2020; Shehata et al., 2021). From Figure 3.17, it is seen that the bentonite-based material consists predominantly of montmorillonite, with small proportions of illite and quartz. Moreover, the spacing between the crystal interlayers of bentonite (i.e., basal spacing) is sensitive to the hydration state of the ions, and the position of the peak in the basal spacing (d_{001}) is affected by the type of interlayer cation. Therefore, the XRD spectrums of the DW sample reveal that the first peak of the Na-montmorillonite is at (2-Theta) 8.92º and d_{001}= 9.9 Å, while the G sample (G23) is at (2-Theta) 6.28º with lower reflection intensity and d_{001}= 14.04 Å. These changes in the position of the peak and the reflection intensity indicate a reduction in the swelling capacity (Moore and Reynolds, 1989). These XRD results are in agreement with those of the TG/DTG analysis in Figure 3.18a and Figure 3.18b. From Figure 3.18a, it can be seen that the TG/DTG results of the specimen mixed and saturated with DW indicate that the initial loss of the mass of water of 2.64 wt. % occurs at a low temperature interval (0–50ºC) because of the removal of the surface water. The second loss of the mass of

water (1.80 wt. %) occurs within the temperature interval of 200–600ºC, which corresponds to water desorption from the interlayers. The last endothermic peak, within the temperature interval of 600–1000ºC, has a mass loss of about 3.22 wt.%, due to the dehydroxylation of the O-H structure and collapse of the smectite crystal structure (Drits et al., 1998; Frost and Ding, 2003; Boudriche et al., 2012). Fig. 18b clearly shows that the total mass loss of the specimen mixed and saturated with G solution within a temperature interval of 50–200ºC is 18.20 wt.%. In addition, the interlayer of chemisorbed water is gradually removed at a temperature interval of 200–600ºC, thus producing a mass loss of 3.85 wt.%. Dehydroxylation of the Al-OH bond structure occurs at a higher temperature interval (600–1000ºC) with an endothermic peak of 9.8 wt.%. Therefore, these TG/DTG results confirm that the B/S microstructure is partially altered in a highly saline solution.

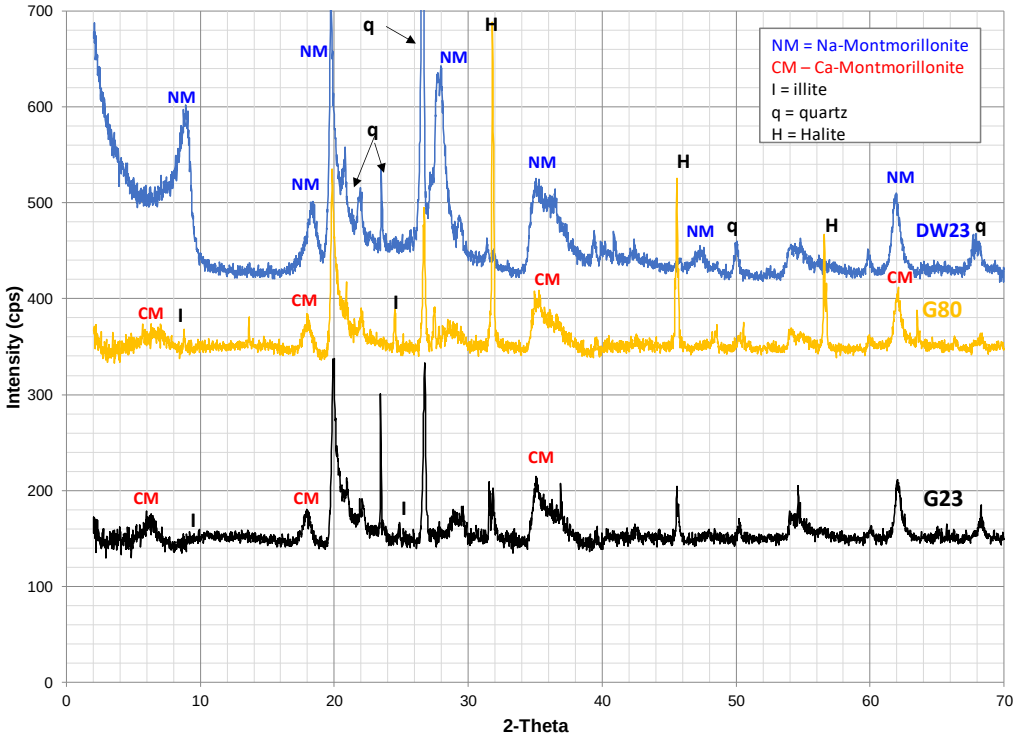

Figure 3.17. XRD patterns of the 30:70 bentonite–sand mixture mixed and saturated with (i) DW at 23 °C, (ii) G solution at 23 °C (G23) and (iii) G solution at 80 °C (G80)

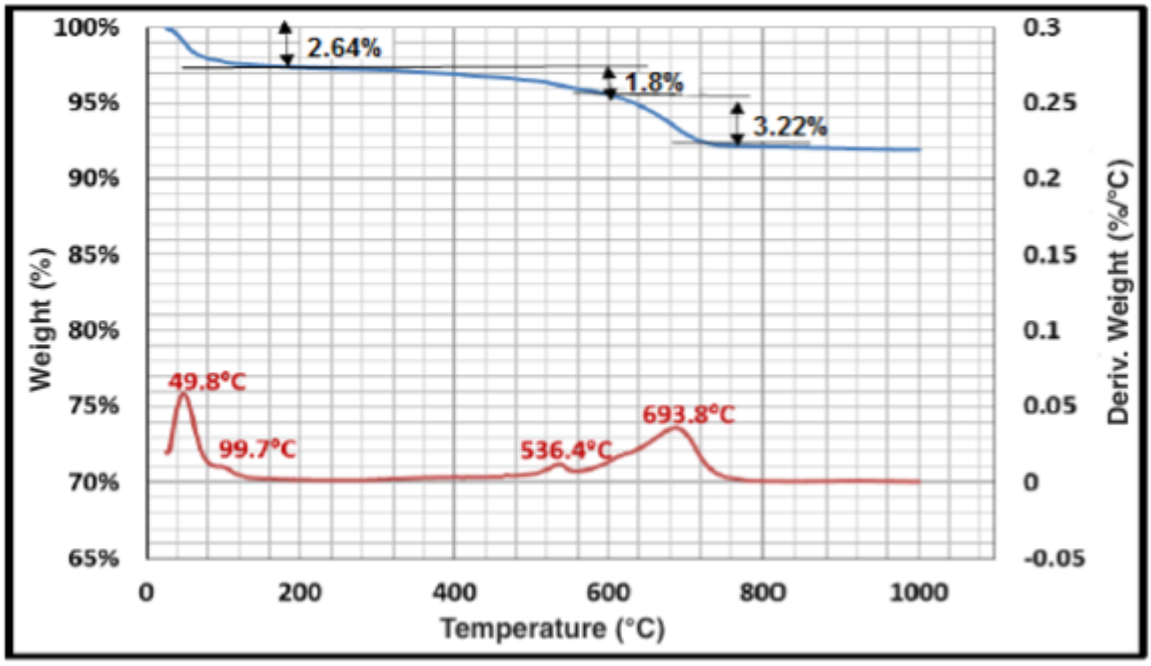

(a)

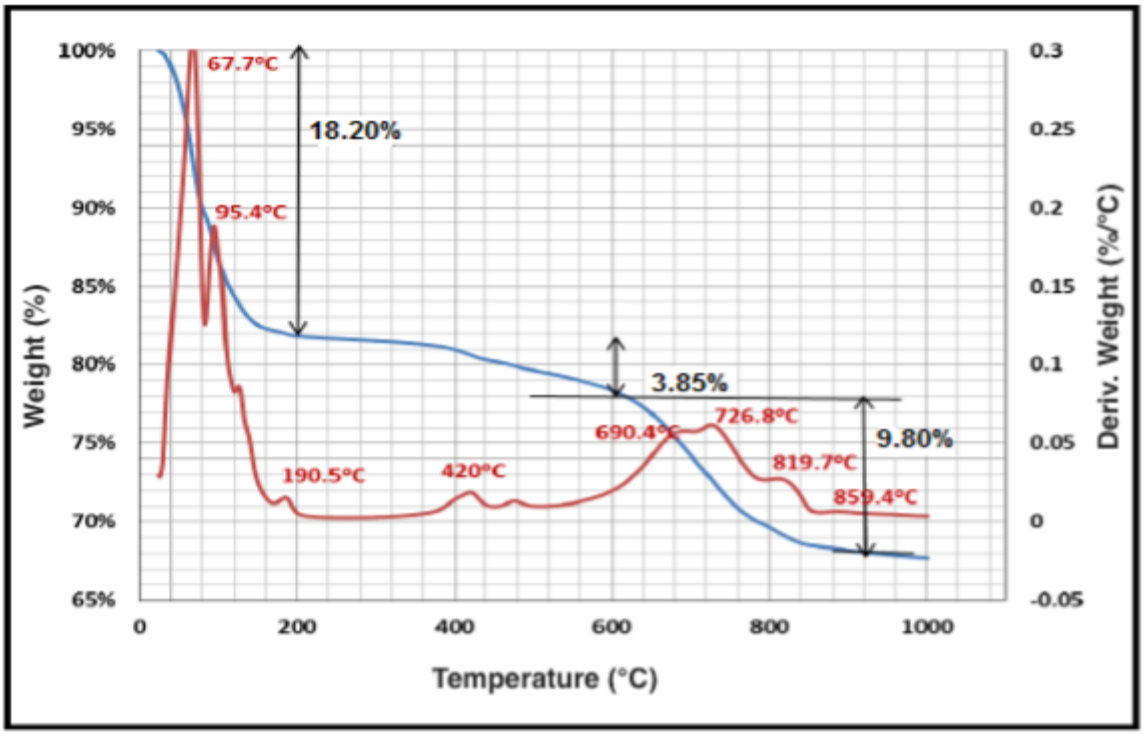

(b)

Figure 3.18. Results of TG/DTG analyses of a 30:70 B/S mixture that is mixed and saturated with: a) DW, and b) G solutions

However, Figures 3.12 to 3.14 show that the reduction in swelling due the saline solutions is smaller for bentonite-based materials with higher dry densities. This reduction in

swelling with increase in dry density can be explained by the mechanisms of crystalline swelling and double layer swelling of the bentonite. Crystalline swelling results from the hydration of exchangeable cations, K+, Na^{+}, Ca^{2+}, and Mg^{2+}, between mineral layers that show a structure with one alumina octahedral sheet sandwiched between two silica tetrahedral sheets. This is a mechanism which shows that the adsorption of the maximum volume of hydrates depends on the nature of the cations (Wang et al., 2014). When three to four water monolayers are formed, the surface hydration mechanism plays a less important role and electric double-layer repulsion becomes the key swelling mechanism (Wang et al., 2014; Suzuki et al., 2005; Bradbury and Baeyens, 2003). For bentonite with high dry density, the low quantity of water adsorbed is essentially pseudo-crystalline interlayer water. Hence, the latter is not enough to build the DDL (Pusch 2000; Wang et al., 2014). Consequently, swelling is largely controlled by the crystalline swelling and the double layer repulsion provides only a slight contribution to the swelling. In this case, bentonite–water interaction is essentially governed by the exchangeable cations (Suzuki et al., 2005; Castellanos et al., 2008; Siddiqua et al., 2011).

3.3.3 Coupled effect of the chemistry of groundwaters and temperature on the bentonite-sand barrier

To properly design the experimental testing program to address the objective of this section as well as to better analyze the results, preliminary investigations were conducted to assess the individual impact of temperature on the swelling ability of the bentonite-sand barrier material saturated with DW (i.e. no chemical effect considered). One-dimension free swelling tests were conducted on compacted B/S material samples with different mix ratios in DW and exposed to different temperatures, 23°C and 80°C. The results indicate that temperature has insignificant effects on the swelling potential of the material. Indeed, the maximum amount of swelling of the samples with DW at 23°C is only 2% higher than that of the 80°C samples. These results agree well with the results from previous studies (e.g., Shehata et al., 2021, Pusch,

2000) that show insignificant changes in the swelling potential of bentonite-based material with increase in temperature (up to 90°C). However, the following question still remains unanswered. Does temperature have a significant effect on the swelling ability of bentonite-based materials saturated with the G groundwater? In other words, how significant is the coupled effect of the chemistry of groundwaters and temperature on the swelling properties of bentonite-sand barrier materials? To address these questions, free swelling tests were carried out on compacted samples with different mix ratios (B/S: 70/30, 50/50) and saturated with the G solution at room and higher temperatures of 23ºC and 80ºC, respectively. Typical results are shown in Figure 3.19. It is seen that, regardless of the mix ratio, the swelling strain is significantly dependent on the temperature and the chemical composition of water. Higher temperature results in more intense chemically-induced degradation of the swelling capacity of the material. It is obvious that the specimens with the G solution at 80ºC have a swelling strain that is lower than those at 23ºC with shorter time to reach the stage of constant rate of swelling and termination of swelling. For example, Figure 3.19 shows that the samples (70:30) tested at 80°C gives a swelling strain of 17% in 25 days, while the specimen exposed to a temperature of 23ºC shows a swelling strain of 30% in 30 days. In other words, the swelling potential of the (70:30) sample in the G solution at 80ºC is decreased by 43% in comparison to that of the 23 ºC sample. Also, the same trend is observed in the samples with a mix ratio of 50:50 which gives a swelling strain of 7% in 26 days at 80°C, while the sample at 23ºC exhibits a swelling strain of 13% in 30 days. The test results show that higher temperatures intensify the chemical reaction of the bentonite in the G solution which reduces the swelling potential of the B/S mixture. Future swelling stress experiments should be performed to determine how this significant loss in free swelling strain translates into loss in swelling stress, and what may be the implications for repository performance. This temperature-induced intensification could be related to the following mechanisms: (i) higher temperatures increase the dissolution rate of

the smectite, which would reduce the amount of expansive minerals (montmorillonites) in the B/S mixture; (ii) higher temperature increases the transformation of Na-montmorillonite minerals to Ca-montmorillonite which has a lower swelling potential; and (iii) higher temperature leads to lattice contraction in different clay structures.

Indeed, a number of previous experimental studies on smectite dissolution kinetics or rates of dissolution in different chemical (pH, different chemical solutions) and thermal (temperature) environments have found that the dissolution rate of smectite increases with temperature. This is in agreement with the findings from previous numerical studies (Zheng et al., 2015, 2017; Xu et al., 2021). For example, Amram and Ganor (2005) investigated the coupled effect of pH and temperature (25°C to 70°C) on the dissolution rate of smectite SAz-1 by conducting dissolution experiments with the use of non-stirred flow-through reactors in thermostatic water. Their results show that the smectite dissolution rate is increased with temperature and decreased with pH. Moreover, Huertas et al., (2001) evaluated bentonite dissolution in granitic solutions (pH 7.6 to 8.5) in a semi-batch reactor at 20°C, 40°C and 60°C. They concluded that temperature increases the dissolution rate of smectite and the effect of temperature on the dissolution rate is a function of the activation energy. These findings on the reduction of the amount of montmorillonites due to a higher dissolution rate at a higher temperature are in agreement with the results of the XRD analyses presented in Figure 3.17. Figure 3.17 shows the XRD patterns of the B/S mixture in the G solution at room temperature (23°C, G23) and higher temperature of 80°C (G80) as well as the XRD pattern of the DW sample. It can be observed that the first peaks for the montmorillonite in the DW, G23 and G80 samples are (2ɵ) 8.92º, 6.288º and 6.632º, with lower reflection intensities and the basal spacings are d (001) = 9.902, 14.044 and 13.1357 Å, respectively. This detected shift to the left of the first peak of the G80 sample is related to the transformation of Na-montmorillonite to Ca-montmorillonite, whereas the observed lower intensity indicates a decrease in the amount

of minerals that undergo swelling. The latter suggests a higher dissolution of montmorillonite in the G80 sample. An additional mechanism can be suggested as a factor that has contributed to the higher decrease in swelling ability observed in the samples saturated with G or T solutions at high temperatures (80°C). The phenomenon can be explained in terms of lattice contraction at high temperature (Chen et al., 2013; Ureana et al., 2013; Chen et al., 2018). Chen et al., (2018) carried out swelling and microstructural tests to investigate the combined effects of temperature (20°C to 60°C) and cation type (in the NaCl and $CaCl_2$ solutions used) on the swelling pressure and microstructure of densely compacted pure GMZ bentonite. They found that lattice contraction at high temperatures decreases the swelling pressure to a greater degree in $CaCl_2$-bentonite with smaller basal spacing. Due to the heating of the saturated $CaCl_2$-bentonite, there is a change of the interlamellar adsorbed water to bulk water which weakens crystalline swelling. The XRD results obtained in this study show that the basal spacing d (001) of the G80 sample (13.1357 Å) is smaller than that of the G23 sample (14.044 Å). In other words, there is a decrease in the basal spacing with temperature. However, it should be noted that more detailed microstructural and mineralogical investigations should be carried out in the future to gain more insight into the changes that take place in the microstructure and mineralogy of compacted MX-80 B/S due to the combined effects of temperature and groundwater chemistry.

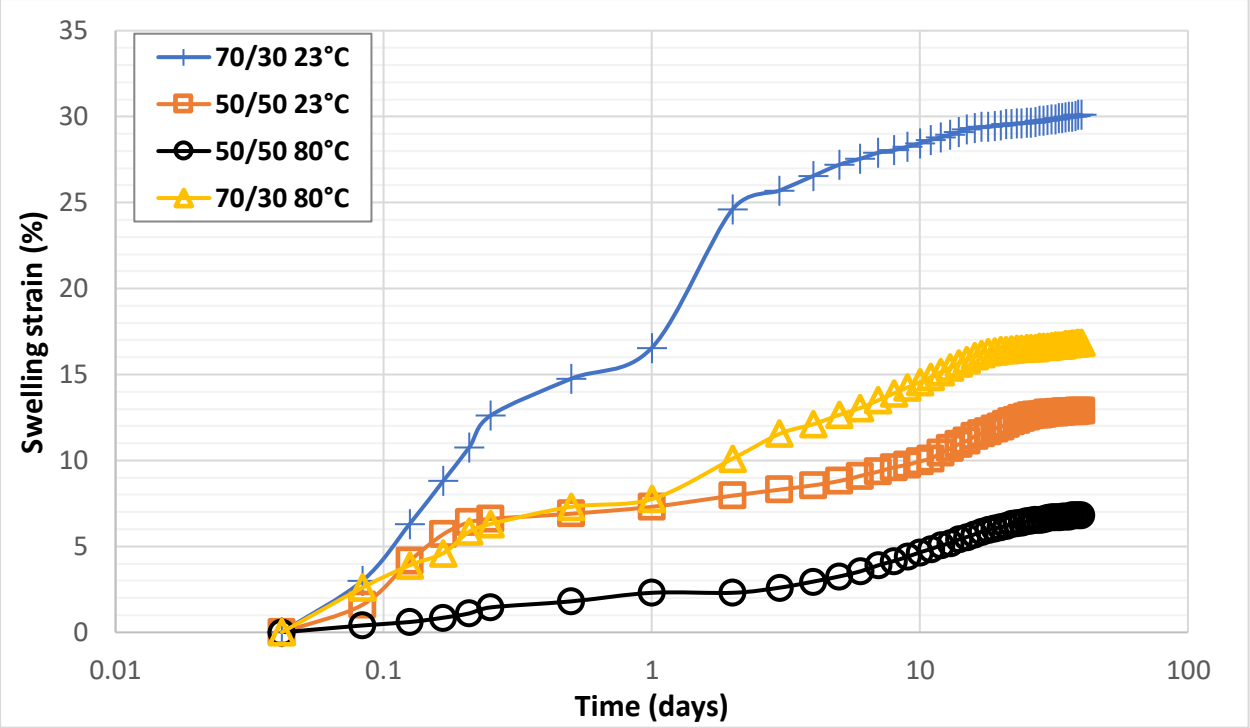

Figure 3.19. Coupled effect of the chemistry in the G solution and temperature on the swelling of: (a) 70:30 bentonite–sand mixtures and (b) 50:50 bentonite–sand mixtures (dry density: 1.6 g/cm^3)

3.4 Conclusions

Based on the results in this study, the following conclusions are made:

- The swelling potential of the studied compacted B/S mixture is significantly dependent on both its initial dry density and bentonite content. Higher dry density and/or larger B/S ratio leads to higher swelling strain of the material. The swelling strain follows a sigmoid relationship with log time, irrespective of the initial dry density and B/S ratio. The maximum swelling strain and the initial dry density follow a linear relationship for densities between 1.4 and 2.0 gm/cm^3.
- The chemical composition of the studied groundwaters significantly decreases the swelling potential of the B/S barrier material, irrespective of its initial dry density and bentonite content. However, the magnitude of this decrease in swelling depends on the

volume of TDS in the solution. The B/S mixture with more sand is better able to reduce the effects of chemicals in the water on the amount of swelling.

- The chemically induced reduction of the swelling potential of the B/S barrier material is caused by (i) the reduction of the DDL thickness of the montmorillonite particles due to a high volume of TDS and (ii) the transformation of Na-montmorillonites to Ca-montmorillonites with less swelling potential due to cation exchange.
- The rate of swelling and swelling potential of the B/S mixture is significantly reduced, not only due to the increase in salinity of the water (chemical factor), but also affected by the combined impact of the chemical factor and the temperature (thermal factor). Higher temperatures lead to more intense chemically induced deterioration of the swelling performance.
- It is recommended that, in the conceptual design of EBSs for HLW repositories in Ontario or Canada, not only the chemistry of the deep groundwater at potential DGR sites, but also the temperature expected within the EBS should be carefully considered to meet the design criteria with respect to swelling potential and swelling pressure of the selected bentonite-based barrier material.
- The findings presented in this paper will contribute to more cost-effective and safer design of EBS and DGR systems in Canada and other regions with similar groundwater chemistry.
- Despite these results, it is still necessary to investigate the swelling potential and swelling characteristics of compacted B/S mixtures at temperatures higher than 80°C in groundwater solutions with different chemical compounds. Moreover, it is necessary to assess the coupling effect of the chemistry of deep groundwater and temperature on the swelling pressure or stress of compacted B/S mixtures. This will be the object of future studies.

3.5 References

Akinwunmi B., Hirvi J. T., Kasa S., Pakkanen T. A. Swelling pressure of Na- and Ca-montmorillonites in saline environments: A molecular dynamics study, Chemical Physics, 528 (2020): 110511.

Amram K., Ganor, J. The combined effect of pH and temperature on smectite dissolution rate under acidic conditions. Geochimica et Cosmochimica Acta 69(10) (2005), 2535-2546.

Bradbury M.H., Baeyens B. Porewater chemistry in compacted re-saturated MX-80 bentonite. J. Contam. Hydrol., 61 (2003), 329-338.

Boudriche L., Calvet R., Hamdi B., Balard H. Surface properties evolution of attapulgite by IGC analysis as a function of thermal treatment. Colloids Surf. A Physicochem. Eng. Aspects 399 (2012), 1–10.

Castellanos E., Villar M.V., Romero E., Lloret A., Gens A. Chemical impact on the hydro-mechanical behaviour of high-density FEBEX bentonite. Phys. Chem. Earth 33 (2008) S516–S526.

Chen Y.-G., Sun Z., Cui Y.-J, Ye W.-M., Liu Q.-L., Effect of cement solutions on the swelling pressure of compacted GMZ bentonite at different temperatures. Construction and Building Materials 229(30) (2019), 116872.

Chen Y. G., Dong X.X., Zhang X-D, Ye W.-M., Cui Y.-J. Combined thermal and saline effects on the swelling pressure of densely compacted GMZ bentonite. Applied Clay Science, Volume 166(15) (2018), 318-326.

Chen Y.-G., Jia L.-Y., Li Q., Ye W.-M., Cui Y.-J., Chen B., 2017. Swelling deformation of compacted GMZ bentonite experiencing chemical cycles of sodium-calcium exchange and salinization-desalinization effect. Applied Clay Science, Volume 141 (2017): 55-63.

Chen, Y.G., Zhu, C.M., Ye, W.M., Cui, Y.J., Wang, Q., 2015. Swelling pressure and hydraulic conductivity of compacted GMZ01 bentonite under salinization-desalinization cycle conditions. Applied Clay Science, 114, 454-460.

Cho W.J., Lee J.O., Chun K.S., Hahn D.S. Basic physicochemical properties of domestic bentonite for use as a buffer material in a high-level radioactive waste repository, J. Korean Nucl. Soc. 31 (1999) 39–50.

Crowe R., Birch K., Freire-Canosa J., Chen J., Doyle D., Garisto F., Gierszewski P., Gobien M., Boyle C., Hunt N., Hirschorn S., Jensen M., Keech P., Kennell-Morrison L., Kremer E., Medri C., Mielcarek M., Murchison A., Parmenter A., Sykes E., Yang T. Technical Program for Long-Term Management of Canada's Used Nuclear Fuel – Annual Report . NWMO-TR-2017-01 December 2017.

Cui Y.-J. On the hydro-mechanical behaviour of MX80 bentonite-based materials. Journal of Rock Mechanics and Geotechnical Engineering 9(3) (2019): 565-574.

Cui SL, Zhang HY, Zhang M. Swelling characteristics of compacted GMZ bentonite–sand mixtures as a buffer/backfill material in China. Engineering Geology 141:65–73 (2012).

Delage P., Marcial D., Cui Y.J., Ruiz X.. Ageing effects in a compacted bentonite: a microstructure approach Géotechnique, 56 (5) (2006), 291-304.

Delage P., Lefebvre G. Study of the structure of a sensitive Champlain clay and its evolution during consolidation. Can. Geotech. J., 21 (1) (1984), 21-35.

DiPietro, J. A. (2018). *Geology and landscape evolution: General principles applied to the United States*. Elsevier.

Drits V., Lindgreen H., Salyn A., Ylagan R., McCarty D. Semiquantitative determination of trans-vacant and cis-vacant 2:1 layers in illites and illite-smectites by thermal analysis and X-ray diffraction, Am. Mineral. 83 (1998) 1188–1198.

European Commision. Third commission report on financing decommissioning, 2011. http://ec.europa.eu/energy/sites/ener/files/documents/seventh_situation_report_corr_version_without_cover_page.pdf.

International Energy Agency (2019), Electricity Information 2011, International Energy Agency Statistics, International Energy Agency, OECD, Paris, France.

Fall, M., Nasir, O., Nguyen, S. A coupled hydro-mechanical model for simulation of gas migration in host sedimentary rocks for nuclear waste repositories. Engineering Geology 176 (2014):24-44.

Frost R.L., Ding Z. Controlled rate thermal analysis and differential scanning calorimetry of sepiolites and palygorskites, Thermochim. Acta 397 (2003), 119–128.

Gleason, M. H., Daniel, D. E., and Eykholt, G. R.. Calcium and sodium bentonite for hydraulic containment applications. Journal of Geotechnical and Geoenvironmental Engineering, 123 (5) (1997): 438–445.

Gobien M., Garisto F., Kremer E., Medri C.. Seventh Case Study: Reference Data and Codes. Report, NWMO-TR-2018-10, Nuclear Waste Management Organization (2018).

Guo, G., Fall, M (2021). Advances in modeling of hydromechanical processes in gas migration within saturated bentonite. Engineering Geology 287: 106123.

Guo, G., Fall, M 2020. A thermodynamically consistent phase field model for gas migration in saturated bentonite accounting for initial stress state. Transport in Porous Media 137(11),1-38.

Guo, G., Fall. M. Modelling of preferential gas flow in heterogeneous and saturated bentonite based on phase field method. Computer & Geotechnics 116 (2019): 103206.

Guo, G., Fall, M. Modelling of dilatancy-controlled gas flow in bentonite based materials with double porosity and double effective stress concepts. Engineering Geology 243(4) (2018):253-271.

He Y, Ye WM, Chen YG, Cui YJ. Effects of K+ solutions on swelling behaviour of compacted GMZ bentonite. Engineering Geology 249 (2019) 241-248.

Hobbs, M.Y., S. Frape, O. Shouakar-Stash and L.R. Kennell. Regional Hydrogeochemistry - Southern Ontario. Nuclear Waste Management Organization Report DGR-TR-2011-12. (2011). Toronto, Canada.

Huertas F.J., Caballero E., Jimenez de Cisneros C., Huertas F., Linares J. Kinetics of montmorillonite dissolution in granitic solutions. Appl. Geochem., 16 (2001), 397-407.

Jensen M., Lam T., Luhowy D., McLay J., Semec B., Frizzell R. Ontario Power Generation's proposed L&ILW deep geologic repository: an overview of geoscientific studies. Canada: N. p., Proceeding from the 62nd Canadian Geotechnical Conference and the 10th Joint CGS/IAH-CNC, GeoHalifax2009.

Karnland O., Olsson S., Nilsson U., Sellin P. Experimentally determined swelling pressures and geochemical interactions of compacted Wyoming bentonite with highly alkaline solutions. Physics and Chemistry of the Earth, Parts A/B/C, 32 (1) (2007), 275–286.

Karnland O., Birgersson M., Montmorillonite stability with respect to KBS-3 conditions, SKB Technical Report (06–11), (2006).

Kim, J.S., Kwon, S.K., Sanchez, M., Cho, G.C., Geological Storage of High Level Nuclear Waste. KSCE Journal of Civil Engineering, 15(4) (2011):721-737.

Komine H., Yasuhara K., Murakami S. Swelling characteristics of bentonites in artificial seawater, Canadian Geotechnical Journal 46 (2009) 177–189.

Lawrence, P. Stability of soil pores during mercury intrusion porosimetry. J. Soil Sci., 29 (1978), 299-304.

Liu L.-N., Chen Y.-G., Ye W.-M., Cui Y.-J., Wu D.-B. Effects of hyperalkaline solutions on the swelling pressure of compacted Gaomiaozi (GMZ) bentonite from the viewpoint of Na+ cations and OH– anions, Applied Clay Science 161(2018), 334-342.

Liu L. Prediction of swelling pressures of different types of bentonite in dilute solutions, Colloids Surf. A: Physico-chem. Eng. Asp. 434 (2013), 303–318.

Mata C M, 2003. Hydraulic behaviour of bentonite based mixtures in engineered barriers: the backfill and plug test at the Äspö Hrl (Sweden). PhD thesis, Universitat Politècnica de Catalunya.

Moore D.M., Reynolds R.C., X-ray Diffraction and the Identification and Analysis of Clay Minerals, Oxford University Press, Oxford, New York, 1989.

Nasir, O., Fall, M., Nguyen, S, Evgin, E. Modeling of the thermo-hydro-mechanical-chemical response of Ontario sedimentary rocks to future glaciations. Canadian Geotechnical Journal 52(7) (2015):836-850.

Nasir, O., Fall, M., Evgin, E, (2014). A Simulator for Modeling of Porosity and Permeability Changes in Near Field Sedimentary Host Rocks under Climate Changes Influences. Tunnelling and Underground Space Technology 42 (2014):122-135.

Nasir, O., Fall, M., Nguyen, S., Evgin, E. Modeling of the thermo-hydro-mechanical-chemical response of sedimentary rocks of Ontario to past glaciations. International Journal of Rock Mechanics and Mining Sciences 64 (2013):160-174.

Navarro V., Yustres Á., Asensio L., De la Morena G., González-Arteaga J., Laurila T., Pintado X. Modelling of compacted bentonite swelling accounting for salinity effects. Engineering Geology 223(7)(2017):48-58.

NWMO. Moving Forward Together: Process for Selecting a Site for Canada's Deep Geological Repository for Used Nuclear Fuel. Nuclear Waste Management Organization Report APM-CORR-06140-23798 (2017). Toronto, Canada.

Nuclear Waste Management Organization. 2011. Geosynthesis. NWMO DGR-TR-2011-11. https://www.ceaa-acee.gc.ca/050/documents_staticpost/17520/49819/geosynthesis-tsd.pdf

Organisation for Economic Co-operation and Development and European Commission. Engineered Barrier Systems and the Safety of Deep Geological Repositories, State-of-the-art Report (2003). EUR 19964 EN. ISBN 92-64-18498-8. European Commission. Luxembourg. OECD. Paris.

Penumadu D., Dean J. Compressibility effect in evaluating the pore-size distribution of kaolin clay using mercury intrusion porosimetry. Can. Geotech. J., 37 (2000), 393-405.

Pusch, R. On the effect of hot water vapor on MX-80 clay. Geodevelopment AB, Lund. Technical Report:TR-00-16, KSB (2000).

Rao F S.M., Thyagaraj T. Role of direction of salt migration on the swelling behaviour of compacted clays, Applied Clay Sciences. 38 (2007a) 113–129.

Rawat A., Baille W., Tripathy S. Swelling behaviour of compacted bentonite-sand mixture during water infiltration. Engineering Geology 257 (26) (2019): 105141.

Rutqvist J., Zheng L., Chen F, Liu H.-H. and Birkholzer J. Modeling of Coupled Thermo-Hydro-Mechanical Processes with Links to Geochemistry Associated with Bentonite-Backfilled Repository Tunnels in Clay Formations. Rock Mechanics and Rock Engineering, 47, 167-186 (2014).

Shehata, A., Fall, M., Detellier C. Impact of groundwater chemistry on the swelling properties of bentonite-based barriers for radioactive wastes repositories. Bulleting of Engineering Geology and the Environment (2021), https://doi.org/10.1007/s10064-020-02020-5.

Siddiqua S., Blatz J., Siemens G.. Evaluation of the impact of pore fluid chemistry on the hydromechanical behaviour of clay-based sealing materials. Canadian Geotechnical Journal, 48 (2011), 199-213.

Sills I.D., Aylmore L.A.G., Quirk J.P. A comparison between mercury injection and nitrogen sorption as methods of determining pore size distributions,Soil Sci. Soc. Am. Proc., 37 (1973), 535-537.

Simms, P.H., Yanful, E.K.: A discussion on the application of mercury intrusion porosimetry for the investigation of soils, including an evaluation of its use to estimate volume change in compacted clay. Géotechnique 54(6) (2004), 421–426.

Sun D.A., Zhang L., Li J., Zhang B.C. Evaluation and prediction of the swelling pressures of GMZ bentonites saturated with saline solution, Applied Clay Sciences. (2015) 105–106, 207–216.

Sun D., Zhang J., Zhang J., Zlang L. (2013). Swelling characteristics of GMZ bentonite and its mixtures with sand. Applied Clay Science 83-84:224-230.

Sun D., Cui H., Sun W., Swelling of compacted sand–bentonite mixtures, Applied Clay Science. 43 (2009) 485–492.

Suzuki S., Prayongphan S., Ichikawa Y., Chae B.G. In situ observations of the swelling of bentonite aggregates in NaCl solution. Applied Clay Sciences 29 (2005) 89–98.

Tang C.S., Tang A.M., Cui Y.J., Delage P., Schroeder C., Shi B., 2011. A study of the hydro-mechanical behaviour of compacted crushed argillite. Engineering Geology, 118 (3–4) (2011), 93-103.

Ureana C., Azañón J.M., Corpas F., Nieto F., León C., Pérez L., Magnesium hydroxide, seawater and olive mill wastewater to reduce swelling potential and plasticity of bentonite soil, Construction and Building Material, 45 (2013), 289–297.

Villar M.V., Lloret A. Influence of dry density and water content on the swelling of a compacted bentonite. Applied Clay Science, 39 (2008) 38–49.

Villar, M.V., 2006. Infiltration tests on a granite/bentonite mixture: Influence of water salinity. Applied Clay Science, 31(1-2), 96-109.

Wang Q., Cui Y.-J., Tang A. M., Delage P., Gatmiri B., Ye W.-M. Long-term effect of water chemistry on the swelling pressure of a bentonite-based material. Applied Clay Science 87 (2014): 157-162.

Wang Q., Tang A. M., Cui Y., Delage P., Gatmiri B., Experimental study on the swelling behaviour of bentonite/claystone mixture, Engineering Geology 124 (2012): 59–66.

Xu H., Zheng L., Rutqvist J., and Birkholzer J. Numerical study of the chemo-mechanical behaviour of FEBEX bentonite in nuclear waste disposal based on the Barcelona expansive model. Computers and Geotechnics 132, 103968 (2021).

Yang, J., Fall, M. 2021. A two-scale time dependent damage model for preferential gas flow in clayey rock materials. Mechanics of Materials 158: 103853.

Yang, J., Fall, M., Guo, G. 2020. A three-dimensional hydro-mechanical model for simulation of dilatancy controlled gas flow in anisotropic claystone. Rock Mechanics and Rock Engineering, 53, 4091-4116, doi: 10.1007/s00603-020-02152-w.

Ye WM, Zheng ZJ, Chen B, Chen YG, Cui YJ, Wang J. Effects of pH and temperature on the swelling pressure and hydraulic conductivity of compacted GMZ01 bentonite. Applied Clay Sciences, 2014, 101: 192-198.

Ye WM, Wan M, Chen B, Chen YG, Cui YJ, Wang J. Temperature effects on the swelling pressure and saturated hydraulic conductivity of the compacted GMZ01 bentonite. Environmental Earth Sciences, 2013, 68(1): 281-288.

Ye WM, Chen YG, Chen B, Wang Q, Wang J. Advances on the knowledge of the buffer/backfill properties of heavily-compacted GMZ bentonite. Engineering Geology, 2010, 116(1-2): 12-20.

Zhang H., Tan Y., Zhu J., He D., Zhua J.Shrinkage property of bentonite-sand mixtures as influenced by sand content and water salinity. Construction and Building Materials 224 (2019), 78-88.

Zhang H.Y., Cui S.L., Zhang M., Jia L.Y. Swelling behaviours of GMZ bentonite-sand mixtures inundated in NaCl-Na2SO4 solutions, Nuclear Engineering and Design, 242 (2012) 115–123.

Zheng L., Rutqvist J., Birkholzer J.T., and Liu H.H. Coupled THMC models for bentonite in an argillite repository for nuclear waste: illitization and its effect on swelling stress under high temperature. Engineering Geology, 230, 118-129 (2017).

Zheng L., Rutqvist J., Birkholzer J.T. and Liu H.H. On the impact of temperatures up to 200ºC in clay repositories with bentonite engineer barrier systems: a study with coupled thermal, hydrological, chemical, and mechanical modeling. Engineering Geology, 197, 278-295 (2015).

Chapter 4: Technical paper II: Saturated Hydraulic Conductivity of Bentonite-Sand Barrier Material for Nuclear Waste Repository: Effects of Physical, Mechanical Thermal and Chemical Factors

Environmental Earth Sciences Journal 81: Article 223 (2022)
Mohammed Alzamel, Mamadou Fall, Sada Haruna

Abstract

Deep geological repositories (DGRs) have been viewed as the most promising technology for the long-term management of nuclear wastes. One of the major functions of the buffer or barrier material used in DGRs for nuclear waste is to prevent the transportation of high-level radioactive chemicals into the biosphere in the case of failure. To achieve that, the buffer is usually designed to have very low hydraulic conductivity. The effects of mix-composition, swelling condition, temperature, and groundwater chemistry on the hydraulic conductivity of compacted bentonite-sand barrier material were investigated. Permeability tests were carried out using flexible wall permeameter after inundating the compacted samples in simulated groundwaters. The obtained results showed that the saline groundwater prevalent in the Guelph region of Canada as well as high temperature have a negative impact on the swelling potentials of the buffer material, consequently increasing the hydraulic conductivity. The saline water reduces the thickness of the diffuse double-layer which is accompanied with low repulsion between the clay minerals. Similarly, high temperature decreases the basal spacing between the bentonite clay minerals which also results in less swelling. Furthermore, it was observed that restricting the swelling of the bentonite-sand mixture produces well-packed material with very low hydraulic conductivity as compared to free swelling. Increasing both the percentage of bentonite and the initial dry density of the mixture were also observed to reduce hydraulic conductivity by eliminating interparticle voids in the material. The research findings presented in this manuscript provide valuable information that will contribute to gain a deeper insight into the impact of field conditions (temperature, groundwater chemistry, confinement) and material characteristics (composition, dry density) on the permeability of bentonite-sand barrier, which is essential for a safe long-term management of radioactive wastes.

Keywords: Bentonite–sand mixture; engineered barrier material; deep geological repository; hydraulic conductivity; pore water chemistry; temperature; nuclear waste management.

4.1 Introduction

Deep geological repositories (DGRs) have been regarded as the most promising technology for the long-term management of nuclear wastes. A critical component of any DGR is the engineered barrier system (EBS). Compacted bentonite is commonly proposed as a buffer and sealing material for the construction EBS in the deep geological repositories (DGRs) for storing radioactive wastes from nuclear power plants (Guo and Fall 2018, 2021; Adamacová and Frankovská, 2009; Ye et al., 2016; Liu et al., 2019). This is because of bentonite's favourable properties, most importantly its high swelling potential owing to its smectite clay minerals contents (Shehata et al., 2015). At the initial stage, the EBS constitutes unsaturated bentonite that begins to swell once it comes in contact with groundwater (Pathak, 2017). Being a clay with high plasticity, the swelling allows the bentonite makes the EBS almost impermeable, thereby stopping or delaying water from percolating into the repository (Cho et al., 2010; Pindato et al., 2018). In addition, the smectite minerals have high adsorption capacity, low thermal conductivity, and high cation exchange capacity (Quintessa, 2011; Pathak, 2017), all of which are important for reducing the chances of contaminant leakage in case of failure. However, pure bentonite does not have sufficient mechanical strength to withstand the stress within and around the deep repository (Martin et al., 2000; Ito, 2006). Moreover, the high swelling pressure of pure bentonite could result in the development of excessive swelling stress that may mechanically damage the canisters (Shehata et al., 2021). This has inspired several research studies in recent years on the use of bentonite-sand mixture as a potential buffer and sealing material in the EBS (Mollins et al., 1996; Akgün et al., 2006; Gatabin et al., 2016; Siddiqua et al., 2018). Furthermore, sand-bentonite mixture, which enables a better control of the swelling pressure, has better thermal conductivity (high thermal conduction facilitates the transport of the heat generated in the canisters) than pure bentonite, decreases material cost, and improves compaction ability (Shehata et al., 2015).

The swelling capacity of bentonite, which governs its hydraulic conductivity, is affected by certain factors, one of which is the chemistry of the pore water it is exposed to, as shown by previous studies (Zhu et al., 2013; Weimin et al., 2014; Navarro et al., 2017; Liu et al., 2018; Shehata et al., 2021). Typically, the smectite minerals that makes up the bentonite absorb water whenever possible, leading to the increase of the total volume of the clay (Önal, 2006). This is achieved either through crystalline swelling, in which water enters into the clay's interlayers to cause repulsion or by osmotic swelling, in which the repulsion comes from the interaction of diffuse double layers water (González, 2013; Jiang et al., 2014). However, the presence of salt in the water limits the swelling capacity of bentonite clays (Komine et al., 2009; Xiang et al., 2019). In one study by Ye et al., (2014), exposing compacted bentonite to NaCl solutions was found to decrease its swelling strain and increase its hydraulic conductivity. The reason was cited to be the domination of the osmotic pressure caused by the fluid within the clay layers by an inward transportation of the salts. Zhu et al. (2013) had similar observations with infiltration solutions containing NaCl and $CaCl_2$.

Both the groundwater chemistry and temperature are key parameters that may vary within deep geological formations where DGRs are located (Fall et al., 2014; Nasir et al., 2015). There is also a tendency for the stored nuclear waste to generate heat during the lifetime of the DGR (Guo, 2016). With respect to salinity, it is important to mention that some of the locations proposed for building DGRs in Canada (e.g., Guelph area in southern Ontario) are in regions known to have groundwater with high level of salinity (Sterling, 2011; Fall et al., 2018; Sheheta et al., 2021). According to Karnland et al. (2007), high salt content in the water may destabilize the chemical structure of minerals such as, but not limited to the transformation of smectite to illite. Likewise, an experimental study by Wang et al. (2012) showed that the swelling pressure of compacted bentonite samples decreases significantly when immersed in water with high salinity as compared to bentonite samples exposed to distilled water. However, their results are

not directly transferable to a bentonite–sand barrier material in Canadian DGR conditions because Canadian groundwaters feature different chemical compositions than the groundwaters examined in previous investigations.

The hydraulic conductivity is a significant parameter in the EBS design as it governs the rate of fluid transport into and out of the repository. In the incidence of cannister failure, a highly permeable barrier material may allow the migration of radioactive compounds through advective flow between the DGR and areas with different hydraulic gradients (Rao et al., 2008; Selvadurai and Glowacki, 2018; Jadda and Bag, 2020). Several factors such as particles size, swelling potential of the bentonite, compacted density, pore water chemistry and temperature play a role on the hydraulic conductivity of bentonite-based barrier materials (Stewart et al., 2003; Ebina et al., 2004; Jadda and Bag, 2020). The use of bentonite-sand mixture as a potential barrier material is a recent proposal, therefore its performance under different ground conditions has not been fully understood. Previous studies have shown that incorporation of sand in the mixture increases the hydraulic conductivity proportionally with respect to the size and percentage of the sand (Sivapullaiah et al., 2000; Sällfors and Öberg-Högsta, 2002). Another study has shown that increasing the initial compacted density by a about 30% reduces the hydraulic conductivity from 10^{-12} to 10^{-14} m/s, which is a significant improvement (Cho et al., 2000). Also, Mishra and Ohtsubo (2009) investigated the effect of NaCl and $CaCl_2$ on the hydraulic conductivity of bentonite-sand mixtures. They observed that increasing the content on each of the salts in the barrier material results in the increase of the hydraulic conductivity. Nevertheless, none of the studies in the literature assessed the hydraulic properties of the bentonite-sand composite in the presence of naturally occurring saline (Canadian) groundwaters with a combined effect of the variation of physical (i.e. density, blending ratio), mechanical (i.e. confinement, free swell) and thermal (i.e. temperature) properties.

Thus, the current study aims at bridging the gap on the current understanding of the behaviour of bentonite-sand buffer material exposed different groundwaters under varying physical, mechanical and thermal factors. The findings will be instrumental on proper design of DGRs for nuclear waste disposal.

4.2 Experimental Program

4.2.1 Materials

Laboratory tests were conducted on bentonite-sand mixtures with 30:70 and 70:30 dry mass ratios. The bentonite clay is an MX-80 type that was extracted from Wyoming, USA with chemical composition presented in Table 4.1. An X-Ray Diffraction (XRD) analysis revealed that montmorillonite is the dominant mineral in the clay, with traces of other minerals, namely quartz, calcite, kaolinite and feldspar (Figure 4.1). The main exchangeable cation in the MX-80 bentonite is Na^+ and it has a cation exchange capacity (CEC) of 105 meq/100 g. The sand used is a GS-20 silica with 99.99% quartz (SiO_2), specific gravity of 2.65 and grain size distribution ranging from 0.2 – 1.9 mm.

Table 4.1. Properties of the MX-80 bentonite

Property	**Description**
Specific gravity	2.66
Liquid limit (%)	530
Plastic Limit (%)	48.5
Cation exchange capacity (mmol/100 g)	105
Montmorillonite content (%)	90

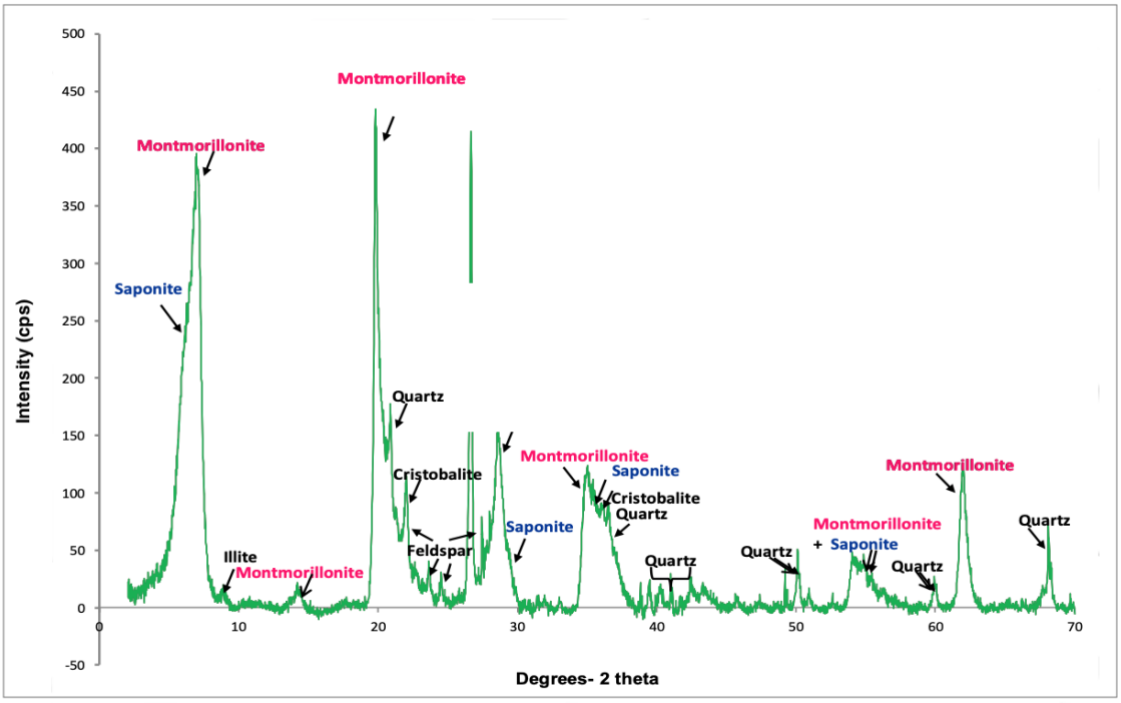

Figure 4.1. Mineralogical content of the MX-bentonite as observed by XRD analysis

To assess the effect of groundwater chemistry on the bentonite-sand mixtures, distilled water (DW) and a solution containing total dissolved solids similar to the groundwater located in the Guelph (G) region of Ontario, Canada were used. Their chemical compositions are given in Table 4.2.

Table 4.2. Chemical composition of the solutions used in the study

Element (g/l)	**DW**	**G**
$CaCl_2$	0	159
NaCl	0	100
$MgCl_2$	0	34.3
KCl	0	6.3
K_2SO_4	0	0.4
TDS	0	300
pH	7	5.7

DW: distilled water; G: Guelph Groundwater

4.2.2 Preparation and curing of specimens

The bentonite and sand were first oven-dried for 24 hours to remove any moisture. Two different mix compositions 70:30 and 30:70 ratios of the dry mass of the bentonite and sand were used. Weighed portions of the materials were first mixed in a bowl using a spoon to achieve a uniform mixture. An amount of water equivalent to the moisture content corresponding to the compacted dry density for each composition was added, and the material was further mixed to achieve homogeneity. The experimental program with the information on the compositions and curing conditions is presented in Table 4.3. An acrylic cylinder of 4.5 cm inside diameter, 5 cm outside diameter and 3 cm height was used to cast the specimen for the permeability test. The curing of the sample was done by inundating the compacted bentonite-sand mixture with DW or G solution as the case may be, and then allowed to swell freely (free swelling) or under confinement (restricted swelling). For the free swelling, the bentonite-sand mixture was compacted in a 6.3 cm diameter by 10 cm height acrylic plastic mould to the desired density as shown in Figure 4.2a. The initial height of the specimens was 2 cm to allow enough room for volume change. After compaction, the mould was filled up with the curing water, covered with a foil to minimize evaporation and then placed in a temperature control chamber for 60 days. The mould was checked regularly and refilled with the curing water whenever needed. At the end of the curing period, a specimen for hydraulic conductivity was cut using the 4.5 cm by 3 cm cylinder as shown in Figure 4.2b. For the restricted swelling, the bentonite-sand mixtures were compacted in the 4.5 cm by 3 cm cylinder to the desired density and then covered on both sides by a porous acrylic disc. The assembly was tied with two metal clips as shown in Figure 4.2c after which it was immersed in the curing water and kept for 60 days as shown in Figure 4.2d. This approach enabled to keep the volume of the bentonite-sand material constant during the immersion phase. At the end of the curing period, the clips and the covers were removed, leaving the specimen in the cylinder for the hydraulic conductivity test.

4.2.3 Hydraulic conductivity test

The saturated hydraulic conductivity of the bentonite-sand specimens exposed to different curing conditions was determined using a flexible wall permeability test in compliance with the ASTM D5084 standard. The curing cylinder containing the specimen was enclosed in a latex membrane and a confining pressure of 40 psi (275 kPa) was used to eliminate seepage between the membrane and the cylinder. A constant head method was used with the pressure difference of 10 psi (69 kPa) between the inflow and outflow. The specimens were fully saturated prior to the test (degree of saturation determined to equal to 100%), therefore no further saturation was necessary. Each hydraulic conductivity test was conducted at least twice to ensure results repeatability, which satisfies the standard error (*Sr*) of 2.9 x 10^{-9} cm/s as specified by the standard.

Table 4.3. Summary of the mix compositions and curing conditions

Sample name	Bentonite content (%)	Sand content (%)	Dry density (g/cm^3)	Mixing Water	Curing[a] water	Curing[b] Temperature (^oC)	Curing time[c] (days)
B/S-70/30-1.63-20C-DW	70	30	1.63	DW	DW	20	60
B/S-30/70-1.63-20C -DW	30	70	1.63	DW	DW	20	60
B/S-70/30-1.63-20C -G	70	30	1.63	G	G	20	60
B/S-30/70-1.63-20C -G	30	70	1.63	G	G	20	60
B/S-70/30-2.0-20C -G	30	70	2.0	G	G	20	60
B/S-30/70-2.0-20C -G	70	30	2.0	G	G	20	60
B/S-70/30-1.63-80C DW	70	30	1.63	DW	DW	80	60
B/S-30/70-1.63-80C -DW	30	70	1.63	DW	DW	80	60
B/S-70/30-1.63-80C -G	70	30	1.63	G	G	80	60
B/S-30/70-1.63-80C -G	30	70	1.63	G	G	80	60
B/S-70/30-2.0-80C -G	30	70	2.0	G	G	80	60
B/S-30/70-2.0-80C -G	70	30	2.0	G	G	80	60

a: the water used when the samples are being subjected to free and confined swelling; b: the temperature to which the samples are subjected during c; c: the duration of the free swelling of all samples is equal to 60 days to enable the comparison of the results. B/S = bentonite-sand mixture; DW: Distilled water; G: Guelph solution

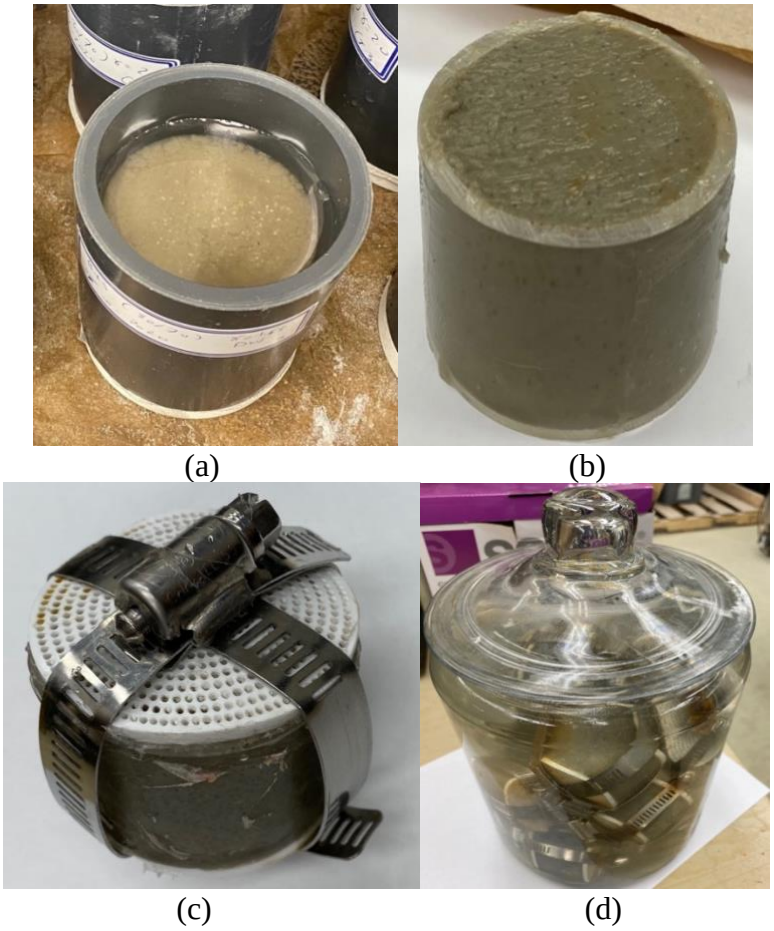

Figure 4.2. Specimens preparation and curing (a) Free Swelling mould (b) Specimen cut for permeability test (c) Restricted swelling assembly (d) Curing of restricted swelling specimens

4.2.4 Microstructural analyses

Two microstructural analysis techniques were adopted to investigate the effect of initial dry density and curing condition on the pore structure of the studied samples and how that affects the hydraulic conductivity. Specimens prepared and cured as described in section 4.3 were oven-dried at 45 ^{o}C over until there was not any moisture in them (when volume change becomes zero). The microstructural techniques are mercury intrusion porosimetry (MIP) and scanning electron microscopy (SEM). The MIP was performed using a Micrometrics AutoPore III 9420 mercury porosimeter (Micrometrcs, Norcross, US) based on ASTM D4404 standard. The MIP test was conducted at the porous materials Inc. (PMI) laboratory facility, New York, USA. The SEM analysis of the specimens was performed using Hitachi S4800 Scanning

Electron Microscope (Hitachi Ltd., Tokyo, Japan). The test was conducted at the Microanalysis lab, University of Ottawa.

4.3 Results and discussion

4.3.1 Effect of swelling condition and groundwater chemistry on the hydraulic conductivity of bentonite-sand mixtures

Effects of mix proportions and swelling conditions on the hydraulic conductivity of compacted bentonite-sand mixture exposed to different solutions are depicted in Figures 4.3. It can be observed that the hydraulic conductivity of mixtures under confinement is generally lower than that of mixtures under free swelling regardless of the chemical composition of the water it is exposed to. The samples under free swelling have hydraulic conductivity values ranging from 2.32×10^{-11} m/s to 7.91×10^{-11} m/s while those under confined conditions have hydraulic conductivity values ranging from 4.52×10^{-13} m/s to 1.79×10^{-12} m/s, respectively. According to Likos and Wayllace (2010), the total volume change of compacted bentonite is greater under free swelling, but the excessive swelling pressure in a confined bentonite leads to less porosity. They associated the large volume change under free swelling to a concurrent expansion of interparticle voids. Specifically, low confining stress conditions (i.e., free swelling) yields a material with higher volume of inter-particles and inter-layer voids as well as more open fabric. Conversely, high confining stress conditions results in densely packed fabric with lower volume of voids. This argument is in agreement with the results MIP tests presented in Figure 4.4. This shows total porosity graphs from an MIP analysis on specimens with a bentonite-sand ratio of 30:70 and cured under the two swelling conditions for 60 days. It can be observed that the confined specimen has pores with a cumulative volume of only 0.21% against 2% for the specimen under free swelling. Also, only pores of diameter 80 and 100 µm were present in the confined specimen, whereas multiple pores with diameter ranging from 0.007 to 100 µm were observed in the free swelling specimen. The two large pore families

were probably generated by shrinkage during the drying process, which takes place before the mercury intrusion test. Thus, optimum sealing from the bentonite-based barrier material is achieved when it is effectively confined. This conclusion is consistent with the results from other experimental studies on compacted bentonite as well as bentonite-sand mixtures (Cui et al., 2008; Gueddouda et al., 2010; Ye et al., 2012; Niu et al., 2020).

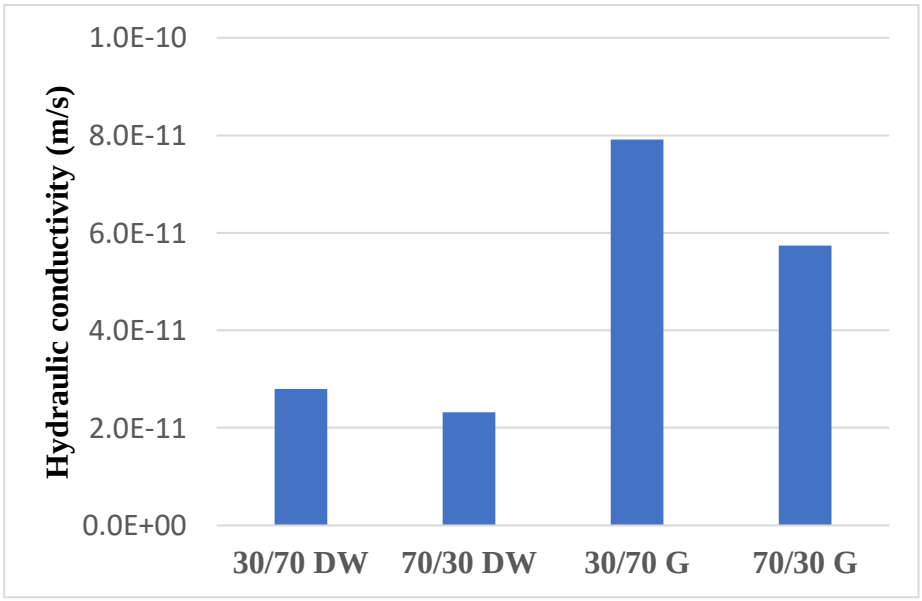

(a)

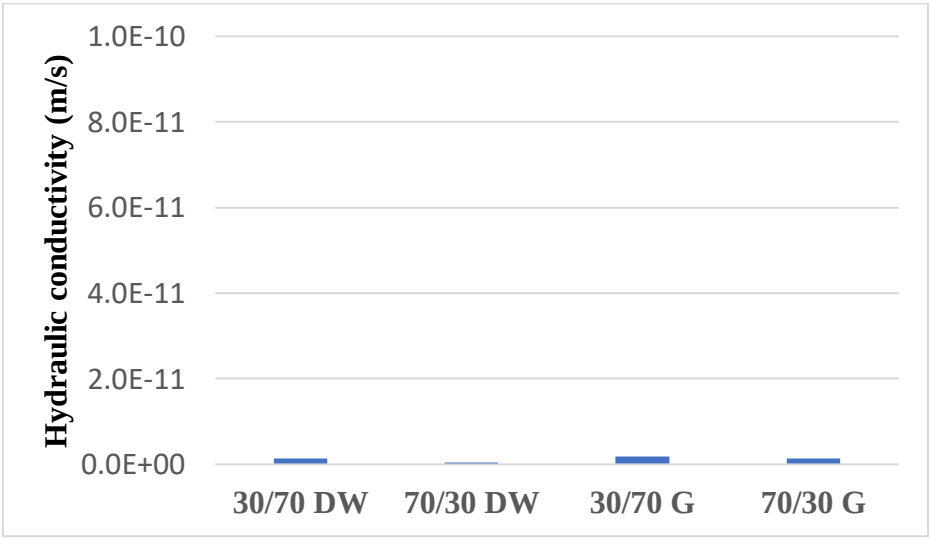

(b)

Figure 4.3. Hydraulic conductivity of bentonite-sand mixtures with different bentonite-sand ratios exposed to two different solutions and swelling conditions at room temperature (a) Free swelling (b) Restricted swelling

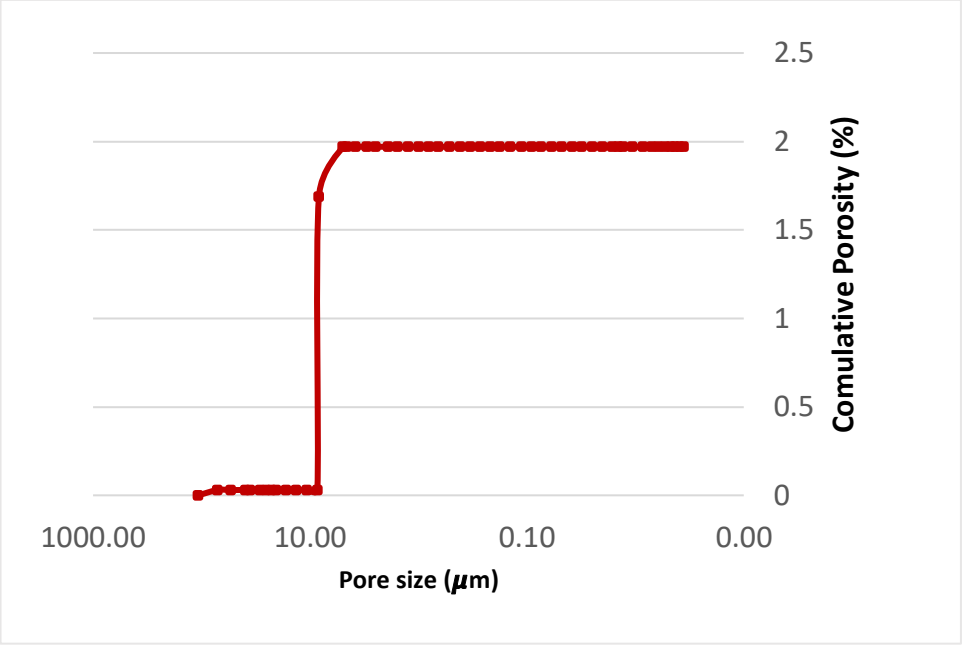

(a)

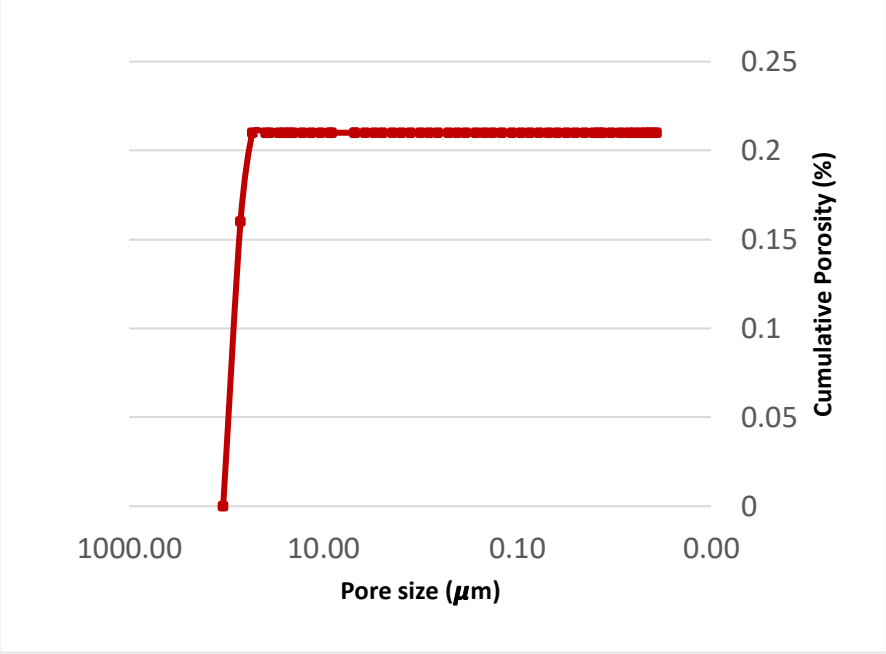

(b)

Figure 4.4. MIP cumulative pore volume for bentonite-sand mixtures cured in distilled water (a) Free swelling (b) Restricted swelling

Beside the effect of swelling condition, it can also be observed from Figure 4.3 that bentonite-sand mixture with 30:70 blending ratio is more permeable than that 70:30 for every curing condition. This means higher bentonite content results in lower hydraulic conductivity

as it would be expected. A previous study by Xu et al. (2016) revealed an increase of hydraulic conductivity of bentonite-sand mixture from 8.39 $x10^{-14}$ m/s to 6.47 x 10^{-13} m/s by increasing the sand content from 10% to 50%. The size of the sand used in the composite buffer material appears to play role on its permeability. Table 4.4 compares the range of hydraulic conductivity from previous studies with that from the present work with the summary of the bentonite-sand proportions and the particle sizes of the sand used. It is evident that the range of the particle size and the proportion of the sand in the mixture have a combined effect on the hydraulic conductivity. The SEM images presented in Figure 4.5 supports this assertion. As it can be observed, the sand particles are clearly seen in the 30/70 specimen, but completely covered by the bentonite clay in the 70/30 specimen. The size and distribution of the pores in the bentonite-sand material will offer a clearer explanation on the different in permeability in the two specimens. Although the total porosity is higher in the 70/30 specimen than the 30/70, the threshold diameter for the mercury intrusion is only about 0.2 µm in the former and 9 µm in the later (Figure 4.6). According to Winslow and Diamond (1969), the threshold diameter represents the pore size at which the rate of mercury flow in the specimen is the highest. Typically taken as the first point of inflection on the total porosity curve, it represents the group of pores that are interconnected, thereby allowing a continuous permeation (Aligizaki, 2006). Thus, hydraulic conductivity of the 30/70 would be higher as it has larger threshold diameter.

Table 4.4. Comparison of hydraulic conductivity values from previous studies

Research work	**Lower limit of k (m/s)**	**Proportion of sand**	**Sand particle size (mm)**
Current study	1×10^{-13}	30-70	0.2 – 1.9
Xu et al., (2016)	1×10^{-14}	0-50	0.075-0.1
Cho et al., (2000)	1×10^{-11}	0-70	0.075-0.84
Zhang et al., (2012)	1×10^{-10}	0-50	0.5-0.1

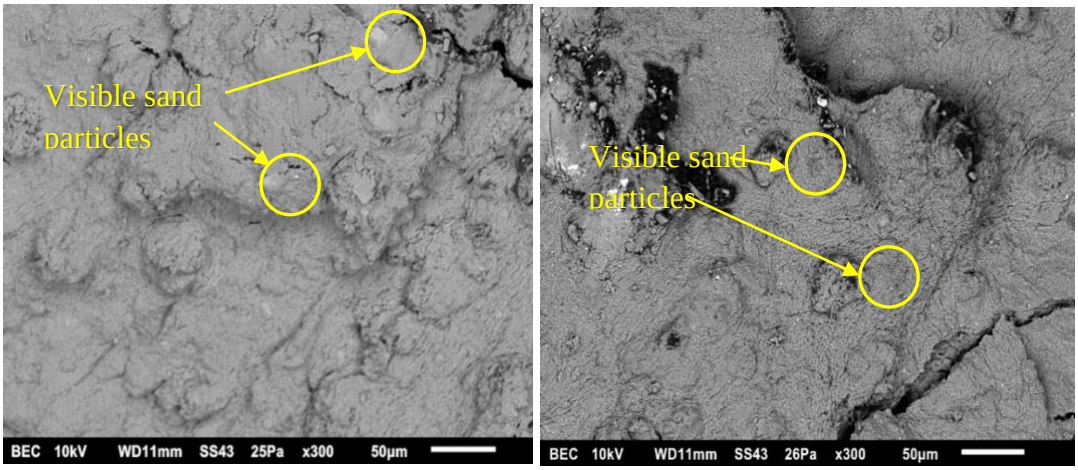

(a) (b)

Figure 4.5. SEM images of compacted bentonite-sand mixture with different bentonite/sand ratios (a) 30/70 mixture (b) 70/30 mixture

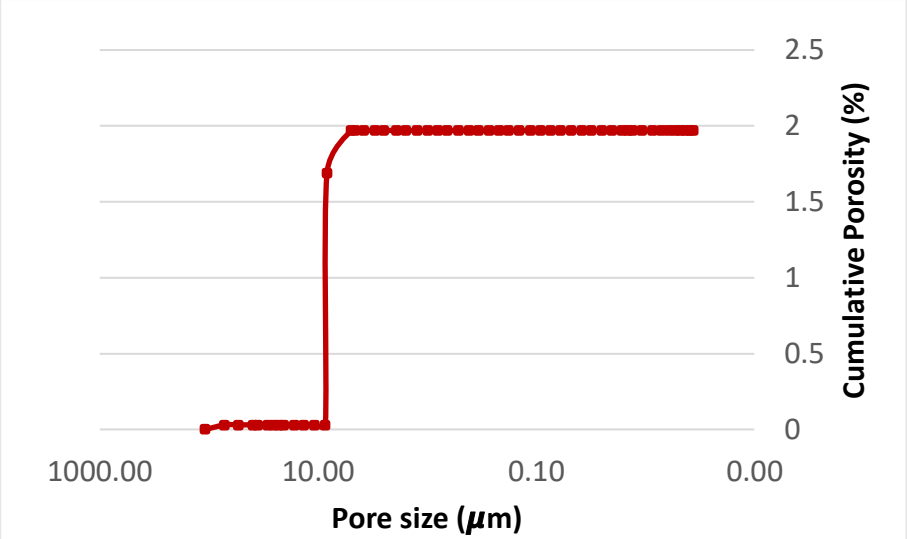

(a)

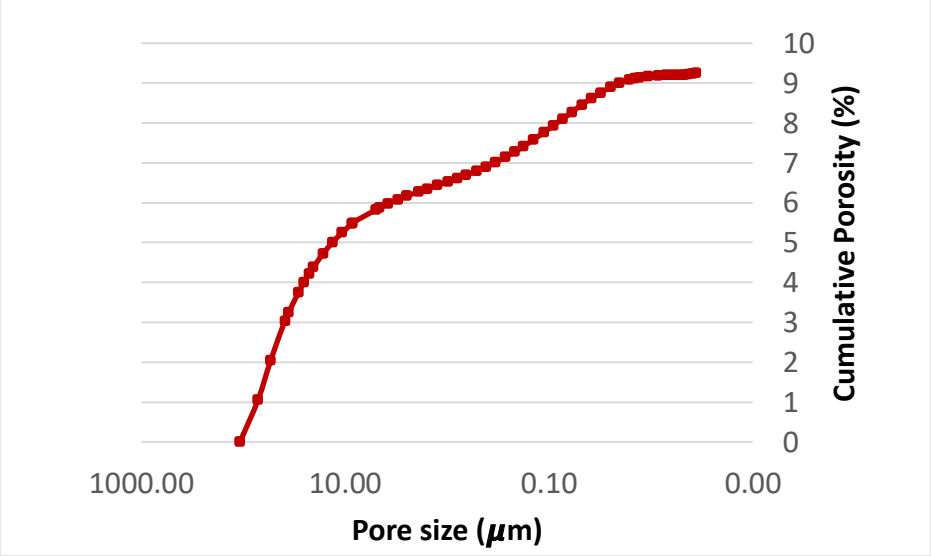

(b)

Figure 4.6. MIP cumulative pore volume for compacted bentonite-sand mixture with different bentonite/sand ratios (a) 30/70 specimen (b) 70/30 specimen

Another important information that can be inferred from Figure 4.3a and 4.3b is the effect of groundwater chemistry on the hydraulic conductivity. Both free and restricted swelling specimens show higher hydraulic conductivity when exposed to solution G. For example, the 30/70 bentonite-sand mixture exposed to DW in a free swelling condition has a hydraulic conductivity of 2.79 x 10^{-11} m/s. Same mixture that was exposed to the G saline

solution has a hydraulic conductivity of 7.91 x 10^{-11} m/s. It is generally accepted that the presence of salt in the hydration water reduces the swelling capacity of clay particles which in turn leads to production of large pores (Studds et al., 1998; Villar et al., 2003; Ye et al., 2014; Navarro et al., 2017; Chen et al., 2019). The variation is largely due to inhibition or reduction of swelling capacity of the capacity mixture in the presence of salt in the solution. When exposed to water, bentonite swells based on two mechanisms: crystalline swelling that occurs due to the hydration of exchangeable cations (e.g. Ca^{2+} and K^{+}); and diffuse double-layer swelling due to repulsion between clay minerals (Bradbury and Baeyens, 2003; Savage, 2005; Puppala et al., 2017). The salt concentration reduces the thickness of the diffuse double-layer, consequently leading to low repulsion between the clay particles (Tripathy et al., 2004; Zhu et al., 2013). With the swelling of the bentonite undermined, the clay particles would be less packed, which will result in higher permeability. This is supported by the SEM images in Figure 4.7 with the specimen exposed to DW having more intact particle structure than the specimen exposed to the saline solution G.

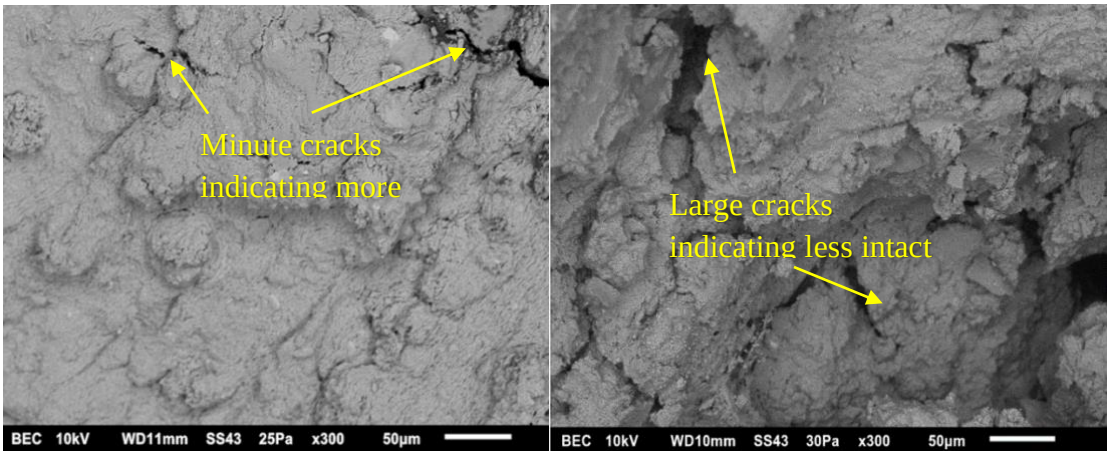

(a) (b)

Figure 4.7. SEM images of compacted bentonite-sand mixture cured in distilled water and G solutions for 60 days (a) DW (b) Solution G

4.3.2 Coupled effect of temperature and ground water chemistry on the hydraulic conductivity of bentonite-sand mixtures

Understanding the effect of high temperature is important for EBS design because the stored spent fuel can generate high amount of heat that may affect the performance of the buffer material (Inoue, 1995; Wersin et al., 2007). Moreover, the high temperature variation in the deep geological formation may also have an influence on the EBS (Zhang et al., 2019). Figure 4.8 show the comparison between the hydraulic conductivity of samples cured at room temperature and those cured at a temperature of 80 ^{o}C. It is evident that the high temperature leads to high hydraulic conductivity for both 30:70 and 70:30 bentonite-sand mixtures. For the 70:30 mixture, the hydraulic conductivity increased by 380% when exposed to DW and by 132% in solution G. Similar increased was observed for the 30:70 mixture. According to Romero et al. (2001), the increased in the hydraulic conductivity can be associated to changes in the clay fabric and redistribution of porosity due caused by high temperature (MIP graphs can be used to support this; Figure 4.9). As described in the previous section, the salt concentration in the permeating solution slows down the diffuse double layer swelling of the bentonite-sand mixtures which subsequently leaves more voids in the sample. At high temperature, the swelling is slower due to the conversion of the interlamellar water into bulk water accompanied by the reduction of the clay lamellae hydration (Chen et al., 2018). In addition, it has been observed from previous studies that high temperature decreases the basal spacing between clay minerals which also contributes to less swelling (Píšková et al., 2010; Shariatmadari and Sehidijam, 2012). Svensson and Hansen (2013) investigated the combined impact of salinity and temperature on the hydration of montmorillonite and their findings are in agreement with the aforementioned observations. Generally, the increase in both the salt concentration and temperature leads to decrease of the swelling pressure of the clay mineral. The observation was associated with the undermining of the interlayer hydration in the montmorillonite which leads to less basal spacing. The total porosity graphs for 30:70 bentonite-sand mixture treated with different solutions and at different temperatures is shown

in Figure 4.9 a-d. It can be observed that the specimen inundated with solution G at a high temperature of 80 ºC has the highest total porosity while the one exposed to distilled water at room temperature is the least porous. These observations agree with the recorded hydraulic conductivity values.

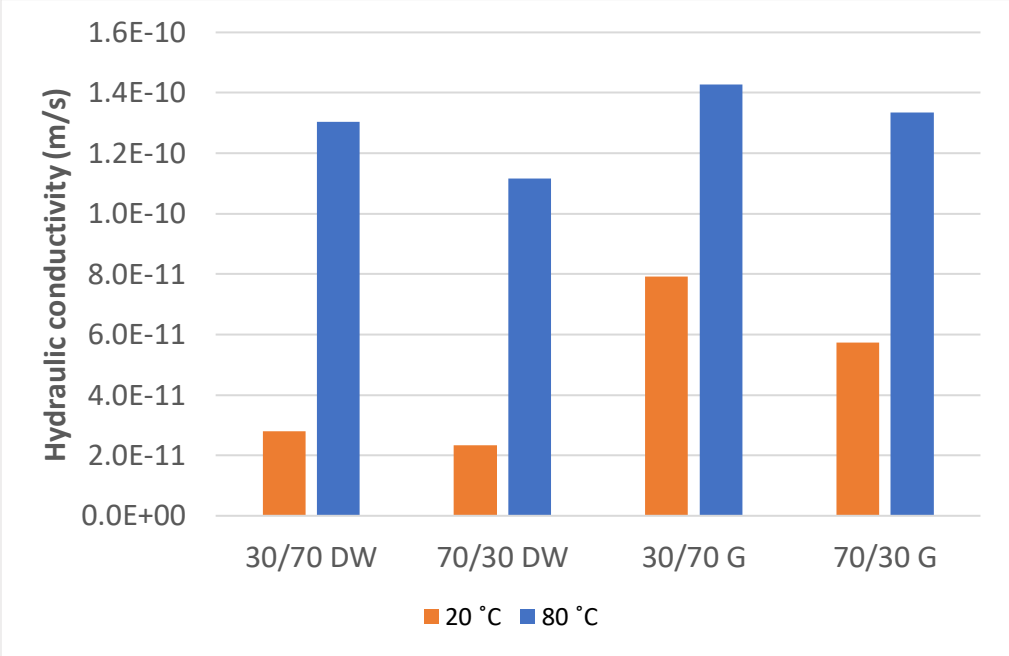

Figure 4.8. Hydraulic conductivity of bentonite-sand mixtures at different curing temperature and groundwater chemistry

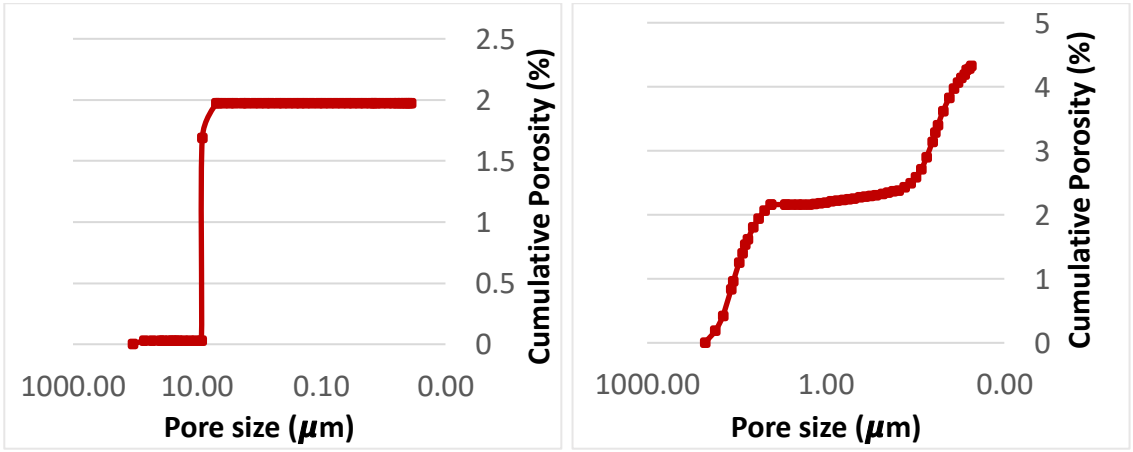

(a) (b)

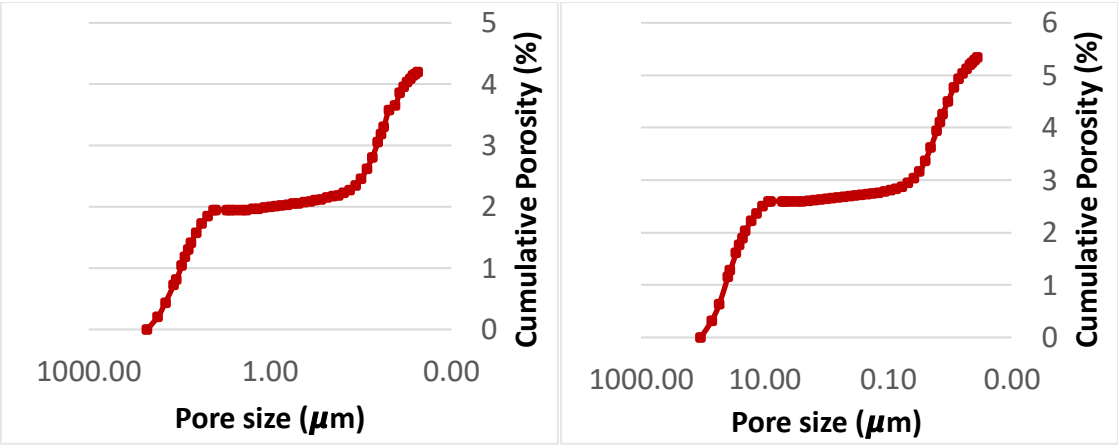

(c) (d)

Figure 4.9. MIP cumulative pore volume for compacted bentonite-sand mixture at different curing temperature and groundwater chemistry (a) DW at 20 °C (b) DW at 80 °C (c) Solution G at 20 °C (d) Solution G at 80 °C

4.3.3 Effect of initial dry density and swelling condition on the hydraulic conductivity of bentonite-sand mixtures

The effect of variation of the initial dry density on the hydraulic conductivity on bentonite-sand mixture exposed to solution G is shown in Figure 4.10. The result shows that the bentonite-sand mixtures compacted to 2.0 g/cm^3 have lower hydraulic conductivity than those with 1.63 g/cm^3 density after being allowed to hydrate for 60 days. The low hydraulic conductivity of the samples with higher initial dry density is largely due to increased swelling pressure as there are more clay particles present. According to Lee et al. (2012), bentonite compacted at a lower dry density tends to have its particles randomly arranged in form of micropeds. These micropeds become fused together eliminating interparticle voids when the bentonite is compacted to a higher dry density. The swelling pressure from such fused clay particles is high that it results in further elimination of voids in the mixture (Pusch, 1999; Cui et al., 2012). Lloret et al., (2004) observed a similar behaviour which they also associated with higher swelling strain for mixtures with higher initial dry density. Figure 4.11 shows the SEM images of specimens with initial dry densities of 1.63 g/cm^3 and 2.0 g/cm^3 exposed to DW

under free swell condition. It can be observed that the denser specimen (Figure 4.11b) has more intact structure with no obvious cracks or pores. Thus, compacting the bentonite-sand barrier mixture to a higher density yields less permeable and ultimately a better performing barrier system.

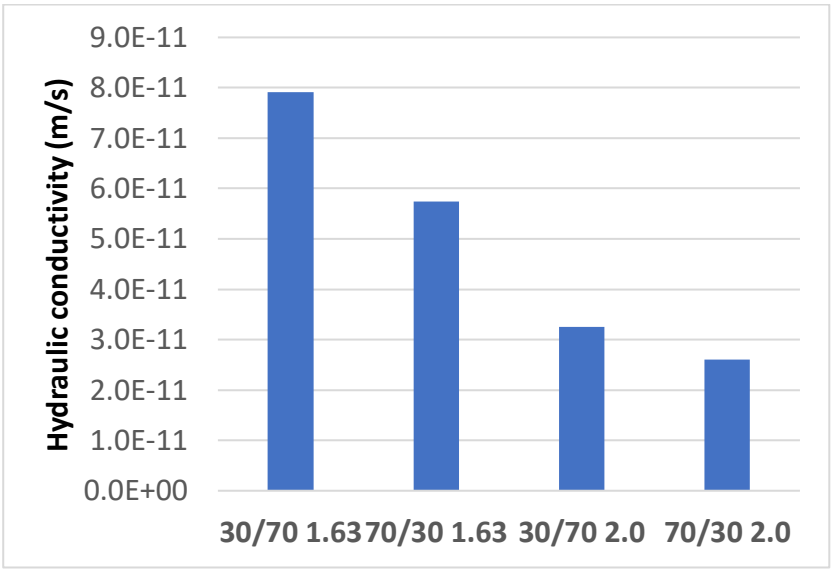

(a)

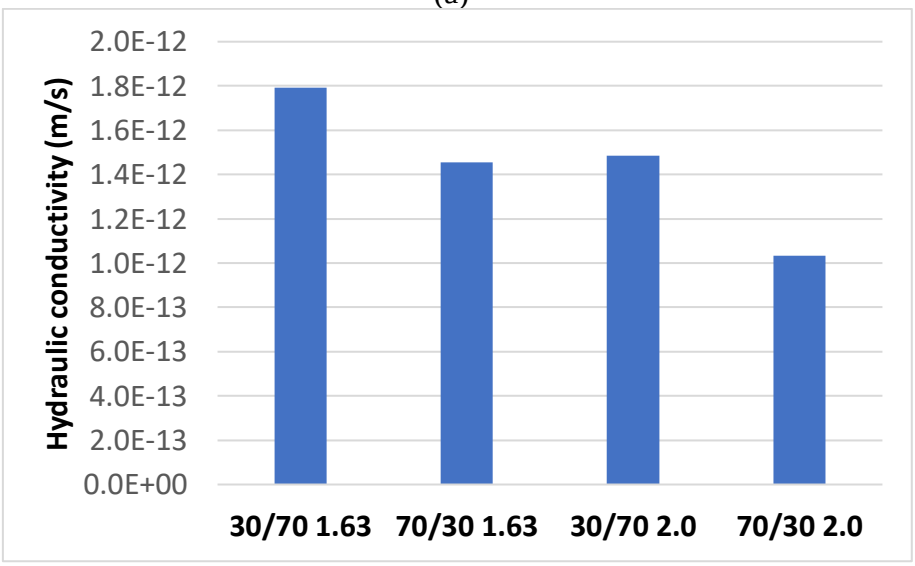

(b)

Figure 4.10. Hydraulic conductivity of bentonite-sand mixtures with different initial dry density inundated with saline solution G (a) Free swelling (b) Restricted swelling

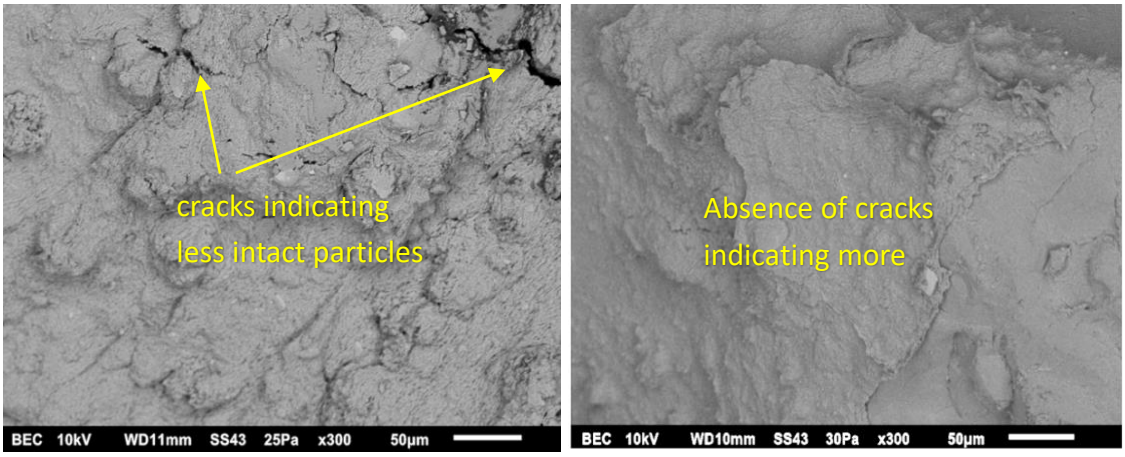

(a) (b)

Figure 4.11. SEM images of compacted bentonite-sand mixture cured in distilled water with different initial dry densities (a) Initial dry density = 1.63 g/cm^3 (b) Initial dry density = 2.0 g/cm^3

4.4 Summary and conclusions

This paper presents and discusses experimental research findings on the combined effects of factors, such as temperature, restricted swelling, bentonite-sand ratio and dry density, and groundwater chemistry, on the hydraulic conductivity of bentonite-sand mixture that has potentials of being used as a buffer material in deep geological repositories. Samples were prepared with different bentonite to sand ratios (30:70 and 70:30), compacted with different initial dry densities (1.63 g/cm^3 and 2.0 g/cm^3), permeated in distilled and Ontario's deep underground water over a period of 60 days under free and confined swelling conditions. The curing temperature during the swelling period was also varied (20 ^{o}C and 80 ^{o}C). Microstructural analyses, namely mercury intrusion porosimetry and scanning electron microscopy were used to study the pore structure and the nature of the bentonite-sand bonding for the different samples. Based on the results obtained, the following conclusions can be made:

a) Confining the bentonite-sand mixture during the swelling process produces a densely packed material with much lower hydraulic conductivity compared to free swelling. High confining stress conditions generates higher swelling pressure from the hydration of clay minerals, which expand to fill up the voids between the sand particles.

b) The mixture containing 70% bentonite attained lower hydraulic conductivity than the mixture containing 30% under same curing conditions. In addition to the high permeability of quartz sand over bentonite clay, higher quantity of bentonite in the mixture ensures that voids are filled up with clay minerals upon hydration.

c) The saline groundwater from Guelph Ontario (simulated as solution G in the study) reduces the swelling pressure of the bentonite-sand mixture, thus resulting in higher permeability. The salt in the permeating water reduces the thickness of the diffuse double-layer, consequently leading to low repulsion between the clay particles.

d) Combination of high temperature and salt concentration have amplified negative effect on the hydraulic conductivity. High temperature decreases the basal spacing between clay minerals which also contributes to less swelling of the clay minerals.

e) Increasing the initial dry density of the bentonite-sand mixture reduces the hydraulic conductivity of the barrier material after permeation. This is because bentonite compacted at a lower dry density tends to have its particles randomly arranged in form of micropeds, which become fused together eliminating interparticle voids when the bentonite is compacted to a higher dry density.

The results presented in this paper suggest that the mix proportions, swelling conditions, Ontario's groundwater chemistry and temperature influence the hydraulic conductivity of bentonite-sand barrier material. All of these factors need to be considered in the design of the EBS for better performance.

4.5 References

Adamcová, R., Frankovská, J., & Durmeková, T. (2009). Engineering geological clay research for a radioactive waste repository in Slovakia. *Acta geologica slovaca*, *1*(2), 71-82.

Akgün, H., Koçkar, M. K., & Aktürk, Ö. Z. G. Ü. R. (2006). Evaluation of a compacted bentonite/sand seal for underground waste repository isolation. *Environmental Geology*, *50*(3), 331-337.

Aligizaki, K. K. (2005). *Pore structure of cement-based materials: testing, interpretation and requirements*. Crc Press.

Bradbury, M. H., & Baeyens, B. (2003). Porewater chemistry in compacted re-saturated MX 80 bentonite. *Journal of Contaminant Hydrology*, *61*(1-4), 329-338.

Chen, Y. G., Dong, X. X., Zhang, X. D., Ye, W. M., & Cui, Y. J. (2018). Combined thermal and saline effects on the swelling pressure of densely compacted GMZ bentonite. *Applied Clay Science*, *166*, 318-326.

Chen, Y. G., Dong, X. X., Zhang, X. D., Ye, W. M., & Cui, Y. J. (2019). Cyclic thermal and saline effects on the swelling pressure of densely compacted Gaomiaozi bentonite. *Engineering Geology*, *255*, 37-47.

Cho, W. J., Lee, J. O., & Kang, C. H. (2000). Hydraulic conductivity of bentonite-sand mixture for a potential backfill material for a high-level radioactive waste repository. *Nuclear Engineering and Technology*, *32*(5), 495-503.

Cho, W. J., Lee, J. O., & Kwon, S. (2010). Analysis of thermo–hydro–mechanical process in the engineered barrier system of a high-level waste repository. *Nuclear Engineering and Design*, *240*(6), 1688-1698.

Cui, S. L., Zhang, H. Y., & Zhang, M. (2012). Swelling characteristics of compacted GMZ bentonite–sand mixtures as a buffer/backfill material in China. *Engineering Geology*, *141*, 65-73.

Cui, Y. J., Tang, A. M., Loiseau, C., & Delage, P. (2008). Determining water permeability of compacted bentonite-sand mixture under confined and free-swell conditions. *Physics and Chemistry of the Earth*, *33*, S462-S471.

Ebina, T., Minja, R. J., Nagase, T., Onodera, Y., & Chatterjee, A. (2004). Correlation of hydraulic conductivity of clay–sand compacted specimens with clay properties. *Applied clay science*, *26*(1-4), 3-12.

Fall, M., Li, Z., Guo, G. &Wei, X. (2018). Simulation of gas migration in Canadian potential host rocks for radioactive waste disposal. Proceedings of 47. Geomechanik-Kolloquium, 2018, Freiberg, Germany, Nov 16, 2018.

Fall, M., Nasir, O., & Nguyen, T.S., (2014). A coupled hydro-mechanical model for simulation of gas migration in host sedimentary rocks for nuclear waste repositories. *Engineering Geology* 176, 24-44.

Gatabin, C., Talandier, J., Collin, F., Charlier, R., & Dieudonné, A. C. (2016). Competing effects of volume change and water uptake on the water retention behaviour of a compacted MX-80 bentonite/sand mixture. *Applied Clay Science*, *121*, 57-62.

González, S. S. (2013). The swelling pressure of bentonite and sand mixtures. *Master of Science Thesis. KTH Chemical Science and Engineering*.

Gueddouda, M. K., Lamara, M., Abou-Bekr, N., & Taibi, S. (2010). Hydraulic behaviour of dune sand-bentonite mixtures under confining stress. *Geomechanics and Engineering*, *2*(3), 213-227.

Guo, G., & Fall, M. (2021). Advances in modelling of hydro-mechanical processes in gas migration within saturated bentonite: A state-of-art review. *Engineering Geology*, 106123, doi: 10.1016/j.enggeo.2021.106123.

Guo, G.& Fall, M. 2018. Modelling of dilatancy-controlled gas flow in bentonite based materials with double porosity and double effective stress concepts. *Engineering Geology* 243(4):253-271.

Guo, R. (2017). Thermal response of a Canadian conceptual deep geological repository in crystalline rock and a method to correct the influence of the near-field adiabatic boundary condition. *Engineering geology*, *218*, 50-62.

Inoue, A. (1995). Formation of clay minerals in hydrothermal environments. In *Origin and mineralogy of clays* (pp. 268-329). Springer, Berlin, Heidelberg.

Ito, H., 2006. Compaction properties of granular bentonite. Applied Clay Science 31, 47–55.

Jadda, K., & Bag, R. (2020). Variation of swelling pressure, consolidation characteristics and hydraulic conductivity of two Indian bentonites due to electrolyte concentration. *Engineering Geology*, *272*, 105637.

Jiang, H., Xiang, G., Xu, Y., & Chen, T. (2014). Study on the Swelling Mechanism and Characteristics of Bentonite. In *Soil Behaviour and Geomechanics* (pp. 43-53).

Karnland, O., Olsson, S., Nilsson, U., and Sellin, P., 2007. Experimentally determined swelling pressures and geochemical interactions of compacted Wyoming bentonite with highly alkaline solutions. Physics and Chemistry of the Earth 32, 275–286. doi: 10.1016/j.pce.2006.01.012.

Komine, H. (2004). Simplified evaluation on hydraulic conductivities of sand–bentonite mixture backfill. Applied Clay Science, 26(1-4), 13-19.

Komine, H., Yasuhara, K., & Murakami, S. (2009). Swelling characteristics of bentonites in artificial seawater. Canadian Geotechnical Journal, 46(2), 177-189.

Lee, J. O., Lim, J. G., Kang, I. M., & Kwon, S. (2012). Swelling pressures of compacted Ca bentonite. *Engineering geology*, *129*, 20-26.

Likos, W. J., & Wayllace, A. (2010). Porosity evolution of free and confined bentonites during

interlayer hydration. *Clays and Clay minerals*, *58*(3), 399-414.

Liu, H., Dang, X., Zhang, H., Dong, J., Zhang, Z., Wang, C., ... & Zhuang, D. (2019, February). Microbial diversity in bentonite, a potential buffer material for deep geological disposal of radioactive waste. In *IOP Conf Ser Earth Environ Sci* (Vol. 227, No. 22010, pp. 1755-1315).

Lloret, A., Romero, E., & Villar, M. V. (2005). *FEBEX II Project: Final report on thermo hydro-mechanical laboratory tests*. Enresa.

Martin, M., Cuevas, J., and Leguey, S., 2000. Diffusion of soluble salts under a temperature gradient after the hydration of compacted bentonites. Applied Clay Science 17, 55–70.

Mishra, A. K., Ohtsubo, M., Li, L. Y., Higashi, T., & Park, J. (2009). Effect of salt of various concentrations on liquid limit, and hydraulic conductivity of different soil-bentonite mixtures. *Environmental geology*, *57*(5), 1145-1153.

Mollins, L. H., Stewart, D. I., & Cousens, T. W. (1996). Predicting the properties of bentonite sand mixtures. *Clay minerals*, *31*(2), 243-252.

Nasir, O., Fall, M., Nguyen, S, Evgin, E, 2015. Modeling of the thermo-hydro-mechanical-chemical response of Ontario sedimentary rocks to future glaciations. *Canadian Geotechnical Journal* 52(7):836-850.

Navarro, V., Yustres, Á., Asensio, L., De la Morena, G., González-Arteaga, J., Laurila, T., & Pintado, X. (2017). Modelling of compacted bentonite swelling accounting for salinity effects. *Engineering Geology*, *223*, 48-58.

Niu, W. J., Ye, W. M., & Song, X. (2020). Unsaturated permeability of Gaomiaozi bentonite under partially free-swelling conditions. *Acta Geotechnica*, *15*(5), 1095-1124.

Önal, M. (2007). Swelling and cation exchange capacity relationship for the samples obtained from a bentonite by acid activations and heat treatments. Applied Clay Science, 37(1-2), 74-80.

Quintessa (2011) Bentonite a Review of key properties, processes and issues for consideration in the UK context. QRS-1378ZG-1, Version 1.1, February.

Pathak, P. (2017). An assessment of strontium sorption onto bentonite buffer material in waste repository. *Environmental Science and Pollution Research*, *24*(9), 8825-8836.

Pintado, X., Romero, E., Suriol, J., Lloret, A., & Madhusudhan, B. N. (2019). Small-strain shear stiffness of compacted bentonites for engineered barrier system. *Geomechanics for Energy and the Environment*, *18*, 1-12.

Píšková, A., Bezdička, P., Hradil, D., Káfuňková, E., Lang, K., Večerníková, E., ... & Grygar, T. (2010). High-temperature X-ray powder diffraction as a tool for characterization of smectites, layered double hydroxides, and their intercalates with porphyrins. *Applied clay science*, *49*(4), 363-371.

Puppala, A. J., Pedarla, A., Pino, A., & Hoyos, L. R. (2017). Diffused double-layer swell prediction model to better characterize natural expansive clays. *Journal of Engineering Mechanics*, *143*(9), 04017069.

Pusch, R. (1999). Microstructural evolution of buffers. *Engineering Geology*, *54*(1-2), 33-41.

Rao, S. M., Kachroo, T. A., Allam, M. M., Joshi, M. R., & Acharya, A. (2008, October). Geotechnical characterization of some Indian bentonites for their use as buffer material in geological repository. In *Proceedings of 12th international conference of international association for computer methods and advances in geomechanics (IACMAG)* (pp. 1-6).

Romero, E., Gens, A., & Lloret, A. (2001). Temperature effects on the hydraulic behaviour of an unsaturated clay. In Unsaturated soil concepts and their application in geotechnical practice (pp. 311-332). Springer, Dordrecht.

Savage, D. (2005). The effects of high salinity groundwater on the performance of clay barriers.

Sällfors, G., & Öberg-Högsta, A. L. (2002). Determination of hydraulic conductivity of sand

bentonite mixtures for engineering purposes. *Geotechnical & Geological Engineering*, *20*(1), 65-80.

Selvadurai, A. P. S., & Głowacki, A. (2018). Estimates for the local permeability of the Cobourg limestone. *Journal of Rock Mechanics and Geotechnical Engineering*, *10*(6), 1009-1019.

Shariatmadari, N., & Saeidijam, S. (2012). The effect of thermal history on thermo-mechanical behaviour of bentonite-sand mixture. *International Journal of Civil Engineering*, *10*(2), 162-167.

Shehata, A., Fall, M., & Detellier, C. (2015). Swelling characteristics of bentonite based barriers for deep geological repository for nuclear wastes: Impact of underground water chemistry and temperature. In Proceedings of 68th Canadian Geotechnical and 7th Canadian Permafrost Conference, Quebec, Canada, September 20–23, 2015.

Shehata, A., Fall, M., Detellier, C., & Alzamel, M. (2021). Effect of groundwater chemistry and temperature on swelling and microstructural properties of sand–bentonite for barriers of radioactive waste repositories. *Bulletin of Engineering Geology and the Environment*, *80*(2), 1857-1873.

Siddiqua, S., Tabiatnejad, B., & Siemens, G. (2018). Impact of pore fluid chemistry on the thermal conductivity of bentonite–sand mixture. *Environmental earth sciences*, *77*(1), 8.

Sivapullaiah, P. V., Sridharan, A., & Stalin, V. K. (2000). Hydraulic conductivity of bentonite sand mixtures. *Canadian geotechnical journal*, *37*(2), 406-413.

Sterling, S. (2011). Bedrock Formations in DGR-7 and DGR-8.

Svensson, P. D., & Hansen, S. (2013). Combined salt and temperature impact on montmorillonite hydration. *Clays and Clay Minerals*, *61*(4), 328-341.

Stewart, D. I., Studds, P. G., & Cousens, T. W. (2003). The factors controlling the engineering properties of bentonite-enhanced sand. *Applied Clay Science*, *23*(1-4), 97-110.

Studds, P. G., Stewart, D. I., & Cousens, T. W. (1998). The effects of salt solutions on the properties of bentonite-sand mixtures. *Clay Minerals*, *33*(4), 651-660.

Tripathy, S., Sridharan, A., & Schanz, T. (2004). Swelling pressures of compacted bentonites from diffuse double layer theory. *Canadian Geotechnical Journal*, *41*(3), 437-450.

Villar, M. V., Romero, E., & Lloret, A. (2005, June). Thermo-mechanical and geochemical effects on the permeability of high-density clays. In *Proceedings of the international symposium on large scale field tests in granite. Advances in understanding engineered clay barriers. In: Alonso EE, Ledesma A (eds) AA Balkema Publishers, Leiden* (pp. 177-191).

Wang, Q., Tang, A., Cui, Y., Delage, P., and Gatmiri, B., 2012. Experimental study on the swelling behaviour of bentonite/claystone mixture. Engineering Geology 124, 59–66.

Weimin, M. Y., Zhang, F., Chen, B., Chen, Y. G., Wang, Q., & Cui, Y. J. (2014). Effects of salt solutions on the hydro-mechanical behaviour of compacted GMZ01 Bentonite. *Environmental earth sciences*, *72*(7), 2621-2630.

Wersin, P., Johnson, L. H., & McKinley, I. G. (2007). Performance of the bentonite barrier at temperatures beyond 100 C: A critical review. *Physics and Chemistry of the Earth, Parts A/B/C*, *32*(8-14), 780-788.

Windslow, D., & Diamond, S. (1969). A mercury porosimetry study of the evolution of porosity in Portland cement: technical publication.

Ye, W. M., Wan, M., Chen, B., Chen, Y. G., Cui, Y. J., & Wang, J. (2012). Temperature effects on the unsaturated permeability of the densely compacted GMZ01 bentonite under confined conditions. Engineering Geology, 126, 1-7.

Ye, W. M., Wan, M., Chen, B., Chen, Y. G., Cui, Y. J., & Wang, J. (2013). Temperature effects

on the swelling pressure and saturated hydraulic conductivity of the compacted GMZ01 bentonite. *Environmental Earth Sciences*, *68*(1), 281-288.

Ye, W. M., Zhu, C. M., Chen, Y. G., Chen, B., Cui, Y. J., & Wang, J. (2015). Influence of salt solutions on the swelling behaviour of the compacted GMZ01 bentonite. *Environmental Earth Sciences*, *74*(1), 793-802.

Ye, W. M., He, Y., Chen, Y. G., Chen, B., & Cui, Y. J. (2016). Thermochemical effects on the smectite alteration of GMZ bentonite for deep geological repository. *Environmental Earth Sciences*, *75*(10), 906.

Xiang, G., Xu, Y., Yu, F., Fang, Y., & Wang, Y. (2019). Prediction of swelling characteristics of compacted GMZ bentonite in salt solution incorporating ion-exchange reactions. *Clays and Clay Minerals*, *67*(2), 163-172.

Xu, L., Ye, W. M., Chen, B., Chen, Y. G., & Cui, Y. J. (2016). Experimental investigations on thermo-hydro-mechanical properties of compacted GMZ01 bentonite-sand mixture using as buffer materials. *Engineering Geology*, *213*, 46-54.

Zhang, M., Zhang, H., Cui, S., Jia, L., Zhou, L., & Chen, H. (2012). Engineering properties of GMZ bentonite-sand as buffer/backfilling material for high-level waste disposal. European journal of environmental and civil engineering, 16(10), 1216-1237.

Zhang, Q., Huang, Y., Sand, W., & Wang, X. (2019). Effects of deep geological environments for nuclear waste disposal on the hydrogen entry into titanium. *International Journal of Hydrogen Energy*, *44*(23), 12200-12214.

Zhu, C. M., Ye, W. M., Chen, Y. G., Chen, B., & Cui, Y. J. (2013). Influence of salt solutions on the swelling pressure and hydraulic conductivity of compacted GMZ01 bentonite. *Engineering Geology*, *166*, 74-80.

Chapter 5: Technical paper III: Thermal conductivity and diffusivity of bentonite-sand backfill materials for a deep geological repository exposed to saline groundwater

Mohammed Alzamel, Mamadou Fall

(Submitted)

Abstract

Compacted bentonite-sand mixture is recognized as a buffer or barrier material in deep geological repositories (DGRs) due to its low hydraulic conductivity, mechanical strength, and chemical stability. However, its engineered properties (e.g. thermal properties) under various field conditions have not been fully understood. This paper presents experimental results on the thermal conductivity and diffusivity of compacted bentonite-sand mixture exposed to saline groundwaters prevalent in some part of Ontario, Canada. Various compositions of the mixture (20/80 30/70, 50/50, and 70/30 bentonite/sand ratios) were compacted to its maximum dry densities and then inundated with distilled water (DW), simulated solution of Guelph (G) and Trenton (T) regions groundwater for up to 60 days at room temperature. The results indicated that an increase in the constituent pore fluid's salt concentration leads to a decrease in the thermal conductivity and diffusivity of the material. Also, the increasing the proportion of the bentonite lowers the thermal conductivity regardless of the chemical composition of the water which is linked to the low conductivity of clay and water as compared to the quartz sand. Increase of void ratio was also observed to affect the thermal conductivity negativity by reducing the compactness of the solid particles and subsequently slowing down the rate of heat transfer. Prediction models were further developed for the estimation of the thermal conductivity of bentonite-sand mixtures in G and T saline waters. The findings from the study will contribute to a safer design of the engineered barrier material for deep geological disposal of radioactive waste.

Keywords: Thermal conductivity; pore water chemistry; deep geological repository; dry density; bentonite–sand mixture; radioactive wastes.

5.1 Introduction

The engineered barrier and backfill material used in deep geological repositories (DGRs) for nuclear waste disposal is required to be nearly impermeable and have mechanical as well as chemical stability to ensure a long-term safe storage (Hicks et al., 2008; Liu et al., 2019; Guo and Fall, 2018, 2019; Orellana et al., 2019). The low permeability of the barrier ensures that the highly radioactive waste is not transmitted into the nearby groundwater through seepage. Mechanical stability of the barrier is also required to withstand earth pressure and other loadings under DGR conditions (Boyle & Meguid, 2015). Likewise, the barrier material should have good thermal conductivity to facilitate the quick and effective dissipation of the heat generated from the cannisters containing the nuclear waste material into the surrounding geoenvironment (Mishra et al., 2017). A composite mixture of bentonite and sand is widely being considered as a promising barrier and backfill material due to its better performance over pure bentonite with respect to the heat transfer ability and mechanical properties (Shehata et al., 2021).

Previous studies have shown that addition of sand to the bentonite improves the overall thermal conductivity of the barrier material. An experimental study by Xu et al. (2016) revealed that the thermal conductivity of a bentonite-sand mixture generally increases with the increase of the sand content. However, the results showed that the rate of the increase of thermal conductivity diminishes at sand contents greater than 30%. Mishra et al. (2017) also compared the thermal conductivity of bentonite-graphite mixtures with that of bentonite-sand mixtures at a drier density and water content at different mixing ratios. Their findings indicated that there was a significant improvement in bentonite's thermal conductivity when graphite was added. Chen et al. (2018) measured thermal conductivity of 17 smectite clays from 13 depositions. Based on their measurement outcomes, the researchers found the value of thermal conductivity to be conjointly influenced by soil structure or characteristics, such as mineral composition,

the microstructure of clay sample, the dry densities and the water contents of the soil. The results reported from the research indicated that the increase in the sand contents led to the increase of bentonite/sand mixtures' thermal conductivity (Chen et al., 2018).

Although both thermal conductivity and diffusivity are associated with the heat conduction characteristics of materials, the latter is rarely used in the design of barrier systems despite being equally important (Salazar, 2003). The thermal diffusivity simply represents the rate of the spread of heat or temperature within a conductive medium (Mishra et al., 2019). Materials with high thermal diffusivity dissipate heat rapidly, which facilitates fast cooling (Zhang, 2016). Within rock formations, the thermal diffusivity has been found to increase with increase in temperatures and water content of the conductive media (Zhang, 2016). Thus, understanding the variation of the thermal conductivity of a barrier material under different conditions is vital for a proper design of DGR structures.

The swelling behaviour of bentonite as well as its resulting strength and thermal characteristics largely depend on the chemistry of the water it is exposed to (Pastina and Hellä, 2006; Santiago et al., 2007). The proposed DGRs locations in Ontario, Canada, are known to have groundwaters with high concentration of salts which may permeate into the engineered barrier system (Jensen et al., 2009; Fall et al., 2014, 2018). Water salinity has been observed to limit the swelling potential of bentonite through the alteration of the clay minerals (Karnland et al., 2007). The inhibition of the clay swelling is proportional to the ionic strength of the saline solutions, which is further exacerbated by molar concentration (Karnland et al., 2007). Similarly, a compacted mixture 50% bentonite and 50% sand showed lower thermal conductivity when exposed to saline water as compared to distilled water (Siddiqua et al., 2017). This has also been observed in other soils, such as clay loam (Abu-Hamdeh & Reeder, 2000), pluvial particulate (Presley et al., 2009) and loess sediment (Yan et al., 2021). None of the previous studies examined the impact of the saline Ontario's groundwater on bentonite-

sand mixture with different blinding ratios. So, the results of these previous studies cannot be directly transferred to a backfill material in Ontario's DGR conditions since the chemical compositions of Ontario's groundwaters are different from those examined in these previous studies. This study is aimed at addressing this research and knowledge gap. In response, this study assesses the thermal conductivity and diffusivity of compacted bentonite-sand materials of different dry densities and blending ratio when exposed to distilled water and saline groundwater in Ontario.

5.2 Experimental Program

5.2.1 Materials

Tests were performed with Na-bentonite and GS-20 silica sand with different blending ratios (20:80, 30:70, 50:50, and 70:30 dry mass). The particle size distributions form the different mixtures are shown in Figure 2. These mixtures were immersed with different chemical compositions of water solutions.

5.2.1.1 Bentonite

An MX-80 bentonite clay extracted from Wyoming; USA was used in this study. Table 5.1 and 5.2 present the physical properties and chemical composition of the bentonite. The dominant mineral in the clay is montmorillonite, with traces of quartz, calcite, kaolinite and feldspar as shown by XRD analysis in Figure 5.1. The major exchangeable cation is Na^+, which has a cation exchange capacity (CEC) of 105 meq/100 g. The grain size distribution curve of the bentonite is given in Figure 5.2. The particle size distribution was determined by conducting a sieve analysis on particle sizes greater than 75 µm and using a sedimentation process on particle sizes less than 75 µm, which follow ASTM standard D422-63.

Table 5.1. Properties of the MX-80 bentonite

Property	**Description**
Specific gravity	2.66
Liquid limit (%)	530
Plastic Limit (%)	48.5
Total specific surface area (m^2/g)	512
Cation exchange capacity (mmol/100 g)	105
Montmorillonite content (%)	90

Table 5.2. Chemical composition of MX-80 bentonite

Chemical Element	**Composition**	**%**
Silicon dioxide	SiO_2	63.59
Aluminium oxide	Al_2O_3	21.43
Iron oxide	Fe_2O_3	3.78
Calcium oxide	CaO	0.66
Magnesium oxide	MgO	2.03
Sodium oxide	Na_2O	2.70
Potassium oxide	K_2O	0.31
Bound water	H_2O	5.50

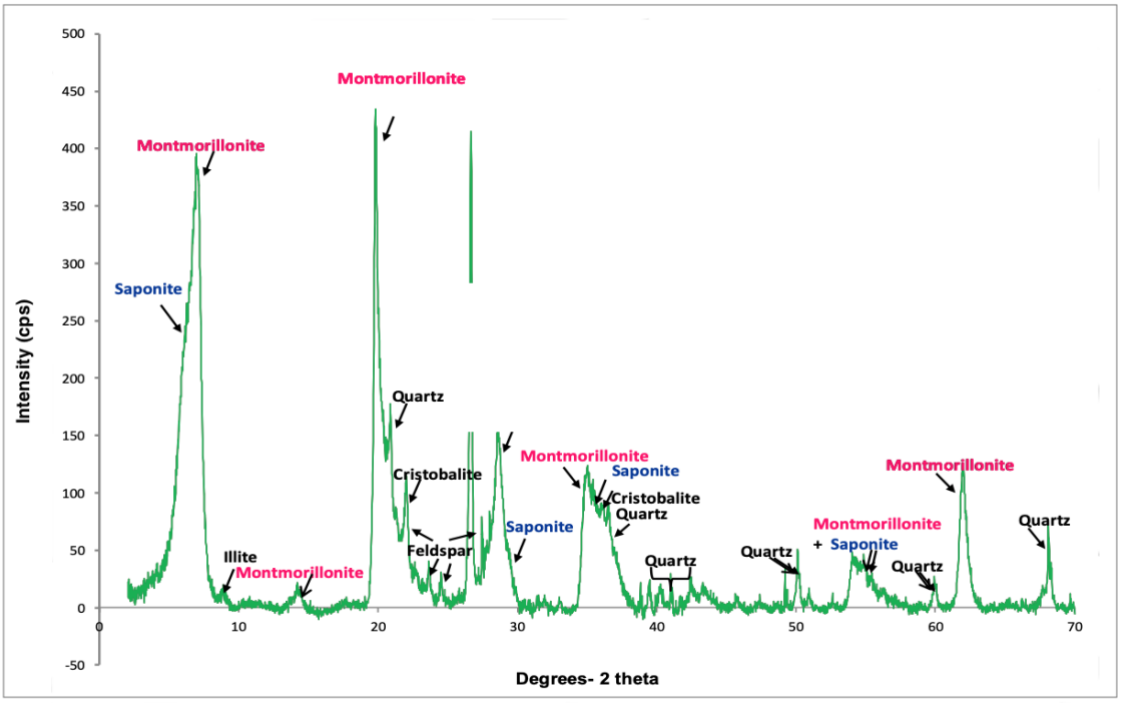

Figure 5.1. Mineralogical content of the MX-bentonite as observed by XRD analysis

5.2.1.2 Sand

Pure quartz sand containing 99.99% silica was used to produce the bentonite-sand mixture. It has a specific gravity of 2.65 and made up of fine to medium particles with size ranging from 0.2 to 1.9 mm (Figure 5.2). A sand sieve analysis was performed by following ASTM standard D6913–04 to develop the grain size distribution of the sand (Figure 5.2),

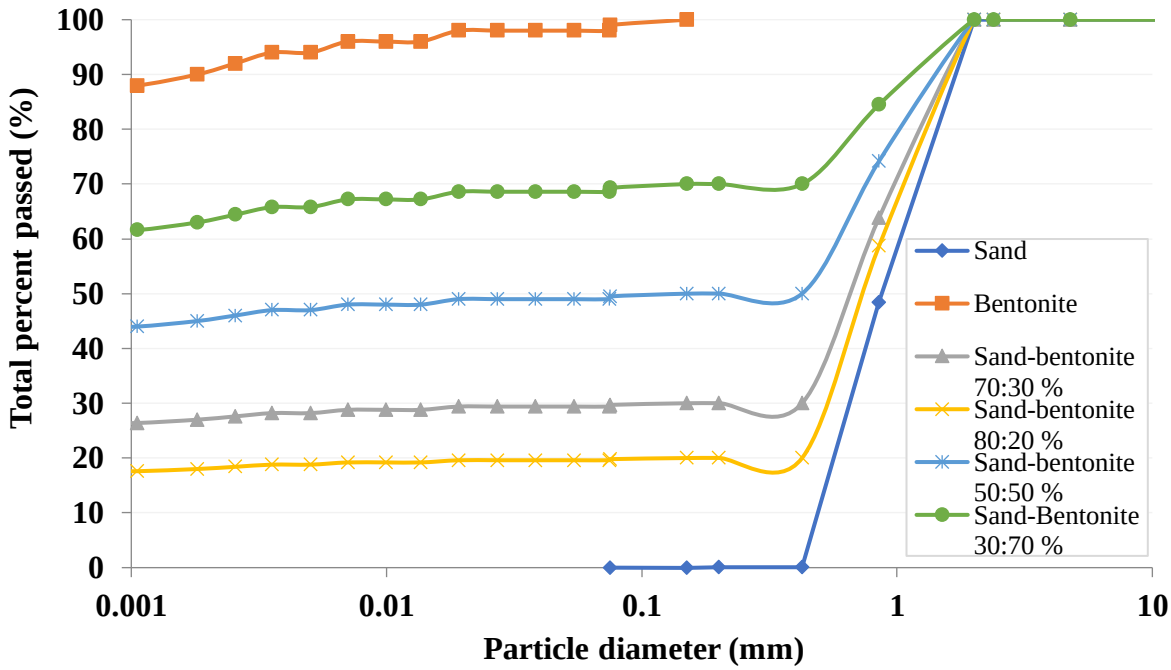

Figure 5.2. Bentonite, sand, and bentonite–sand grain size distribution

5.2.1.3 Solutions

Two solutions were prepared in the laboratory with chemical compositions as found in the groundwaters in the Guelph and Trenton regions of Ontario. Distilled water was used as a control solution. The chemical compositions and properties of the solutions are presented in Table 5.3. The main constituent salts in the Guelph and Trenton solutions are calcium chloride ($NaCl_2$) and sodium chloride (NaCl).

Table 5.3. Main chemical composition and characteristics of the synthesized groundwaters

Element	Distilled Water (DW)	Guelph Water (G)	Trenton Water (T)
Ca (g/l)	0	57	23.0
Na (g/l)	0	39.0	40.0
Mg (g/l)	0	8.7	5.5
K (g/l)	0	3.9	2.0
Cl (g/l)	0	191.0	121.0
SO_4 (g/l)	0	0.2	0.6
TDS (g/l)	0	300	192
pH	7	5.7	6.5

5.2.2 Specimen preparation and mix proportions

5.2.2.1 Compaction tests

To obtain the maximum dry densities of the various bentonite-sand mixtures, compaction tests were conducted in accordance with ASTM D698 standard. Each bentonite-sand mixture was compacted at varying moisture contents using standard Proctor mold and an intermediate energy level. The maximum dry density and optimum moisture contents (Figure 3) were determined and used for the determination of the thermal conductivity and other tests.

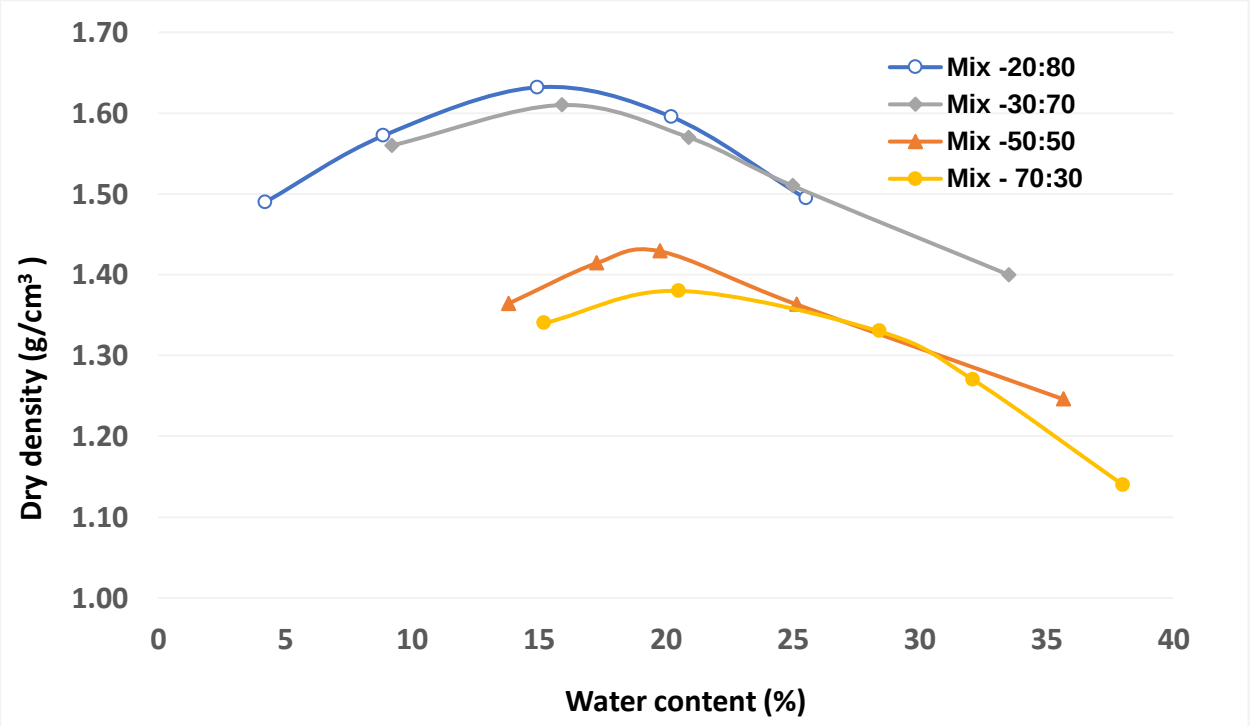

Figure 5.3. Dry density and moisture content curves of different bentonite–sand mixtures

5.2.2.2 Treatment of specimens

The different ratios of bentonite -sand mixtures (20:80, 30:70, 50:50, and 70:30 dry mass) were mixed with DW to achieve the desired water content obtained from Figure 5.3. The prepared mixtures were then sealed in plastic bags at room temperature (24 ºC) for 72 hours to ensure an even moisture distribution. Afterward, the mixtures were used to prepare compacted specimen based on the target dry density. A calculated amount of the bentonite–sand mixtures

were statically compacted to a polycarbonate tube with a diameter of 50 mm and a height of 100 mm. For each specimen, an appropriate amount of the mixtures corresponding to dry densities of 1.4, 1.6, 1.7, 1.8, or 2.0 g/cm^3 was compacted to 20 mm height in the tube. The remaining height of 80 cm was left to allow for free swelling. The specimens were placed into a reservoir containing an inundation water, DW, G or T as shown in Figure 5.4. The tube was covered with a porous disk at the bottom to allow capillary based permeation but left open at the top to allow free swelling.

Figure 5.4. Compacted specimens placed in a water reservoir for inundation

5.2.2.3 Thermal properties measurements

Cured specimens were tested for thermal conductivity and thermal diffusivity using KD2 Pro analyzer by Decagon Devices (Pullman WA, USA). The instrument measures thermal properties based on infinite line heat source theory, and thus determines the thermal conductivity by evaluating the rate of heat dissipation from a metallic probe into the material being monitored (Decagon, 2006). For this study, a KS-1 probe with a length of 60 mm and diameter of 1.27 mm was used to measure the thermal conductivity. The needle has an accuracy of ± 5% for measurement values in the range of 0.2 to 2 W/mK. Thermal diffusivity was

measured using an SH-2 dual needle sensor, which has an accuracy of ± 10% for measurements values over 0.1 mm^2/s. Calibration was done before the actual testing using pure glycerol liquid. For each specimen, measurements were taken by inserting the KS-1 needle into the sample and the thermal conductivity was displayed on the sensor monitor after equilibrating for few minutes. The measurement was repeated at a minimum of 3 different locations and the average was calculated as the thermal conductivity of the sample. The variation between values obtained in repeated tests was less than 5%.

5.2.2.4 Specific gravity and void ratio determination

After inundating the bentonite-sand mixtures in solutions with different chemical compositions, transformations were observed. To compare these changes for the various samples prepared in the study, specific gravity (Gs) was determined in accordance with the ASTM D854 using a pycnometer. Void ratio was determined based on the dry density (ρ_d) and the G_s as follows

$$e = \frac{G_s - \rho_d}{\rho_d}$$

5.2.2.5 Microstructural analyses

To have a better understanding of the mechanisms responsible for the thermal behaviour of the bentonite-sand mixtures, additional tests or analyses were carried to study the microstructural variation of the samples. The tests are mercury intrusion porosimetry (MIP) and scanning electron microscopy (SEM). For both tests, cured specimens were first oven-dried at 45 ^oC temperature for 4 days. MIP was performed using Micrometrics AutoPore III 9420 porosimeter (Micrometrcs, Norcross, US) to determine the distribution and volume of pores by mercury intrusion. The MIP test was conducted at the porous materials Inc. (PMI) laboratory facility, New York, USA. On the other hand, the SEM was conducted using Hitachi 3500-N microscope (Hitachi Ltd., Tokyo, Japan), with which microscopic texture and

materials configuration of the specimens were observed. The SEM test was performed at the Microanalysis lab, University of Ottawa.

5.3 Results and Discussion

5.3.1 Time dependent change of thermal conductivity and diffusivity of bentonite-sand mixture.

Figure 5.5a shows the thermal conductivity of 30/70 bentonite-sand mixture compacted to an initial dry density of 1.63 g/cm^3 and inundated in three different solutions (DW, G and T) for up to 60 days. Measurements were taken when the specimens were fully saturated. As it can be observed from the figure, the thermal conductivity decreased with time for all the three waters. Most of the reduction (up to 15%) occurred during the first 14 days and only slightly decreased thereafter until 60 days (6%). This is because bulk of the change in the structure of the composite material due to swelling occurs at the initial stage since there is availability of sufficient absorption water. Generally, the swelling pressure in expansive clays tends to change exponentially after being exposed to water and then maintain a near uniform trend after a reaching a peak value (Montes-H et al., 2003; Komine, 2004; Kolay and Ramesh, 2015; Shehata et al., 2021). The swelling of the mixture controls some of the parameters that are responsible for how heat is transferred in soils. These parameters include the degree of contact between solid particles, the soil structure, and the amount of voids (filled with air or water) (Côté and Konrad, 2005; Wang et al., 2017). Based on the SEM and MIP results presented in Figure 5.6 and Figure 5.7, the compacted bentonite-sand evidently has less total porosity after 3 days of inundation (swelling) than it has after 60 days. The cumulative pore volume in the 60 day-specimen is 0.05 mL/g as opposed to 0.04 mL/g in the 3 days specimen. With high degree of swelling, the mixture contains more water after 60 days, which translates to air voids in the MIP test. It can be clearly seen from the SEM image that the 60 days (Figure 5.6b) specimen has some pores while 3 days (Figure 5.6a) appears to be intact. It should be mentioned

that the thermal conductivities of distilled water, bentonite clay and quartz sand in pure forms are respectively about 0.6 W/mK, 0.7 W/mK and 7.5 W/mK (Li et al., 2013; Zhang et al., 2015). When fully saturated, bentonite and quartz sand have thermal conductivities of about 1.5 W/mK and 3.4 W/mK, respectively (Zhang et al., 2015; Carpenter, 2019). This range of values indicate that the thermal conductivity of clay particles increases with the increase of the amount of the absorbed pore water while that of quartz sand decreases with the increase of absorbed pore water. Considering that there is 70% sand in the mixture, and the effect of water on sand thermal behaviour is more pronounced, the observed drop in thermal conductivity of the mixture is largely due to the change in the amount of absorbed water in the mixture and the interparticle spacing due to swelling.

Similarly, the thermal diffusivity of the compacted bentonite/sand mixture show a steady decrease with time regardless of the inundation solution (Figure 5.5b). The change can also be discussed based on the variations of the thermal diffusivity of the individual elements, in pure form and as composites. Thermal diffusivities of water, bentonite clay, and quartz sand in pure form are about 0.14, 0.25 and 1.4 mm^2/s respectively (Salazar, 2003; Sun and Hu, 2019; Xu et al., 2021). Thus, as the barrier material swells by absorbing more water, the thermal diffusivity will continue to decrease. This is consistent with what has been observed in previous studies on heat transfer within wet soils. According to Tikhonravova (2007), wetting a soil containing either saline or non-saline results in the decrease of heat flux within the soil mass provided the water content is above the maximum hygroscopic level. The hygroscopic water refers to the water content that is tightly held in the soil due to adhesion, which is much less than the saturated water content (Amer, 2009). Thus, as the bentonite-sand mixtures absorbed more water beyond the hygroscopic water level, the thermal diffusivity of the material become less.

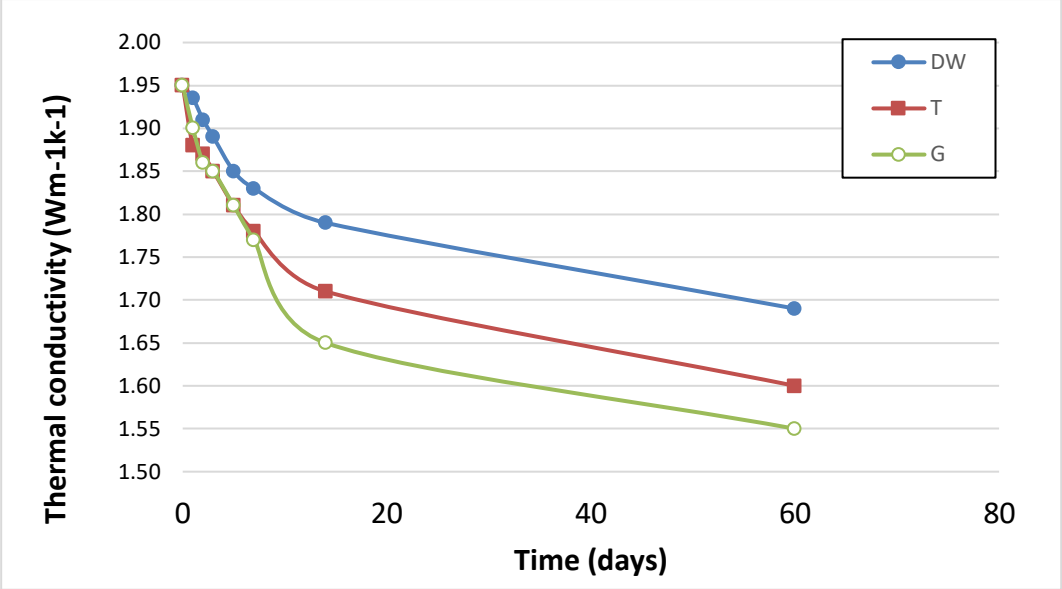

(a)

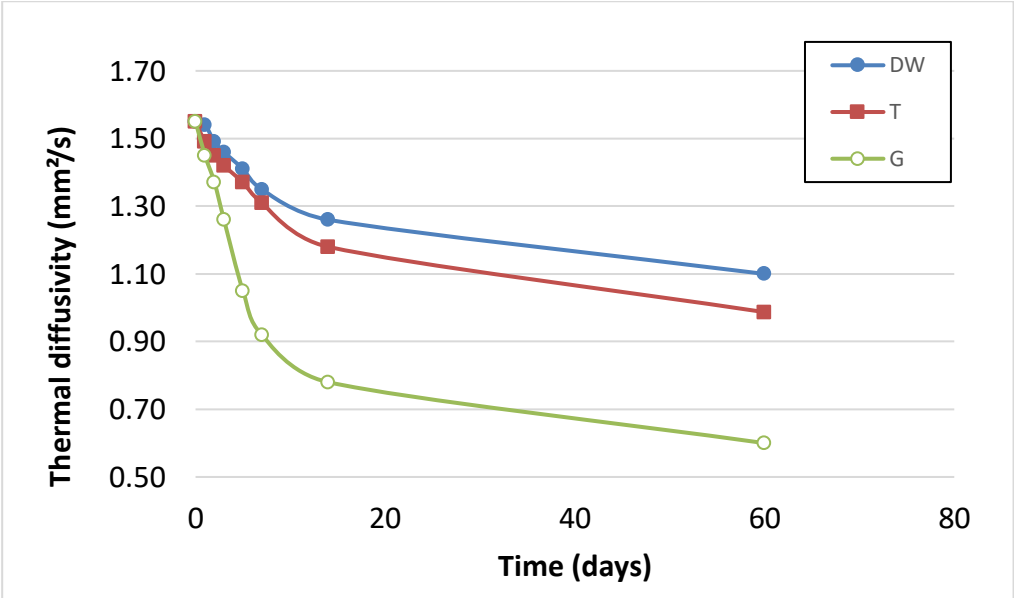

(b)

Figure 5.5. Time-dependent change of the thermal (a) conductivity and (b) diffusivity of the 30/70 bentonite-sand samples exposed to various solutions

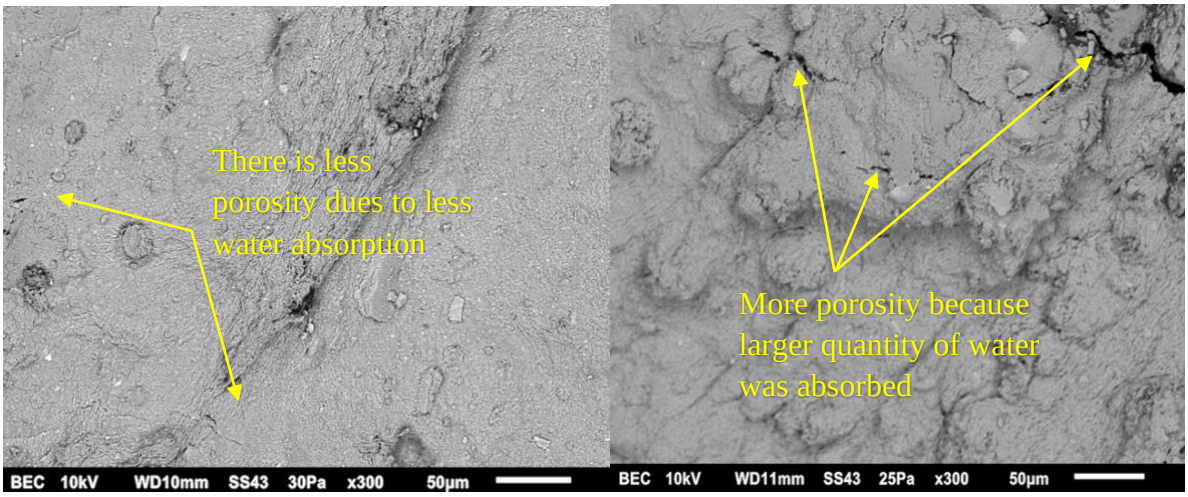

(a) (b)

Figure 5.6. SEM images of compacted bentonite-sand mixture cured in distilled water (a) 3 days specimen (b) 60 days specimen

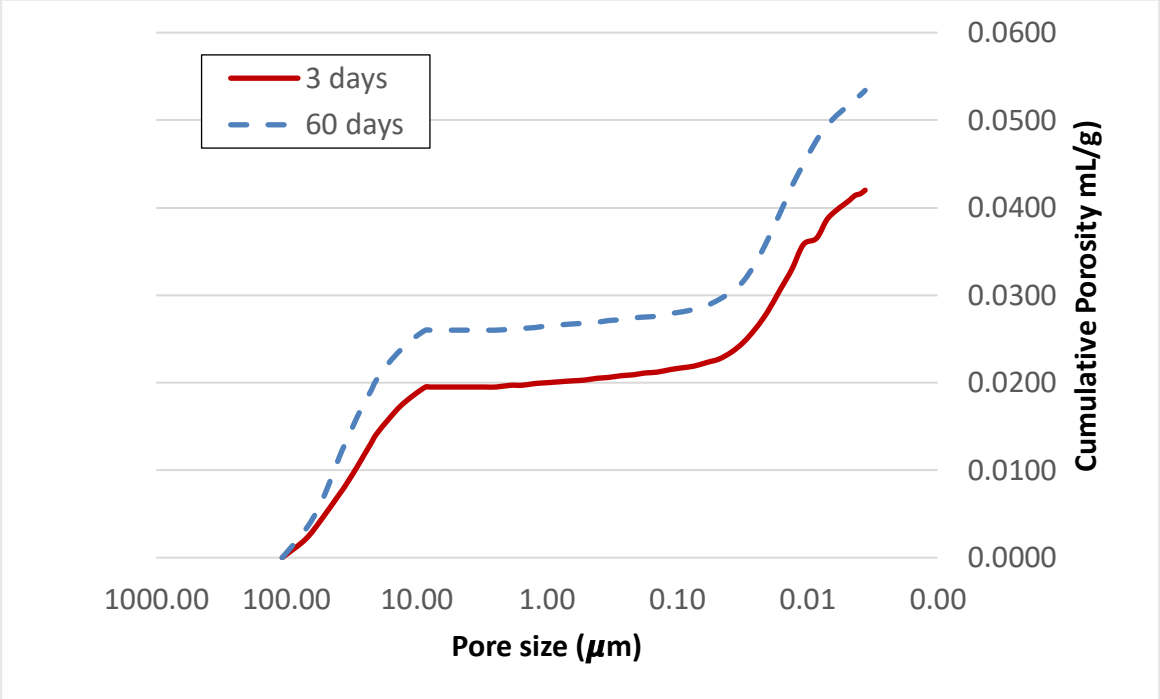

Figure 5.7. MIP cumulative pore volume for bentonite-sand mixtures cured in distilled water for 3 days and 60 days

5.3.2 Effect of pore water chemistry on the thermal conductivity and diffusivity of bentonite-sand mixture.

On the other hand, Figure 5.5a and 5.5b also reveal that the groundwater chemistry has a negative effect on the thermal conductivity and diffusivity of bentonite-sand mixture. Specimens inundated with distilled water has the highest thermal conductivity (1.83 W/mK after 7 days and 1.69 W/mK after 60 days), followed by solution T (1.78 W/mK after 7 days and 1.60 W/mK after 60 days) and solution G with the lowest (1.77 W/mK after 7 days and 1.55 W/mK after 60 days). Similarly, the thermal diffusivity varied from 1.55 mm^2/s to 1.1 mm^2/s; 1.55 mm^2/s to 0.99 mm^2/s; 1.55 mm^2/s 0.6 mm^2/s for the DW, T, and G solutions, respectively. As provided in Table 2, the total dissolved solids in solutions G and T are respectively 300 g/L and 192 g/L signifying higher level of salinity in the former, which is dominated by Na and Ca salts. This lower thermal conductivity values of the samples exposed to the saline solutions G and T results from the combined effects of the following factors. Firstly, high water salinity has been reported to cause chemical and/or mineralogical transformations in bentonite-based buffer materials (Honty el al., 2004; Karnland et al., 2007; Elert et al., 2008). These changes would affect the swelling capacity of the mixture, which determines the pore structure and configuration of the bentonite-sand particles. Generally, the swelling pressure in a bentonite-based material is mainly generated by either crystalline swelling or double layer swelling (Wang et al., 2014; Zhang et al., 2019). The hydration of the exchangeable cations (i.e., Na^+, K^+, Mg^{2+}, and Ca^{2+}) in the mineral layers is the source of the crystalline swelling. Na-montmorillonite, which is the dominant mineral in the MX-80 bentonite (Table 2), is the most expansive of all the montmorillonite minerals that give the clay its high swelling capacity (Odriozola and Guevara-Rodriquez, 2004). The higher salt concentration in the solutions T and G reduced the swelling ability of the clay by partially transforming the Na-montmorillonite into Ca-montmorillonite through cation exchange

(Charlet and Tournassat, 2005; Segad et al., 2010; Karpinski and Szkodo, 2015). Both solutions have high amount of the Ca^{2+} ions (Table 3), which have greater affinity for the montmorillonite minerals than the univalent Na^{+} ions (Tournassat et al., 2011; Akinwunmi et al., 2020). The transformations can be observed from the XRD diagrams in Figure 5.8 for mixtures exposed to both DW and G solutions. The predominantly Na-montmorillonite minerals in the DW, were extensively converted into Ca-montmorillonite when saturated with the saline solution. The effect of this on the swelling of the mixture can be vividly observed from the SEM images (Figure 5.9), with the specimen exposed to DW having more intact particle's structure or finer pore structure (less void) and the one exposed to solution G has the most spacing or voids (coarse pore structure). Packed clay and sand particles with less spacing improves the thermal conductivity (Abu-Hamdeh and Reeder, 2000; Ochsner et al., 2001). Another way the saline solution affects the swelling capacity of the bentonite clay is weaking the repulsive forces between the clay particles. This occurs due to the negative effect the dissolved saline ions have on the diffuse double layer (DDL) of the montmorillonite particles in the mixture (Shiranzi et al., 2011; Weiman et al., 2014). According to Tessier (2013), increasing the salt concentration decreases the double-layer swelling between the clay quasicrystals which consequently reduces the overall swelling pressure in the mixture.

Beside the transformations on the clay, the salt concentration in the pore water of the compacted bentonite-sand mixture has a strong negative correlation with the thermal conductivity, as noted by Siddiqua et al., (2018) too. The primary reason for this is the fact that saline solutions have lower thermal conductivities than pure distilled water (Ramires and Nieto de Castro, 1994; Casás et al., 2013; Siddiqua et al., 2018). It is important to point out the positive correlation between the thermal conductivity and thermal diffusivity for the three different solutions. Mixtures exposed to distilled water has the highest values for both properties consistently, followed by solution T and then solution G. Previous studies have

shown that the thermal diffusivity of materials has a direct relation with their thermal conductivity as (Tikhonravova, 2007; Casás et al., 2013).

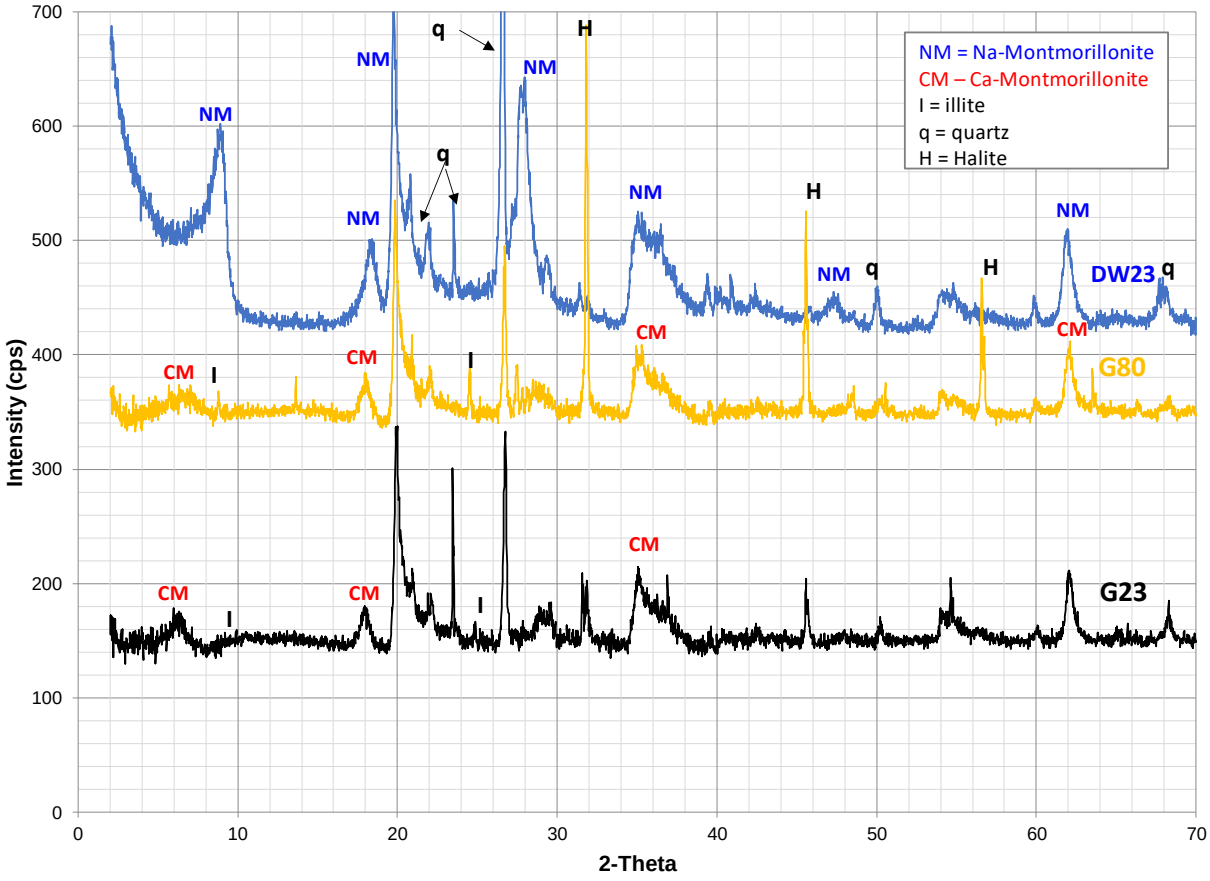

Figure 5.8. XRD patterns of the 30:70 bentonite–sand mixture mixed and saturated with (i) DW at 23 ºC, (ii) G solution at 23 ºC (G23) and (iii) G solution at 80 ºC (G80)

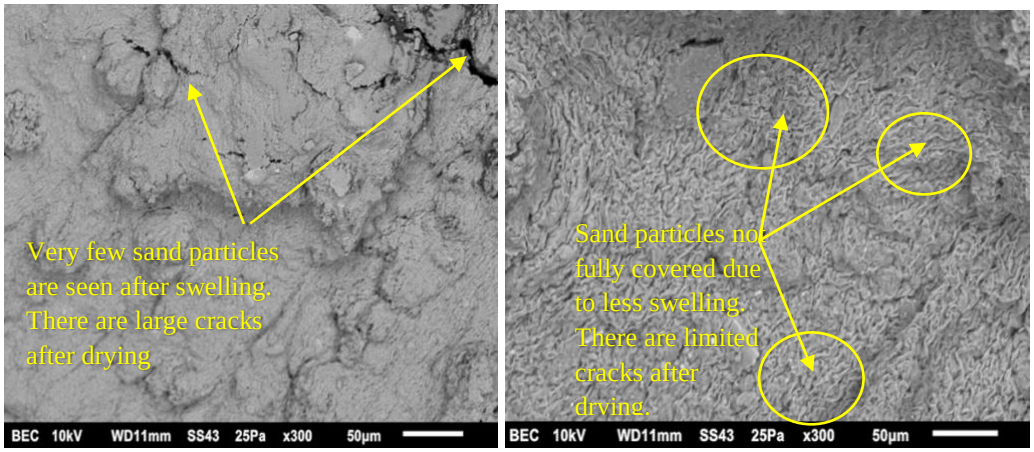

(a) (b)

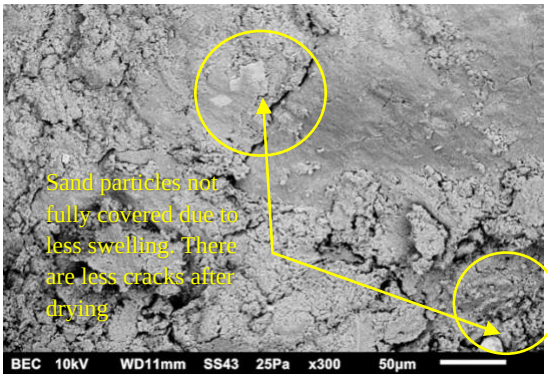

(c)

Figure 5.9. SEM images of compacted bentonite-sand mixture cured in distilled water and saline solutions for 60 days (a) DW (b) Solution T (c) Solution G

5.3.3 Effect of bentonite content on the thermal conductivity and thermal diffusivity

Regardless of the water salinity, the thermal conductivity of the bentonite-sand mixture decreases with the increase of the clay proportion as shown in Figure 5.11. As pointed out in the previous section, quartz sand has higher thermal conductivity as compared to bentonite, therefore, the variation observed is largely govern by the thermal behaviours of the materials. Liu et al. (2019b) observed that any increase in the bentonite fraction in a quartz sand-bentonite-carbon fiber composite beyond 10% is accompanied by the decrease of the thermal conductivity. They associated the impact with the low thermal conductivity of bentonite compared to other materials in the mixture. Besides that, high percentage of bentonite clay in the mixture leads to absorption of more water due to its swelling potential. As the amount of water within the mixture increases, the contact between the solid particles is weakened, thereby lowering down the rate of heat transfer of the material (Yun and Santamarina, 2008; Dong et al., 2015). This in agreement with the pore structure or particles arrangement of the 30/70 and 70/30 specimens as seen from the SEM images in Figure 10 a and b. The grains of sand in 30/70 specimen can be seen clearly with the bentonite serving as a filler. For the 70/30 specimen, the sand is not obvious, and the material has a lot more pores that were formed by the drying of absorbed water. The evidence of the high porosity can be seen from Figure 5.12,

with the mixture containing 70% bentonite having a total porosity of 0.09 mL/g while that containing 30% bentonite has only 0.05 mL/g. Thus, having an adequate amount of sand in the mixture does not only improve the mechanical strength of the barrier material, but also improves the thermal conductivity.

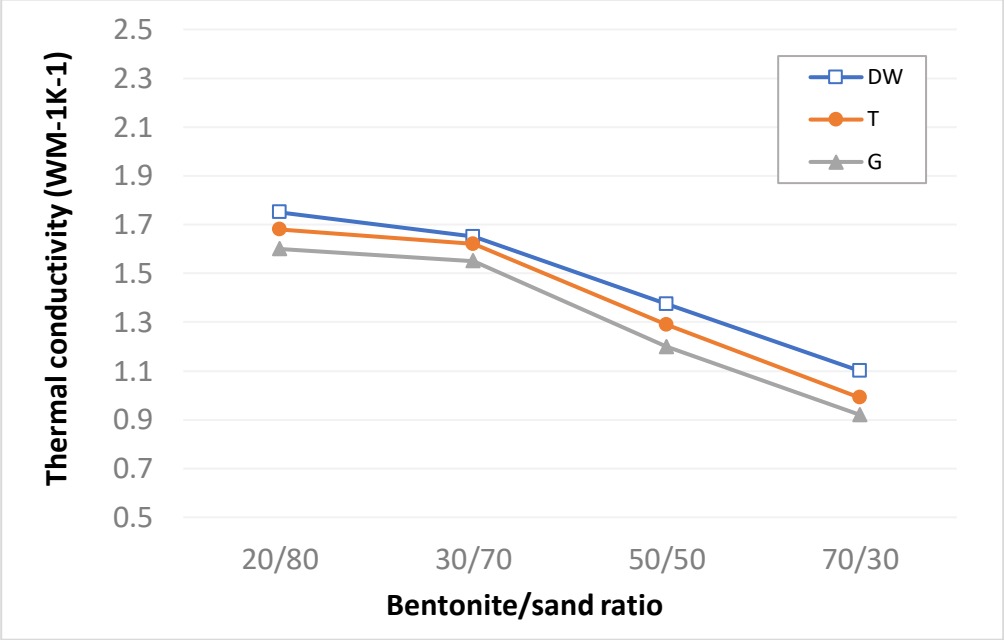

(a)

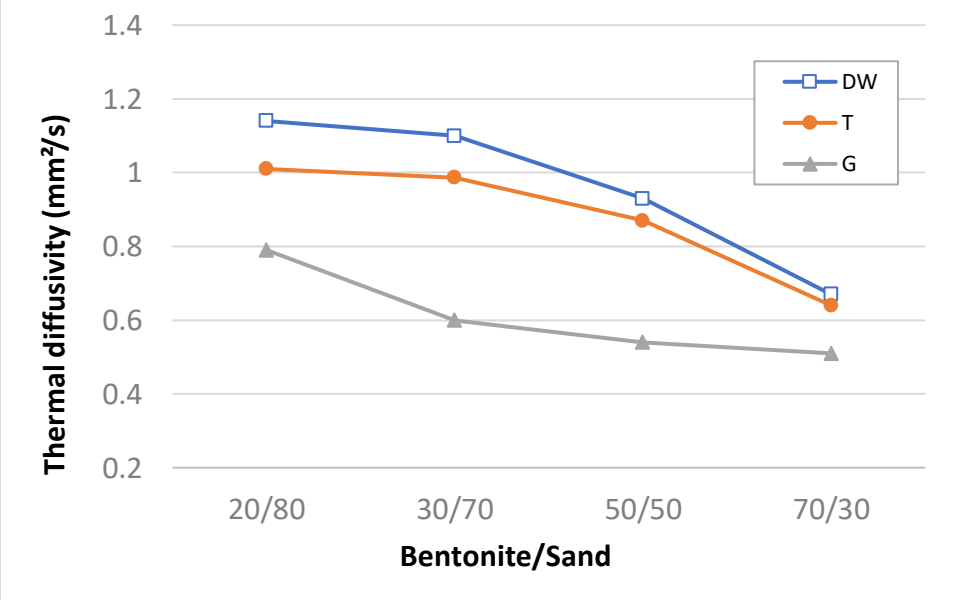

(b)

Figure 5.10. Effect of bentonite/sand ratio on the thermal conductivity (a) Thermal conductivity (b) Thermal diffusivity

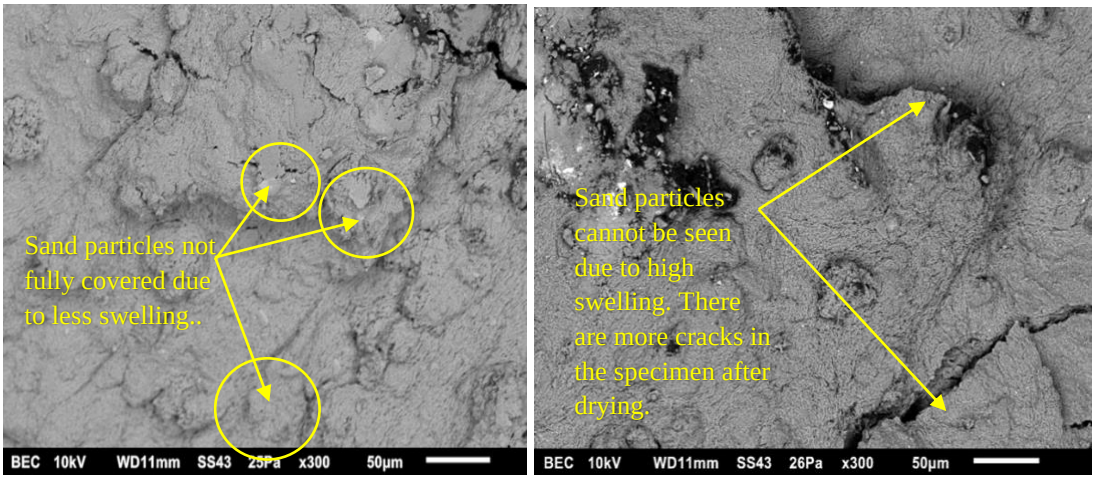

(a) (b)

Figure 5.11. SEM images of compacted bentonite-sand mixture with different bentonite/sand ratios (a) 30/70 (b) 70/30

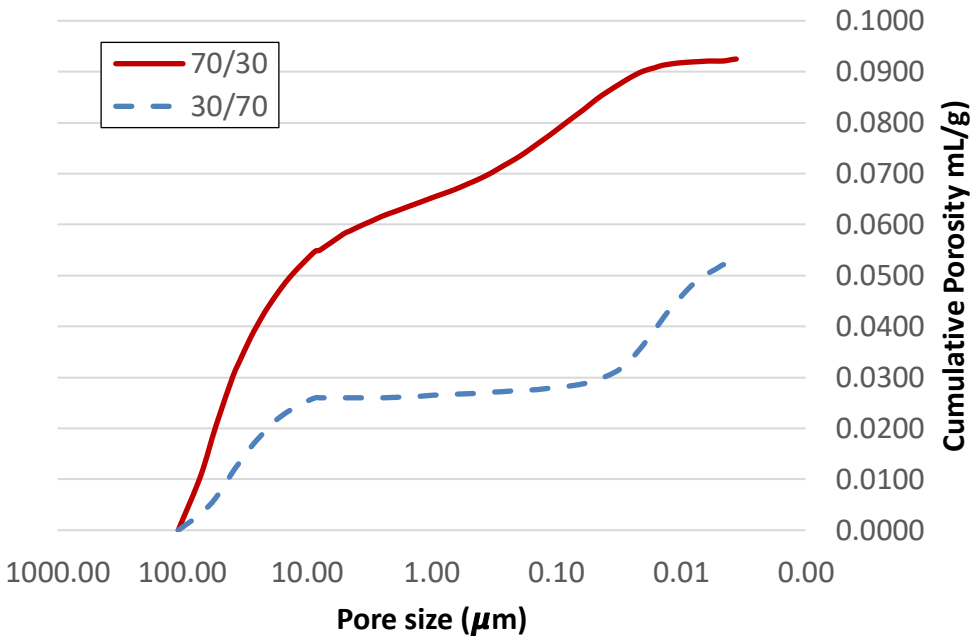

Figure 5.12. MIP cumulative pore volume for compacted bentonite-sand mixture with different bentonite/sand ratios

5.3.4 Prediction of thermal conductivity in of bentonite-sand mixture in saline solution

Multiple researchers have attempted to model the thermal conductivity of clayey soils as well as clay-based mixtures based on different input variables. Most of the mathematical models used geomaterial properties such as particle size, density, clay content, water content

and mineral contents as the main parameters (Gualtieri et al., 2010; Mishra et al., 2017). Perhaps, the choice of the input variables relies on the manner by which heat is transferred through conduction (Mishra et al., 2017). In soils, the conduction occurs through the packed solid particles and available water molecules, if not dry. The magnitude of thermal conductivity would, therefore, depends on the nature of the materials and how densely there are packed (Mishra et al., 2017). As summarized in Table 5.4, the reviewed models have limited applicability on the barrier material made of bentonite/sand mixture exposed to different groundwaters.

Table 5.4. Accuracy and limitations of various predictive models of thermal conductivity of compacted clay materials

Model	**Model expression**	**Notes**
Bruggeman (1935)	$\left(\frac{k_{m,p}}{k_c}\right)^{\frac{1}{3}}(1-P_d)=\frac{\left[\lambda-\left(\frac{k_{m,p}}{k_c}\right)\right]^{\frac{1}{3}}}{\lambda-1}$	With $\lambda=\frac{k_d}{k_c}$. Where $k_{m,p}$ is the predicted thermal conductivity, k_d is the thermal conductivity of suspended particles, k_c is the thermal conductivity of the continuous phase, P_d is the volume of fraction of spherical particles. This model is only limited to a 50:50 bentonite/sand mixture with sand being considered in a suspended phase.
Kersten (1949)	For sandy soils: $k_u = 0.1442[0.7\log(w) - 0.4] \times 10^{0.6243\gamma_d}$ $k_f = 0.001096 \times 10^{0.8116\times\gamma_d} + 0.00461w \times 10^{0.9115\gamma_d}$ For Fine grained soils: $k_u = 0.1442[0.9\log(w) - 0.2] \times 10^{0.6243\gamma_d}$ $k_f = 0.001442 \times 10^{0.373\times\gamma_d} + 0.001226w \times 10^{0.4994\gamma_d}$	k_u is the thermal conductivity of unfrozen soil, k_f is the thermal conductivity of frozen soil, w is the moisture content, and γ_d is the dry unit weight. Even though the model has a relatively high correlation coefficient (R = 0.72), it is only suitable for either purely sandy or fined grained soils.

Johansen (1975)	For sandy soils: $k_{ru} = 0.7\log(S_r) + 1$ $k_{rf} = S_r$ For fine grained soils: $k_{ru} = \log(S_r) + 1$ $k_{rf} = S_r$ $k{=}k_r\left(k_{sat} - k_{dry}\right) + k_{dry}$	k_{sat} is the thermal conductivity of the soil in saturated conditions, k_{dry} is the thermal conductivity at completely dry conditions, k_r is termed Kersten number, which is the influence of the degree of saturation on normalized thermal conductivity, S_r is the degree of saturation, k_{rf} is the normalized thermal conductivity of frozen soil, k_{ru} is the normalized thermal conductivity of unfrozen soil. This model is only suitable for pure sandy soils on one hand or for fined-grained soils having a degree of saturation above 20% (Mishra et al., 2017; Siddiqua et al., 2018).
de Vries (1963)	$k = \frac{\chi_f k_{fl} + f_s\chi_s k_s + f_a\chi_a k_a}{\chi_f + f_s\chi_s + f_a\chi_a}$	$k_s$is the thermal conductivity of solids, k_s is the thermal conductivity of air, k_{fl} is the thermal conductivity of the fluid, $f_s$is the weight factor for the solids, f_a is the weight factor for the air, $\chi_a$is the fraction of air in the soil, $\chi_f$is the fraction of fluid in the soil, χ_s is the fraction of solids, The correlation coefficients for this model are very low due to errors causing overprediction (R = 0.32) and underprediction (R = 0.39).
McInnes (1981)	$k(\theta) = A + B\theta - (A - D)\exp[-(C\theta)^E]$ $A = 0.65 - 0.78\rho_b + 0.6\rho_b^2$ $B = 1.06\rho_b\theta$ $C = 1 + 26\sqrt{f_{clay}}$ $D = 0.03 + 0.1\rho_b^2$ E = 4	The parameters A, B, C, D, and E are empirical terms determined based on soil properties. ρ_b is the bulk density of the soil, θ is the moisture content, and f_{clay} is the clay fraction in the soil. This model considered soils that are very closely similar to the barrier material used in the current study. However it did not put into consideration the chemistry of the water in the soils.

MDD Therm by Arnepalli et al. (2004)	$\frac{1}{k} = 0.01 \times (a \times 10^{-3+0.6243 \times \gamma_d})$	a is an empirical parameter that is a function of the water content and the type of soil, γ_d is the dry unit weight of the soil. The model has a very low prediction accuracy with a coefficient of correlation, R = 0.32.
Cote and Konrad (2005)	$k = (k_{sat} - \chi^{10-\eta n}) \left[\frac{\lambda S_r}{1 + (\lambda - 1)S_r}\right] + \chi^{10-\eta n}$	k_{sat} is the thermal conductivity of the soil in saturated conditions, χ and η are material properties related to the particles shape, λ is texture factor for the soil, and n is the porosity. The soils used to develop the model were classified into crushed rocks, gravels, sand, silt, clay, and peat, limiting its applicability on soils with mixed compositions.
Lu et al. (2007)	$k = k_s(k_{sat} - k_{dry}) \times k_r + k_{dry}$ $k_r = \exp[\alpha(1 - S_r^{\alpha-1.33})]$ $k_{dry} = -an + b$	Improved version of Johansen (1975) model with the additional parameters: a and b are empirical terms, α is a soil texture parameter, and n is the porosity of the soil. The soil modeled in this case is coarse textured with sand fractions > 40% which limits the model's applicability.
Chen (2008)	$k = k_{sat}[(1 - 0.0022)S_r + 0.0022]^{0.78n}$	k_{sat} is the thermal conductivity of the soil in saturated conditions, S_r is the degree of saturation, and n is the porosity. The model was developed for purely sandy soils with different gradations.

The thermal conductivity of a mixture of sand and clay can be estimated using the equation proposed by McInnes (1981) as shown by the equation below.

$$k(\theta) = A + B\theta - (A - D)\exp[-(C\theta)^E] \qquad (1)$$

Where θ is the water content, and the coefficients A, B, C, D, and E are calculated based on the soil properties. For a saturated mixture, Campbell (1985) stated that the last term of equation (1) becomes zero. Thus, the thermal conductivity would be

$$k = A + B\theta \qquad (2)$$

The coefficients are determined from curve fitting using data from DeVries (1963) as follows

$$A = 0.65 - 0.78\rho_d + 0.60\rho_d^2 \qquad (3)$$

$$B = 1.06\rho_d \qquad (4)$$

Where ρ_d is the density of the mixture in kN/m^3.

Because the thermal conductivity results recorded in this research are all for saturated samples, equation (2) is used to fit the thermal conductivity of bentonite-sand mixtures permeated with solution G and T. The terms in equations (3) and (4) can be rewritten with four unknown constants to simplify the modelling process.

$$A = C_1 - C_2\rho_d + C_3\rho_d^2 \qquad (5)$$

$$B = C_4\rho_d \qquad (6)$$

Moreover, densities recorded in this research are the initial compacted densities, which differ from the densities of the mixtures after permeation. However, the final densities of the samples would be a function of the initial densities, but lower in magnitude. Thus, the equations can be modified as follows

$$A = C_1 - C_2[\rho_d - (\rho_d * \theta * C_5)] + C_3[(\rho_d - (\rho_d * \theta * C_5)]^2 \qquad (7)$$

$$B = C_4[(\rho_d - (\rho_d * \theta * C_5)] \qquad (8)$$

a) Model for estimating thermal conductivity for bentonite-sand mixture permeated in solution G

For the mixtures permeated in solution G, the coefficients are estimated as follows:

C_1 = 0.79; C_2 = 0.0031; C_3 = 0.0029; C_4 = 0.0548; C_5 = 0.31

The model for the mixture in G becomes

$$k = 0.79 - 0.0031[\rho_d - 0.31(\rho_d * \theta)] + 0.0029[(\rho_d - 0.31(\rho_d * \theta)]^2 + 0.0548[(\rho_d - 0.31(\rho_d * \theta)]$$

Figure 5.13 show the comparison between the predicted values of thermal conductivity with those obtained experimentally. It is obvious the model predictions and experimental values agree well.

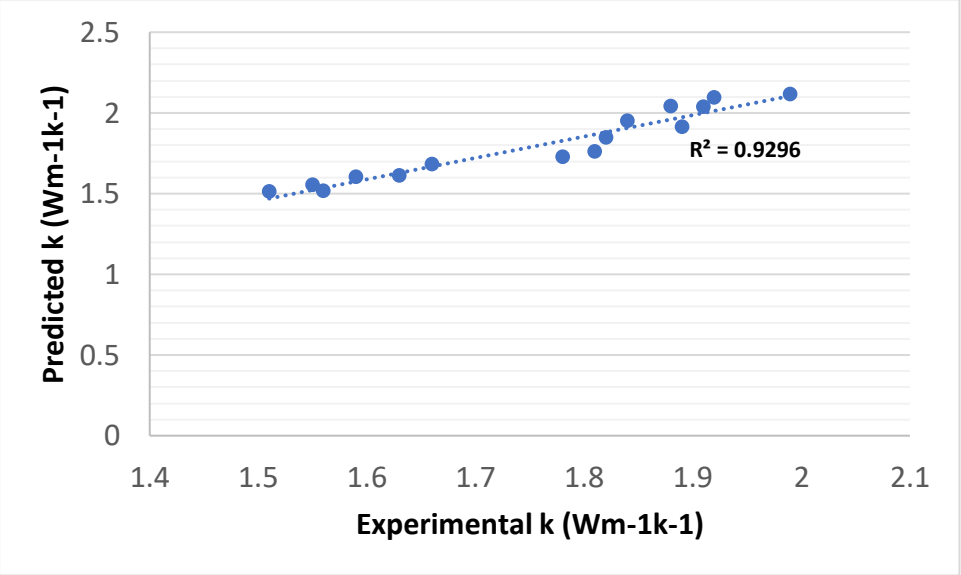

Figure 5.13. Correlation between experimental and predicted data for G solution

b) Model for estimating thermal conductivity for bentonite-sand mixture permeated in solution T

For the mixtures permeated in solution T, the coefficients are estimated as follows:

C_1 = 0.80; C_2 = 0.003; C_3 = 0.0032; C_4 = 0.06; C_5 = 0.31

The model for the mixture in T becomes

$$k = 0.80 - 0.003[\rho_d - 0.31(\rho_d * \theta)] + 0.0032[(\rho_d - 0.31(\rho_d * \theta)]^2 + 0.06[(\rho_d - 0.31(\rho_d * \theta)]$$

The results of the model predictions are compared with experimental, and the comparison is shown in Figure 5.14. It can be seen that there is a good agreement between model predictions and experimental results.

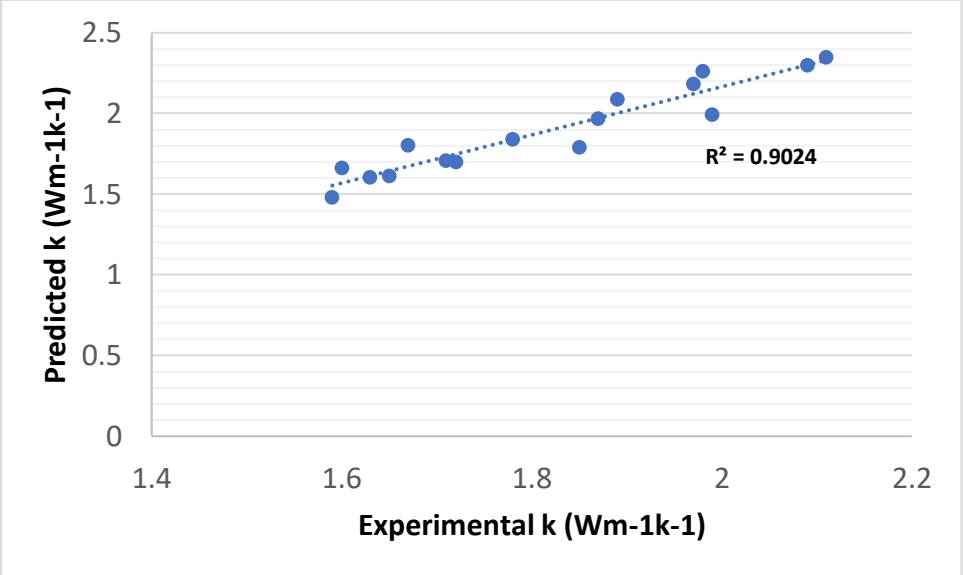

Figure 5.14. Correlation between experimental and predicted data for T solution

5.4 Summary and Conclusions

The thermal conductivity and diffusivity of compacted bentonite-sand mixture exposed to waters of different chemical composition (distilled water, Guelph and Trenton saline groundwaters) were experimentally investigated and discussed in this paper. Based on the results, the following conclusions are drawn.

1. The high thermal conductivity of quartz sand dominates the heat transfer behaviour of the composite buffer material made up of bentonite and sand. Increasing the proportion of sand in the mixture significantly increases the thermal conductivity as well as the thermal diffusivity, regardless of the chemical composition of the water. The material has the greatest thermal conductivity when it is initially compacted as the solid's particles are packed closely together allowing the fast transmission of heat. As the clay particles absorb water, whether pure or saline, the contact between the weakens, which

lowers down the thermal conductivity. This is because water is the least conductive material in comparison to bentonite and quartz sand, especially when it contains dissolved salts.

2. The pore water chemistry or the chemical composition of Ontario's groundwaters has a significant influence on the thermal conductivity and diffusivity of compacted bentonite-sand mixture. Dissolved salts lower the conductivity of the pore water and also triggers the transformation of the Na-montmorillonite mineral into less swelling Ca- montmorillonite. Also, increasing the salt concentration decreases the double-layer swelling between the crystals of the clay which consequently reduces the overall swelling pressure in the mixture.
3. The porosity of the bentonite-sand mixture, whether filled with air or water, plays a significant role on the thermal conductivity and diffusivity, irrespective of the chemical composition of the water. The thermal conductivity was observed to decrease with the increase of void ratio. Spacing between the solid particles slows down the rate of heat transfer within the buffer material.
4. Using the volumetric water content and the dry density of the bentonite-sand mixture, a model was developed to predict the thermal conductivity of a buffer material exposed to Guelph and Trenton saline groundwaters. Both models agree with experimental studies and have an R-squared values of 0.93 and 0.90 respectively.

The findings from this study shed light on the thermal properties of compacted bentonite-sand mixture used as a buffer material in saline groundwaters prevalent in some parts of Ontario, Canada. It will help in a more effective design of the engineered barrier material for deep geological disposal of radioactive waste.

5.5 References

Abu-Hamdeh, N. H., & Reeder, R. C. (2000). Soil thermal conductivity effects of density, moisture, salt concentration, and organic matter. *Soil science society of America Journal*, *64*(4), 1285-1290.

Amer, A. M. (2009). Moisture adsorption capacity and surface area as deduced from vapour pressure isotherms in relation to hygroscopic water of soils. *Biologia*, *64*(3), 516-521.

Boyle, C. H., & Meguid, S. A. (2015). Mechanical performance of integrally bonded copper coatings for the long-term disposal of used nuclear fuel. *Nuclear Engineering and Design*, *293*, 403-412.

Bruggeman, D. A. G. (1935). Dielectric constant and conductivity of mixtures of isotropic materials. *Ann. Phys.(Leipzig)*, *24*, 636-679.

Campbell, G. S. (1985). *Soil physics with BASIC: transport models for soil-plant systems*. Elsevier.

Carpenter, T. (2019). Thermal Properties of Dry and Saturated Soils. *Master's Thesis, University of Tennessee*.

Casás, L. M., Pozo, M., Gómez, C. P., Pozo, E., Bessières, L. D., Plantier, F., & Legido, J. L. (2013). Thermal behaviour of mixtures of bentonitic clay and saline solutions. *Applied clay science*, *72*, 18-25.

Chen, Y. G., Liu, X. M., Mu, X., Ye, W. M., Cui, Y. J., Chen, B., & Wu, D. B. (2018). Thermal conductivity of compacted GO-GMZ bentonite used as buffer material for a high-level radioactive waste repository. *Advances in Civil Engineering*, *2018*.

Côté, J., & Konrad, J. M. (2005). A generalized thermal conductivity model for soils and construction materials. *Canadian Geotechnical Journal*, *42*(2), 443-458.

Dong, Y., McCartney, J. S., & Lu, N. (2015). Critical review of thermal conductivity models

for unsaturated soils. *Geotechnical and Geological Engineering*, *33*(2), 207-221.

Elert, K., Sebastián, E., Valverde, I., & Rodriguez-Navarro, C. (2008). Alkaline treatment of clay minerals from the Alhambra Formation: Implications for the conservation of earthen architecture. *Applied Clay Science*, *39*(3-4), 122-132.

Fall, M., Li, Z., Guo, G. &Wei, X. (2018). Simulation of gas migration in Canadian potential host rocks for radioactive waste disposal. Proceedings of 47. Geomechanik-Kolloquium, 2018, Freiberg, Germany, Nov 16, 2018.

Fall, M., Nasir, O., & Nguyen, T.S., (2014). A coupled hydro-mechanical model for simulation of gas migration in host sedimentary rocks for nuclear waste repositories. *Engineering Geology* 176, 24-44.

Guo, G., & Fall, M. (2021). Advances in modelling of hydro-mechanical processes in gas migration within saturated bentonite: A state-of-art review. *Engineering Geology*, 106123, doi: 10.1016/j.enggeo.2021.106123.

Guo, G.& Fall, M. 2018. Modelling of dilatancy-controlled gas flow in bentonite based materials with double porosity and double effective stress concepts. *Engineering Geology* 243(4):253-271.

Hicks, T. W., Baldwin, T. D., Hooker, P. J., Richardson, P. J., Chapman, N. A., McKinley, I. G., & Neall, F. B. (2008). Concepts for the geological disposal of intermediate-level radioactive waste. *Sign*, *736*(1).

Honty, M., Uhlík, P., Sucha, V., Caplovicová, M., Franců, J., & Biron, A. (2004). Smectite to illite alteration in salt-bearing bentonites (the East Slovak Basin). *Clays and Clay Minerals*, *52*(5), 533-551.

Jensen, M., Lam, T., Luhowy, D., McLay, J., Semec, B., & Frizzell, R. (2009). Ontario

power generation's proposed L&ILW deep geologic repository: an overview of geoscientific studies. *Nuclear Waste Management Organization, GeoHalifax2009/GéoHalifax2009*.

Johansen, O. (1975). "Thermal conductivity of soils." Ph.D. thesis, Institute for Kjoleteknikk, Trondheim, Norway.

Karnland, O., Nilsson, U., Weber, H., & Wersin, P. (2008). Sealing ability of Wyoming bentonite pellets foreseen as buffer material–laboratory results. *Physics and Chemistry of the Earth, Parts A/B/C, 33*, S472-S475.

Karpinski, B., & Szkodo, M. (2015). Clay minerals-mineralogy and phenomenon of clay swelling in oil & gas industry. *Advances in Materials Science*, *15*(1), 37.

Kersten, M. S. (1949). "Laboratory research for the determination of the thermal properties of soils." ACFEL Technical Rep. No. 23, Univ. of Minnesota, MN.

Kolay, P. K., & Ramesh, K. C. (2016). Reduction of expansive index, swelling and compression behaviour of kaolinite and bentonite clay with sand and class C fly ash. Geotechnical and Geological Engineering, 34(1), 87-101.

Komine, H. (2004). Simplified evaluation for swelling characteristics of bentonites. Engineering geology, 71(3-4), 265-279.

Li, X., Zhang, C., & Röhlig, K. J. (2013). Simulations of THM processes in buffer-rock \ barriers of high-level waste disposal in an argillaceous formation. *Journal of Rock Mechanics and Geotechnical Engineering*, *5*(4), 277-286.

Liu, X., Cai, G., Liu, L., Liu, S., & Puppala, A. J. (2019). Thermo-hydro-mechanical properties of bentonite-sand-graphite-polypropylene fiber mixtures as buffer materials for a high-level radioactive waste repository. *International Journal of Heat and Mass Transfer*, *141*, 981-994.

Liu, L., Cai, G., Liu, X., Liu, S., & Puppala, A. J. (2019b). Evaluation of thermal-mechanical

properties of quartz sand–bentonite–carbon fiber mixtures as the borehole backfilling material in ground source heat pump. *Energy and Buildings*, *202*, 109407.

McInnes, K. J. (1981). Thermal Conductivities of Soils from Dryland Wheat Regions of Eastern Washington. *MS Thesis, Washington State University*.

Mishra, R., Militky, J., & Venkataraman, M. (2019). Nanoporous materials. *Nanotechnology in Textiles*, 311-353.

Mishra, P. N., Surendran, S., Gadi, V. K., Joseph, R. A., & Arnepalli, D. N. (2017). Generalized approach for determination of thermal conductivity of buffer materials. *Journal of Hazardous, Toxic, and Radioactive Waste*, *21*(4), 04017005.

Montes-H, G., Duplay, J., Martinez, L., & Mendoza, C. (2003). Swelling–shrinkage kinetics of MX80 bentonite. *Applied Clay Science*, *22*(6), 279-293.

Tikhonravova, P. I. (2007). Effect of the water content on the thermal diffusivity of clay loams with different degrees of salinization in the Transvolga region. *Eurasian Soil Science*, *40*(1), 47-50.

Ochsner, T. E., Horton, R., & Ren, T. (2001). A new perspective on soil thermal properties. *Soil science society of America Journal*, *65*(6), 1641-1647.

Odriozola, G., & Guevara-Rodríguez, F. D. J. (2004). Na-montmorillonite hydrates under basin conditions: Hybrid Monte Carlo and Molecular Dynamics simulations. *Langmuir*, *20*(5), 2010-2016.

Orellana, L. F., Giorgetti, C., & Violay, M. (2019). Contrasting mechanical and hydraulic properties of wet and dry fault zones in a proposed shale-hosted nuclear waste repository. *Geophysical Research Letters*, *46*(3), 1357-1366.

Pastina, B., & Hellä, P. (2006). *Expected evolution of a spent nuclear fuel repository at Olkiluoto* (No. POSIVA--06-05). Posiva Oy.

Presley, M. A., Craddock, R. A., & Zolotova, N. (2009). The effect of salt crust on the

thermal conductivity of one sample of fluvial particulate materials under Martian atmospheric pressures. *Journal of Geophysical Research: Planets*, *114*(E11).

Ramires, M. L., Nieto de Castro, C. A., Fareleira, J. M., & Wakeham, W. A. (1994). Thermal conductivity of aqueous sodium chloride solutions. *Journal of Chemical and Engineering Data*, *39*(1), 186-190.

Salazar, A. (2003). On thermal diffusivity. *European journal of physics*, *24*(4), 351.

Santiago, F., Mucientes, A. E., Osorio, M., & Rivera, C. (2007). Preparation of composites and nanocomposites based on bentonite and poly (sodium acrylate). Effect of amount of bentonite on the swelling behaviour. *European polymer journal*, *43*(1), 1-9.

Segad, M., Jonsson, B., Åkesson, T., & Cabane, B. (2010). Ca/Na montmorillonite: structure, forces and swelling properties. *Langmuir*, *26*(8), 5782-5790.

Shehata, A., Fall, M., Detellier, C., & Alzamel, M. (2021). Effect of groundwater chemistry and temperature on swelling and microstructural properties of sand–bentonite for barriers of radioactive waste repositories. *Bulletin of Engineering Geology and the Environment*, *80*(2), 1857-1873.

Shirazi, S. M., Wiwat, S., Kazama, H., Kuwano, J., & Shaaban, M. G. (2011). Salinity effect on swelling characteristics of compacted bentonite. *Environment Protection Engineering*, *37*(2), 65-74.

Siddiqua, S., Tabiatnejad, B., & Siemens, G. (2018). Impact of pore fluid chemistry on the thermal conductivity of bentonite–sand mixture. *Environmental earth sciences*, *77*(1), 8.

Sun, Q., & Hu, J. (2019). The effect of rapid cooling on the thermal diffusivity of granite. *Journal of Applied Geophysics*, *168*, 71-78.

Tessier, D. (2013). Behaviour and Microstructure of. *Soil Colloids and Their Associations in Aggregates*, *214*, 387.

Tikhonravova, P. I. (2007). Effect of the water content on the thermal diffusivity of clay loams with different degrees of salinization in the Transvolga region. *Eurasian Soil Science*, *40*(1), 47-50.

Tournassat, C., Bizi, M., Braibant, G., & Crouzet, C. (2011). Influence of montmorillonite tactoid size on Na–Ca cation exchange reactions. *Journal of Colloid and Interface Science*, *364*(2), 443-454.

Charlet, L., & Tournassat, C. (2005). Fe (II)-Na (I)-Ca (II) cation exchange on montmorillonite in chloride medium: evidence for preferential clay adsorption of chloride–metal ion pairs in seawater. Aquatic Geochemistry, 11(2), 115-137.

Wang, Q., Cui, Y. J., Tang, A. M., Delage, P., Gatmiri, B., & Ye, W. M. (2014). Long-term effect of water chemistry on the swelling pressure of a bentonite-based material. *Applied clay science*, *87*, 157-162.

Wang, Y., Cui, Y. J., Tang, A. M., Tang, C. S., & Benahmed, N. (2016). Changes in thermal conductivity, suction and microstructure of a compacted lime-treated silty soil during curing. *Engineering geology*, *202*, 114-121.

Weimin, M. Y., Zhang, F., Chen, B., Chen, Y. G., Wang, Q., & Cui, Y. J. (2014). Effects of salt solutions on the hydro-mechanical behaviour of compacted GMZ01 Bentonite. *Environmental earth sciences*, *72*(7), 2621-2630.

Xu, L., Ye, W. M., Chen, B., Chen, Y. G., & Cui, Y. J. (2016). Experimental investigations on thermo-hydro-mechanical properties of compacted GMZ01 bentonite-sand mixture using as buffer materials. Engineering Geology, 213, 46-54.

Xu, Y., Zhou, X., Sun, D. A., & Zeng, Z. (2021). Thermal properties of GMZ bentonite pellet mixtures subjected to different temperatures for high-level radioactive waste repository. *Acta Geotechnica*, 1-12.

Yan, X., Duan, Z., & Sun, Q. (2021). Influences of water and salt contents on the thermal conductivity of loess. *Environmental Earth Sciences*, *80*(2), 1-14.

Yun, T. S., & Santamarina, J. C. (2008). Fundamental study of thermal conduction in dry soils. *Granular matter*, *10*(3), 197-207.

Zhang, N., Yu, X., Pradhan, A., & Puppala, A. J. (2015). Thermal conductivity of quartz sands by thermo-time domain reflectometry probe and model prediction. *Journal of Materials in Civil Engineering*, *27*(12), 04015059.

Zhang, Z. X. (2016). *Rock fracture and blasting: theory and applications*. Butterworth Heinemann.

Zhang, F., Ye, W. M., Wang, Q., Chen, Y. G., & Chen, B. (2019). An insight into the swelling pressure of GMZ01 bentonite with consideration of salt solution effects. *Engineering Geology*, *251*, 190-196.

Chapter 6 Synthesis and Integration of Results

6.1 Introduction

For a better understanding of the effects of pore water chemistry and temperature on the properties (swelling capacity, thermal behaviour, and hydraulic conductivity), the results obtained from the three technical papers are integrated and discussed in this chapter. Each of the technical papers has a main objective of investigating a particular performance property, but the key findings are inter-related. Table 6.1 gives a summary of the tests conducted.

Table 6.1. Summary of influential factors studied in the research work

Technical Paper	Chapter	Mix composition	Curing (permeation) Time	Pore water chemistry	Initial compaction density	Curing Temperature	Microstructural tests
1	**3**	**x**	**x**	**x**	**x**	**x**	XRD, MIP, TG/DTG, SEM
2	**4**	**x**	**x**	**x**	**x**	**x**	MIP, TG/DTG, SEM
3	**5**	**x**	**x**	**x**	**x**		XRD, MIP, TG/DTG, SEM

In the following sections, the key factors responsible for the variation of the swelling, thermal, and hydraulic properties of the bentonite-sand barrier material will be discussed. These factors are i) mix proportion ii) initial density iii) curing time iv) pore water chemistry v). curing temperature.

6.2 Effect of mix proportion

Quartz sand is introduced in the barrier material mainly its better mechanical and thermal property as compared with bentonite clay. The experiments conducted used different bentonite-sand blending ratios (20/80, 30/70, 50/50, 70/30, and 80/20) to study the properties of the composite barrier material. As shown in Figure 6.1 A major influence observed from the

results is on the swelling behaviour, which in turn dictates other properties. As measured by a one-dimensional swelling strain, increasing the proportion of sand in the mixture results in the decrease of the swelling strain. For example, with an initial compacted density of 2.0 g/cm3, the specimens containing 30% and 70% sand reached maximum swelling strains of 305% and 191% respectively. Also, specimens with high sand content attain maximum swelling strain much earlier than the specimens with low sand content. Understandably, the swelling is mainly caused by the clay particles, therefore mixtures with high bentonite content would undergo more swelling after being exposed to water. Because the hydraulic conductivity is also dependent on the swelling, mixtures containing higher sand contents were observed to be more permeable. Beside its lack of swelling potentials, the range of the particle sizes of the sand also influences the hydraulic conductivity. Large sand particles increase the hydraulic conductivity of the mixture. On the other hand, incorporation of sand in the barrier material has beneficial effects on the thermal properties. Due to its higher thermal conductivity, increasing the proportion of sand leads to an increase in both thermal conductivity and diffusivity. Also, high percentage of bentonite clay in the mixture leads to absorption of more water due to its swelling potential. When the pore water within mixture increases, the contact between the solid particles is weakened, thereby lowering down the rate of heat transfer of the material.

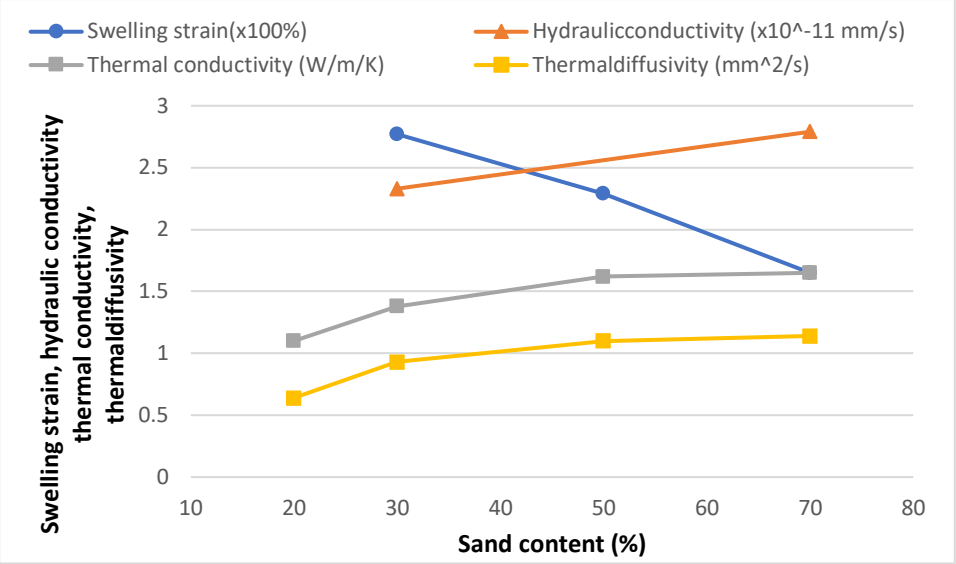

Figure 6.1. Effect of sand content on the properties of the bentonite-sand mixture

6.3 Initial compacted density

The initial density of the bentonite-sand mixture plays a significant role on its behaviour after being exposed to water. The results from this study revealed that compacting the mixture to a higher initial density significantly improves the swelling strain and other performance properties. For any given bentonite-sand ratio, higher dry density is associated with a smaller volume of voids in the mixture, which in turn increases the swelling strain and swelling rate. In other words, increasing the density means that there is more clay in the barrier material per unit volume, which would be available for hydration when exposed to water. Thus, mixtures with higher compaction density will have higher swelling strain mainly from the cumulative expansion of the clay minerals. As indicated earlier, high swelling pressure leads to more compact barrier material with low hydraulic conductivity. Moreover, compaction alone is a common means of reducing the permeability of engineering materials. Likewise, when the clay and sand particles are intact, the rate of heat transfer becomes high, which translates to high thermal conductivity and diffusivity.

6.4 Curing (permeation) time

The permeation time is also an important determinant of the properties of the bentonite-sand mixture because it governs the water intake by the bentonite clay. Typically, the mixture continues to swell (as shown by the one-dimensional swelling test) after being inundated with water until reaching a maximum swelling. The time to reach the maximum swelling strain depends on different factors namely, the initial dry density, the bentonite-sand proportion, and the salinity of the permeation water. For lower values of initial compacted density, the mixture reaches maximum swelling strain earlier than the 100 days employed in the study, while denser mixtures continued to swell. A 70:30 bentonite-sand mixture with an initial density of 1.4 g/cm3 reached its maximum swelling strain of 265% after about 60 days, and then stays constant. However, the same mixture compacted to 2.0 g/cm3 reached a swelling strain of 305% after 100 days while still expanding. However, a general trend has been observed in all the swelling strain curves. The swelling mechanism of the bentonite-sand mixture is divided into three stages: initial swelling (inter-void swelling), primary swelling, and secondary swelling (Cui et al., 2012; Rao and Thyagaraj 2007; Suzuki et al., 2005). Most of the swelling occurs during the primary swelling stage of the clay, whereby the cations exchanged between the crystal layers are hydrated. The primary swelling has typically been observed to span between 0.1 days to about 10 days of permeation and its curve is non-linear. The secondary stage of swelling follows a linear relationship (Cui 2019; Rawat et al., 2019) and is characterized by the creation of double layer. Moreover, the swelling of the bentonite-sand mixture is what mainly governs the hydraulic conductivity which decreases with the permeation time. As the clay expand, the pores in the mixture are eliminated making it less permeable. The thermal conductivity and diffusivity also have a negative correlation with the permeation time. The decrease is caused by the absorption of water which has very low thermal conductivity.

6.5 Porewater chemistry

The three solutions used for the permeation of the barrier material are distilled water (DW), simulated Guelph groundwater (G), and simulated Trenton groundwater (T). Highest rate of swelling of the bentonite-sand mixtures was achieved when exposed to DW, followed by the T solution and finally the G solution having the least swelling. Thus, the swelling capacity of the bentonite clay diminishes when exposed to the saline solutions, with the TDS in the solution being the key determinant factor. Higher volume of TDS causes a reduction in the thickness of the double diffused layer (DDL) of the montmorillonite minerals which leads to a decrease in the repulsive forces between the clay particles (Siddiqua et al., 2011). Also, the cations present in the solutions G and T causes partial transformation of Na-montmorillonite minerals into Ca-montmorillonite, which less expansive. The reduction of the swelling capacity by the saline water leads to high porosity in the bentonite-sand mixture, and consequently resulting in high hydraulic conductivity.

Likewise, thermal conductivity and diffusivity of the barrier material have both been observed to decrease in the presence of the saline waters. Also, the hinderance on the swelling capacity of the clay by the saline solutions is the main reason for the decrease in the thermal properties. In addition, saline water have lower thermal conductivity than pure distilled water (Ramires and Nieto de Castro, 1994; Casás et al., 2013), and also contribute to the changes observed.

6.6 Curing temperature

In addition to room temperature, the experimental tests were also conducted at a temperature of 80 oC to investigate how heat may affect the performance of the barrier material. Using DW for permeation, the high temperature only reduces the swelling strain of the bentonite-sand mixture by only about 2%, which is insignificant. However, when permeated with solution G, the swelling strain of the material was observed to significantly decrease. The mixture containing 70% bentonite recorded the highest decrease in swelling strain of up to 43%

when the curing temperature was increase from room to 80 ^{o}C. This is because higher temperature accelerates the chemically induced degradation of the swelling capacity of the material (Cuevas et al., 2022). The chemical degradation could be a) the dissolution rate of the smectite, which would reduce the amount of expansive minerals (montmorillonites) in the B/S mixture; b) the transformation of Na-montmorillonite minerals to Ca-montmorillonite which has a lower swelling potential; and c) the lattice contraction in different clay structures. Both b and c were confirmed by the microstructural analyses performed in the study. Like the other factors, reduction of the swelling strain by high temperature consequently influences other properties of the bentonite/sand mixture. Interestingly, even though the change in swelling strain for DW is insignificant, the hydraulic conductivity was observed to increase considerably at the high curing temperature. Main reason for that is the redistribution of the pores in the mixture when the temperature increases (Romero et al., 2001).

6.7 Novel Contributions of the Research

The use of bentonite-sand mixture as buffer material in DGRs is new, its performance characteristics are still being studied by many researchers in the field. Some of these studies have shown the benefits of the incorporation of sand in the mixture such as improvement of mechanical strength and thermal properties (Akgün et al., 2006; Gatabatin et al., 2016; Shehata et al., 2015; Siddiqua et al., 2018). However, to ascertain the long-term potentials of the composite barrier material, its performance under varying ground conditions needs to be fully understood. One of these conditions is the groundwater chemistry. This PhD research has been motivated by the recent proposal of locations in Guelph and Trenton, Ontario, for the construction of DGRs for storing spent nuclear fuel generated by the province (Fall et al., 2018. The groundwater in these two regions is known to have very high salinity. Previous studies on the effects of saline water on bentonite-based barrier material have only utilized common salts, such as NaCl and KCl (e.g., Suzuki et al., 2005; Batenipour, 2008; Shirazi et al., 2011; Zhang

et al., 2012). The saline groundwaters from the proposed locations contain several other salts with a total dissolved solids of 300 g/l and 192 g/l for Guelph and Trenton respectively. This is the first time full-scale experimental research is being conducted to specifically study the influence of the saline waters from these two regions. Furthermore, the research also investigated the combined effect other variabilities, namely initial compacted density, bentonite-sand ratio, permeation time, and temperature on the properties of the composite material. This is a novel approach as there has not been any research in the literature that investigated the combined effects of these properties on a bentonite-sand buffer material.

6.8 References

Akgün, H., Koçkar, M. K., & Aktürk, Ö. Z. G. Ü. R. (2006). Evaluation of a compacted bentonite/sand seal for underground waste repository isolation. *Environmental Geology*, *50*(3), 331-337.

Batenipour, H., 2008. Effect of water salinity on the hydro-mechanical behaviour of granular bentonite as light backfill material. Volume 1, Pages 499-505, 61st, Canadian Geotechnical Conference; 2008; Edmonton, Alberta, Canada.

Casás, L. M., Pozo, M., Gómez, C. P., Pozo, E., Bessières, L. D., Plantier, F., & Legido, J. L. (2013). Thermal behaviour of mixtures of bentonitic clay and saline solutions. *Applied clay science*, *72*, 18-25.

Cui SL, Zhang HY, Zhang M. Swelling characteristics of compacted GMZ bentonite–sand mixtures as a buffer/backfill material in China. Engineering Geology 141:65–73 (2012).

Cui Y.-J. On the hydro-mechanical behaviour of MX80 bentonite-based materials. Journal of Rock Mechanics and Geotechnical Engineering 9(3) (2019): 565-574.

Cuevas, J., Villar, M. V., Martın, M., Cobena, J. C., & Leguey, S. (2002). Thermo-hydraulic

gradients on bentonite: distribution of soluble salts, microstructure and modification of the hydraulic and mechanical behaviour. *Applied Clay Science*, *22*(1-2), 25-38.

Fall, M., Li, Z., Guo, G. &Wei, X. (2018). Simulation of gas migration in Canadian potential host rocks for radioactive waste disposal. Proceedings of 47. Geomechanik-Kolloquium, 2018, Freiberg, Germany, Nov 16, 2018.

Gatabin, C., Talandier, J., Collin, F., Charlier, R., & Dieudonné, A. C. (2016). Competing effects of volume change and water uptake on the water retention behaviour of a compacted MX-80 bentonite/sand mixture. *Applied Clay Science*, *121*, 57-62.

Ramires, M. L., Nieto de Castro, C. A., Fareleira, J. M., & Wakeham, W. A. (1994). Thermal conductivity of aqueous sodium chloride solutions. *Journal of Chemical and Engineering Data*, *39*(1), 186-190.

Rao F S.M., Thyagaraj T. Role of direction of salt migration on the swelling behaviour of compacted clays, Applied Clay Sciences. 38 (2007) 113–129.

Rawat A., Baille W., Tripathy S. Swelling behaviour of compacted bentonite-sand mixture during water infiltration. Engineering Geology 257 (26) (2019): 105141.

Romero, E., Gens, A., & Lloret, A. (2001). Temperature effects on the hydraulic behaviour of an unsaturated clay. In Unsaturated soil concepts and their application in geotechnical practice (pp. 311-332). Springer, Dordrecht.

Shehata, A., Fall, M., & Detellier, C. (2015). Swelling characteristics of bentonite based barriers for deep geological repository for nuclear wastes: Impact of underground water chemistry and temperature. In Proceedings of 68th Canadian Geotechnical and 7th Canadian Permafrost Conference, Quebec, Canada, September 20–23, 2015.

Shirazi, S. M., Wiwat, S., Kazama, H., Kuwano, J., & Shaaban, M. G. (2011). Salinity effect on swelling characteristics of compacted bentonite. *Environment Protection Engineering*, *37*(2), 65-74.

Siddiqua, S., Blatz, J., & Siemens, G. (2011). Evaluation of the impact of pore fluid chemistry on the hydromechanical behaviour of clay-based sealing materials. *Canadian Geotechnical Journal*, *48*(2), 199-213.

Siddiqua, S., Tabiatnejad, B., & Siemens, G. (2018). Impact of pore fluid chemistry on the thermal conductivity of bentonite–sand mixture. *Environmental earth sciences*, *77*(1), 8.

Suzuki S., Prayongphan S., Ichikawa Y., Chae B.G. In situ observations of the swelling of bentonite aggregates in NaCl solution. Applied Clay Sciences 29 (2005) 89–98.

Zhang H.Y., Cui S.L., Zhang M., Jia L.Y. Swelling behaviours of GMZ bentonite-sand mixtures

inundated in NaCl-Na2SO4 solutions, Nuclear Engineering and Design, 242 (2012) 115–123.

Chapter 7 General Conclusions and Recommendations

7.1 General conclusions

Experimental investigations were conducted in this study to understand the performance characteristics of bentonite-sand mixture as a barrier material in DGRs. Four main properties, namely swelling strain, hydraulic conductivity, thermal conductivity, and thermal diffusivity were studied. Effects of different parameters (mix composition, initial dry density, chemistry of the permeation water, curing temperature, and curing time) were also studied. The following conclusions are drawn based on the findings from the research study.

- The swelling strain, hydraulic conductivity, thermal conductivity, and thermal diffusivity of bentonite-sand mixtures are significantly influenced by the salinity of the groundwater.
- The saline water reduces of the swelling potential of the barrier material mainly through (i) the reduction of the DDL thickness of the montmorillonite particles due to a high volume of TDS and (ii) the transformation of Na-montmorillonites to Ca-montmorillonites with less swelling potential due to cation exchange.
- The bentonite/sand mix ratio, dry density, and temperature are other influential factors on the performance of the bentonite-sand barrier material.
- High temperature amplifies the degradation of bentonite clay swelling by accelerating the transformation of the clay minerals.
- Using the volumetric water content and the dry density of the bentonite-sand mixture, a model was developed to predict the thermal conductivity of a buffer material exposed to Guelph and Trenton saline groundwaters. Both models agree with experimental studies and have an R-squared values of 0.93 and 0.90 respectively.

7.2 Recommendations

The following are recommended for future studies.

- The temperature of 80°C used in the PhD study is based on the maximum temperature observed from a modeling of DGRs located at 300-700 m deep rocks. A broader study of the effect of different range of temperatures would be beneficial towards understanding the behaviour of the barrier material in different scenarios.
- More work needs to be done on the effects of other saline groundwaters beyond those found in Guelph and Trenton regions of Canada.
- Additional laboratory and field experiments should be performed for the validation of the modeled developed for the prediction of thermal conductivity of bentonite-sand mixture in saline environment.
- New models can be developed for the prediction of the hydraulic conductivity and thermal diffusivity of bentonite-sand mixture in saline environment.